Transcutaneous Co-Delivery of Therapeutic Agents Using Liposomes to Treat Cancer

THESIS

Submitted in partial fulfillment

of the requirements for the degree of

DOCTOR OF PHILOSOPHY

by

ANUP JOSE

ID. No. 2013PHXF0012H

Under the supervision of

Dr. VENKATA VAMSI KRISHNA VENUGANTI

BITS Pilani

Pilani | Dubai | Goa | Hyderabad

BIRLA INSTITUTE OF TECHNOLOGY AND SCIENCE, PILANI

2017

BIRLA INSTITUTE OF TECHNOLOGY AND SCIENCE, PILANI

CERTIFICATE

This is to certify that the thesis entitled **"Transcutaneous Co-Delivery of Therapeutic Agents Using Liposomes to Treat Cancer"** and submitted by **Anup Jose** ID. No. **2013PHXF0012H** for award of Ph.D. of the Institute embodies original work done by him under my supervision.

Signature of the supervisor :

Name in capital letters : VENKATA VAMSI KRISHNA VENUGANTI

Designation : Assistant Professor

Date :

Acknowledgements

I would like to remember and express my sincere gratitude to all the people who contributed in some way to the completion of my doctoral degree.

First and foremost, I thank my supervisor Dr. Venkata Vamsi Krishna Venuganti for giving me the opportunity to complete my PhD thesis at BITS Pilani, Hyderabad campus. During my tenure, he has been a tremendous mentor for me with his unconditional support, encouragement and valuable guidance. A person with outstanding commitment and dedication, he has always made himself available with his immense care and support in my professional as well as personal life throughout my PhD tenure. Without his guidance and constant feedback this PhD would not have been achievable.

I am extremely grateful to my Doctoral Advisory Committee (DAC) members Prof. Punna Rao Ravi and Dr. Swati Biswas for simultaneously encouraging, guiding, and supporting my research.

I express my profound gratitude to Prof. D. Sriram, Professor and Head, Department of Pharmacy, for his support and extending the facilities to work at the institute.

My sincere thanks to Prof. P. Yogeeswari, Associate Dean, Sponsored Research and Consultancy Division, BITS-Pilani Hyderabad for her invaluable suggestions and support.

My special thanks to Dr. Shrikant Yashwant Charde, Technical manager, Neo Pharma, Dubai and former Associate Professor & Head, Department of Pharmacy, for sharing his vast experience and technical knowledge with me at needy times. It was a memorable experience to work with him as a teaching assistant.

I would like to thank Prof. A. Sajeli Begum, Dr. Onkar Prakash Kulkarni, Dr. Arti Dhar and Dr.Balaram Ghosh, Faculty, Department of pharmacy for their support and invaluable suggetsions.

My sincere gratitude to Prof. Souvik Bhattacharyya, Vice Chancellor, Prof. G Sundar, Director, BITS Pilani, Hyderabad Campus, Prof. S. C. Sivasubramanian, Acting Registrar, Prof. Sanjay Kumar Verma, Dean, Academic Research, Prof. M. B. Srinivas, Dean, General Administration and Prof. Vidya Rajesh, Associate Dean, Academic Research (Ph.D. Programme) BITS-Pilani, Hyderabad, for providing necessary support to accomplish my research work.

My heartfelt gratitude to all labmates Dr.Praveen Kumar, Dr.Suman Labala, Ms. Shubhmita Bhatnagar, Dr. Sudeep Kumar, Mr. Naga Thirumalesh, Mr.Girdhari Roy, Mr. Kunal Ninave, Mr. Omkaraswami, Ms. Preeti Kumari, Mr. Vishnu Kiran and Mr. Himanshu Bhat.

Special thanks to all my colleagues Dr. Jean, Dr. Manoj, Dr. Bobesh, Dr. Aditya, Dr. Rahul, Dr.Madhubabu, Dr. Saketh, Dr. Brahmam, Dr. Ganesh S., Dr. Ganesh P., Dr. Mahibalan, Dr. Ram, Dr.Koushik, Dr.Renuka, Dr. Rukaiyya, Dr.Poorna, Dr.Srikanth, Mr.Shailender, Mr. Santhosh, Mr.Gangadhar, Ms. Reshma, Mrs. Prakruti, Mrs. Hasitha, Mrs. Priyanka, Ms. Nikhila, Mrs. Prasanthi, Mr. Shubham, Mr. Siva Krishna, Mr. Suresh, Ms. Rimpy, Ms. Ekta, Ms. Avantika, Mr.Teja, Ms. Jaspreet, Ms. Kalyani, Ms. Kavitha, Ms. Kirti, Ms.Ravali, Ms. Amala, Ms. Pooja, Ms. Janaki, Ms. Deepthi.

My sincere gratitude to the supporting staff Mrs. Saritha, Mr. Rajesh, Mr. Praveen, Ms. Laxmi, Mr. Srinivas and Ms. Rekha for their unconditional support.

My heartfelt gratitude to the Department of Science and Technology (DST), Government of India for providing funding to pursue my doctoral degree as well as for providing international travel support to present my research work at conference abroad.

I also appreciate Centre for International Co-operation in science (CICS) and Amgen (USA) for providing international travel support for presenting my research highlights at various conferences.

Of course no acknowledgments would be complete without giving thanks to my family members, the strong pillars of my life. No words can mention my heartfelt gratitude to my beloved parents, Mr. M. P. Joseph and Mrs. Gracy Joseph. Their unconditional love, care and prayers guided my journey till here. Special thanks to my sister Nisha Tom and brother Anish M Jose for their love and support. My sincere gratitude to my parents-in-law Prof. Jose P Varghese and Mrs. Rose Mary Jose for their love, prayers and support.

Special thanks to Tom Jose, Mable Anish, Lijo Joseph, Nissa Lijo, Gautam Varghese, Arjun John, Anjana Gautam, Anna, Issakiya, Nikitha, Kripa and Issa.

Finally, and most importantly, I would like to thank my wife and best friend, Ann Mary Jose. Our friendship began when we entered the B.Pharm course at College of Pharmaceutical Sciences, Medical College, Trivandrum in 2004. We immediately became friends and have remained so ever since. Her unwavering love, support, encouragement and quiet patience were undeniably the bedrock upon which the past twelve years of my life have been built. She took all the pain to find out various universities offering PhD and completed all the formalities for getting my admission at BITS Pilani. I could not have completed this journey without Ann by my side. Last but not least, a sweet kiss to my 6 months old beloved son, Joseph M Mathew.

Abstract

Co-delivery of more than one therapeutic agent is a promising strategy to improve the therapeutic outcome of cancer therapy. Recently, a better understanding of the fact that cancers arise from the genetic disorders in cell signaling prompted the use of combination therapy involving drug and gene. Among the various nanocarriers explored for the topical delivery of nucleic acids, liposomes have emerged as the most preferable candidates. In the present work, different liposomal formulations were investigated for the transcutaneous co-delivery of either two anticancer drugs or an anticancer drug with siRNA for the treatment of breast and skin cancer respectively.

Initially, we have focussed on transcutaneous co-delivery of tamoxifen and imatinib mesylate using flexible temperature-sensitive liposomes for the treatment of breast cancer. Tamoxifen and imatinib co-encapsulated liposomes were prepared using DPPC, MPPC, Span 80 (70:15:15 w/w) and characterised for average particle size, zeta potential, drug encapsulation efficiency, elasticity, in-vitro drug release at different temperatures and storage stability. Further, the impact of this co-delivery system on breast cancer cells were studied using MCF-7 (estrogen receptor positive) and MDA-MB-231 cells (estrogen receptor negative). Skin permeation studies using porcine skin were carried out to investigate the impact of temperature on permeation parameters of the temperature-sensitive liposomes. Results of in-vitro drug release studies showed more than 80% release of both drugs within 30 minutes at 40^{o}C. Cell viability studies showed enhanced cell growth inhibition upon combination therapy compared to individual therapeutic agents in case of both cell lines.

Later, we have investigated the liposomal co-delivery of curcumin and STAT3 siRNA by non-invasive topical iontophoretic application to treat skin cancer. Curcumin was encapsulated in cationic liposomes and then complexed with STAT3 siRNA. The liposomal nanocomplex was characterized for particle size, zeta-potential, drug release and stability. Human epidermoid (A431) cancer cells were used to study the cell uptake, growth inhibition and apoptosis induction of curcumin loaded liposome-siRNA complex. Topical iontophoresis was applied to study the skin penetration of nanocomplex in excised porcine skin model. Results showed that curcumin loaded liposome-siRNA complex was rapidly taken up by cells preferentially through clathrin mediated endocytosis pathway. The co-delivery of curcumin and STAT3 siRNA using liposomes resulted in significantly ($p<0.05$) greater cancer cell growth inhibition and apoptosis events compared with neat curcumin and free STAT3 siRNA treatment. Furthermore, topical iontophoresis application enhanced skin penetration of nanocomplex to penetrate viable epidermis.

Further, in-vivo studies were carried out to evaluate the efficacy of transcutaneous co-delivery of curcumin and STAT3 siRNA in mouse melanoma model using cationic liposomes. Co-administration of the curcumin and STAT3 siRNA using liposomes significantly ($p<0.05$) inhibited the tumor progression as measured by tumor volume and tumor weight compared with either liposomal curcumin or STAT3 siRNA alone. Furthermore, the iontophoretic administration of curcumin loaded liposome-siRNA complex showed similar effectiveness in inhibiting tumor progression and STAT3 protein suppression compared with intratumoral administration. Taken together, cationic liposomes can be developed for topical iontophoretic co-delivery of small molecule and siRNA for effective treatment of skin diseases.

Table of contents

List of Tables

List of figures

List of abbreviations and symbols

ANOVA	Analysis of variance
BCC	Basal cell carcinoma
BRAF	Murine sarcoma viral (v-raf) oncogene homolog B1
BSA	Bovine serum albumin
CO_2	Carbon dioxide
Cy3	Cyanine3
Da	Dalton
DAPI	4, 6-Diamidino-2-phenylindole
DC	Direct current
DCIS	Ductal carcinoma in situ
DLS	Dynamic light scattering
DMEM	Dulbecco's modified eagle's medium
DMSO	Dimethyl sulfoxide
DNA	Deoxyribonucleic acid
DOPE	1, 2-Dioleoyl-*sn*-glycero-3-phospho-ethanolamine
DOTAP	1, 2-Dioleoyl-3-trimethylammonium propane
DPPC	1, 2-Dipalmitoyl-*sn*-glycero-3-phosphocholine
DSC	Differential scanning calorimeter

ED&C	Electrodesiccation and curettage
EDTA	Ethylene diamine tetra acetic acid
EE	Encapsulation efficiency
FBS	Fetal bovine serum
FITC	Fluorescein Isothiocyanate
FTIR	Fourier transform infrared spectroscopy
g	Gram
h	Hour
HER2	Human epidermal growth factor receptor 2
Hh	Hedgehog
HPLC	High performance liquid chromatography
HPV	Human papillomavirus
kDa	kilodalton
kg	kilogram
kHz	kilohertz
kΩ	kiloohm
L	Litre
M	Molar
MΩ	Megaohms

mA	milliampere
MAPK	Mitogen-activated protein kinase
MEK	Mitogen-activated, extracellular signal-regulated kinase
MEM	Minimum esssential medium Eagle
mg	Milligram
min	Minute
mm	Millimetre
mM	Millimolar
MPa	Megapascal
MPPC	Monopalmitoyl-2-hydroxy-*sn*-glycero-3-phosphocholine
MMS	Mohs micrographic surgery
MRI	Magnetic resonance imaging
MTT	Thiazolyl blue tetrazolium bromide
mV	Millivolt
MW	Molecular weight
NFkB	Nuclear factor kB
NLC	Nanostructured lipid carrier
nm	Nanometer
nM	Nanomolar

N/P	Nitrogen to phosphate
PBS	Phosphate buffered saline
PDI	Polydispersity index
PI3K	Phosphoinoside-3 kinase
R^2	Regression coefficient
RNAi	Ribonucleic acid interference
RP-HPLC	Reverse phase – high performance liquid chromatography
rpm	Revolutions per minute
s	Seconds
SC	Stratum corneum
SCC	Squamous cell carcinoma
SD	Standard deviation
SDS	Sodium dodecyl sulphate
SDS-PAGE	Sodium dodecyl sulphate polyacrylamide gel electrophoresis
SERM	Selective estrogen receptor modulator
siRNA	Small interference ribonucleic acid
SLN	Solid lipid nanoparticle
STAT3	Signal transducer and activator of transcription 3
TDD	Transdermal drug delivery

TEM	Transmission electron microscopy
TEMED	N, N‘tetra methyl ethylene diamine
UV	Ultraviolet
VE	Viable epidermis
w/w	weight/weight
λmax	Wavelength maxima for UV-absorbance
%	Percentage
^{o}C	Degree Celsius
µg	Microgram
µm	Micrometer
µM	Micromolar
µs	Microsecond

Chapter 1

Introduction

1.1. Cancer

Cancer is a generic term used to express a group of diseases that are capable of affecting any part of the body characterized by uncontrolled multiplication of cells. Malignant tumors and neoplasms are the terms used as synonyms to cancer. One of the defining features of cancer is the development of abnormal cells that grow out of control and spread to the adjoining organs, the latter process referred to as metastasis. Cancer is the second leading cause of death worldwide and accounted for more than 8.8 million deaths in 2015. Majority of cancer related deaths (>70%) occur in low and middle income countries. The estimated number of new cancer cases in India will be more than 17 lakhs by the year 2020 (Jain 2017). Globally, the common forms of cancer that contribute to majority of cancer deaths in men are lung, liver, colorectal, esophagus and stomach cancer. Similarly, cancers of breast, cervix, lung, colorectal and stomach accounts for majority of cancer deaths in women.

Cancer arises as a result of multistage transformation process of normal cells to tumor cells that gradually progresses from benign lesion to malignant tumor. It occurs as a result of the molecular interaction between the genetic factors of an individual with various physicochemical and biological agents. Physical carcinogens mainly include UV and ionizing radiation. Common chemical carcinogens are arsenic, heavy metals, asbestos, constituents of tobacco smoke and aflatoxin, a food contaminant. Biological carcinogens include some chronic infections like Helicobacter pylori, Hepatitis B and C virus, Human papillomavirus (HPV) and Epstein-Barr virus. Tobacco use is the single major preventable cause of cancer, leading to more than 22% of cancer deaths globally (Forouzanfar, Afshin et al. 2016). Other risk factors include high body mass index, alcohol consumption, low fruit and vegetable intake and lack of physical activity.

In general, most of the cancer chemotherapeutic agents are administered either orally or through parenteral routes. Unfortunately, majority of these drugs cause severe unwanted side effects wherein they cause damage to healthy cells along with cancer cells. So, in case of cancers that are accessible through topical or transdermal routes, the transcutaneous administration is preferred to minimize unwanted side effects. Breast cancer and skin cancers are types of cancers where, the cancer cells can be accessed through topical/transdermal drug delivery.

1.1.1. Breast cancer

Breast cancer is the most common form of cancer that is responsible for majority of cancer deaths in women globally (Jemal, Bray et al. 2011). It is a type of cancer in which malignant cells form in the tissues of the breast. Breast cancer cases in male are very rare and it accounts for less than one percentage of total breast cancer cases. Symptoms of breast cancer include, swelling of all or part of the breast, breast pain, presence of lump, nipple discharge other than milk, pain or changes in nipple shape, thickening or redness of the nipple or breast skin and a lump in the underarm area (Bish, Ramirez et al. 2005). The common risk factors for breast cancer include, age, genetics, being a woman, family history of breast cancer, radiation to chest or face, race or ethnicity, being obese, pregnancy and breast feeding history, menstrual history, use of hormone replacement therapy, lack of exercise, smoking and alcohol consumption (McPherson, Steel et al. 2000).

1.1.1.1. Types of breast cancer (Weigelt and Reis-Filho 2009)

- Ductal carcinoma in situ (DCIS) – It is a non-invasive form of breast cancer in which cancer cells occur in the lining of milk ducts in breast.

- Invasive ductal carcinoma – Cancer cells are associated with the lining of breast milk duct that invades the nearby tissues.
- Triple negative breast cancer – Cancer cells are negative for estrogen, progesterone and HER2 (Human epidermal growth factor receptor 2)/neu receptors.
- Inflammatory breast cancer – Rare type of breast cancer that may not form tumor and usually affects the surrounding skin.
- Metastatic breast cancer – Cancer cells spread from breast tissues to other parts of body including, lungs, bones and brain.
- Medullary, tubular and mucinous carcinoma – Less common types of breast cancer.

1.1.1.2. Diagnosis and treatment approaches for breast cancer

Breast cancer could be diagnosed by proper examination of the symptoms associated with breast cancer like presence of lump or other change in the breast or armpit. Use of screening modalities like mammogram, where a low dose X-ray of the compressed breast tissue helps to identify the presence of abnormalities in the breast. Further, detailed investigative techniques like breast ultrasound, breast biopsy and breast magnetic resonance imaging (MRI) can be employed to confirm the diagnosis of breast cancer (Mangasarian, Street et al. 1995).

Based on the size of tumor and extension of invasion, breast cancer is mainly divided into four stages

- Stage I: Localized breast cancer with a tumor size of less than 2 cm.
- Stage II: Cancer spread to axillary lymph node with a tumor size of more than 2 cm but smaller than 5 cm.

- Stage III: Cancer cells spread to nearby tissues with extensive axillary nodal involvement. Tumor size more than 5 cm.
- Stage IV: Tumor metastasized to areas outside breast tissues like, lungs, liver, bones and brain. It is referred to as metastatic breast cancer.

Breast cancer treatment should be individualized and based on several factors like, stage of cancer, age and overall health of the patient.

- Surgery: Two types of surgical procedures are used for the treatment of early stage localized breast cancer. Removal of the breast (mastectomy) and breast conserving surgery that involves removal of the malignant tissue (lumpectomy).
- Adjuvant therapy: It involves the use of systemic anti-cancer agents to eliminate or prevent the growth of any cancer cells that have metastasized to other organs. There are mainly three types of adjuvant systemic therapy. Depending on the tumor characteristics, individual or combination of anticancer agents are used in adjuvant therapy.
    - Endocrine therapy (hormone/anti-estrogen therapy): Recommended for women with estrogen receptor positive breast cancer. There are two types of endocrine therapy, one which uses selective estrogen receptor modulators (SERM) like tamoxifen and raloxifen and aromatase inhibitors.
    - Anti-HER2 therapy: Recommended for those patients with HER2 overexpression. Trastuzumab and pertuzumab are mainly used in anti-HER2 therapy.
    - Chemotherapy: Depending on the stage and grade of tumor, different anti-cancer agents are employed in breast cancer chemotherapy.

1.1.2. Skin cancer

Skin cancer is the most common of all cancer types and every year more than 5 million new skin cancer cases are diagnosed in the United States alone (Siegel, Miller et al. 2016). It is estimated that each year, the number of new cases of skin cancer exceeds the combined incidence of cancers of the breast, lung, prostate and colon (Siegel, Miller et al. 2016). The occurrence of skin cancer is more common in fair skinned populations around the world.

Exposure to ultraviolet radiation (UV) from sun is the primary cause of skin cancer (Kricker, Armstrong et al. 1994). Other risk factors include ionizing radiation, chemical carcinogens, environmental pollutants and work-related exposures (Saladi and Persaud 2005). Certain treatment modalities like radiation therapy, phototherapy and long-wave ultraviolet radiation (PUVA) can also cause skin cancers. In some cases, viral infections caused by the human papilloma virus can act as trigger for squamous cell carcinomas.

There are mainly three types of skin cancers that include basal cell carcinoma (BCC), squamous cell carcinoma (SCC) and cutaneous malignant melanoma (Armstrong and Kricker 2001). BCC and SCC are collectively called as nonmelanoma skin cancers.

1.1.2.1. Basal cell carcinoma

It is a type of non-melanoma skin cancer commonly occur in fair skinned people, and its incidence is increasing worldwide (Wong, Strange et al. 2003). Approximately 80 percent of all nonmelanoma skin cancers are BCC (Rubin, Chen et al. 2005).

Exposure to ultraviolet radiation is considered as the major cause for the pathogenesis of basal cell carcinoma (Tan and Billis 2004). Other risk factors include physical factors like fair skin

complexion, red or blond hair, and blue or green eye color (Goldberg 1996). Sun burn in childhood, family history of skin cancer and exposures to ionizing radiation, arsenic and oral methoxsalen (psoralen) are also been reported as trigger factors for the development of BCC. Another contributing factor is immunosuppression, that predisposes persons to BCC (Wong, Strange et al. 2003).

Basal cell carcinomas predominantly appears in body parts that are more exposed to sun like head and neck (80 percent of BCC cases), the trunk (15 percent) and on arms and legs. Even though not common, BCC may occur in unusual sites like the breasts, axillae, perianal area, palms, soles and genitalia (Rubin, Chen et al. 2005).

There are mainly three types of BCC, namely nodular, superficial and infiltrative (morphoea-form and nonmorphoea-form) but a single patient may have more than one type of BCC (Goldberg 1996). These tumors may sometimes associate with bleeding, ulceration, regression, and getting fibrotic, creating variable clinical presentations among the three forms.

Among the three, nodular BCC occurs as a pearly papule or nodule with a rolled border and sometimes exhibits a central crusting or ulceration (Rubin, Chen et al. 2005). Superficial BCC tumors are mostly red in color, finely scaled, finely wrinkled and with small superficial ulcerations. The shape of these tumors may be round or oval with scalloped or ill-defined border and sometimes they appear with a pearly border (especially upon compression with a glass slide) (Goldberg 1996). Infiltrative morphoea-form of BCC appears as a patch of morphoea (scleroderma) in white or yellow color mainly due to the fibrotic response of tissues to the presence of BCC islets. Infiltrative non-morphoea-form of BCC appears almost same as that of the morphoea form BCC except the absence of color change, which makes it less visible.

1.1.2.2. Squamous cell carcinoma (SCC)

It is the second most common type of skin cancer after BCC and its number of incidences are increasing worldwide (Marks 1996). It occurs as result of the malignant proliferation of epidermal keratinocytes, the most common form of epidermal cells (Schwartz 1988). Although majority of SCC can be completely cured by proper treatment, a very few lesions may recur or metastasize (Hawrot, Alam et al. 2003). These types of SCC that metastasize are responsible for the deaths associated with nonmelanoma skin cancers.

Among the various factors leading to the pathogenesis of SCC, exposure to UV radiation is the major trigger (Brash, Rudolph et al. 1991). Like BCC, people with fair skin color, green or blue eyes and those associated with childhood sunburn are more prone to SCC. Those who are under long-term immunosuppressive therapy like renal transplant patients are at high risk of acquiring SCC (Bouwes Bavinck, Vermeer et al. 1994). Other risk factors for SCC include chronic cutaneous ulcers, arsenic ingestion and chronic radio dermatitis (Marks 1996). Infection with human papillomavirus (HPV) also triggers the occurrence of SCC.

Squamous cell carcinoma occurs mainly on areas which are exposed to sunlight, such as head and neck (approximately 50-60% of SCC cases), upper trunk, lower leg, hands and forearms. The diagnostic feature to malignant transformation of SCC tumor is tenderness and thickening on palpation. Occasionally they may bleed and it is difficult to identify a definite edge upon stretching of these tumors which makes them different from BCC (Marks 1996).

1.1.2.3. Malignant melanoma

It is the most dangerous form of skin cancer with the possibility of spreading to other body parts, like lymph nodes, if not detected and treated early. The number of incidences of cutaneous melanoma has increased rapidly over the past three decades (Rosko, Vankoevering et al.). Even though melanoma accounts for only less than 10% of total skin cancers, it is responsible for the majority of deaths associated with skin cancers due to its high metastatic potential and resistance to therapy (Pfeifer and Besaratinia 2012, Society 2012). It occurs in all classes of people irrespective of their sex, age and race but the incidences are much higher in fair skinned populations.

Melanoma cancer growth occurs when unrepaired DNA damage to skin cells cause mutations (genetic defects) that triggers uncontrolled multiplication of these skin cells leading to the formation of tumors (Sarasin 1999). Melanoma originates in melanocytes in the basal layer of epidermis, the cells responsible for the production of the brown pigment called melanin (Thomson, Mattes et al. 1985). This melanin gives color and protects the lower layers of skin from the harmful effects of sunlight.

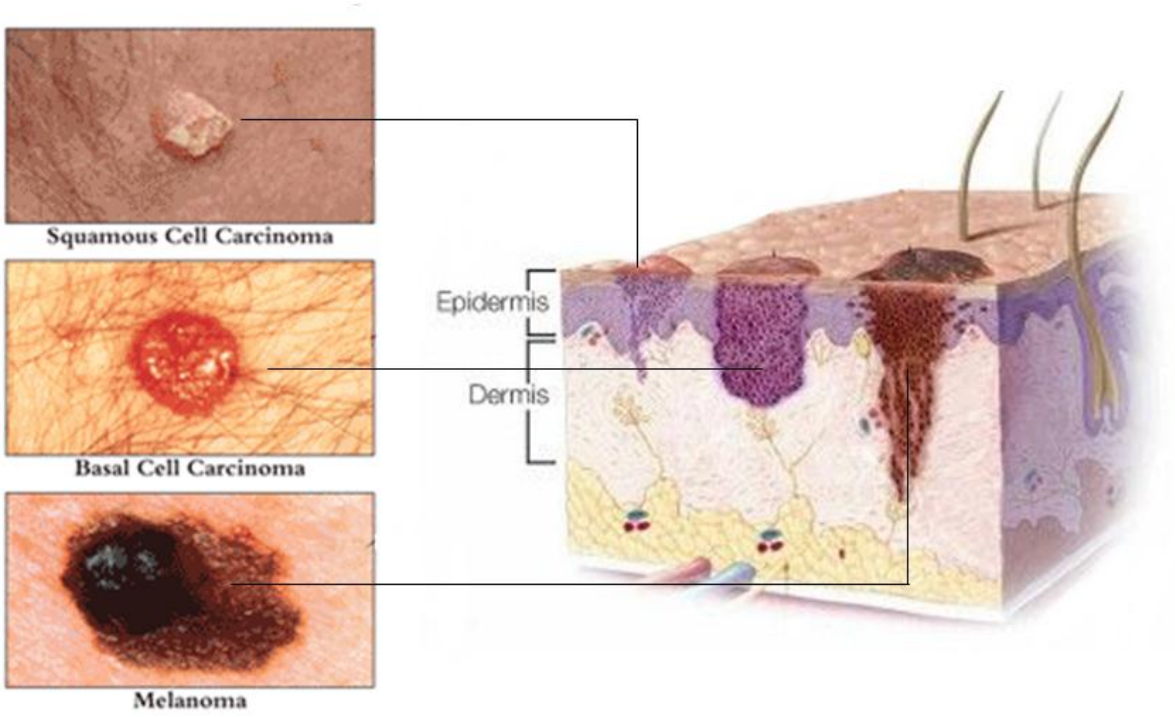

Fig.1.1. Types of skin cancer. Reproduced from web page http://anatomyandphysiologyi.com/skin-cancer

Melanomas sometimes resemble moles and even evolve from moles also. Majority of melanoma tumors appear in black or brown color, but sometimes they appear as skin colored patches, pink, red, purple or even white in color (Steiner, Pehamberger et al. 1987). Melanoma occurs mostly on the trunk region of men and lower legs in case of women, even though it can be found on the head, neck or anywhere on the skin (Gilchrest, Eller et al. 1999).

Exposure to UV radiation is the major cause for the development of melanoma (Gandini, Sera et al. 2005). Ultraviolet radiation produces gene mutations, DNA damage, immunosuppression, oxidative stress and inflammatory reactions, that contribute to the photo ageing of the skin and development of skin cancer (Meeran, Punathil et al. 2008). Other risk factors include fair skin color, history of sunburn, living at higher altitudes or close to the equator, presence of unusual moles, deficient immune system and genetic factors (Muhrer 2009).

1.1.2.4. Skin cancer signaling pathways

Recent findings in the complex mechanisms involved in skin cancer proliferation and progression have led to the development targeted therapeutic agents for the effective management of skin cancer. A thorough understanding of the various signaling pathways that contribute to the initiation and progress of skin cancer has led to the discovery of novel targets for skin cancer therapy. Few of the important signaling pathways that act as promising targets for the treatment of skin cancer include hedgehog pathway, Ras/Raf/MEK/ERK (MAPK) pathways, PI3K/AKT/mTOR pathway, NFκB pathway and STAT3 signaling pathway.

1.1.2.4.1. Hedgehog pathway

The Hedgehog pathway (Hh) is one of the fundamental signal transduction pathways that play a vital role in the embryonic development (Ming, Roessler et al. 1998). Inappropriate activation of Hedgehog (Hh) pathway is found to be one of the most common cause for BCC, the most common form of skin cancer (Bonilla, Parmentier et al. 2016). There are mainly three Hh proteins in mammals, namely sonic hedgehog (Shh), Desert hedgehog (Dhh) and Indian hedgehog (Ihh) (Athar, Tang et al. 2006). The Hh pathway gets initiated upon binding of any ligands and leads to inactivation of the Hh receptor, protein patched homologue 1 (PTCH- 1). As a result of this, smoothened (SMO) receptor, a trans membrane protein, transmits signals to downstream targets like gli, PTCH, and members of THF-β family (Göppner and Leverkus 2010) (Kalderon 2005).

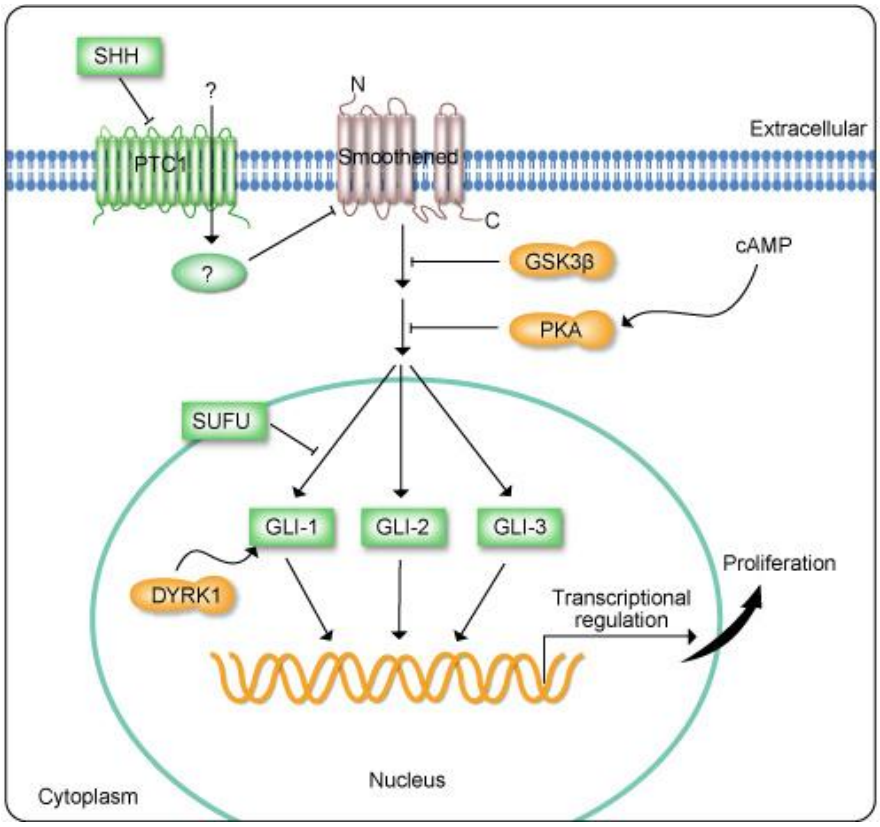

Fig.1.2. Hedgehog pathway. Reproduced from web page http://www.genecopoeia.com

In normal conditions, the Hh pathway remains ligand dependent and actively repressed as a result of the constant inhibition of SMO by PTCH- 1. However hyper activation of Hh pathway due to mutations within this cascade leads to the development of many cancers including BCC (Scales and de Sauvage 2009).

1.1.2.4.2. Ras/Raf/MEK/ERK (MAPK) pathways

The Ras/Raf/MEK/ERK pathway, or the MAPK (mitogen-activated protein kinase) pathway, is a signaling pathway that relays on extracellular signals from cell membrane to nucleus through series of phosphorylation events (Garnett and Marais 2004). Ras gets activated by various stimuli, like growth factor-mediated activation of receptor tyrosine kinases (RTKs) and leads to

the uptake of Raf from the cytoplasm to the cell membrane where it gets activated (Marais, Light et al. 1995). Activated Raf in turn, leads to activation of MAP kinase extracellular signal regulated kinases 1 and 2 (MEK1/MEK2), which further activates extracellular signal-regulated kinases 1 and 2 (ERK1/ERK2) (Xu, Robbins et al. 1995, Marais, Light et al. 1997). The translocation of activated ERK to the nucleus leads to phosphorylation of various nuclear transcription factors associated with several genes that are involved in cell proliferation, differentiation, and survival (Russo, Torrisi et al. 2009).

Mutations in Ras/Raf/MEK/ERK (MAPK) pathways play a vital role in the development of various types of cancer including melanoma (McCubrey, Milella et al. 2008). Dysregulation of these signaling pathways leads to uncontrolled proliferation and survival of cells leading to tumorigenesis. More than 50 percent of melanomas reported to have mutations in B-Raf gene leading to proliferation and survival of melanoma cells by the activation of MAPK pathway (Russo, Torrisi et al. 2009). The most common B-Raf mutation, that accounts for more than 90% of melanomas due to B-Raf mutation involves the substitution of valine by glutamic acid at codon 600 in exon 15 (Davies, Bignell et al. 2002).

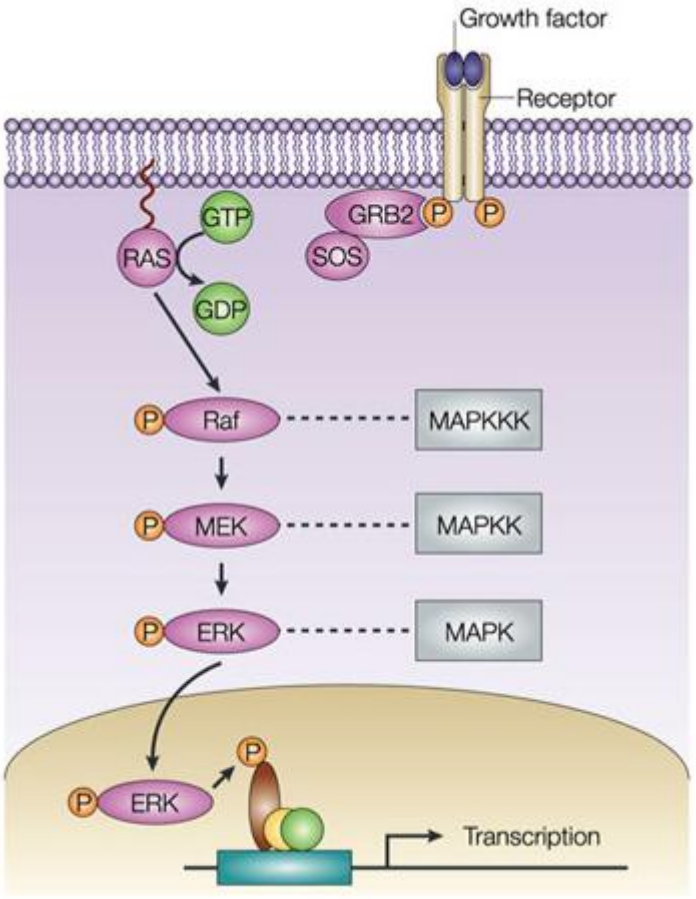

Fig.1.3. Ras/Raf/MEK/ERK (MAPK) pathways. Reproduced from web page http://flipper.diff.org

1.1.2.4.3. PI3K/AKT/mTOR pathway

The Akt family of protein kinases include three members, namely Akt1, Akt2 and Akt3 (Testa and Bellacosa 2001). Even though these three isomers act in similar manner, their regulation mechanisms vary according to different cell types (Testa and Bellacosa 2001). There are series of events that occurs in PI3K/AKT pathways in normal cells. Phosphoinoside-3 kinase (PI3K) gets activated upon binding of growth factors to cell membrane receptors or through G-protein coupled receptors. This activated PI3K in turn phosphorylates phosphatidylinositol -4,5-bisphosphate (PIP2) and leads to the activation of second messenger known as

phosphatidylinositol -3,4,5-trisphosphate (PIP3) (Vanhaesebroeck and Alessi 2000). PIP3 helps in the translocation of AKT to the plasma membrane. The activity of AKT is regulated by phosphorylation at different threonine and serine for different AKT isomers. In normal cells, the AKT activity is balanced between positive signals from elevated PIP3 levels and negative signals that lead to dephosphorylation and inactivation of AKT (Robertson 2005).

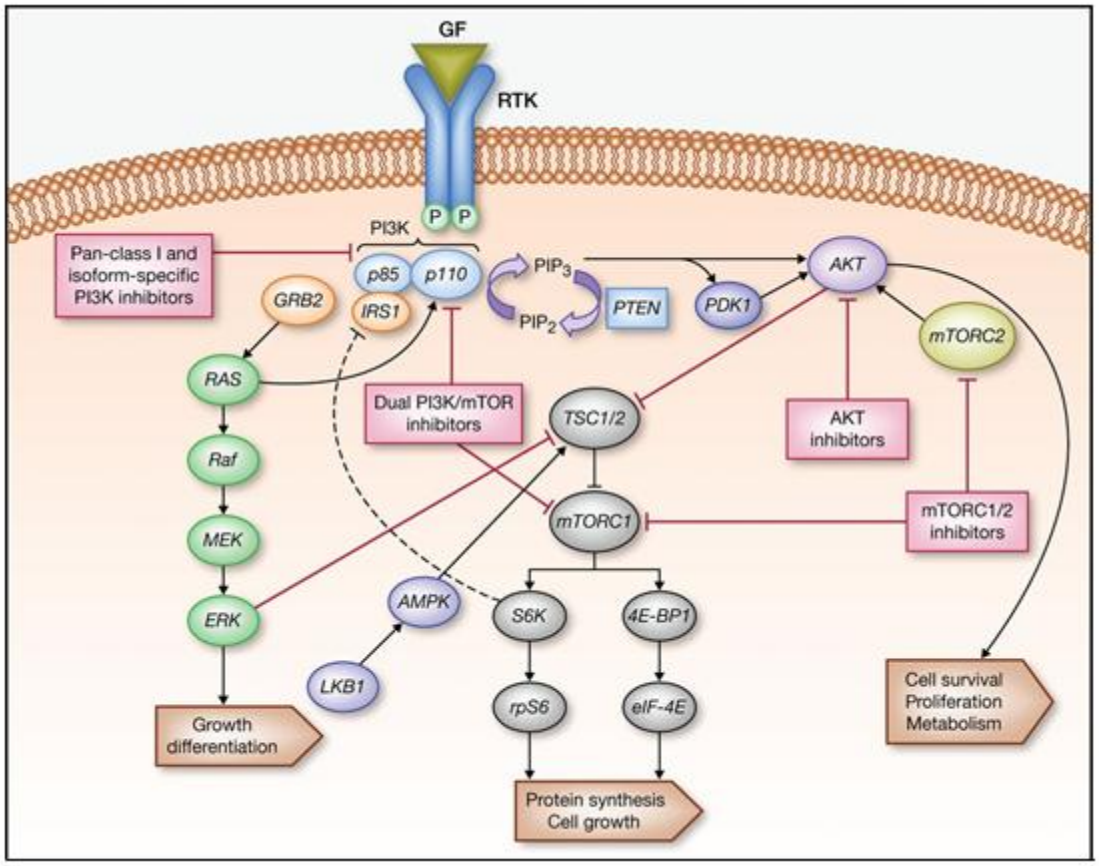

Fig.1.4. PI3K/AKT/mTOR pathway. Reproduced from (Dienstmann, Rodon et al. 2014).

There have been reports of increased AKT activity associated with melanoma, indicating that AKT plays vital role in the development of melanoma (Stahl, Sharma et al. 2004). Dysregulation of PI3K/AKT/mTOR pathway via mutation or increased gene copy numbers of PI3K isoforms or

pathway suppressor inactivation leads to the development of various cancers including melanoma (Russo, Ficili et al. 2014).

1.1.2.4.4. NFκB pathway

The nuclear factor kB (NFkB) encompass a family of transcription factors with five genes, namely NF-κB1 (p50/p105), NF-κB2 (p52/p100), RelA (p65), RelB and c-Rel which are involved in the regulation of biological responses (Dolcet, Llobet et al. 2005). These genes are responsible for the development of seven proteins with a common Rel Homology Domain (RHD) in their sequence.

In majority of cells, the NFκB dimers exist predominantly in the cytoplasm and are being regulated by the inhibitors of NFκBs (IkBs) which make them transcriptionally inactive. The IkBs comprise a family of proteins which interact with RHD domains of NFκB proteins and are responsible for retaining them within the cytoplasm.

NFκBs gets activated by different signaling pathways that are triggered by growth factors, cytokines and tyrosine kinases. Other factors that contribute to the activation of NFκBs include enhanced expression of epidermal growth factor receptor, insulin growth factor receptor and tumor necrosis factor receptor. In certain cases, the activation of other signaling pathways like Ras/MAPK and PI3K/AKT also triggers the activation of NFκBs (Dolcet, Llobet et al. 2005).

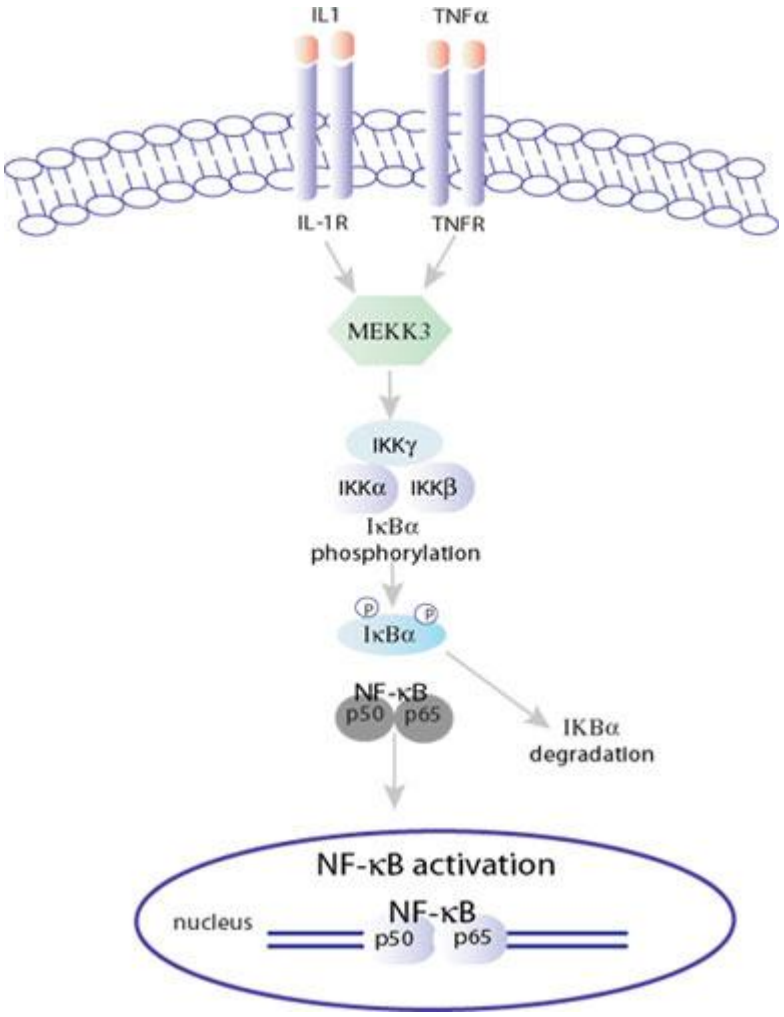

Fig.1.5. NFκB pathway. Reproduced from web page http://www.isogen-lifescience.com

NFκB activation has been reported to be involved in the development of many tumors including SCC of head and neck. Various mechanisms by which NFκB activation triggers cancer development include transcription of genes engaged in the suppression of cell death and inducing the expression of apoptosis inhibitors (Deveraux, Roy et al. 1998, Wang, Mayo et al. 1998). IkB family of proteins plays a vital role in regulation of NFκB activation and any alteration in these genes alter the ability of IkB to inhibit NFκB leading to NFκB activation (Dolcet, Llobet et al. 2005).

1.1.2.4.5. Signal Transducer and Activator of Transcription 3 (STAT 3) signaling

STATs comprise a family of seven latent transcription factors that occur in the cytoplasm and are activated by many cytokines and growth factors. They include Stat1 (a and b isoforms), Stat2, Stat3 (a and b isoforms), Stat4, Stat5a, Stat5b, and Stat6 that are encoded by seven specific genes (Yu and Jove 2004). The characteristic feature of STAT proteins is their dual roles, in transducing signals through cytoplasm and act as transcription factors inside nucleus (Darnell Jr, Kerr et al. 1994)

STATs activation is dependent upon phosphorylation of tyrosine residues in STAT proteins, that induces dimerization via domain interactions of reciprocal phosphotyrosine–SRC homology 2 (SH2). Activated STATs then get translocate to the nucleus wherein they activates the transcription of target genes by binding to their consensus promoter sequences. Each STAT protein is activated by a defined set of cytokines and are responsible for the regulation of a group of specific genes (Yu, Pardoll et al. 2009).

In normal cells, the STAT tyrosine phosphorylation is a short term process that lasts for few minutes to many hours. Whereas, in many cancer cells and primary tumors, STATs, especially STAT3 remains persistently tyrosine phosphorylated either due to the effects of deregulated positive effectors of STAT activation like tyrosine kinases or negative regulators of STAT phosphorylation (Bromberg 2002).

STATs, especially STAT3 are reported to be activated in many of human malignancies, including lung, prostate, breast, brain and squamous cell carcinomas (Pedranzini, Leitch et al. 2004). They play a crucial role in both extrinsic and intrinsic pathways that lead to cancer inflammation (Kortylewski, Xin et al. 2009). STAT3 proteins act as transcription factors for the

regulation of genes involved in tumor cell proliferation, angiogenesis, survival and invasion, other than genes encoding many tumor promoting inflammatory mediators (Darnell 2002, Yu and Jove 2004).

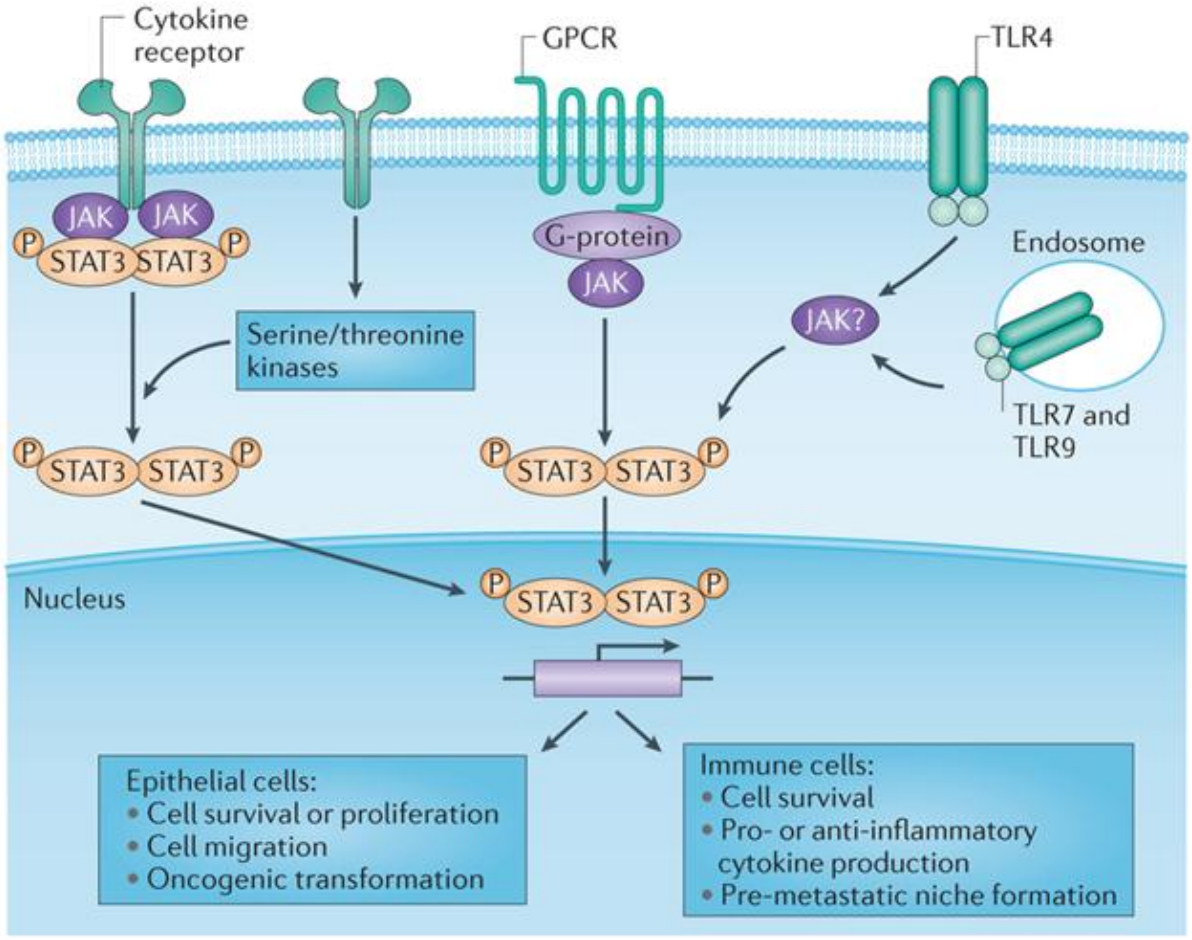

Fig.1.6. JAK-STAT3 pathway in cancer. Reproduced from (Yu, Lee et al. 2014)

Even though STAT3 pathway is vital mediators of cancers that are begin by genetic changes in transformed cells, it is also important for inflammatory conditions due to environmental and other etiological factors associated with higher cancer risk. Many infectious agents causing inflammation-induced cancer are known to activate STAT3 by different mechanisms.

1.1.2.5. Diagnosis and treatment approaches for skin cancer

Skin cancers can be diagnosed by performing thorough physical examination of skin followed by biopsy of suspected skin tissue (Sober 1983). The biopsy provides information about histopathologic growth pattern of cancer and thereby ensures more accurate diagnosis. Non-invasive optical technologies like optical coherence tomography (non-invasive imaging test of retina using light radiation) and dermatoscopy (imaging of skin to identify thickening of layers, borders of a lesion and epidermal organization) are helpful in increasing the accuracy of skin cancer diagnosis (Deinlein, Richtig et al. 2016, Giavedoni, Puig et al. 2016). Early detection and appropriate treatment helps in improving the outcome of patients with skin cancer.

Multiple treatment modalities are available for the management of both melanoma and non-melanoma skin cancers. The choice of treatment depends on various factors like type of skin cancer, anatomic location, tumor size, ease of defining margins, depth of invasion, patient age and physician's skill and training (Martinez and Otley 2001). The various treatment approaches for skin cancer include, Mohs micrographic surgery, excisional surgery, electrodessication and curettage (ED&C), cryosurgery, radiotherapy, chemotherapy and immunotherapy (Martinez and Otley 2001).

1.1.2.5.1. Excisional surgery

Excisional surgery is one of the most common and effective treatment strategies for nonmelanoma skin cancers as it gives acceptable cure rates and is cheap (Nguyen and Ho 2002). Unlike other surgical techniques, this method helps in histopathological examination of excised tissue and accurate determination of excisional margins. In many cases, this particular treatment

strategy is preferred because of its superior cosmetic effects and rapid healing rates (Martinez and Otley 2001).

1.1.2.5.2. Mohs micrographic surgery (MMS)

MMS is the most commonly used treatment strategy for the management of high risk nonmelanoma skin cancers. This is a special type of excisional surgery that provides up to 100 % microscopically controlled histologic margins (Nelson, Railan et al. 1997). This technique involves removal of serial horizontal sections of tumor, mapping of excised tissue, and microscopic evaluation of the surgical specimen and the procedure is repeated until a tumor free margin is attained (Martinez and Otley 2001). The ultimate goal of MMS is to identify and complete excision of the entire tumor while preserving the healthy tissue.

1.1.2.5.3. Electrodessication and curettage (ED&C)

This is probably the most commonly used treatment strategy for the management of low risk BCC and SCC in situ. It is a type of superficial ablative therapy that is safe, easy to perform and efficacious (Martinez and Otley 2001).This method involves the use of a sharp curette to scrape off the tumor tissue until normal, firm dermis is felt. Initially, the tumor area is electrodessicated to kill the cells and the necrotic debris is then curetted to the base of the wound (Neville, Welch et al. 2007). This cycle is repeated up to two more times until the complete removal is ensured.

1.1.2.5.4. Cryosurgery

Cryosurgery is a technique of destroying tumor cells by freezing and vascular stasis using liquid nitrogen at –196.5 °C (Neville, Welch et al. 2007). Intracellular and extracellular ice crystal formation results in the destruction of concerned tissues. In order to maximize the efficacy of

therapy, several factors like spray technique, duration and number of freeze thaw cycles are performed in different patterns. This technique is useful in the treatment of tumors with well-defined margins in elderly and debilitated patients.

1.1.2.5.5. Radiation therapy (RT)

Radiation therapy can be used either as a primary or adjuvant therapy for the treatment of various skin cancers. In RT, usually fractionated doses of radiation is administered in the form of superficial or deep X-rays, or electron-beam therapy (Neville, Welch et al. 2007). Fractionation permits normal tissue to recover between therapies while tumor tissues get damaged as they require more time to recover. Radiotherapy is reported to provide best functional and cosmetic result in SCC of the lip, ear and nasal vestibule. Radiotherapy adjuvant to surgery is one of the best treatment strategy for the management of aggressive SCC with nodal metastases and perineural invasion (Sedda, Rossi et al. 2008).

1.1.2.5.6. Chemotherapy

Chemotherapy involves the use of anticancer drugs designed for killing or slows down the growth of rapidly growing cancer cells. In case of skin cancer, chemotherapy is preferred in patients with advanced skin cancer that has spread to other body parts. Various anticancer drugs like, 5-Fluorouracil, imiquimod, dacarbazine and temozolomide are reported to be effective in the treatment of skin cancers. Curcumin, a flavonoid obtained from the plant Curcuma longa, having anti-inflammatory and anticancer activity shows promising activity against skin cancer.

1.1.2.5.7. Targeted therapy

Targeted therapies aim to inhibit those targets on which the cancer cells depend for their further progression. Generally, cancer cells are more dependent on hyper activated pathways compared to normal cells and thereby rely more on activated oncogenes that regulate these pathways (Gray-Schopfer, Wellbrock et al. 2007). Some of the targeted therapeutic agents which are found to be effective in the management of melanoma include Ipilimumab, Vemurafenib, Dabrafenib, and Trametinib (Olszanski 2014).

1.1.2.5.8. RNA interference technology

RNA interference technology involves the selective post transcriptional down regulation of specific genes in the cells, and thereby inhibiting the synthesis of protein of interest. This is mediated by a special kind of small double stranded RNA, having a sequence of 21-23 pairs of nucleotide, known as small interfering RNA (siRNA) (Prabha, Vyas et al. 2016). RNA interference can be used as a treatment approach for various diseases wherein the post-transcriptional levels of a particular disease-causing protein is regulated in a sequence-specific manner.

Skin cancers are reported to be associated with overexpression of various proteins like STAT3 (Pedranzini, Leitch et al. 2004). RNA interference technology can be used as a targeted therapy in skin cancers wherein the post transcriptional expression of proteins of interest is regulated in a sequence specific manner.

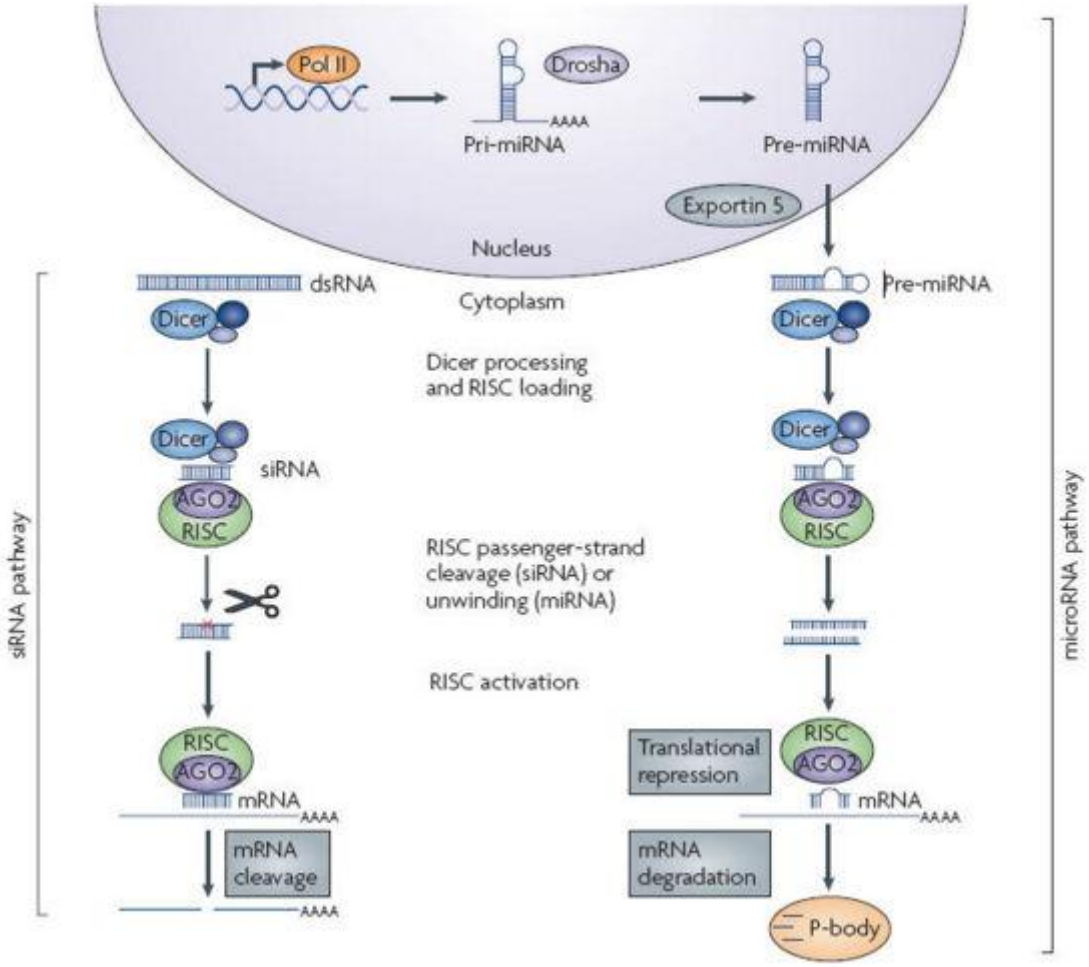

Fig.1.7. Mechanism of RNA interference. Reproduced from webpage https://dolcera.com

1.1.2.5.9. Immunotherapy

Immunotherapy in cancer relies on the host immune system's ability to reject the carcinogens and it is achieved through the administration of cancer vaccines, monoclonal antibodies and cytokines (Ghafouri-Fard and Ghafouri-Fard 2012). The various approaches used in immunotherapy include nonspecific stimulation of immune responsive cells that infiltrate tumors, immunotherapy using tumor antigens, induction of specific immune response using antitumor vaccines, and inhibiting the expression of immunosuppressive cytokines (Strickland

and Kripke 1997).In recent years, various immunotherapeutic strategies have been indicated for the treatment of both melanoma and nonmelanoma skin cancers.

1.2. Co-delivery of therapeutic agents in cancer therapy

Chemotherapy is one of the most commonly used and effective treatment modality in the management of various cancers. There are several cytotoxic agents that act by various mechanisms like blocking cellular or metabolic pathways for controlling the growth of tumor tissues. However, most of these chemotherapeutic agents do not achieve satisfactory therapeutic levels due to poor water solubility, low stability and rapid metabolism (Iwamoto 2013). Moreover non targeted body distribution of these agents causes similar cytotoxic effects in cancerous as well as healthy cells leading to many unwanted side effects (Khan, Ong et al. 2012). To overcome these limitations and improve the efficacy of chemotherapeutic agents, various novel drug delivery systems that are capable of targeted drug delivery have been established (Nitta and Numata 2013). The commonly used vectors for targeted drug delivery include liposomes, micelles, lipoplexes, polymeric and metal nanoparticles.

Although these strategies are effective in improving the accumulation of chemotherapeutic agents in cancer cells, the molecular complexities of cancer cells eventually leads to alternate mechanisms of drug resistance to escape the drug induced apoptosis (Igney and Krammer 2002, Tsuruo, Naito et al. 2003). There are several mechanisms of drug resistance including, efflux pumps that reduce the cellular drug concentration, membrane lipid alterations leading to reduced cellular uptake, alterations in drug targets, metabolic alteration of active ingredients, damaged DNA repair, apoptosis inhibition and cell cycle checkpoint alterations (Borst, Evers et al. 2000, Gottesman, Fojo et al. 2002, Szakács, Paterson et al. 2006). The multiple mechanisms that enable

cancer cells to evade programmed cell death combined with various complex signaling pathways associated with tumor genesis and progression make the cancer treatment extremely challenging (Teo, Cheng et al. 2016).

In past two decades gene therapy using various macromolecules like siRNA, microRNA (miRNA) and plasmid DNA (pDNA) has been extensively investigated for the successful treatment of various cancers (Kang, Gao et al. 2015, Teo, Cheng et al. 2016). pDNA acts as supplement to down regulated or replace the mutated genes where as siRNA and miRNA acts by inhibition of overexpressed target proteins via RNA interference (Kay 2011). As the tumor suppressor protein gene like p53 can induce apoptosis, pDNA encoding p53 can be employed for the cancer therapy. On the other hand, gene silencing using siRNA and miRNA introduces some time lag during which the resistant cells transiently become sensitized to anticancer drugs and thereby increasing the efficacy of cancer therapy.(Hannon 2002, McManus and Sharp 2002).

Even though the initial preclinical and clinical trials are promising, the molecular complexity of various forms of cancer suggests that the use of single chemotherapeutic agent or a gene therapy may not be sufficient for the control of many cancers. In recent years, scientists have investigated the possibility of co-delivery of chemotherapeutic drugs and genes to maximize the efficacy of cancer therapy (Yang, Gao et al. 2015, Teo, Cheng et al. 2016).

Rational combination of either two chemotherapeutic agents or a chemotherapeutic drug and gene focuses on the advantages of an additive or synergistic effect which is more efficient in comparison with individual therapies for the treatment of cancers (Kang, Gao et al. 2015). There are several reports of improved therapeutic efficacy and patient compliance with combination therapy using drugs and genes, mainly because of reduced dose and decreased multidrug

resistance (Gandhi, Tekade et al. 2014, Tsouris, Joo et al. 2014).

In order to get the maximum therapeutic capability of drug as well gene, an ideal carrier system should be employed for the co-delivery of drugs and genes in cancer therapy. According to the recent researches, nanocarriers have been extensively investigated as potential vehicles for the co-delivery of drugs and genes. An ideal co-delivery carrier should be capable of simultaneously carrying drugs and genes and deliver them in a controlled manner in required therapeutic dose at the target site (Kang, Gao et al. 2015). Moreover, these carriers should be biocompatible and biodegradable with adequate circulatory stability in order to elicit maximum therapeutic efficiency of the co-delivered therapeutic agents.

1.3. Modes of drug delivery in cancer therapy

Administration of chemotherapeutic agents for the treatment of cancers includes various modes like oral, parenteral and topical or transdermal.

1.3.1. Oral drug delivery

Oral drug delivery is associated with various disadvantages like poor bioavailability due to first pass metabolism, unwanted side effects and requires large quantity of dose. Moreover this route of drug administration cannot be used for the delivery of various biological products as it leads to their enzymatic degradation. Since skin cancer is a superficial disease occurring on the surface of skin, local drug delivery using topical or transdermal routes of drug administration is found to be a better choice than oral or parenteral methods of drug administration.

1.3.2. Parenteral drug delivery

Parenteral drug delivery involves the direct injection of therapeutic agents in to body tissue via the primary protective systems of our body like skin and mucous membrane (Jain 2008). Parenteral formulations include injections, infusions, implants, powder for injections or infusions, concentrates for injections or infusions, and gels for injections. Immediate therapeutic response is the prime advantage with parenteral drug delivery systems. Additionally, they are employed in case of those drugs which are not effective orally or that are degraded by the enzymes in digestive system. Since the therapeutic agents are directly entering into blood circulation, chemotherapy using parenteral formulations is associated with many unwanted side effects in cancer therapy (Moses, Brem et al. 2003).

1.4. Transdermal drug delivery (TDD)

Transdermal drug delivery ensures the transport of drugs across the skin for absorption into systemic circulation. TDD represents an attractive alternative to oral drug delivery as well as to painful hypodermic injections (Prausnitz and Langer 2008). It ensures local drug delivery at the targets of concern, lower systemic exposure and minimizes the toxicity compared to oral drug delivery (Marwah, Garg et al. 2016).

1.4.1. Advantages and disadvantages of TDD

Advantages of transdermal drug delivery

- It helps to avoid first pass metabolism wherein active drug molecules are converted to inactive forms or sometimes even to toxic forms leading to unwanted side effects.

- Avoids the acidic gastric environment wherein the drug can get degraded (Singh, Arora et al. 2012).
- Helps to maintain steady plasma levels
- Non-invasive and can be self-administered
- Improves patient compliance
- Improves bioavailability
- Drug input can be discontinued at any time
- Toxicity due to overdosing can be avoided
- Better choice for pediatric, unconscious and vomiting patients (Marwah, Garg et al. 2016)

Disadvantages of transdermal drug delivery

- Intra and inter variability in dosing due the difference in permeability of intact and diseased skin (Larsen, Nielsen et al. 2003).
- Issues with geriatric patients as the skin undergoes various deformations and alteration in elderly patients
- Pre-systemic metabolism of drugs by enzymes present in the skin (Steinsträsser and Merkle 1995).
- Irritation and sensitization of skin associated with topical and transdermal drug delivery referred to as the "Achilles heel" (Murphy and Carmichael 2000).

1.4.2. Skin anatomy and physiology

Skin, the integument of human body, covers an area of approximately 1.5-2 m^2, receives one third of blood circulating through the body and accounts for about 10% of total body mass

(Singh and Morris 2011, Ashara, Paun et al. 2014). It represents the outermost complex barrier that separates the biological system from the external environment. The major protective functions of skin includes protection against mechanical stress, prevents excessive water loss, prevents the ingress of foreign bodies and facilitates transpirational cooling (Jain, Patel et al. 2017). An average adult human skin surface has approximately 40-70 hair follicles and 200-300 sweat ducts per square meter of skin and the pH of skin is slightly acidic (4.0-5.6) (Ashara, Paun et al. 2014)

Histologically, the skin consists of three distinguishable layers such as the epidermis, the dermis and the hypodermis with specific physical and functional characteristics (Fig.1.8). The outermost layer, epidermis predominantly consists of keratinocytes, but also includes the melanocytes and dendritic cells such as the Langerhans cells (Menon 2015). Based on keratinocyte proliferation and differentiation, the epidermis is subdivided into 5 different layers. These layers consists of the outermost stratum corneum (SC), stratum lucidum, stratum granulosum, stratum spinosum and stratum basale (Singh and Morris 2011).

SC consists of the end product of epidermal cell differentiation process and the overall SC structure is the major contributor to the skin barrier functions (Yang, Bugno et al. 2013). This layer has approximately 10-20 μm thickness and is considered to be metabolically inactive. (Walters 2002). The SC is composed of approximately 10-60 layers of dead corneocytes that are predominantly made up of cross linked keratin, embedded in a lipid intercellular matrix composed mainly of long chain ceramides, triglycerides, free fatty acids, cholesterol, sterol/wax esters and cholesterol sulfate (Lampe, Williams et al. 1983, Huzil, Sivaloganathan et al. 2011).

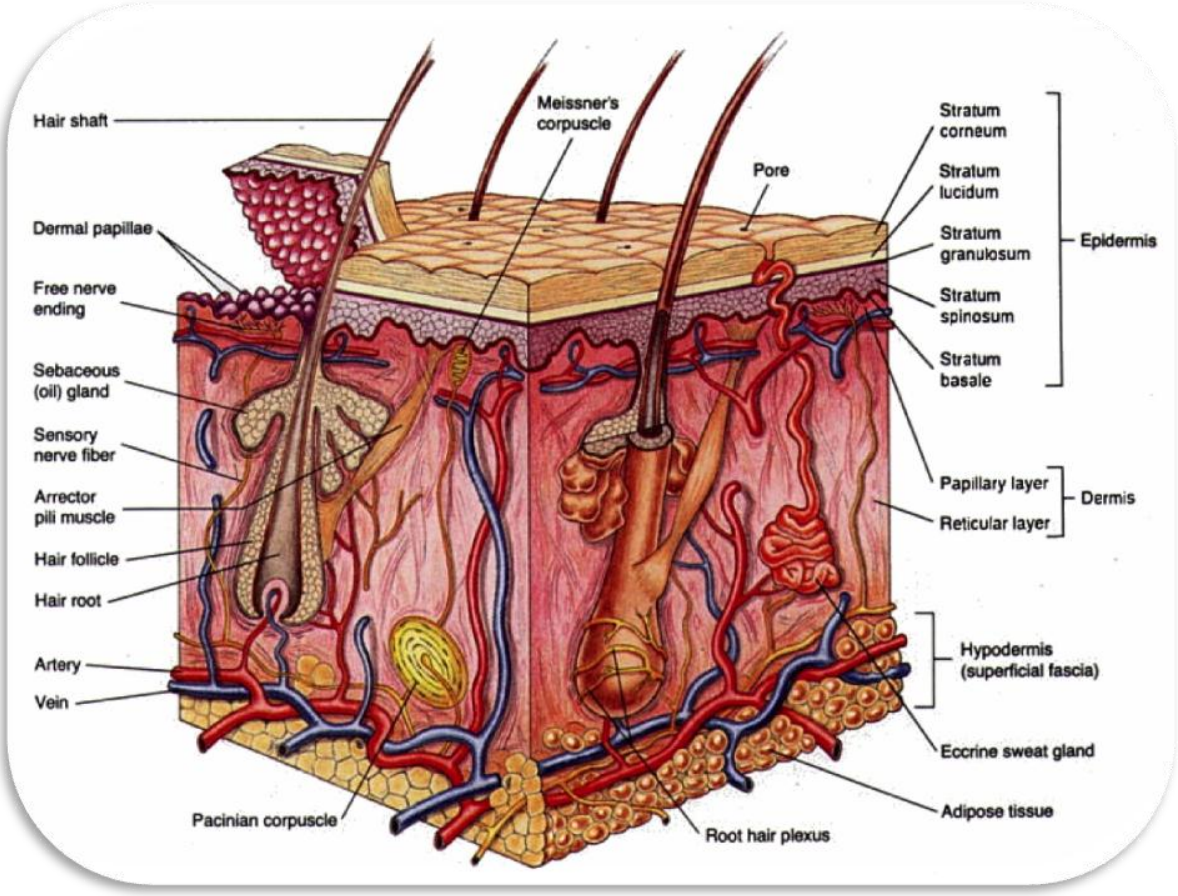

Fig.1.8. Anatomy of the skin. Reproduced from web page http://www.bionebio.com

As per the 'bricks and mortar' model of SC, the hydrophilic corneocytes represents the bricks and the intercellular space containing hydrophobic lipids represents the mortar (Elias 1983, Tojo 1987, Abraham and Downing 1992). The lipid lamellae structure of SC was further investigated by Forslind and he proposed a domain mosaic model (Forslind 1994). According to this model, the lipids are differentiated in a crystalline lipid region, giving SC its barrier function and are surrounded by fluid lipids that facilitates water uptake that helps the keratinocytes to remain hydrated. This hydration helps to prevent the development of cracks and fissures on skin surface. The SC shows selective permeability that allows only relatively lipophilic molecules to traverse

to the lower layers. In every 2-3 weeks, the SC undergoes a total turnover (Singh and Morris 2011).

Below the SC, there occurs the viable epidermis with thickness of approximately 50-100 µm (Feingold 2007). These layers of cells are different from SC and they have more physiological resemblance to other living cellular tissues and contain many metabolizing enzymes. Viable epidermis is responsible for the generation of SC and helps in metabolism of foreign bodies that tries to invade our body (Jain, Patel et al. 2017). The presence of Langerhan cells in viable epidermis makes it responsible for the immune response of the skin (Klareskog, Tjernlund et al. 1977).

In between the epidermis and dermis, there is a band called basement membrane zone (BMZ) or the dermal epidermal junction of approximately 0.5-1.0 µm thickness whose primary function is to hold the epidermis to the dermis (Menon 2015).

Dermis layer is composed mainly of proteins like collagen and elastin, an interfibrillar gel composed of glycosaminoglycans, water and salts (Jain, Patel et al. 2017). Dermis layer accommodates blood and lymph vessels, hair follicles, nerve endings, sweat and sebaceous glands. The hair follicles and sweat glands in dermis provides a direct contact between the dermis and skin surface, bypassing the SC, and thereby facilitates the appendageal route of skin permeation (Otberg, Richter et al. 2004).

The lowermost layer, the hypodermis or the subcutaneous fat tissue is composed mainly of adipose tissue that contains cells with large quantities of fat (Walters 2002). The dermis and epidermis are linked to the underlying structure of the skin by the collagen between these fat

cells (Jain, Patel et al. 2017). The main function of hypodermis is to act as a heat insulator, shock absorber and also as a reservoir of high energy triglycerides (Singh and Morris 2011).

1.4.3. Pathways for skin penetration

There are mainly three different pathways for the transport of molecules across the skin namely, intercellular or paracellular route, intra cellular or transcellular route and transappendageal route.

1.4.3.1. Intercellular pathway/Paracellular pathway

This is the most common pathway for the transport of drug molecules across the skin. In this pathway, molecules pass through the lipid domain in between the cells and is more suitable for the transport of lipid soluble molecules (Parnami, Garg et al. 2014).

1.4.3.2. Intracellular pathway/Transcellular pathway

In this pathway, the molecules get transported across the cells to reach systemic circulation. This is the straight pathway of dug permeation across the skin as it allows passage of molecules through both keratinocytes and lipids (Ghaffarian and Muro 2013)

1.4.3.3. Transappendageal pathway

In transappendageal pathway of drug delivery, molecules passes through continuous channels associated with hair follicles and sweat ducts (Sharma, Agarwal et al. 2011).

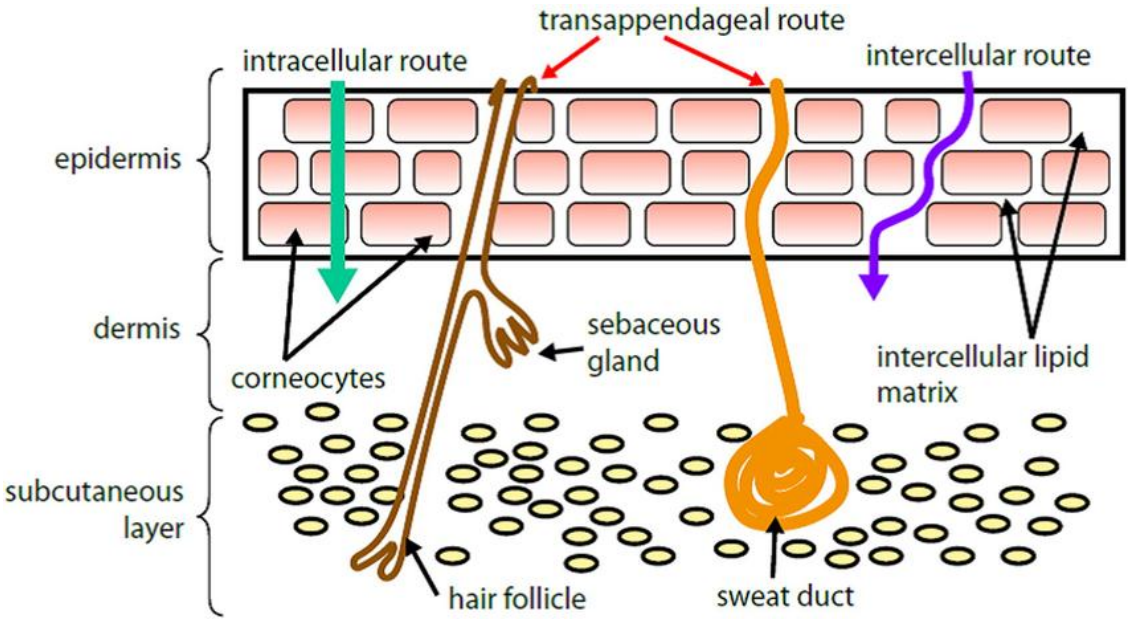

Fig.1.9. Pathways of skin permeation. Reproduced from (Erdő, Hashimoto et al. 2016)

1.4.4. Factors affecting transdermal drug delivery

Transport of drug molecules across the skin are affected by various factors associated with the drug molecule, drug delivery system and physiology of skin (Marwah, Garg et al. 2016).

1.4.4.1. Physicochemical properties of drug molecule

- Molecular size: Molecules with less than 500 Da molecular weight are considered to be suitable candidates for TDD (Bos and Meinardi 2000).
- Partition coefficient : Sufficient lipid and aqueous solubility, Log P value between 1-3 is required for the efficient permeation of molecules across the SC (Yano, Nakagawa et al. 1986)
- Ionization: Unionized drug molecules permeate easily through the skin compared to ionized molecules as per pH-Partition hypothesis.

- Diffusion coefficient: Permeation of molecules across the skin is affected by their diffusion coefficient which in turn depends on the properties of drug molecule, diffusion medium and their interactions.

1.4.4.2. Physicochemical properties of drug delivery system

- Composition of drug delivery system: Composition of the carrier affects the permeability of molecules across the skin as those with lipoidal vehicles permeate better than other carriers.

- Drug release characteristics: Release of drug from the carrier system depends on the partition coefficient of the drug from carrier system to the tissue. The rate of transdermal permeation increases upon release of drug from the carrier system.
- Addition of permeation enhancers: Incorporation of permeation enhancers like propylene glycol and dimethyl sulphoxide in delivery system enhances the permeation of molecules across the skin.

1.4.4.3. Physiology of skin

- Barrier properties of neonatal skin: The skin of new born babies will be relatively dry and hydrophobic compared with older infants. Stabilization of stratum corneum occurs by the age of three months.
- Barrier properties of elderly skin: The moisture content in human skin decreases after the age of 65 years along with destruction of epidermal junctions. These factors contribute to the reduction in area available for dermal transmission.
- Temperature of skin: The normal temperature of human skin varies from 32-37^{o}C.

Increase in temperature enhances the diffusion of molecules across the skin.

- Race: There is some difference in anatomical and physiological features of the skin in black and fair skinned people. Increased lipid content in black skin leads to enhanced intracellular permeation compared to fair skin.

1.5. Challenges & techniques for enhancement of skin permeation

The most important challenge in transdermal drug delivery lies crossing the barrier function offered by SC. Different approaches have been utilized to cross this barrier, including passive methods using chemical permeation enhancers, active methods which uses various physical techniques to breach the SC and formulation optimization like application of nanocarriers.

1.5.1. Passive methods

Passive methods of permeation enhancement make use of various chemical agents including water to disrupt the barrier function of stratum corneum.

1.5.1.1. Horny layer modification by hydration

Hydration of skin leads to the swelling of keratin and influences the lipid packing which ultimately causes the opening of polar and nonpolar routes of skin permeation (Haftek, Teillon et al. 1998).

1.5.1.2. Chemical permeation enhancers

Chemical permeation enhancers act by different strategies to improve the permeation of molecules across the SC. These mechanisms include disruption of the highly ordered structure of SC, interaction with intercellular proteins and enhancement of drug partition into the SC (Garg, Singh et

al. 2013). The various commonly used chemical permeation enhancers are classified according to their chemical class like, hydrocarbons (alkanes, alkenes, mineral oil), alcohols (ethanol, glycerol, glycol, polyglycol), acids (oleic acid), esters (isopropyl myristate), surfactants (sodium lauryl sulfate, sorbitan monolaurate, polysorbate 80), sulfoxides (dimethyl sulfoxide), terpenes and essential oils (menthol, limonene) and lipids (phospholipids) (Marwah, Garg et al. 2016).

1.5.2. Active methods

Active methods of permeation enhancement make use of various physical methods including electrically and mechanically assisted techniques to improve the permeation of molecules across the SC.

1.5.2.1. Electrical methods

Two commonly used electrical methods for permeation enhancement are electroporation and iontophoresis.

1.5.2.1.1. Electroporation

Electroporation make use of electricity to disrupt the cell membranes (Sammeta, Vaka et al. 2010). This method involves application of DC electric pulses (>100 V) for 10 μs - 10 ms , that leads to the formation of aqueous pores in SC lipid bilayers as well as reversible disruption of cell membranes (Denet, Vanbever et al. 2004, Schoellhammer, Blankschtein et al. 2014). Even though the electric field provides a driving force, permeation occurs mainly through passive diffusion along the long-lived pores due to the short duration of electric pulses (typically milliseconds) (Zorec, Becker et al. 2013). This technique can be used for the delivery of various molecules like proteins, oligonucleotides, insulin, heparin, vitamin C and dextran.

There are two types of electroporation techniques namely, reversible and irreversible electroporation. In reversible method, the electric pulses leads to short term improvement in permeation and the cell survives after treatment, whereas, in irreversible method, the electric pulses leads to enhanced permeation that ultimately results in cell death (Marwah, Garg et al. 2016).

1.5.2.1.2. Iontophoresis

Iontophoresis make use of electrical current to permeate charged molecules across the skin through electrostatic effects (Herr, Kile et al. 2008). Typically the range of current applied varies from 0.1 to 1.0 mA/cm^2 (Dubey and Kalia 2010). The instrument consists of a cathode and an anode wherein, one electrode pushes the likely charged molecules across the skin via electrostatic forces of repulsion while the other electrode attracts the oppositely charged molecule (Garg and Kumar Goyal 2012).

Iontophoresis acts in two ways namely, electromagnation in which the charged molecules are attracted towards the oppositely charged electrode and electro-osmosis in which neutral molecules permeates along the direction of solvent (Dhote, Bhatnagar et al. 2011). Depending on the charge of molecule to be permeated, iontophoresis can be anodal (for the permeation of positively charged ions) and cathodal (for the negatively charged ions). Iontophoresis is a better choice for the delivery of high molecular weight drugs like inulin, calcitonin, gonadotropin releasing hormone and nucleic acids effectively across the skin (Garg, Malik et al. 2014). Sometimes electroporation and iontophoresis are coupled to achieve greater enhancement in the permeation of molecules across the skin (Schoellhammer, Blankschtein et al. 2014).

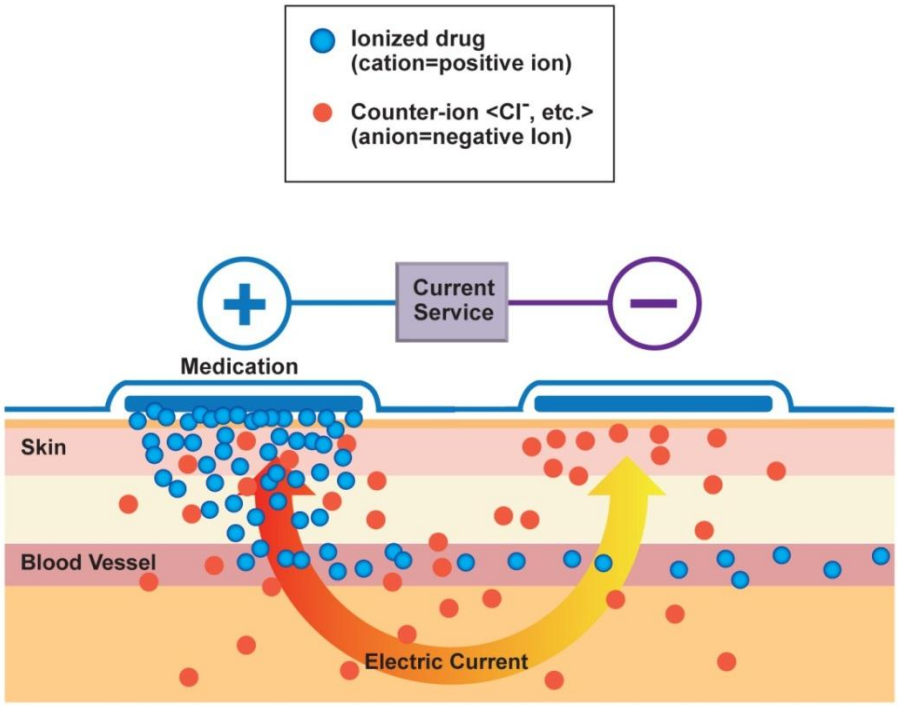

Fig.1.10. Mechanism of iontophoresis. Reproduced from web page http://electronicsmaker.com

1.5.2.2. Mechanical methods

Mechanical methods involve various physical or mechanical techniques to breach the SC barrier function to enable the permeation of molecules across the skin.

1.5.2.2.1. Microneedles

Microneedles consists of a drug pool and thin projectiles having length of few microns which are capable of piercing the SC (Schoellhammer, Blankschtein et al. 2014). This device has the functions of both hypodermic needles and transdermal patches. Typically these needles are of 200–750 microns in length arranged in groups called arrays which usually contains 150–650 microneedles/cm2 (Marwah, Garg et al. 2016). Commonly used materials for the manufacture of microneedles include metal, silicon, plastics and sugar (Duan, Moeckly et al. 2011).

Microneedles are capable of penetrating through the epidermis up to a depth of 70–200 μm whereas, their small size limits their penetration to the dermis layer with its nerves, enabling painless drug delivery (Xie, Xu et al. 2005).

There are four types of microneedles namely, i) poke and patch approach (rupturing SC using microneedles and application of medicated patch on the treated surface thereafter.), ii) coat and poke approach (microneedles coated with drug solution), iii) poke and release approach (microneedles made up of polymers and polysaccharides that dissolve or degrade after administration) and iv) poke and flow approach (after piercing, drug flows through the hollow microneedles from the reservoir) (Marwah, Garg et al. 2016).

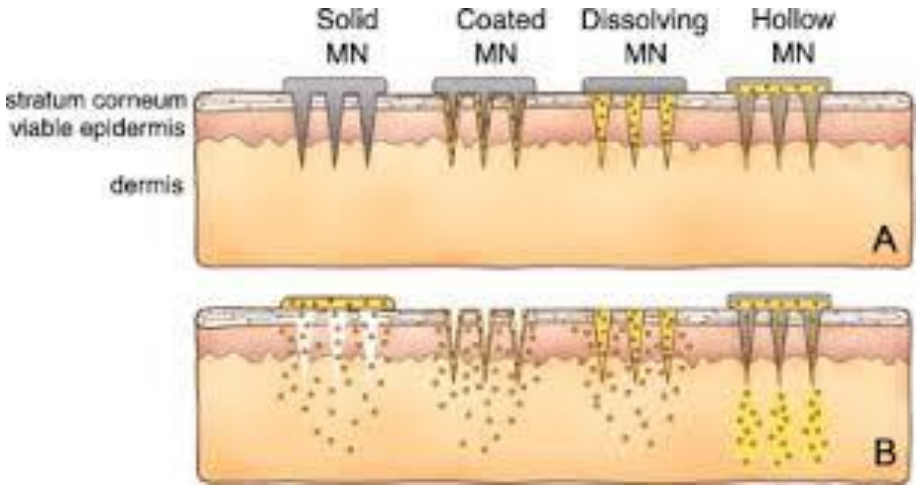

Fig.1.11. Mechanism of drug release from different types of microneedles. Reproduced from web page http://www.kj-microneedle.com. A (before) and B (after) administration.

1.5.2.2.2. Abrasion

This technique involves the disruption or removal of the upper skin layers in order to allow the permeation of molecules across the skin (Brown, Martin et al. 2006). Various devices used by dermatologists in the treatment of acne, scars and hyperpigmentation are reported to be employed in abrasion mediated drug delivery also. In this method, the permeability of

molecules across the skin remains independent of the physicochemical properties of the molecule and it is reported to enhance the permeability of hydrophilic molecules, vaccines and biopharmaceuticals across the skin (Mikszta, Britingham et al. 2001, Mikszta, Brittingham et al. 2003).

1.5.2.2.3. Skin puncture and perforation

This technique of enhancing transdermal permeability of molecules make use of needle like structures to make small punctures in SC through which the topically applied permeants reaches the deeper skin layers (Brown, Martin et al. 2006). Imprinter™ , A device that make use of blunt needles, designed by Imprint Pharmaceuticals are reported to be capable of delivering low to high viscosity formulations across the skin (Crocker, Maynard et al. 2001). Since it is a rapid application technique, it helps to avoid the pain and bruising associated with needle injection.

1.5.2.2.4. Needleless injection

Needleless injection involves the firing of liquid or solid particles at supersonic speeds across the outer skin layers using particular energy source (Brown, Martin et al. 2006). It is a painless method of drug administration across the skin. Many such devices have been introduced for the delivery of liquid (Iject®, Intraject®, Ped-O-Jet®, Medi-jector®, Biojector2000®, Dermajet®, Preci-jet® and Injex™) and powder (PMED™, previously known as powderject® injector) formulations. Powderject® injector has been reported to be used for the transdermal delivery of molecules like lidocaine hydrochloride, testosterone and macromolecules like insulin and calcitonin (Longbridge, Sweeney et al. 1998, Burkoth, Bellhouse et al. 1999).

1.5.2.2.5. Suction ablation

This technique involves the creation of a suction blister by applying vacuum or negative pressure that leads to the removal of epidermis while keeping the dermis layer as such (Svedman 1995). This technique also known as skin erosion is a painless method of drug permeation as this technique avoids dermal invasion. Cellpatch® (Epiport Pain Relief) is a marketed product works on this mechanism for the delivery of morphine (Brown, Martin et al. 2006). This technique has been reported to be used for the successful transdermal delivery of molecules like various molecular weight dextran (Svedman, Lundin et al. 1996) and vasopressin (Svedman, Svedman et al. 1991).

1.5.2.2.6. Skin stretching

In this technique, the skin is maintained under tension in multidirectional or unidirectional manner by using an expandable stretching device (Brown, Martin et al. 2006). It is reported that a tension of approximately 0.01 to 10 mP leads to the formation of reversible micropores in the skin through which the drug molecules get permeated. Once the tension is removed, the skin returns to its original configuration.

1.5.2.3. Miscellaneous

1.5.2.3.1. Ultrasound

Ultrasound mediated permeation enhancement involves the application of ultrasonic energy to breach the barrier properties of SC, and this technique is known as sonophoresis or phonophoresis (Svedman, Svedman et al. 1991). In this technique, the drug molecules can be permeated simultaneously along with the application of ultrasound energy or it can be used as a pretreatment to enhance the permeation of

molecules. The probable mechanisms by which the drug permeation enhances include, i) ultrasound application increases the fluidity of skin lipids that indirectly leads to enhanced transcellular permeation and ii) Bubbles formed within the skin layers leads to the formation of micropores through which drug molecule gets permeated easily (Marwah, Garg et al. 2016). The various factors that affect this mode of permeation enhancement include duration of treatment, intensity and frequency of ultrasound energy (Brown, Martin et al. 2006). There are several reports of combined use of microneedle and ultrasound to enhance the transdermal permeation of various molecules.

1.5.2.3.2. Magnetophoresis

In this technique, an external magnetic field is applied around the permeant to enhance the transdermal permeation of diamagnetic molecules (Brown, Martin et al. 2006). Exposure of skin to magnetic field may contribute to structural changes in the well packed SC and indirectly helps in pushing molecules across the skin. There are reports of enhanced skin permeation of molecules like benzoic acid (Murthy 1999) and terbutaline sulphate (Murthy and Hiremath 2001) by the application of magnetophoresis.

1.5.2.3.3. Radiofrequency

Radiofrequency thermal ablation involves the application of high frequency alternating current (~100 kHz) to create micro-channels within the skin layers. These micro-channels enhances the permeation of molecules across the skin (Brown, Martin et al. 2006). The rate of drug permeation using this technique can be controlled by the depth and number of pores formed, which in turn depends on the nature of micro-electrodes used for the therapy.

1.5.2.3.4. Laser and photomechanical waves

Exposure of skin to direct and controlled laser radiation leads to the disruption of SC without

causing damage to the deep skin layers. This technique has been reported to be effective in the enhanced permeation of both lipophilic and hydrophilic molecules across the SC (Marwah, Garg et al. 2016) (Lee, Shen et al. 2001, Lee, Shen et al. 2003). Various advantages associated with laser mediated transdermal drug delivery include painless method, short duration of therapy, controlled disruption of SC and less adverse effects(Brown, Martin et al. 2006).

1.5.2.3.5. Thermal Approaches

The technique of enhancing transdermal drug delivery by the application of temperature is known as thermophoresis (Brown, Martin et al. 2006). Previous in-vitro studies have reported that every 7–8^{o}C increase in skin surface temperature is associated with 2-3 fold rise in flux values (Clarys, Alewaeters et al. 1998, Akomeah, Nazir et al. 2004). The heat mediated enhanced permeation of molecules across the skin is attributed to increased diffusion of drug from the dosage form and into the skin, the latter in turn caused by an increase in fluidity of skin lipids (Ogiso, Hirota et al. 1998). In in-vivo conditions, the increased blood circulation to the skin upon application of temperature also plays vital role in enhanced permeation of topically applied molecules (Klemsdal, Gjesdal et al. 1992).

1.5.2.3.6. Combination methods

Combination methods for the enhancement of skin permeation usually make use of combinations of a skin permeabilizing technology with a driving force (Schoellhammer, Blankschtein et al. 2014). The commonly reported combinations for enhanced transdermal permeation include microneedles with electrical techniques, microneedles with ultrasound and ultrasound pretreatment followed by iontophoresis

1.5.3. Formulation optimization

Along with employing various techniques to breach the skin barrier, formulation optimization also plays critical role in improving transdermal drug delivery. It includes addition of permeation enhancers within the formulation as well as design of drug carriers that are capable of squeezing through the micropores of skin. In novel drug delivery systems, nanocarriers play vital role in the efficient transdermal delivery of micro as well as macromolecules.

1.6. Nanocarriers for transdermal drug delivery

After the turn of the millennium, nanoparticulate drug delivery systems became an inevitable part of the research in novel drug delivery systems, especially in cancer therapy. There are numerous reasons why tremendous efforts are being entrusted on nanoparticulate drug delivery systems. For instance, they are effective in improving the solubility and bioavailability of low-soluble drugs, protects vulnerable molecules from degrading environment by encapsulation and most importantly, helps in site specific delivery of drugs without affecting the surrounding normal cells (Sultana, Khan et al. 2013).

Nanocarriers offer a promising vehicle for the effective delivery of drugs topically as well as transdermally, owing to their ability to penetrate across the SC and targeting properties (Gupta, Agrawal et al. 2012). Based on the material of construction they are mainly classified into polymeric nanoparticles, metal nanoparticles and lipid based nanocarriers.

1.6.1. Polymer based nanoparticles

1.6.1.1. Polymeric nanocapsules/nanoparticles

These are rigid nanosystems made up of various polymers in which the drug molecules will be either encapsulated within the core (nanocapsule) or dispersed in the polymeric matrix (nanoparticles) (Venuganti and Perumal 2009). Moreover, the drug molecules can be adsorbed, conjugated or complexed on to the surface of polymeric nanocarriers. Polymeric nanocarriers can be prepared by various biodegradable and non-biodegradable polymers.

1.6.1.2. Dendrimers

Dendrimers are novel class of polymeric nanocarriers composed of perfectly branched spherical polymers with core–shell nano-architecture (Esfand and Tomalia 2001). In general, the particle size of dendrimers varies from 1 to 10 nm (Venuganti and Perumal 2009). An interesting feature about dendrimers is the presence of large number of surface functional groups that can carry high drug payload and are capable of interacting with biological membranes (Esfand and Tomalia 2001). Drug molecules can either be encapsulated within the core or complexed or conjugated with the surface functional groups of dendrimers.

1.6.2. Metal based nanoparticles

Metal based nanoparticles especially; gold and silver nanoparticles are capturing much attention during the recent years due to their effective application in the field of targeted drug delivery.

1.6.2.1. Gold nanoparticles

Gold nanoparticles (AuNPs) are biocompatible nanoparticles in a size range of 1–150 nm with a unique combination of physical, chemical, optical, and electronic properties for drug delivery (Goyal, Macri et al. 2016).

1.6.2.2. Silver nanoparticles

Silver nanoparticles (AgNPs) consists of particles with size range of 1- 100 nm which are reported to possess antiseptic and antimicrobial activity against gram positive and gram negative bacteria (Marin, Mihail Vlasceanu et al. 2015). The various techniques used in the preparation of silver nanoparticles include, i) chemical synthesis, ii) physical dispersion, iii) biological synthesis and iv) photochemical synthesis (Singh, Shedbalkar et al. 2015).

1.6.3. Lipid based nanocarriers

Lipid based nanocarriers remain inevitable candidates in the field of nanoparticulate drug delivery owing to their properties like biocompatibility and biodegradability (Sezer 2012). Their proven safety and efficacy make the lipid based delivery systems, an attractive candidate as pharmaceutical carriers for the delivery of drugs (Allen and Cullis 2004) and genes (del Pozo-Rodríguez, Delgado et al. 2010) , vaccines (Watson, Endsley et al. 2012), imaging (Dunne, Zheng et al. 2011), neutraceuticals and cosmeceuticals.

The first nanoscale drug delivery system was introduced by Alec Bangham as swollen phospholipid bilayer structures known as liposomes in 1960’s (Desmet, Van Gele et al. 2017). The concept of using liposomes as drug carriers was first introduced by Gregory Gregoriadis in the early 1970’s (Allen and Cullis 2013). Topical drug delivery using liposomes was first

reported in early 1980s by Mezei and Gulasekharam (Mezei and Gulasekharam 1982). The lipophilic nature of these carriers allows them to partition into the skin layers, enabling them to penetrate across the skin (Jain, Patel et al. 2016). To date, numerous lipid based nanocarriers has been emerged as efficient carriers for the topical and transdermal delivery of various therapeutic agents.

1.6.3.1. Vesicular carriers

Vesicular carriers typically consists of biocompatible lipids and aqueous phase (water, buffer solutions, or co-solvents) wherein, the lipids form concentric lamellae entrapping the aqueous phase (Jain, Patel et al. 2016). In order to improve the skin permeation, researchers have modified the vesicular carriers with various structural and functional properties during the last three decades.

1.6.3.1.1. Liposomes

Liposomes are submicroscopic vesicular structures formed by the spontaneous arrangement of amphipathic lipids in one or more concentric bilayers entrapping an aqueous core. The term liposomes originates from two Greek words ‘lipos’ (fat) and ‘soma’ (body) (Aparajita and Ravikumar 2014). The bilayered structure of liposomes are contributed by the self-assembly of amphiphilic lipids in such a way that the polar head group faces the aqueous media and hydrophobic hydrocarbon chains get arranged against the aqueous media. The amphiphilic nature of liposomes enables them to incorporate both hydrophilic (within the aqueous core) and hydrophobic (in between lipid bilayers) molecules within them (Desmet, Van Gele et al. 2017)

Based on their size and lamellarity, liposomes are categorized into small unilamellar vesicles (20-100 nm), large unilamellar vesicles (>100 nm), giant unilammelar vesicles (>1000nm), oligolamellar vesicles (100-500 nm) and multilamellar vesicles (>500 nm) (Pattni, Chupin et al. 2015). In general, liposomes within the size range of 50 to 450 nm are employed in therapeutic applications (Etheridge, Campbell et al. 2013).

Different methods used for the preparation of liposomes include i) thin film hydration, ii) reverse-phase evaporation, iii) solvent injection, iv) detergent depletion, v) low-pressure extrusion, vi) high-pressure homogenization, vii) size reduction sonication and viii) supercritical fluid (Goyal, Macri et al. 2016).

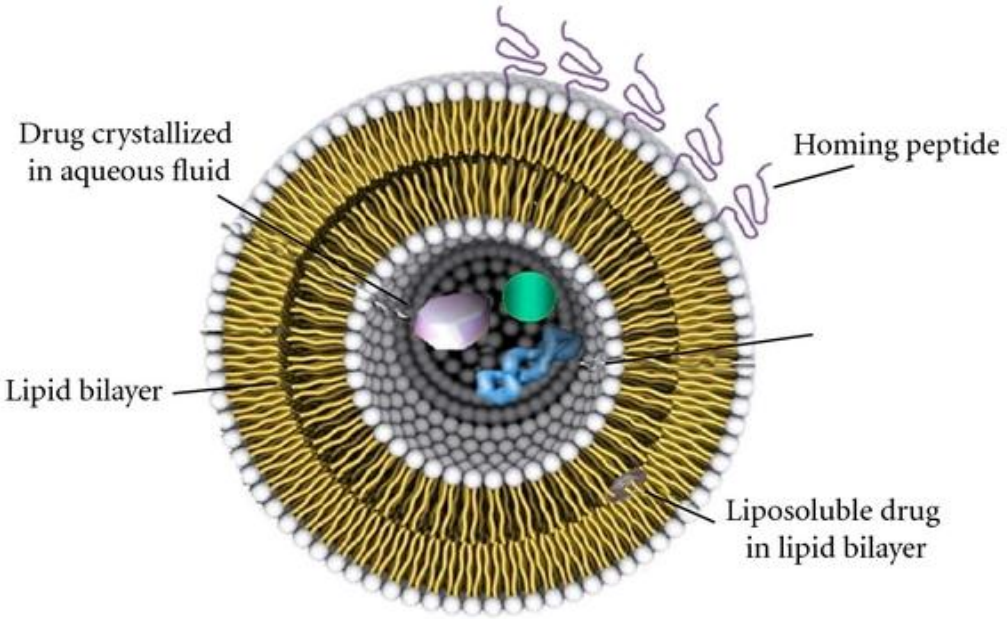

Fig.1.12. Liposome in drug delivery. Reproduced from (Bitounis, Fanciullino et al. 2012)

Various factors that limits the use of liposomes in therapeutic applications include vesicular leakage, alteration in size and zeta potential due to aggregation, degradation by oxidation and ester hydrolysis (Desmet, Van Gele et al. 2017). Inclusion of epidermal lipids (ceramides and

cholesterol) along with phospholipids and embedment in gel matrix are recommended alterations for improving the stability of liposomes (Pattni, Chupin et al. 2015).

General liposome characteristics like size, zeta potential, flexibility, stability and encapsulation efficiency can be altered by the addition of various natural or synthetic lipids in different proportions (Pattni, Chupin et al. 2015). Inclusion of PEGylated lipids extends the circulation time of liposomes in blood by avoiding the uptake by reticuloendothelial system (RES) enabling them as 'stealth' drug carriers.

The ability of liposomes in topical and transdermal drug delivery can be enhanced by converting liposomes into ultra-deformable liposomes/transfersomes.

1.6.3.1.2. Ultra deformable liposomes/transfersomes

Ultra deformable liposomes or transfersomes are prepared by the addition of edge activators like surfactants in the liposome composition (Desmet, Van Gele et al. 2017). These single chain surface active agents (sodium cholate, span, tween etc.) cause destabilization of lipid bilayer leading to increased elasticity, fluidity and deformability of the vesicles. These features enable them to squeeze through the intercellular regions and permeate to the deeper skin layers (Cevc and Blume 1992).

In early 1990s, Cevc and Blume introduced the idea of transfersomes for the first time. Compared to conventional liposomes, transfersomes have the advantages of increased skin penetration owing to the enhanced elasticity of vesicles (Pradhan, Singh et al. 2013). So they are more preferred over conventional liposomes for topical as well as transdermal applications. The

driving force that causes increased flux of transfersomes is the osmotic gradient generated by the difference in moisture content of SC and viable epidermis (Cevc and Blume 1992).

1.6.3.1.3. Ethosomes

Ethosomes are liposomes containing high amount of alcohol (usually ethanol) which makes them capable of penetrating into the deeper skin layers (Fireman, Toledano et al. 2011). Ethanol content of up to 45% is reportedly used in the preparation of ethosomes. The increased skin permeation of ethosomes is attributed to ethanol that plays a significant role in the ethosome-skin lipids interactions. Intercalation of ethanol with intercellular lipids increases lipid fluidity and leads to increased permeability across the skin layers. Another proposed mechanism of increased ethosome permeation is the fusion of ethosomes with intercellular lipids that makes them capable of delivering therapeutics into the deeper skin layers (Barry 2001).

Recently, there are reports of formulations combining the technology of transfersomes and ethosomes like, flexible nanosomes called SECosomes for the topical delivery of siRNA (Geusens, Van Gele et al. 2010, Bracke, Carretero et al. 2014).

1.6.3.2. Lipid nano particulate systems

Lipidic nanoparticles composed of various lipids serves as excellent drug carriers in topical delivery of therapeutic agents (Jensen, Petersson et al. 2011). Commonly employed lipid nanoparticulate systems include lipospheres, solid lipid nanoparticles (SLN) and nanostructured lipid carriers (NLC).

1.6.3.2.1. Lipospheres

These are lipid based solid particles composed of a solid lipid core wherein the drug molecules are dissolved or dispersed in a solid lipid matrix and stabilized by a single external layer of phospholipids (Dudala, Yalavarthi et al. 2014). The particle size of lipospheres typically varies from 0.01 to 100 µm in diameter and are mainly used for the parenteral and topical delivery of bioactive compounds (Domb 2005).

Various factors that make lipospheres a superior drug delivery system over other particulate drug delivery systems include improved stability of the drug in the formulation, controlled particle size, freeze dry and reconstitution properties, no carrier toxicity, high drug load and well controlled drug release (Reithmeier, Herrmann et al. 2001, Almeida and Souto 2007).

1.6.3.2.2. Solid lipid nanoparticles

Solid lipid nanoparticles (SLN) are submicron sized lipid particles made up of solid lipids (0.1-30% w/w) dispersed in an aqueous medium and sometimes stabilized with a surfactant (Kamel Hassan and Elshafeey 2010). The mean particle size of SLN varies from 40-1000 nm (Lucks and Müller 1991). The characteristic features of SLNs that makes them ideal drug carriers include increased physical stability as well as prolonged drug release. The rate of drug release from SLNs can be altered by using lipids that are solid at body temperature (Desmet, Van Gele et al. 2017).

There are two methods of incorporating drug molecules in SLNs namely, drug coating on the external shell and dissolving the drug in the core solid lipid matrix. In first case, there will be initial burst release due to the adsorbed drugs on the shell followed by a gradual release from the

core whereas in latter, prolonged drug release occurs due to increased drug diffusional area (Martins, Sarmento et al. 2007). Drawbacks associated with SLNs include drug expulsion during storage and loading limitations based on lipid solubility of drugs.

1.6.3.2.3. Nanostructured lipid carriers

The drawbacks associated with SLNs were overcome by the introduction of nanostructured lipid carriers (NLC) composed of both fluid and solid lipids, usually in a ratio of 70:30 (Singhal, Patel et al. 2011). In NLCs, the fluidic lipid phase can either be embedded within the solid lipid matrix or localized on the external surface of the particles.

Compared to SLNs, NLCs possess higher drug loading efficiency due to their less organized crystalline structure (Singhal, Patel et al. 2011). The difference in melting point between the solid and fluid lipids in NLCs contribute to the characteristic drug release pattern of initial burst release followed by sustained release (Desmet, Van Gele et al. 2017).

1.6.4. Surfactant based nanocarriers

1.6.4.1. Neosomes

Neosomes are self-assembled vesicles composed mainly of nonionic surface active agents introduced in 1999 (van den Bergh, Vroom et al. 1999). Compared to liposomes, neosomes are much stable to oxidation and chemical incompatibilities and thereby require no special conditions of storage and preparation (Fireman, Toledano et al. 2011). They can be prepared by using different amphiphiles that possess a hydrophilic head group and hydrophobic tail.

The most commonly used surfactants for the preparation of neosomes include Span and Brij. Additives like cholesterol are included in neosomes to increase their stability by preventing

aggregation of vesicles (Venuganti and Perumal 2009). It has been reported that the encapsulation efficiency of neosomes increases with an increase in surfactant/lipid ratio(Florence 1993).

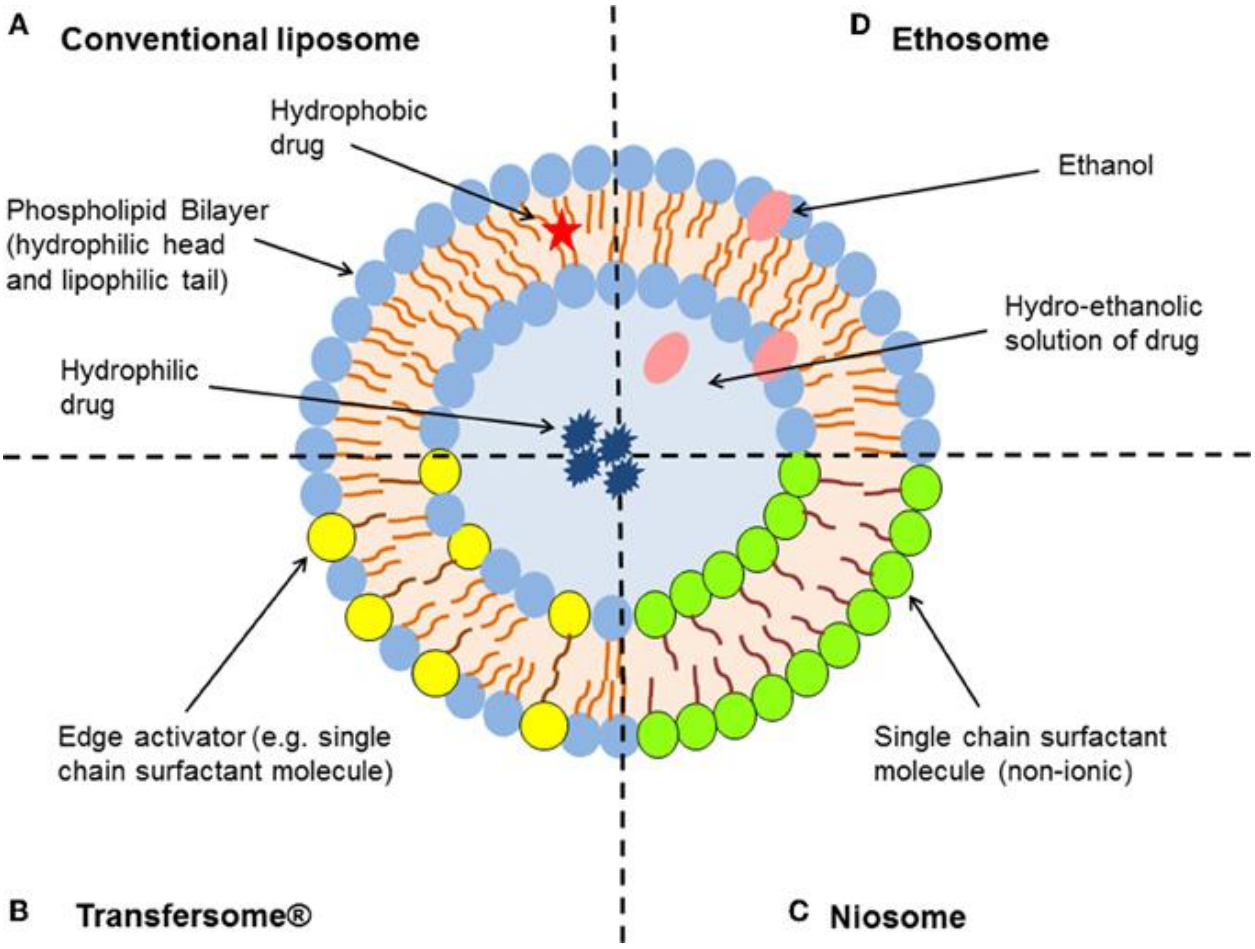

Fig.1.13. A. Conventional liposomes, **B.** Transfersomes, **C.** Niosomes and **D**. Ethosomes. Reproduced from (Hua 2015)

1.7. Advantages of liposomes in transdermal drug delivery

Among the various nanocarriers discussed in the above sections, liposomes are considered to be the best choice, especially for the topical or transdermal drug delivery. The unique ability of liposomes to incorporate both hydrophilic and lipophilic molecules enables them to deliver wide

range of therapeutic agents (Sercombe, Veerati et al. 2015). The large aqueous core and biocompatible external lipid membrane allows them to incorporate micromolecules as well as macromolecules like DNA, RNA, proteins and imaging agents (Ulrich 2002). Various other advantages of liposomes as drug delivery systems include biocompatibility, nontoxic, nonirritant, ability of self-assembly, ease of preparation, sustained and triggered release of payload and targeted drug delivery (Sercombe, Veerati et al. 2015). The lipid components of liposome gets degraded by the endogenous enzymes and thereby making them one of the most biocompatible nanocarrier (Shim, Kim et al. 2013).

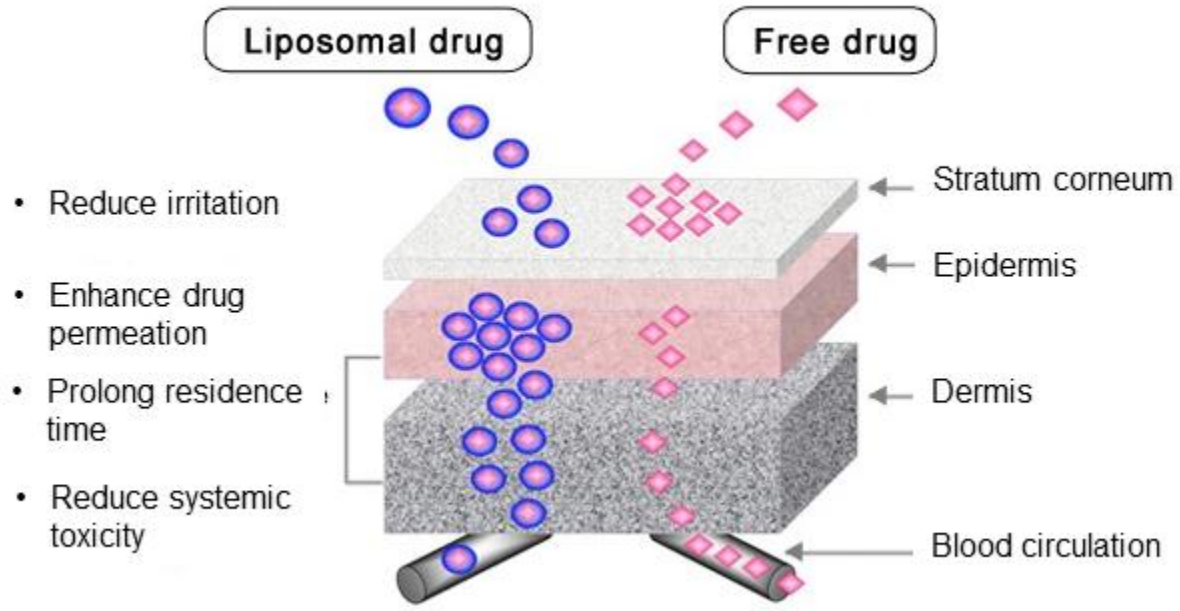

Fig.1.14. Advantages of liposomal drug over free drug in topical drug delivery. Reproduced from web page http://en.charitesnature.com/a_34448_14906_Nano-liposome-system.htm.

As a carrier for the topical and transdermal drug delivery, their advantages include the ability to interact with skin lipids and thereby enhanced permeation, lipids help to minimize the drug-serum protein interaction and thereby increases the drug circulation time. Based on the charge of

liposomes, molecules with different charge can be incorporated for the effective therapeutic application. The inclusion of PEGylated lipids, other functional lipids and surface active agents enable the functional alteration of liposomes according to our requirements (Shim, Kim et al. 2013). Since skin has negative charge, cationic liposomes act as ideal carriers by which the molecules can be permeated across the skin.

1.7.3. Cationic liposomes and lipoplexes

As a delivery system, cationic liposomes are the most extensively studied nanocarrier for the delivery of nucleic acids. The complex formed between cationic liposome and nucleic acid is known as lipoplex. The presence of positive charge on these liposomes enables efficient binding of negatively charged nucleic acids via electrostatic interactions and thereby helps in the therapeutic delivery of nucleic acids.

In general, cationic liposomes are prepared using a mixture of positively charged lipids (cationic lipids) and a co-lipid (helper lipid) such as DOPE (Hui, Langner et al. 1996). Some of the commonly used cationic lipids for the preparation of cationic liposomes include 1,2-dioleoyl-3-trimethylammonium-propane (DOTAP), dimethyl dioctadecyl ammonium bromide (DDAB), 1,2-di-O-octadecenyl-3-trimethylammonium propane (DOTMA), dioctadecyl amidoglycylspermine (DOGS) and N,N-dimethyl-N-[2-(sperminecarboxamido)ethyl]-2,3-bis(dioleyloxy)-1-propaniminium pentahydrochloride (DOSPA) (Mahato, Rolland et al. 1997).

The exceptional biocompatibility of cationic liposomes among other nanocarriers enable them to be the ideal candidates for nucleic acids delivery in-vivo (Oh and Park 2009). There are various reports of cationic liposomes being used for the delivery of nucleic acids like siRNA, plasmid DNA and antisense oligonucleotides (Xiong, Mi et al. 2011, Bhavsar, Subramanian et al. 2012).

Moreover, inclusion of hydrophobic molecules within the lipid bilayers of cationic liposomes enable co-delivery of anticancer drugs along with nucleic acids for more effective anticancer therapies (Jose, Labala et al. 2016).

1.7.4. Stimuli-responsive liposomes

In order to achieve targeted drug delivery with lipid based carriers, stimuli-responsive liposomal vehicles have proved their efficient candidature. Stimuli-responsive lipids are lipids that respond sharply to a trigger, i.e. small changes in physical or chemical conditions with relatively large changes in phase or property. These lipids are also referred as "smart", "intelligent" or "environmentally-sensitive" lipids. The principle behind stimuli-responsive drug carriers include a specific stimulus of physical, chemical, biological or a combination of any of these causes an abrupt change in structural composition/conformation of the carrier resulting in the release of active component in the specific area of concern (Fleige, Quadir et al. 2012)

1.7.4.1. Temperature-sensitive liposomes

Among the various triggered drug release mechanisms investigated so far for the lipid based delivery of therapeutic agents, the one that has progressed to the point where clinical trials have been completed, involves the combinatory use of mild hyperthermia (HT) and thermo-sensitive liposomes (TSLs). Thermo-sensitive liposomes are usually formulated by using a combination of lipids like dipalmitoyl phosphatidylcholine (DPPC) and distearoyl phosphatidylcholine (DSPC), which exhibits a phase transition temperature of few degrees above the normal body temperature (37°C). It is essential that these liposomes remain stable at the normal physiological temperature (37°C), and should release their contents upon application of hyperthermia (39-44°C).

1.7.4.2. pH-sensitive liposomes

One of the most investigated strategies for pH triggered drug delivery is the development of pH-sensitive liposomes. These vesicles remain stable at normal physiological pH (~7.4) but to become unstable and fusogenic upon exposure to acidic conditions resulting in the release of encapsulated contents (Kim, Lee et al. 2008).

1.7.4.3. Light-sensitive liposomes

In order to achieve efficient targeted delivery using liposomes, the use of light as a source of trigger has been investigated for decades. Several investigations have proven the application of photo reactive lipids to design stimuli-responsive drug carriers that can be triggered by a suitable source of light (Bisby, Mead et al. 2000). Light triggered drug delivery from liposomes mostly involves the activation of photosensitive molecules, leading to the destabilization of liposomal membrane resulting in the release of entrapped contents (Lamparski, Liman et al. 1992).

1.8. Objectives

Co-delivery of either two chemotherapeutic agents or a chemotherapeutic drug and nucleic acid is a promising strategy to improve the therapeutic outcome in cancer therapy. It focuses on the advantages of an additive or synergistic effect which is more efficient in comparison with individual therapies for the treatment of cancers. An ideal carrier that is capable of co-delivering more than one therapeutic agent to the target site is the primary requirement for combination therapy. Liposomes are well established nanocarriers proven to be efficient in the delivery of both hydrophilic and hydrophobic micro molecules as well as macromolecules.

The overall objective of this study was to investigate the feasibility of using liposomes as a carrier for the transcutaneous co-delivery of small and macromolecule therapeutics. Breast cancer and skin cancer were selected as model diseases to prove our hypothesis. Micro molecules like tamoxifen and imatinib mesylate were employed in our studies. Similarly, macromolecule STAT3 siRNA was used along with curcumin to investigate the effectiveness of co-delivery in skin cancer

Objective I. Transcutaneous co-delivery of tamoxifen and imatinib mesylate using temperature-sensitive liposomes to treat breast cancer.

Specific aims:

(i) Preparation and characterisation of flexible temperature-sensitive liposomes loaded with tamoxifen and imatinib mesylate.

(ii) Evaluation of temperature dependent in-vitro release of tamoxifen and imatinib mesylate from temperature-sensitive liposomes.

(iii) Evaluation of the cell growth inhibitory effect of tamoxifen and imatinib, alone or in combination using MCF-7 and MDA-MB231 cells.

Objective II. Transcutaneous co-delivery of curcumin and STAT3 siRNA using flexible cationic liposomes to treat skin cancer – *in vitro* studies

Specific aims:

(i) Preparation and characterisation of curcumin loaded cationic liposomes and curcumin loaded liposome-siRNA complex.

(ii) To study the cell inhibitory effect, apoptotic potential and in-vitro gene silencing effect of curcumin and STAT3 siRNA in A431 cells.

(iii) To study the skin penetration of curcumin and STAT3 siRNA delivered using flexible cationic liposomes with the assistance of iontophoresis.

Objective III. Transcutaneous co-delivery of curcumin and STAT3 siRNA using flexible cationic liposomes to treat skin cancer – *in vivo* studies

Specific aims:

(i) To study the cell inhibitory effect of curcumin and STAT3 siRNA co-delivered using cationic liposomes in B16F10 cells.

(ii) Development of mice melanoma model in C57BL/6 mice by subcutaneous injection of B16F10 cells.

(iii) To study the effect of transcutaneous iontophoretic co-delivery of curcumin and STAT3 siRNA using cationic liposomes in mice melanoma model.

Chapter 2

Transcutaneous co-delivery of tamoxifen and imatinib mesylate using temperature-sensitive liposomes to treat breast cancer

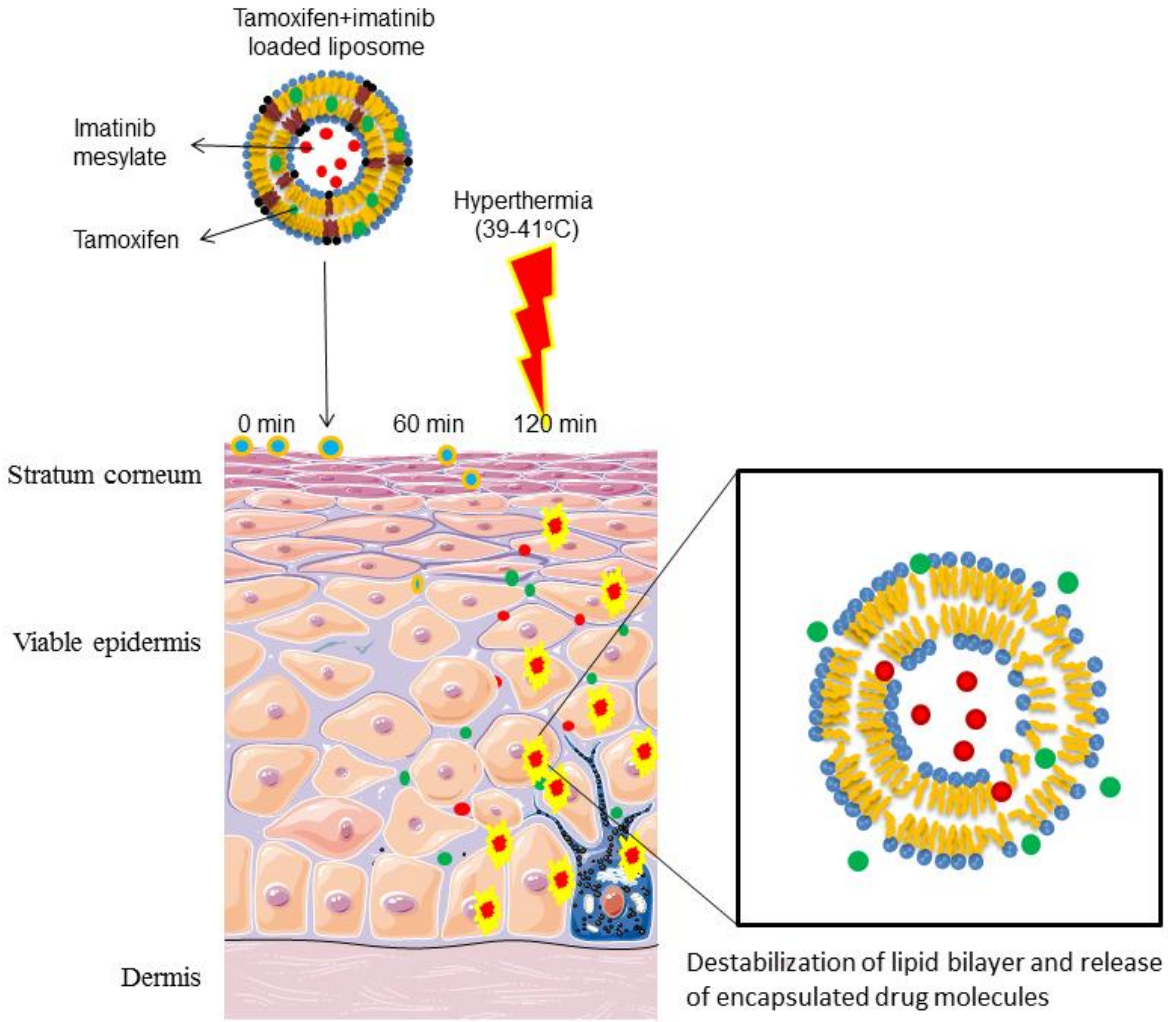
Tamoxifen+imatinib
loaded liposome
Imatinib
mesylate
Tamoxifen
Hyperthermia
(39-41°C)
0 min
60 min
120 min
Stratum corneum
Viable epidermis
Dermis
Destabilization of lipid bilayer and release
of encapsulated drug molecules

2.1. Introduction

Breast cancer is the leading cause of cancer related deaths in women worldwide. In 2016, nearly 1.7 million new breast cancer cases were reported with an estimated death of over 595,690 women globally (Siegel, Miller et al. 2016). The causative factors of breast cancer include genetic factors, hormonal changes and environmental factors among others (McPherson, Steel et al. 2000). Histologically, breast cancer can be classified as invasive lobular carcinoma and invasive ductal carcinoma (Li, Anderson et al. 2003). Lobular carcinoma is characterized by small, noncohesive cells that infiltrate the stroma in a linear pattern, whereas ductal tumors tend to form glandular structures (Korkola, DeVries et al. 2003). Breast cancer progresses through different stages where first stage involves tumor localized in breast tissue; in the second stage, the tumor is either in breast and/ or in the nearby lymph nodes; third stage involves spread of cancer from breast to lymph nodes or skin close to the breast; in the fourth stage, cancer spreads to other distant parts of the body.

The tumors are surgically resected in the first and second stages of breast cancer. This is followed by radiation therapy and/ or chemotherapy (Krag, Weaver et al. 1993). In the third and fourth stages of the cancer, chemotherapy is the choice of treatment (Joy, Ghosh et al. 2015). More recently, with the advent of personalized medicine, chemotherapy is targeted against the cancer causative factors (La Thangue and Kerr 2011). For example, estrogen receptor positive tumors are treated with agents such as tamoxifen and anastrozole among others (Bonneterre, Buzdar et al. 2001). Newer chemotherapeutic agents including monoclonal antibodies (e.g. trastuzumab) with greater efficacy have been developed (Slamon, Leyland-Jones et al. 2001).

One of the major challenges associated with administration of potent and efficacious chemotherapeutic agents is effective drug delivery. Majority of the chemotherapeutic agents are administered as intravenous injections where the drug distributes to the entire body resulting in adverse drug reactions (Kalepu and Nekkanti 2015). Furthermore, prolonged administration of the same agent would result in development of cancer resistance (Chaudhary and Roninson 1993). Therefore, the two main challenges associated with delivery of anti-cancer agents are i) targeting to the tumor site, ii) reducing cancer resistance. Drug targeting has emerged as an important concept with the innovations in drug delivery technologies (Danhier, Feron et al. 2010). Especially, nanoparticle-based systems have been extensively investigated to target the cancer tissue through enhanced permeation and retention strategy. In addition to the nanoparticle-based systems, for the tumors that are accessible, topical route of administration would provide greater localized drug deposition (Sinico and Fadda 2009).

On the other hand, dual drug therapy has been reported to be more effective clinically compared with monotherapy (Wang, Zhao et al. 2011). Multi-drug administration would also render cancer cells more sensitive to individual drugs and minimize the development of drug resistance (Fan, Li et al. 2010). To this end, the objective of the present study was to deliver two chemotherapeutic agents with different mechanisms of action, tamoxifen and imatinib mesylate using liposomal nanocarrier system. Localized topical application was investigated to overcome the unwanted systemic distribution of drugs. The two drugs were encapsulated in temperature-sensitive liposomes to achieve temporal and spatial control over their release. To the best of our knowledge, this is the first study to investigate non-invasive transcutaneous application of temperature-sensitive liposomes containing two drugs.

The two model anti-cancer agents used in this study include tamoxifen and imatinib mesylate. Tamoxifen is a selective estrogen receptor modulator widely used in the treatment of early and advanced estrogen receptor positive breast cancer (O'Regan and Jordan 2002, Lin, Chen et al. 2016). Tamoxifen acts by inhibiting the binding of estrogen to its receptors (Shiau, Barstad et al. 1998). The orally administered tamoxifen is reported to cause several adverse effects including increased risk of thromboembolism, uterine and endometrial cancers, hot flashes among others (Fisher, Costantino et al. 1998, Samson 2014).

On the other hand, imatinib acts by inhibiting several protein kinases including c-kit and platelet-derived growth factor receptor (PDGFR), which are expressed in tumors including breast cancer (Cristofanilli, Morandi et al. 2008). The mechanism of action of tamoxifen and imatinib is shown in figure 2.1.

2.2. Materials and methods

2.2.1. Materials

1, 2-dipalmitoyl-*sn*-glycero-3-phosphocholine (DPPC) and monopalmitoyl-2-hydroxy-*sn*-glycero-3-phosphocholine (MPPC) were purchased from Avanti Polar lipids, USA. Tamoxifen, imatinib mesylate (IM), sodium cholate, tween 80, span 80, paraformaldehyde, Triton X-100 and DAPI were purchased from Sigma Aldrich Chemical Company (Bangalore, India). Dulbecco's modified Eagle's medium (DMEM), minimum essential medium Eagle (MEM), fetal bovine serum (FBS), Dulbecco's phosphate buffered saline (PBS), trypsin EDTA solution and thiazolyl blue tetrazolium bromide (MTT) were purchased from Himedia laboratories (Mumbai, India). All chemicals were used as such and milli-Q water (Millipore, USA) with 18 MΩ cm^{-1} resistivity was used in all experiments.

2.2.2. Preparation of liposomes

Temperature sensitive liposomes were prepared using DPPC, MPPC and different surface active agents like sodium cholate or tween 80 or span 80 by thin film hydration method. Briefly, chloroform solutions of DPPC, MPPC, sodium cholate/tween 80/span 80 were mixed with methanolic solutions of tamoxifen/imatinib mesylate or both in a round bottom flask and the organic solvent was removed using rotary evaporator at 50±2^{o}C and 80 rpm under reduced pressure. Then hydrated the lipid film using phosphate buffered saline (PBS - pH 7.4) to obtain a final lipid concentration of 10 mg/ml. Bath sonicated the liposome suspension for 3 min and extruded through 800 nm pore size polycarbonate membrane for 15-times followed by 100 nm pore size membrane for 11 times (Mini extruder, Avanti Polar Lipids Inc., USA). Different weight ratios of lipids, surfactants and active agents were evaluated to optimize the liposome formulation with desired characteristics as shown in table 2.1.

2.2.3. Characterization of liposomes

Individual drug loaded liposomes as well as dual drug loaded liposomes were characterized for average particle size, polydispersity index and zeta-potential by dynamic light scattering using Zetasizer Nano ZS (Malvern Instruments, UK). For the determination of zeta potential, liposome suspensions were diluted with PBS and 0.75 mL of the dispersion was injected into clear folded capillary cell (DTS1060). Zeta potential measurements were carried out using Smoluchowski model in automatic mode. All the results are expressed as mean value of three different experiments (n=3).

Fourier transform infrared (FTIR) spectroscopic analysis was performed to evaluate the compatibility of tamoxifen with imatinib as well as combination of tamoxifen and imatinib with

lipids used in liposome (FT/IR-4200, Jasco Inc, USA). Samples of individual drugs, mixture of drugs and mixture of drugs with lipids were mixed with potassium bromide at 1:100 ratio and a pellet was prepared using high pressure hydraulic press (Riken Seiki, Tokyo, Japan) by applying pressure of 20 MPa. IR spectra were recorded in the range of 4000–400 cm^{-1} at a spectral resolution of 2 cm^{-1}.

Thermal transitions, especially phase transition of liposomes were studied using differential scanning calorimeter (DSC-60, Shimadzu, Japan). Liposome suspensions (≈3 mg) were placed in an aluminum liquid sample analyzing pan and thermograms were recorded from 30 to 60^{o}C at a heating rate of 0.5^{o}C per min. Liposomes containing only DPPC, DPPC: MPPC (85:15) and DPPC: MPPC: Span 80 (70:15:15) were analyzed for thermal transitions.

TEM analysis samples were prepared by placing a drop of liposomal suspension (diluted to 1mg/ml) on a carbon-coated copper grid, followed by evaporation of solvent. Images were acquired using JEM-2100F (JEOL Ltd., Japan).

2.2.4. Loading & encapsulation efficiency

Loading & encapsulation efficiency of individual drugs as well as combination of drugs within the liposomes were determined by separating the free drug/drugs from the liposome suspension by centrifuging the liposomes using Amicon 10 kDa filters at 6000 rpm for 12 min at 4^{o}C. Concentrations of total drug/drugs in liposome suspension (free as well as entrapped in liposomes) were determined by lysing the liposomes using 6% v/v Triton X-100. Later, concentration of free dug/drugs (from filtrate) and concentration of total drug/drugs in liposome suspension were determined using RP-HPLC system equipped with UV-detector (Shimadzu, Japan). The HPLC analysis was performed using a Phenomenex C18 column with mobile phase

containing methanol and 0.5 M ammonium acetate (85: 15% v/v)) at a flow rate of 1.0 ml/min. 10 µl of sample was injected and both tamoxifen and imatinib mesylate were simultaneously detected at 276 nm wavelength. A representative chromatogram is shown in figure 2.2.The loading & encapsulation efficiency was calculated using Equations (1) & (2) respectively.

$$Loading\ efficiency\ (\%) = \frac{Total\ amount\ of\ drug\ trapped\ in\ liposomes\ (mg)}{Total\ amount\ of\ lipids\ (mg)}\ X\ 100 \qquad (1)$$

$$Encapsulation\ efficiency\ (\%) = 1 - \frac{Concentration\ of\ free\ drug/drugs}{Concentration\ of\ total\ drug/drugs} \times 100 \qquad (2)$$

2.2.5. Elasticity value

Elasticity value of temperature sensitive liposomes (DPPC: MPPC - 85: 15 w/w) was compared with that of deformable temperature sensitive liposomes (DPPC: MPPC: Span 80 - 70: 15:15 w/w). Elasticity value of liposomal vesicles was calculated using Equation (3)

$$\text{Elasticity value} = Jflux\ \times\ (\frac{rv}{rp})^2 \qquad (3)$$

Where J_{flux} is the rate of penetration of liposomes through a permeable membrane (mg sec^{-1} cm^{-2}), r_v is the mean diameter of liposomes after extrusion (nm) through polycarbonate membrane and r_p is the pore size of the barrier/polycarbonate membrane (nm). J_{flux} was determined by extruding the liposomes through a polycarbonate membrane (Nuclepore, Whatman Inc., USA) with a pore size of 100 nm (r_p) for 5 minutes at a pressure of 0.5 MPa. Later, weighed the extrudate and the mean diameter of vesicles after extrusion (r_v) was determined using Zetasizer.

2.2.6. *In vitro* drug release

In vitro drug release from temperature sensitive liposomes was studied at two different temperature conditions (35^{o}C and 40^{o}C) using dialysis bag method (Panwar, Pandey et al. 2010). Briefly, soaked the dialysis membrane (3.0 kDa MW cut off) in deionized water for 12 hours at room temperature to remove the preservatives. Drug release experiments were performed by placing liposomes equivalent to 600 µg drug (200 µl liposome suspension diluted up to 1 ml using PBS). Tightly bound both the ends of dialysis bag with threads after putting the formulation inside. These dialysis bags were then placed in beaker containing 50 ml PBS (pH 7.4) with 20 % methanol. Methanol was used to enhance the solubility of tamoxifen in the receptor medium. The beaker was kept on a magnetic stirrer and solution was cautiously stirred at 100 rpm and the required temperature conditions (35^{o}C and 40^{o}C) were maintained using a thermostat. Individual drug loaded liposomes (tamoxifen & imatinib mesylate) as well as dual drug loaded liposomes were evaluated for drug release at two different temperature conditions. Samples (1.0 ml) were withdrawn from the beaker at predetermined time points (0.25, 0.5, 1, 2, 3, 4, 6, 8, 12, 24 and 48 h) and replaced with fresh media. The collected samples were analyzed using HPLC method as described above. The amount of tamoxifen and imatinib released was determined using a standard calibration curve with a concentration range of 1 to 25 µg/ml and a correlation coefficient of 0.998.

In order to study the temperature dependent drug release from temperature sensitive liposomes, 50 µl liposome suspensions was mixed with 5 ml PBS maintained at different temperature conditions (25, 35-42 & 45^{o}C) and incubated for 5 minutes in a thermomixer (Heidolph, Germany). After 5 minutes incubation, samples were immediately transferred to ice bath to stop further drug release from liposomes. Later, the samples were centrifuged using Amicon 10 kDa

filters at 6000 rpm for 10 min at 4^{o}C and the filtrate was analysed using HPLC method as described above to determine the concentrations of released drug contents.

2.2.7. Stability studies

The stability of temperature sensitive liposomal formulations including tamoxifen loaded liposomes, imatinib loaded liposomes and dual drug loaded liposomes was evaluated for up to two months. Liposomal suspensions were stored in amber colored glass vials closed with screw caps at 2-8°C for two months. Samples were withdrawn at regular time points including 7, 14, 28, 45 and 60 days, and analyzed for particle size, polydispersity index, zeta potential and % drug retained.

2.2.8. Cell culture studies

Estrogen receptor positive (MCF-7) and estrogen receptor negative (MDA-MB-231) breast cancer cells were employed to evaluate the efficacy of tamoxifen, imatinib and dual drug loaded temperature sensitive liposomes. Both the cell lines were obtained from National Centre for Cell Science (Pune, India). Minimum essential medium Eagle (MEM) supplemented with 10% fetal bovine serum and 1% antibiotic solution (penicillin and streptomycin) was used for culturing MCF-7 cells whereas, Dulbecco's modified Eagle's medium (DMEM) was used instead of MEM in case of MDA-MB-231 cells. Maintained the ells at 37°C temperature, 95% humidity and 5% CO_2.

2.2.9. Cell uptake studies

Uptake of temperature sensitive liposomes by MCF-7 and MDA-MB-231 cells was studied using coumarin loaded temperature sensitive liposomes. These liposomes had the same composition as

that of our optimized temperature sensitive liposomes (DPPC: MPPC: Span 80 – 70:15:15). Both MCF-7 and MDA-MB-231 cells were seeded in separate 12 well plates (1 x 10^5 cells/well) and incubated for 24 h. Later, removed the spent media, washed the cells with PBS and incubated the cells with 200 µl of coumarin loaded liposomes dispersed in 800 µl of DMEM for different time periods including 15, 30, 60 and 120 minutes. After specified time point, removed the media followed by washing the cells with ice cold PBS. Fixed the cells using 4% paraformaldehyde. Then, permeabilized the cells using 0.1% Triton X-100 followed by incubation with 4, 6-diamidino-2-phenylindole (DAPI, 1 µg/mL) for 5 min. Later, washed the cells with PBS and observed under fluorescence microscope (Olympus IX53, Olympus Corporation, Japan). Images were acquired after excitation of DAPI and coumarin at 358 and 488 nm lasers, respectively under 20X objective lens. Further, image analysis was carried out using Image J software (version 1.47 V, National Institutes of Health, USA).

2.2.10. Cell viability study

Cell viability of both MCF-7 and MDA-MB-231 cells after incubation with different concentrations of tamoxifen, imatinib and dual drug loaded liposomes was investigated. Additionally, influence of temperature dependent drug release from thermosensitive liposomes upon cell viability was studied. Cell viability was studied using thiazolyl blue tetrazolium bromide (MTT) assay. Briefly, cells were seeded in 96 well plates (1 x 10^4 cells/well) and incubated for 24 h. Later, cells were treated with different formulations including liposomal tamoxifen (2, 5 and 10 µM tamoxifen), liposomal imatinib mesylate (1.5, 3.75 and 7.5 µM imatinib) and liposomal tamoxifen+imatinib (2+1.5, 5+3.75 and 10+7.5 µM tamoxifen and imatinib, respectively). Free tamoxifen and imatinib (5+3.75 and 10+7.5 µM tamoxifen and imatinib, respectively dissolved in 1% DMSO) and blank liposomes were used as controls.

Liposomal formulations were diluted in DMEM and incubated with cells for 8 h at 37ºC. To study the effect of drug release beyond transition temperature of liposomes on cell viability, two different heating strategies were followed. In the first experiment, cells along with the formulations were incubated at 40ºC for 15 min followed by incubation at 37ºC for 7 h 45 min. In the second experiment, cells along with formulations were incubated at 37ºC for 2 h followed by incubation at 40ºC for 15 min, and again followed by incubation at 37ºC for the remaining 5 h 45 min. Later, the formulations were aspirated and cells were washed with ice cold PBS, and incubated with complete media for further 48 h. The cells were then treated with MTT solution for 4 h. The formazan crystals formed were solubilized using DMSO and absorbance was measured at 572 nm wavelength using multimode plate reader (SpectraMax M4, Molecular Devices, USA).

Furthermore, to study the nature of interaction between tamoxifen and imatinib mesylate, a combination index (CI) has been calculated using Equation (4).

$$CI = \frac{D1}{ID1} + \frac{D2}{ID2} \qquad (4)$$

Where, D1 and D2 are concentrations of drug 1 and 2 that produce a certain effect if applied together and ID1 and ID2 are the concentrations that produce the same effect when given alone (Chou 2010). A CI value of >1 indicates antagonistic effect; CI value of 1 indicates additive effect and a CI value of <1 indicates synergistic effect.

2.2.11. Skin permeation studies

Excised porcine ear skin was used for performing skin permeation studies in Franz diffusion cell apparatus. Porcine ears were procured from a local abattoir immediately after kill and washed thoroughly with tap water. Removed the hairs on dorsal side of ears using a hair clipper (HC70, Remington, China). Later, the complete skin from dorsal side of ears was carefully excised using

scalpel and forceps. Scrapped off the underlying fat tissue completely using a blunt scalpel. The thickness of each skin samples were measured using a digital micrometer (Baker gauges India Pvt. Ltd, Mumbai, India). Resistance (R) of skin samples was measured to check the integrity of skin. In order to check the resistance, direct current (I, 1 mA) was applied on skin using a DC power supply unit (V-care Meditech Pvt. Ltd, Bangalore, India) and the voltage drop (V) at that point was measured using a digital multimeter (17B, Fluke Corporation, China). Later, resistance (R) was calculated using Ohm's law (V=IR).

Mounted skin samples between the receptor and donor compartments of Franz diffusion cells with SC facing the donor compartment. Each diffusion cell was having 5 ml receptor volume with an effective diffusional area of 0.637 cm^2. PBS (pH 7.4) containing 20 % methanol maintained at 37±0.5^oC was used as receptor medium. The receptor medium was kept under magnetic stirring throughout the experiment using magnetic beads. Liposomal tamoxifen+imatinib (200 µl) as well as free drug solution (dissolved in methanol) containing similar amount of tamoxifen and imatinib were charged in the donor compartment. 300 µL samples were withdrawn at predetermined time points (0.25, 0.5, 1, 2, 4, 6, 8, 12, 24, 30, 36 and 48 hours) from receptor compartment and replaced with fresh PBS containing 20 % methanol. Later, the samples were analyzed using HPLC method as mentioned earlier.

In order to check the impact of temperature dependent drug release from liposomes on skin permeation characteristics, a separate set of experiments were performed. Mounted the skin samples and treated with formulations (liposomal tamoxifen+ imatinib as well as solution of tamoxifen+imatinib) at 37±0.5^oC for 2 h. Later, hyperthermia (40^oC) was applied on the dorsal side of skin treated with formulation for 15 minutes. Further, permeation studies were carried out in the same manner as mentioned in earlier experiment for 48 h.

Skin permeation parameters were calculated from the cumulative amount of tamoxifen/imatinib permeated per unit area of skin vs. time profile. The flux (J) and lag time (t_{lag}) was calculated from the slope of linear portion of the curve and by extrapolating the linear portion of the curve onto the time axis respectively.

The amount of tamoxifen/imatinib retained within skin layers was determined by tape stripping method. After 48 h of treatment, carefully removed the skin samples from Franz diffusion cell, washed with PBS and tape stripping was performed using scotch book tape (845, 3M, USA). Tape stripping was repeated until the complete stratum corneum was removed, which was ensured by checking skin resistance. The weight of SC removed during each stripping was measured using a microbalance (XP6, Excellence plus, Mettler Toledo, USA). Tapes along with stripped SC were placed in micro centrifuge tubes (2 mL), added 1 ml methanol and kept overnight to extract the drugs from SC. Tamoxifen/imatinib retained in the viable epidermis was extracted by cutting the skin after tape stripping, into small pieces, mixed with methanol and probe sonicated. All the samples were centrifuged at 10000 rpm for 10 minutes and supernatant was analyzed using HPLC method mentioned earlier to determine the concentrations of tamoxifen and imatinib.

2.2.12. Statistical Analysis

All experimental results are presented as mean (n=3) ± standard deviation. Further, statistical analysis was performed using analysis of variance (ANOVA) (GraphPad Prism V6), where $p<0.05$ was considered to be minimum level of significance.

2.3. Results

2.3.1. Characterization of temperature sensitive liposomes

Temperature-sensitive liposomes were prepared at different weight ratios of DPPC, MPPC and surface active agents. Table 2.1 shows the composition of liposomal formulations loaded with tamoxifen and/ or imatinib, average particle size, polydispersity index (PDI) and zeta-potential. The average particle size of all the formulations was <200 nm after extrusion through polycarbonate membranes. After storage at 2-8^{o}C for 24 h, there was significant ($p<0.05$) increase in particle size in the case of liposomes containing sodium cholate and polysorbate 80. On the other hand, liposomes containing sorbitan monooleate remained stable. The average particle size, polydispersity index and zeta-potential of tamoxifen (3 mg/ml) loaded liposomes were found to be 147.3 ± 4.4 nm, 0.25 ± 0.01 and 14.26 ± 3.76 mV, respectively. In the case of imatinib (3 mg/ml) loaded liposomes, these parameters were found to be 155.8 ± 4.0 nm, 0.25 ± 0.01 and 12.33 ± 1.15 mV, respectively. Similarly, the average particle size, polydispersity index and zeta-potential of dual drug loaded liposomes (tamoxifen+imatinib, 3 mg/ml each) were 168.5 ± 7.2 nm, 0.23 ± 0.02 and 16.7 ± 3.6 mV, respectively. The liposomes prepared using 4 mg/ml drug concentrations were found to be unstable.

Figure 2.3 shows the FTIR spectra of neat tamoxifen and imatinib, physical mixture of tamoxifen and imatinib, and physical mixture of drugs and lipids. The characteristic peaks of tamoxifen and imatinib remained unchanged for the physical mixtures of drugs and lipids.

Figure 2.4 shows the thermal transitions of different liposomal formulations studied using DSC. The phase transition temperature of liposomes prepared with only DPPC was 41.6 ^{o}C. The phase transition temperature reduced to 39.8^{o}C after addition of 15% w/w MPPC (DPPC: MPPC,

85:15). Further addition of sorbitan monooleate did not significantly alter the phase transition temperature (39.4^{o}C) of liposomes.

Figure 2.5 shows the TEM images of temperature sensitive liposomes before and after encapsulation of tamoxifen and imatinib. The elasticity value of sorbitan monooleate containing liposomes was 13.95 ± 1.31 mg sec^{-1} cm^{-2}. This elasticity value was 3-fold greater than that of liposomes without sorbitan monooleate (4.53 ± 0.67 mg sec^{-1} cm^{-2}).

2.3.2. Loading & encapsulation efficiency

Encapsulation and loading efficiency of tamoxifen and imatinib alone and in combination in the temperature-sensitive liposomes were studied at different lipid: drug ratios (Table 2.2). In the case of tamoxifen loaded liposomes, all the formulations with lipid to drug ratios (10: 2, 10: 3 and 10: 4) showed more than 90% encapsulation efficiency. In the case of imatinib loaded liposomes encapsulation efficiency increased with increase in drug proportion from 54.6 ± 2.7% at 10: 2 lipid: drug to 71.4 ± 3.3% at 10: 3 lipid: drug ratio. Further increase in drug concentration to 4 mg/ml (10: 4, lipid: drug) did not increase encapsulation efficiency (73.2 ± 1.6%). The encapsulation efficiency of drugs in dual drug loaded liposomes was similar to encapsulation efficiency of individual drugs.

The loading efficiency of tamoxifen in liposomes increased from 18.6 ± 1.2% to 27.6 ± 1.0% upon increasing lipid: drug ratio from 10: 2 to 10: 3. Similarly, in the case of imatinib loaded liposomes, the loading efficiency increased from 10.9 ± 0.8% to 21.4 ± 1.2%, when lipid: drug ratio was increased from 10: 2 to 10: 3. For dual drug loaded liposomes, loading efficiency of tamoxifen and imatinib were found to be 27.8 ± 2.1% and 22.1 ± 1.8%, respectively, at 10: 3: 3 lipid: tamoxifen: imatinib proportions.

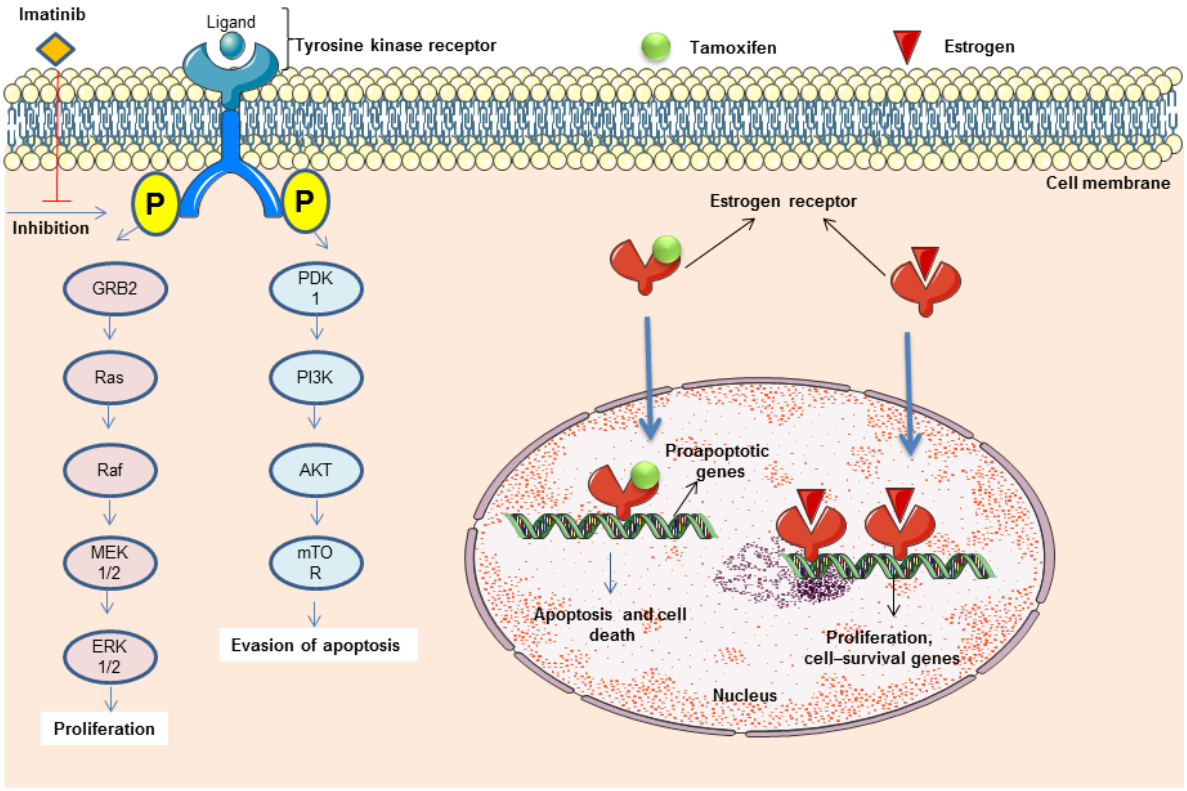

Fig.2.1. Schematic representation of the mechanism of action of tamoxifen and imatinib mesylate.

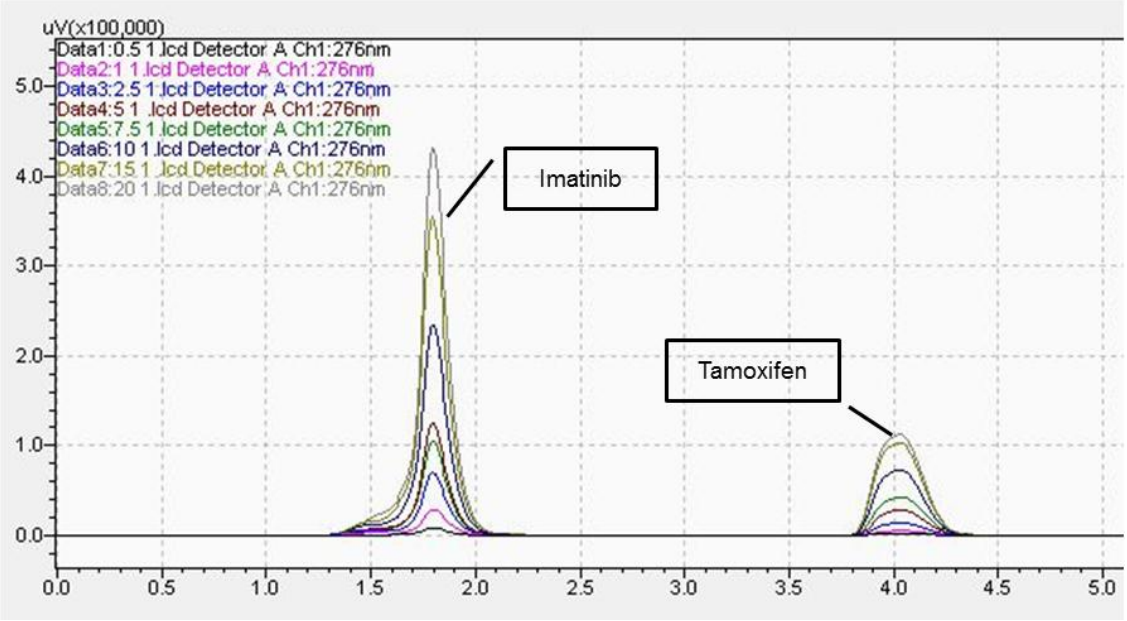

Fig.2.2. HPLC chromatogram representing simultaneous estimation of tamoxifen and imatinib

Table 2.1. Composition, average particle size, polydispersity index and zeta potential of temperature sensitive liposomes.

Formulation	DPPC (% w/w)	MPPC (% w/w)	Sodium cholate (% w/w)	Tween 80 (% w/w)	Span 80 (% w/w)	Tamoxifen (mg/ml)	Imatinib Mesylate (mg/ml)	Particle size (nm)	PDI (Polydispersity index)	Zeta potential (mV)
1	80	10	10	-	-	-	-	112.26 ± 3.45	0.28 ± 0.05	-10.06 ± 1.51
2	80	10	10	-	-	2	-	141.30 ± 20.11	0.35 ± 0.10	-6.13 ± 21.55
3	75	15	15	-	-	2	-	190.30 ± 70.24	0.28 ± 0.07	-4.47 ± 2.24
4	80	20	-	-	-	2	-	174.13 ± 11.63	0.51 ± 0.05	5.91 ± 0.25
5	70	15	-	15	-	2	-	165.76 ± 20.18	0.46 ± 0.06	0.84 ± 3.37
6	70	15	-	-	15	2	-	146.60 ± 19.67	0.30 ± 0.01	11.98 ± 0.64
7	70	15	-	-	15	-	2	188.30 ± 6.38	0.30 ± 0.01	14.73 ± 0.85
8	70	15	-	-	15	3	-	147.33 ± 4.38	0.25 ± 0.01	14.26 ± 3.76
9	70	15	-	-	15	-	3	155.83 ± 4.04	0.25 ± 0.01	12.33 ± 1.15
10	70	15	-	-	15	2	2	180.03 ± 4.17	0.31 ± 0.01	14.50 ± 1.17
11	70	15	-	-	15	3	3	168.50 ± 7.20	0.23 ± 0.02	16.70 ± 3.60

Data are presented as mean (n=3) ± standard deviation.

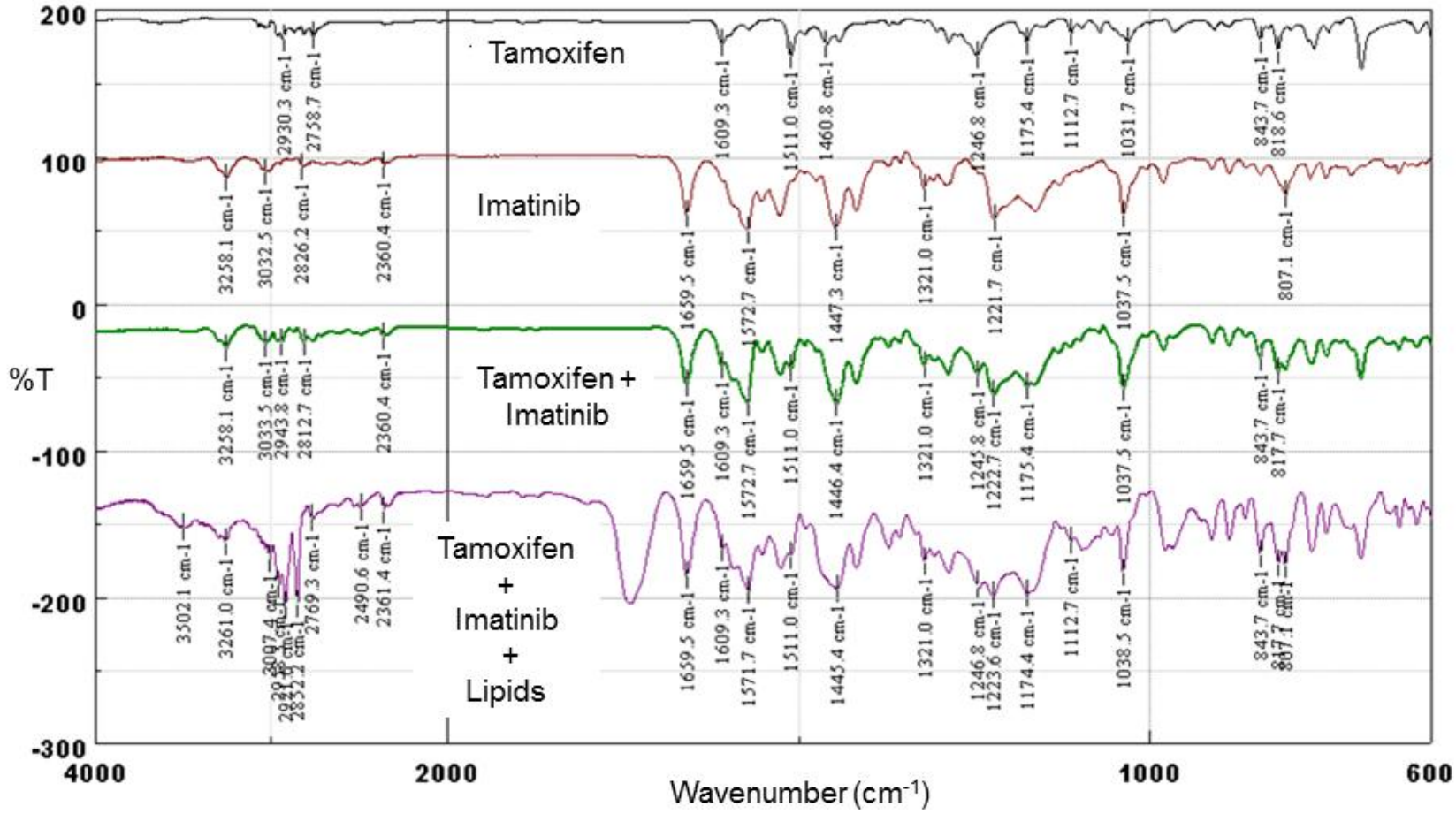

Fig.2.3. FTIR spectra of tamoxifen, imatinib mesylate, mixture of tamoxifen & imatinib mesylate and mixture of tamoxifen, imatinib mesylate, DPPC, MPPC and span 80

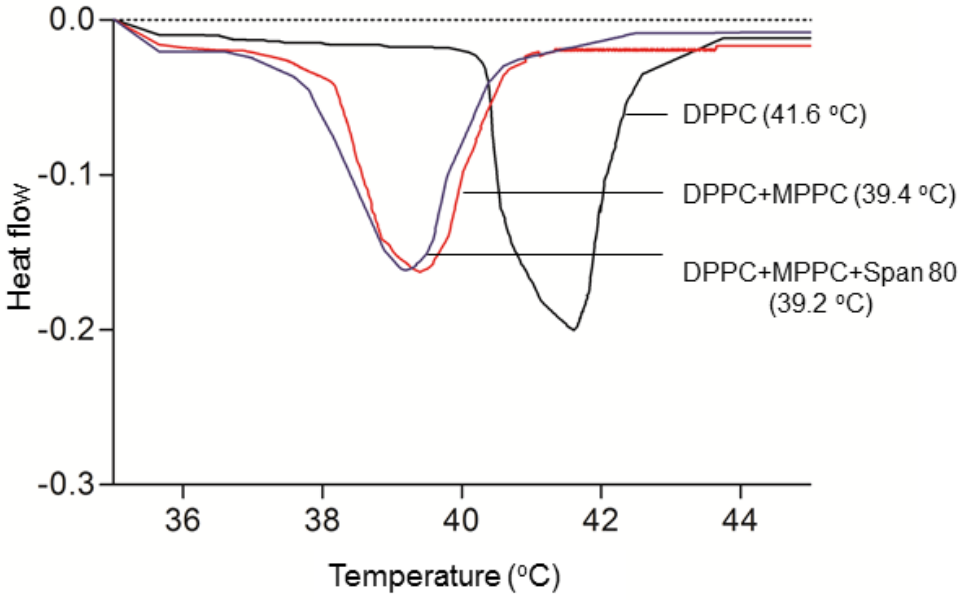

Fig.2.4. DSC thermogram of DPPC liposomes, DPPC+MPPC liposomes and DPPC+MPPC+span 80 liposomes.

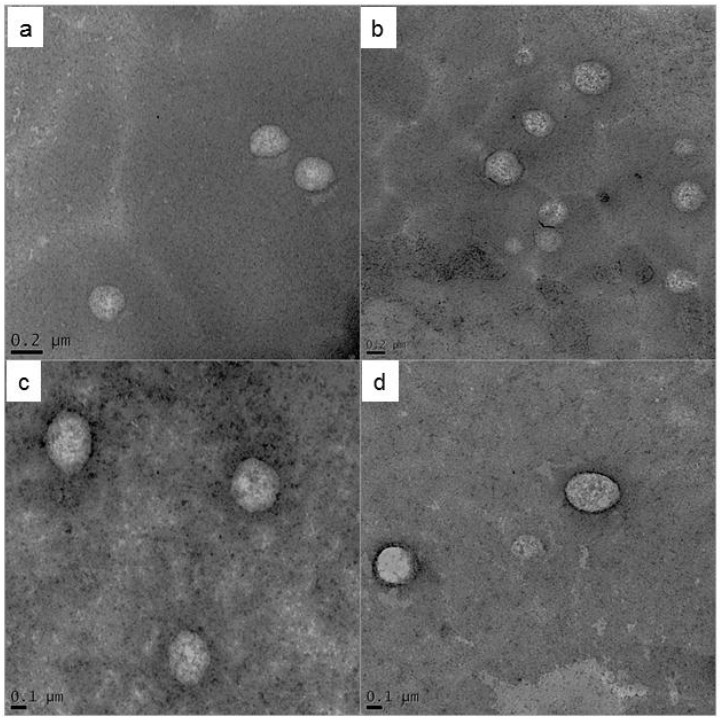

Fig.2.5. TEM images of liposomes. a. Blank liposomes, b. Imatinib loaded liposomes, c. Tamoxifen loaded liposomes, d. Tamoxifen+Imatinib loaded liposomes.

Table 2.2. Lipid: drug ratio, encapsulation efficiency and loading efficiency of tamoxifen and/or imatinib loaded temperature sensitive liposomes.

Formulation	Lipid: drug ratio	Encapsulation efficiency (% EE)		Loading efficiency (%)	
		Tamoxifen	Imatinib	Tamoxifen	Imatinib
1	10:2	92.93 ± 1.30	-	18.58±1.24	-
2	10:3	91.96 ± 1.98	-	27.58±1.02	-
3	10:4	93.18 ± 1.25	-	37.27±2.11	-
4	10:2	-	54.62 ± 2.72	-	10.92±0.84
5	10:3	-	71.44 ± 3.34	-	21.43±1.22
6	10:4	-	73.22 ± 1.55	-	29.28±1.41
7	10:2:2	92.30 ± 0.69	67.26 ± 4.92	18.46±1.13	13.45±1.02
8	10:3:3	92.78 ± 1.47	73.76 ± 4.45	27.83±2.14	22.13±1.82

Data are presented as mean (n=3) ± standard deviation.

2.3.3. *In vitro* drug release

In vitro release of tamoxifen and imatinib was studied at two different temperature conditions, below (35^{o}C) and above (40^{o}C) the phase transition temperature of liposomes. Figure 2.6a shows the drug release profiles of tamoxifen and imatinib at 35^{o}C and 40^{o}C from the respective liposomes. At 35^{o}C, <30% of tamoxifen released after 24 h, whereas at 40^{o}C, >80% of tamoxifen released within 30 min and 98% was released within 4 h. In the case of imatinib loaded liposomes, only 43% of total imatinib released after 24 h incubation at 35^{o}C, whereas at 40^{o}C, >80% of imatinib released within 30 min and 99% of imatinib released in 4 h. Similarly, dual drug loaded temperature-sensitive liposomes showed significantly ($p<0.05$) greater release rate of both the drugs at 40^{o}C compared with release at 35^{o}C temperature (Figure 2.6b). There was no significant change in the release profile of drugs when loaded in liposomes alone or in combination.

The phase transition of temperature-sensitive liposomes was also determined using drug release studies. Figure 2.6c shows the amount of tamoxifen and imatinib released from temperature-sensitive liposomes in 5 min after incubation at different temperature conditions ranging from 25 to 45^{o}C. At temperatures below the phase transition temperature of liposomes (<38^{o}C), there was

negligible amount of drug released. The release of both the drugs increased at phase transition temperature (38^{o}C) followed by a maximum amount of drug released at temperature >39^{o}C. More than 80% of both tamoxifen and imatinib released within 5 min at 40^{o}C.

2.3.4. Stability studies

Stability of liposomes loaded with tamoxifen and/ or imatinib was determined after storage at 5±3°C for up to 60 days. Table 2.3 shows the average particle size, zeta-potential and percentage drug retained within liposomes after storage. There was no significant ($p>0.05$) change in the average particle size and zeta-potential of all the formulations up to 45 days. At 60 days storage, the average particle size and zeta-potential of all the formulations increased significantly ($p<0.05$). Similarly, percentage of tamoxifen and imatinib retained within liposomes reduced to 67.2±5.2% and 61.7±9.1%, respectively after 60 days of storage.

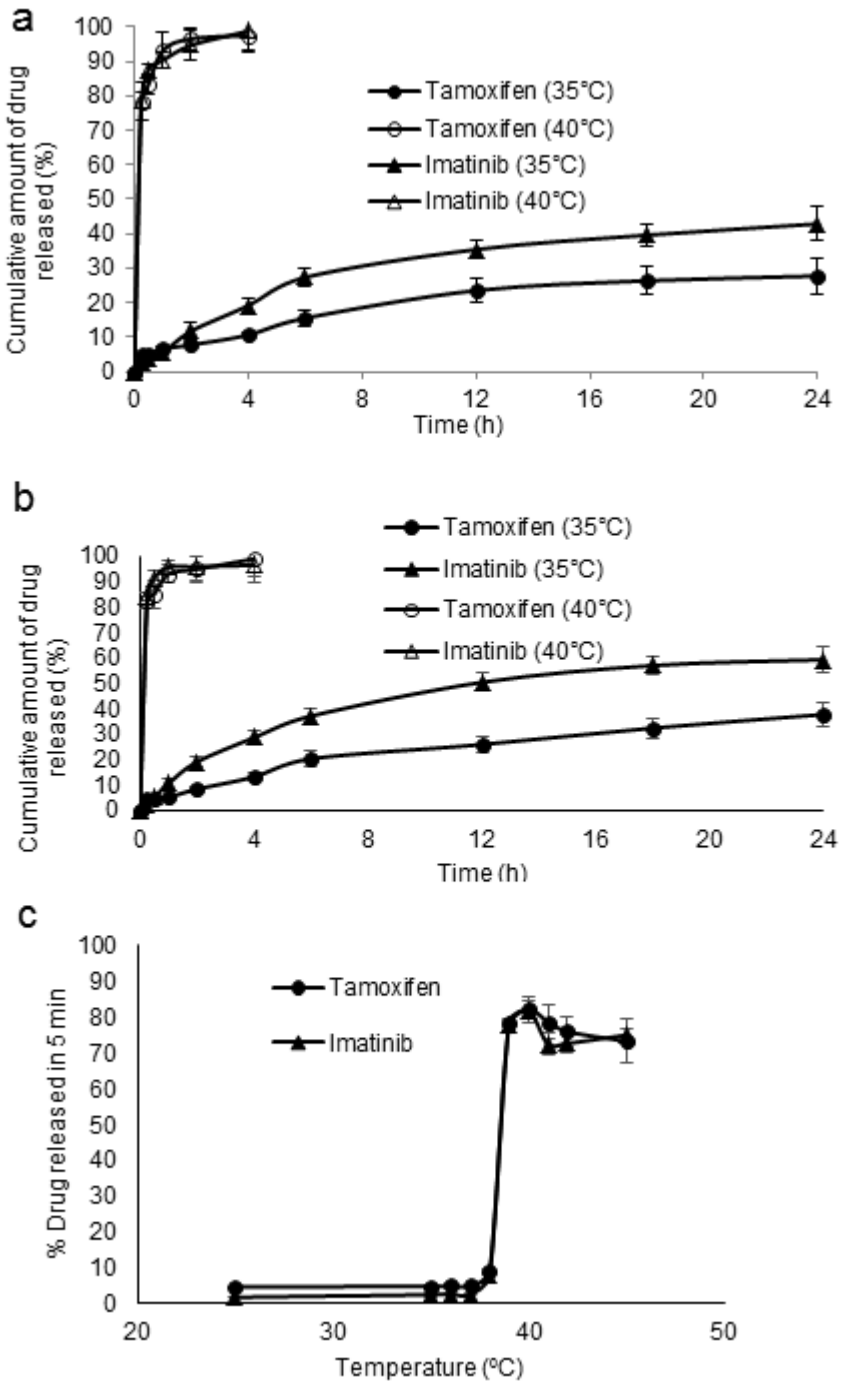

Fig. 2.6. a. *In vitro* release of tamoxifen and imatinib from respective temperature sensitive liposomes at 35°C and 40°C. **b.** *In vitro* release of tamoxifen and imatinib from temperature sensitive liposomes at 35°C and 40°C. **c.** Temperature dependent release of tamoxifen and imatinib from temperature sensitive liposomes. Data represents mean (n =3) ± standard deviation.

Table 2.3. Stability data of tamoxifen and/or imatinib loaded temperature sensitive liposomes stored at 2-8^{o}C.

	Day 1	Day 7	Day 14	Day 28	Day 45	Day 60
Tamoxifen loaded liposomes						
Size (nm)	147.33±4.38	158.83±3.60	162.33±5.14	179.46±5.00	189.24±4.21	265.34±8.25
PDI	0.25±0.01	0.24±0.02	0.26±0.04	0.31±0.04	0.33±0.04	0.35±0.09
Zeta-potential (mV)	14.26±3.76	13.73±1.29	16.56±1.71	15.80±2.90	14.54±1.58	12.25±2.01
Tamoxifen retained (%)	100.00	98.72±6.24	95.45±4.25	92.68±5.16	89.74±4.67	86.26±6.21
Imatinib Mesylate loaded liposomes						
Size (nm)	155.83±4.04	144.86±4.65	157.80±4.73	162.57±8.39	169.58±7.58	298.52±9.24
PDI	0.26±0.01	0.28±0.04	0.30±0.02	0.29±0.05	0.32±0.05	0.41±0.11
Zeta-potential (mV)	12.33±1.15	13.53±2.91	14.10±1.46	13.46±3.59	14.48±1.65	12.35±3.45
Imatinib retained (%)	100.00	96.84±4.32	92.75±6.14	85.46±7.12	78.27±6.27	67.18±5.19
Dual drug (tamoxifen+imatinib) loaded liposomes						
Size (nm)	168.50±7.20	170.16±12.95	188.43±6.67	189.32±5.97	201.24±11.21	281.73±13.95
PDI	0.23±0.02	0.26±0.06	0.27±0.02	0.31±0.02	0.34±0.08	0.39±0.09
Zeta-potential (mV)	16.70±3.60	16.40±1.35	16.80±1.44	15.50±2.79	16.54±4.25	11.26±3.58
Tamoxifen retained (%)	100.00	97.45±6.23	96.28±3.56	94.57±7.32	91.83±5.32	88.17±7.91
Imatinib retained (%)	100.00	95.71±4.84	90.47±7.11	83.66±5.66	72.84±8,34	61.72±9.14

Data are presented as mean (n=3) ± standard deviation. PDI – Polydispersity index.

2.3.5. Cell uptake studies

To visualize the cell uptake of temperature-sensitive liposomes, coumarin, a fluorescent dye was loaded in liposomes. Cell uptake studies were performed in MCF-7 and MDA-MB-231breast cancer cells. Figure 2.7a shows the fluorescence micrographs of MCF-7 cells after incubation with coumarin loaded liposomes at different time periods including 15, 30, 60 and 120 min. The coumarin loaded liposomes were taken up by the cells after 30 min of incubation. The background corrected cell associated fluorescence intensity significantly ($p<0.05$) increased with the increase in incubation time from 15 to 120 min (Figure 2.7b).

Figure 2.8a shows the images of MDA-MB-231 cells after incubation with coumarin loaded temperature-sensitive liposomes at different time periods. It was observed that the cell uptake of liposomes was negligible within 15 min of incubation. However, the fluorescence intensity associated with cells increased with the increase in the incubation time from 30 to 120 min. Similarly, background corrected cell associated fluorescence was shown in figure 2.8b).

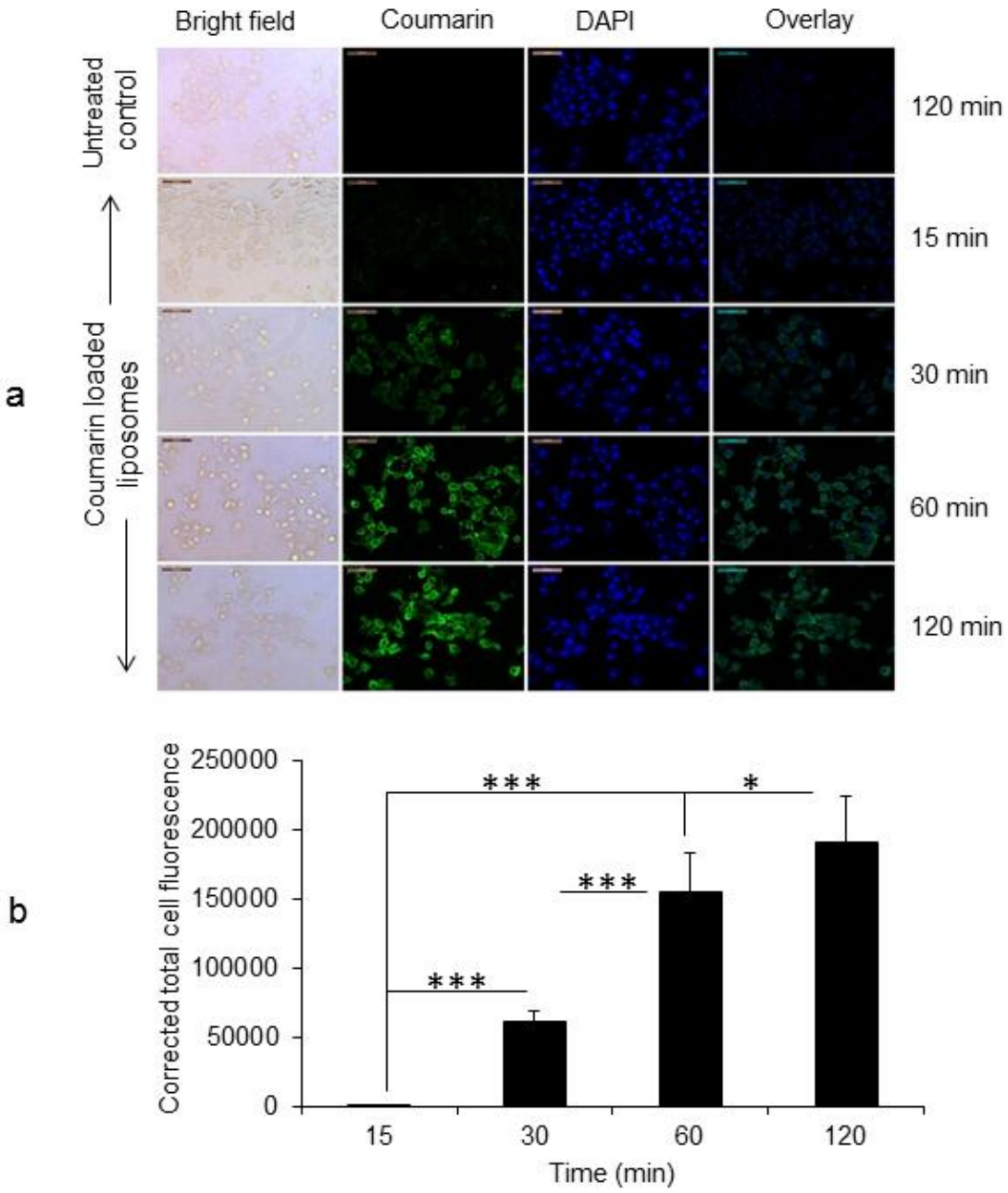

Fig.2.7. a. Cellular uptake of coumarin loaded temperature sensitive liposomes by MCF-7 cells after incubating for 15, 30, 60 and 120 min. Images were representative of at least three experimental groups. **b.** Corrected total cell fluorescence calculated using Image J image analysis software. Data represents mean (n =3) ± standard deviation. *** and * indicates that the value is significantly different at $p < 0.001$and $p < 0.05$.

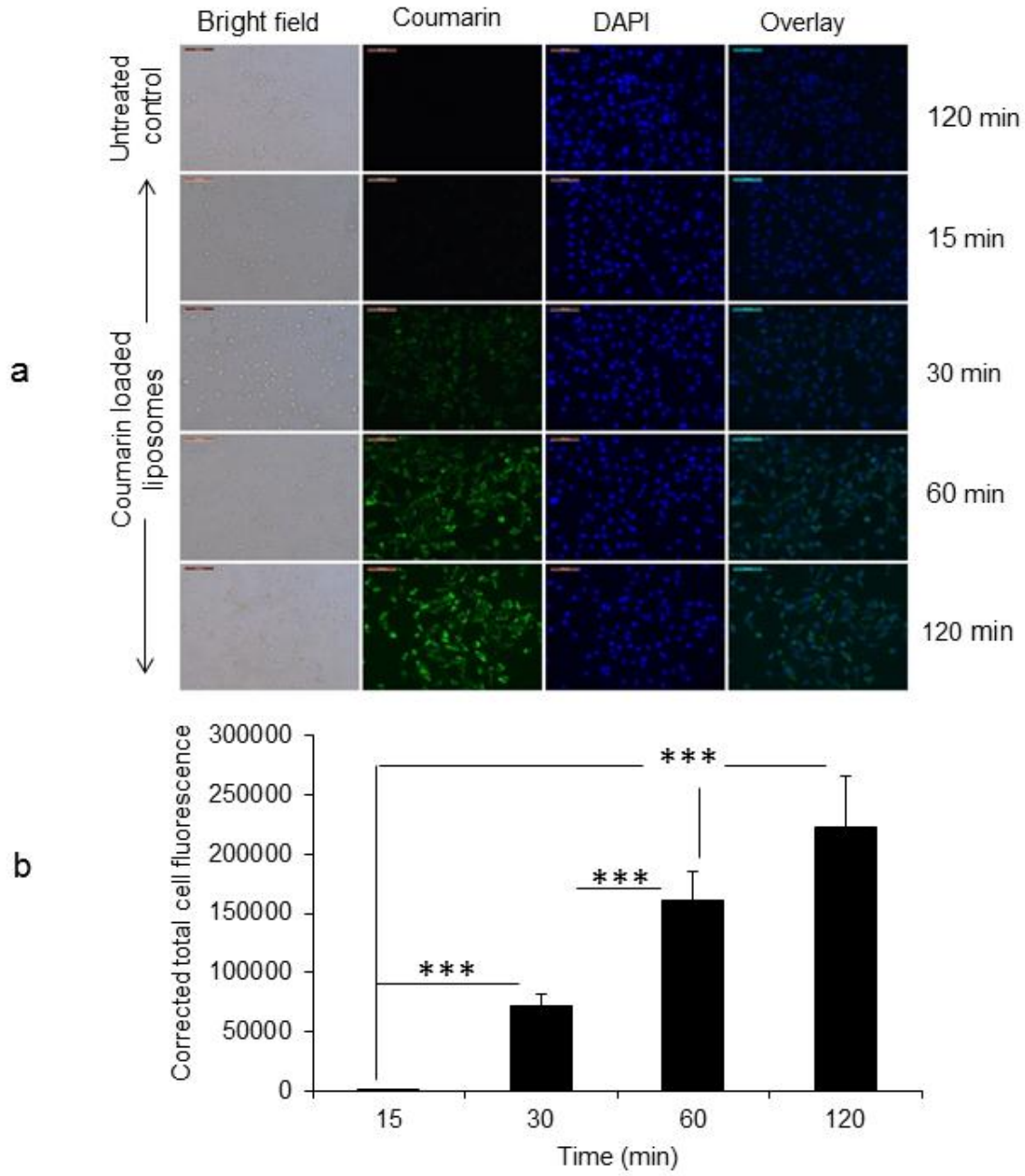

Fig.2.8. a. Cellular uptake of coumarin loaded temperature sensitive liposomes by MDA-MB-231 cells after incubating for 15, 30, 60 and 120 min. Images were representative of at least three experimental groups. **b.** Corrected total cell fluorescence calculated using Image J image analysis software. Data represents mean (n =3) ± standard deviation. *** indicates that the value is significantly different at $p < 0.001$.

2.3.6. Cell viability study

Growth inhibition of MCF-7 and MDA-MB-231 cells was studied after treatment with different liposomal formulations of tamoxifen and imatinib. The influence of drug release before and after cell uptake on cell viability was evaluated by heating the liposomes above transition temperature at two different time points. Figure 2.9 shows the growth inhibition of MCF-7 cells after treatment with different formulations of tamoxifen and imatinib at 37^{o}C and 40^{o}C. Blank liposomes showed 3.6 ± 0.5% and 4.2 ± 0.8% growth inhibition at 37^{o}C and 40^{o}C, respectively. At 37^{o}C, increase in the tamoxifen concentration (2 to 10 μM) in liposomes increased the growth inhibition from 6.1 ± 0.7% to 33.2 ± 4.2%. After incubating at 40^{o}C for the initial 15 min, the growth inhibition increased from 18.3 ± 1.4% to 58.9 ± 2.9% with the increase in concentration of tamoxifen from 2 to 10 μM. On the other hand, when the liposomes were heated at 40^{o}C for 15 min after 2 h incubation, the growth inhibition was 23.6 ± 2.4% and 70.6 ± 2.4% at 2 and 10 μM concentrations, respectively. Similarly, imatinib loaded liposomes incubated at 37^{o}C at different concentrations (1.5, 3.75 and 7.5 μM) showed 14.8 ± 3.3%, 35.2 ± 1.2% and 42.5 ± 2.7% growth inhibition, respectively. After incubating at 40^{o}C for initial 15 min, imatinib (1.5, 3.75 and 7.5 μM concentrations) loaded liposomes showed 28.2 ± 2.6%, 58.3 ± 4.1% and 65.3 ± 4.0% growth inhibition, respectively. On the other hand, when the liposomes were heated at 40^{o}C for 15 min after 2 h incubation, the growth inhibition was found to be 19.3 ± 1.4%, 43.0 ± 3.3% and 51.9 ± 2.8% at 1.5, 3.75 and 7.5 μM imatinib concentrations, respectively.

Dual drug loaded liposomes at concentrations (2+1.5, 5+3.75 and 10+7.5 μM, tamoxifen+imatinib) showed 48.4 ± 3.3%, 61.8 ± 3.0% and 70.7 ± 2.1% growth inhibition at 37^{o}C. The growth inhibition increased to 68.3 ± 2.2%, 79.5 ± 4.9% and 88.2 ± 2.7% when the liposomes were incubated with cells at 40^{o}C for the initial 15 min. On the other hand, when the

incubation temperature was increased after 2 h, growth inhibition was 74.1 ± 1.8%, 86.3 ± 1.5% and 92.5 ± 1.1% at 2+1.5, 5+3.75 and 10+7.5 μM concentrations of tamoxifen+imatinib, respectively. The tamoxifen and imatinib (5+3.75 μM; tamoxifen+imatinib) free drug solutions showed 78.8 ± 3.4% and 74.9 ± 3.4% growth inhibition at 37^{o}C and 40^{o}C, respectively. At higher concentration (10+7.5 μM tamoxifen+imatinib), the percentage cell growth inhibition increased to 84.9 ± 2.9% and 86.3 ± 3.7% at 37 and 40^{o}C, respectively.

Figure 2.10 shows the growth inhibition of MDA-MB-231 cells after treatment with different drug loaded liposomal formulations at 37^{o}C and 40^{o}C. There was no significant ($p>0.05$) difference in growth inhibition after treatment of MDA-MB-231 with blank liposomes (4.4 ± 0.8% and 5.8 ± 0.7% growth inhibition at 37^{o}C and 40^{o}C). At 37^{o}C, increase in the concentration of tamoxifen loaded liposomes (2, 5 and 10 μM) increased the growth inhibition at 9.8 ± 0.5%, 14.9 ± 1.4% and 32.4 ± 1.3%, respectively. When the cells were incubated at 40^{o}C with formulations for the initial 15 min before cell uptake, the growth inhibition for the same concentrations was 9.2 ± 0.5 %, 21.7 ± 0.6% and 46.9 ± 2.9%. On the other hand, when the liposomal tamoxifen is treated at 40^{o}C after 2 h of incubation (allowing for the cell uptake), the growth inhibition increased to 16.8 ± 3.6%, 32.5 ± 3.4% and 54.7 ± 4.2%. After treatment of MDA-MB-231 cells with imatinib loaded liposomes (1.5, 3.75 and 7.5 μM concentrations) at 37^{o}C, the growth inhibition was found to be 25.9 ± 1.1%, 39.1 ± 3.6% and 46.0 ± 2.9%. The growth inhibition increased after increase in incubation temperature to 40^{o}C (42.6 ± 1.0%, 59.1 ± 3.9% and 64.9 ± 1.7% for initial 15 min incubation at 40^{o}C; and 34.8 ± 1.7%, 47.6 ± 0.5% and 56.0 ± 1.2% growth inhibition when the temperature was increased at 40^{o}C after 2 h of incubation.

Dual drug loaded liposomes (2+1.5, 5+3.75 and 10+7.5 μM, tamoxifen+imatinib) increased the growth inhibition to 46.1 ± 4.9%, 56.1 ± 2.5% and 67.9 ± 3.5%, respectively compared with individual drug treatments after incubation at 37^{o}C. After incubation at 40^{o}C for the initial 15 min (before cell uptake), the growth inhibition for the same concentrations was 63.9 ± 3.7%, 74.2 ± 2.7% and 81.2 ± 2.7%. Alternatively, when the temperature was increased to 40^{o}C after 2 h (allowing for cell uptake), the dual drug loaded liposomes showed 58.6 ± 3.2%, 66.5 ± 3.9% and 75.5 ± 0.9% growth inhibition. Treatment of cells with free tamoxifen and imatinib mixture (5+3.75 and 10+7.5 μM tamoxifen+imatinib) showed 69.1 ± 3.6% and 76.7 ± 2.8% growth inhibition at 37^{o}C. There was not significant ($p>0.05$) difference in growth inhibition after increasing the incubation temperature to 40^{o}C (68.3 ± 1.8% and 78.3 ± 2.4% growth inhibition).

A combination index of <1 indicating synergistic effect was found after treatment of MCF-7 and MDA-MB-231 cells with tamoxifen and imatinib at lower concentrations (2+1.5 μM, 5+3.75 μM tamoxifen+imatinib). On the other hand, at higher concentration (10+7.5 μM tamoxifen+imatinib), combination index was close to 1.

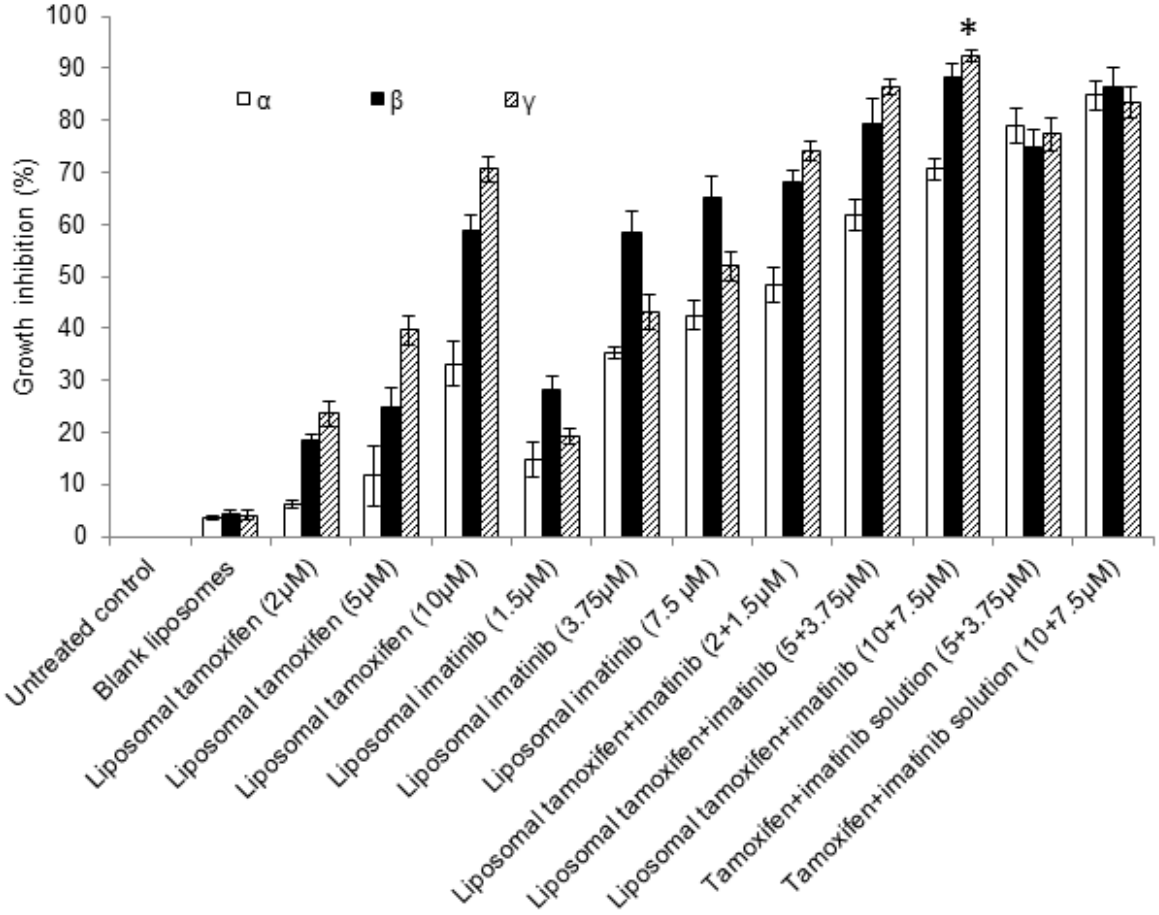

Fig.2.9. Inhibition of MCF-7 breast cancer cell growth after treatment with different formulations of tamoxifen and imatinib mesylate (α – incubated at 37°C for 8 h, β – incubated at 40°C for 15 min followed by 37°C for 7h 45 min, γ – incubated at 37°C for 2 h followed by 40°C for 15 min followed by 37°C for 5h 45 min). Results are presented as mean (n=5) ± standard deviation. Asterisk (*) indicates that the values are significantly ($p < 0.05$) different from all other treatment groups except liposomal tamoxifen+imatinib (5+3.75 μM) at 40^{o}C, tamoxifen+imatinib solution (5+3.75 μM) at 35 & 40^{o}C and tamoxifen+imatinib solution (10+ 7.5 μM) at 35 & 40^{o}C.

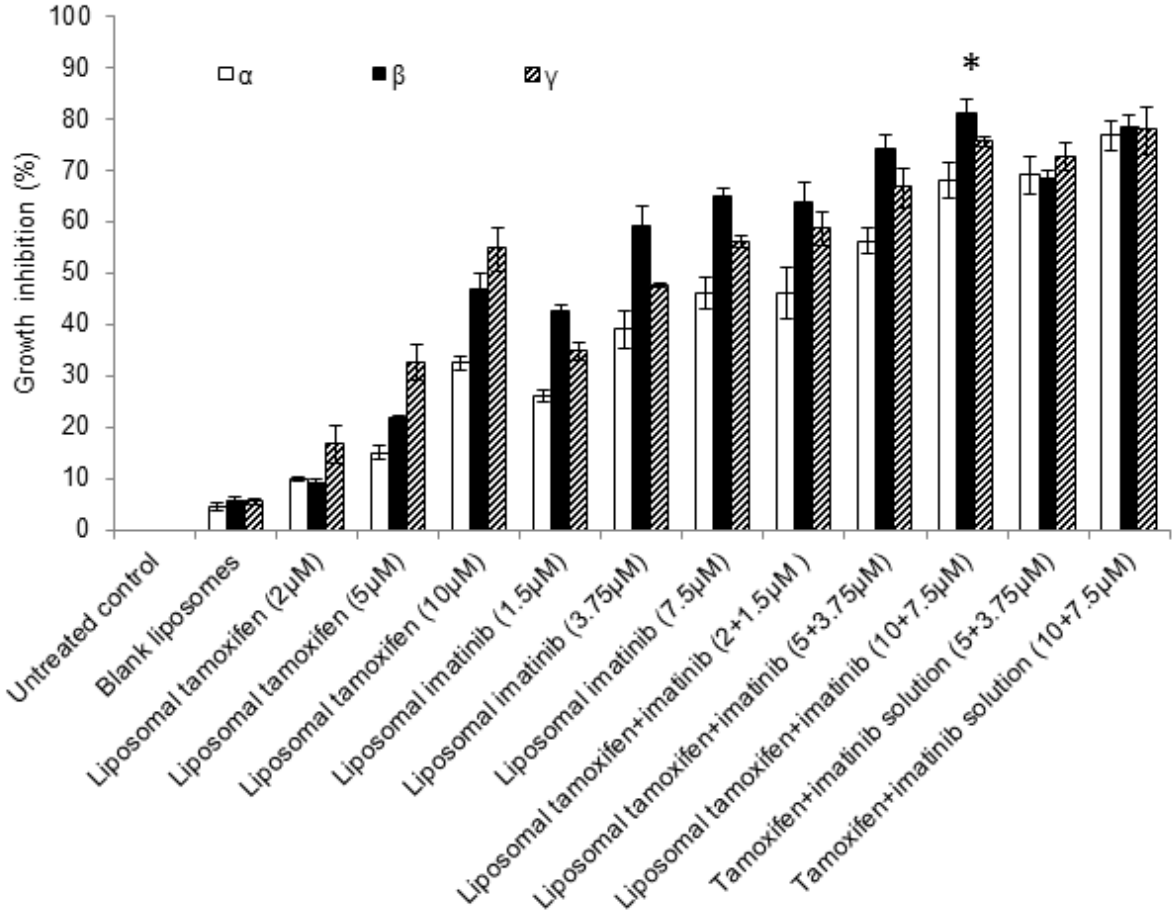

Fig.2.10. Inhibition of MDA-MB-231 breast cancer cell growth after treatment with different formulations of tamoxifen and imatinib mesylate (α – incubated at 37°C for 8 h, β – incubated at 40°C for 15 min followed by 37°C for 7h 45 min, γ – incubated at 37°C for 2 h followed by 40°C for 15 min followed by 37°C for 5h 45 min). Results are presented as mean (n=5) ± standard deviation. Asterisk (*) indicates that the values are significantly ($p < 0.05$) different from all other treatment groups except liposomal tamoxifen+imatinib (5+3.75 μM) at 40^{o}C, tamoxifen+imatinib solution (5+3.75 μM) at 35 & 40^{o}C and tamoxifen+imatinib solution (10+ 7.5 μM) at 35 & 40^{o}C.

2.3.7. Skin permeation studies

The average thickness of porcine ear skin used for *ex vivo* permeation studies was found to be 0.90 ± 0.07 mm. The electric resistance of skin samples used for experimentation was found to be 4.89 ± 1.35 kΩ. Skin samples were treated with liposomal formulations of tamoxifen and imatinib for 48 h. Free tamoxifen or liposomal tamoxifen was not detected in the receptor medium after treating the skin for 48 h. Similarly, tamoxifen was not detected in the receptor medium even after heat application (40°C) for 15 min. On the other hand, imatinib permeated through the skin into receptor medium from free and liposomal formulations. Skin permeation parameters of imatinib were presented in table 2.4.

Tape stripping was performed to evaluate the amount of tamoxifen and imatinib retained within SC and viable epidermis. Complete stripping of stratum corneum was ensured by measuring skin resistance. Figure 2.11a shows the total amount of drug retained in stratum corneum and viable epidermis after treatment for 48 h. In general, SC retained more amount of drug compared with viable epidermis. The cumulative amount of imatinib retained in stratum corneum at 37°C was 82.8 ± 10.8 and 87.4 ± 9.7 µg/mg of tissue for free and liposomal imatinib, respectively. After heating the skin samples at 40°C for 15 min, the cumulative amount of imatinib retained in stratum corneum increased to 101.5 ± 17.9 and 108.5 ± 6.9 µg/mg of tissue for free and liposomal imatinib, respectively. For tamoxifen, the cumulative amount retained in stratum corneum at 37°C was 66.5 ± 5.5 and 25.1 ± 7.9 µg/mg of tissue for free and liposomal tamoxifen, respectively. After heating the skin samples at 40°C for 15 min, the cumulative amount of tamoxifen retained in stratum corneum was 65.0 ± 11.1 and 51.0 ± 5.9 µg/mg of tissue for free and liposomal tamoxifen, respectively.

Figure 2.11b shows the amount of tamoxifen and imatinib retained in viable epidermis. The amount of imatinib retained in viable epidermis was 9.7 ± 5.4 and 8.0 ± 3.0 µg/mg of tissue for free and liposomal imatinib at 37°C. Whereas at 40°C, 22.4 ± 5.6 and 17.7 ± 4.8 µg/mg of tissue for free and liposomal imatinib was retained. Similarly, the amount of tamoxifen in viable epidermis at 37°C was 6.3 ± 3.0 and 5.7 ± 1.9 µg/mg of tissue for free and liposomal tamoxifen, respectively. Similarly, after heating skin samples at 40°C for 15 min, 17.1 ± 6.6 and 13.9 ± 6.7 µg/mg was retained in viable epidermis after application of free and liposomal tamoxifen, respectively.

Table 2.4. Skin permeation parameters of imatinib from tamoxifen and imatinib loaded temperature sensitive liposomes.

Treatment	Lag time (h)	Flux (µg/cm^2/h)	Cumulative amount permeated (µg/cm^2)	Diffusion coefficient	Permeability (cm^2/h)
Drug solution (37^{o}C)	2.56±0.37	6.14±1.17	447.76±32.51	0.00053	0.01124±0.0007
Drug solution (40^{o}C)	1.78±0.49	8.93±1.21	592.81±24.26	0.00077	0.01489±0.0005
Liposomes (37^{o}C)	5.45±1.25	1.99±0.35	211.53±17.45	0.00025	0.00332±0.0003
Liposomes (40^{o}C)	3.04±0.98	5.59±1.35	402.82±21.23	0.00045	0.00931±0.0002

Data are presented as mean (n=3) ± standard deviation.

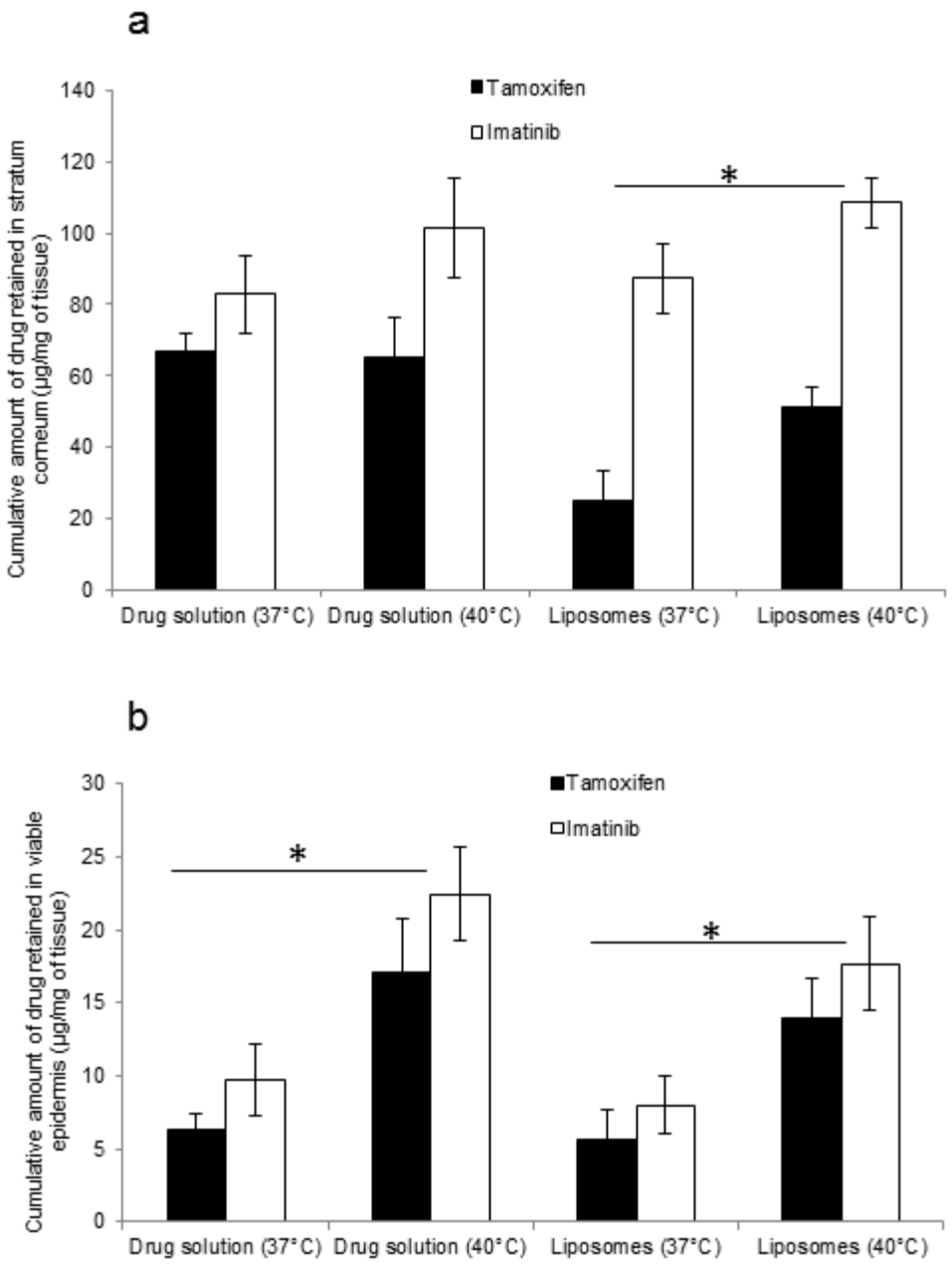

Fig.2.11. a. Cumulative amount of tamoxifen & imatinib retained within stratum corneum (SC) after treatment with different formulations at 37 & 40^{o}C. **b.** Cumulative amount of tamoxifen & imatinib retained within viable epidermis (VE) after treatment with different formulations at 37 & 40^{o}C. Results are presented as mean (n=3) ± standard deviation. Asterisk (*) indicates that the values are significantly ($p < 0.05$) different compared with other treatment groups.

2.4. Discussion

Tamoxifen and imatinib mesylate were selected as the two model anti-cancer molecules to investigate their transcutaneous delivery after encapsulation in temperature-sensitive liposomes. Tamoxifen has a molecular weight of 371.5 Da and a log P of 7.9 (Monteagudo, Gándola et al. 2012). It is a poorly water soluble compound at ~0.4 µg/ml solubility (Hu, Neoh et al. 2006). On the other hand, imatinib mesylate is a weakly basic drug with molecular weight of 589.7 Da and water solubility of 10 mg/ml (van Leeuwen, van Gelder et al. 2014). Liposomes preferentially encapsulate hydrophobic agents with greater efficiency compared with hydrophilic drugs (Schwendener and Schott 2010). This is attributed to the greater partitioning of lipophilic agents in phospholipid containing medium before liposome formation, and then entrapment in phospholipid bilayer after liposome formation (Kulkarni, Betageri et al. 1995). In the case of hydrophilic agents, the partitioning in phospholipid containing medium is less. The hydrophilic agent is expected to be entrapped in the aqueous core of liposomes (Immordino, Dosio et al. 2006). Therefore, the encapsulation and loading efficiency of water insoluble tamoxifen in liposomes was significantly ($p<0.05$) greater than water soluble imatinib. Furthermore, this difference in partitioning and spatial location of drugs within liposomes allowed for lower drug-drug interactions as observed from the infrared spectroscopic studies.

The encapsulated drugs should release from liposomes into the aqueous release medium. In general, the polar molecules release at a greater rate compared with non-polar molecules. To that end, tamoxifen with greater log P value released at a slower rate compared with polar imatinib at both 35^{o}C and 40^{o}C incubation temperature. However, beyond the transition temperature of lipids at 40^{o}C, the release rate of both the drugs was significantly ($p<0.05$) greater compared with release rate at 35^{o}C, below transition temperature. The molecular changes that occur above

the transition temperature in DPPC include conversion of lipid acyl chains from all-trans configuration to the one with increased number of gauche "kinks," leading to conformational disorder and mobility (Nagarajan, Schuler et al. 2012). However, a transition temperature of 38-39^{o}C is most suitable for clinical application of temperature-responsive systems. The transition temperature of the liposomes reported here was 39.4^{o}C, which is between the 37^{o}C body temperature and ~40^{o}C solid tumor temperature that allows for cancer targeted drug release (Li, Wu et al. 2015).

The >40^{o}C transition temperature of liposomes made of DPPC was decreased by addition of lysolipid MPPC. Conical molecular shape attributed to single chain and large head group along with tendency to form spherical micelles in aqueous solution, makes lysolipids suitable candidates to form head group lined pores (McIntosh, Advani et al. 1995, Mills and Needham 2005). Above transition temperature, the grain boundary regions liquefy and the lysolipids make defect structures which stabilize pores along the liquid–solid boundaries and allow drug release (Mills and Needham 2005). The rapid release of drug molecules at temperatures above gel-liquid crystal phase transition is attributed to the presence of MPPC within liposomal membrane (Mills and Needham 2005).

The rational co-delivery of anti-cancer agents should provide additive or more than additive synergistic effect in cancer cell growth inhibition. Tamoxifen is a selective estrogen receptor modulator (SERM) that competes with endogenous estrogen and has been used as first line of treatment in estrogen receptor positive breast cancer for more than three decades (Jiang, Zheng et al. 2013). Imatinib is a selective tyrosine kinase inhibitor including c-kit (Demetri, Von Mehren et al. 2002). Tamoxifen and imatinib affect different downstream signaling pathways that lead to cancer cell death (figure 2.1). The combination delivery of tamoxifen and imatinib showed

synergistic activity when administered at lower concentrations. Interestingly, tamoxifen also showed growth inhibition in estrogen receptor negative MDA-MB-231 cells. This is attributed to the downregulation of cancer inhibitor of protein phosphatase 2A (CIP2A) and phospho-Akt (Manna and Holz 2016). Imatinib is clinically approved for the treatment of chronic myelogenous leukemia and acute lymphocytic leukemia (Cohen, Williams et al. 2002). Furthermore, it is under clinical investigation against melanoma and gastrointestinal stromal tumors (Heinrich, Owzar et al. 2008, Guo, Si et al. 2011). The c-kit surface receptor has been identified as a potential target for the treatment of triple negative breast cancer (Cleator, Heller et al. 2007). The greater cell growth inhibition after heating the medium at 40^{o}C compared with 37^{o}C is attributed to greater release of dual drugs from liposomes.

It should be noted that the two target receptors for tamoxifen and imatinib, estrogen and c-kit are majorly localized in cytoplasm and cell surface, respectively (Greene, Sobel et al. 1984, Cleator, Heller et al. 2007). This is evident from significant ($p<0.05$) increase in cell growth inhibition when imatinib was released from liposomes at 40°C immediately after incubating with cells (extracellularly) compared with growth inhibition after liposomal imatinib cell uptake. In contrary, liposomal tamoxifen showed greater cell growth inhibition when the tamoxifen was released inside the cells compared with growth inhibition after extracellular tamoxifen release. Therefore, it is important to understand and coordinate the stimuli-responsive drug release before and after cell uptake based on the location of target site. To the best of our knowledge, this is the first report to show importance of extracellular and intracellular drug release using stimuli-responsive systems.

Application of external hyperthermia after intravenous administration of temperature-sensitive carriers has been shown to provide targeted drug release (Needham, Anyarambhatla et al. 2000).

However, application of hyperthermia to tumors located in deeper tissues is still a technical problem (Szmigielski, Zielinski et al. 1988). To that end, the most suitable cancer types for hyperthermia-based targeted drug release would be skin cancer, breast cancer and few forms of head and neck cancers. Therefore, it was hypothesized that topical application of anti-cancer agents using flexible liposomes would penetrate the outer layers of skin; and then application of hyperthermia would result in drug release within the target breast cancer site. Furthermore, hyperthermia in skin would also increase the microcirculation and local perfusion (Petersen, Rousing et al. 2011). The preliminary skin penetration and temperature-responsive drug release studies showed penetration and deposition of drugs in skin. However, the drug disposition within the skin was similar to application of free drug solutions. This is attributed to the preparation of drug solutions in methanol that has skin permeation enhancement properties (Aungst, Blake et al. 1990). While imatinib was found to diffuse across the skin to reach receptor chamber, tamoxifen was retained within the skin. Earlier studies also reported poor permeability of tamoxifen across the intact skin due to its high lipophilic property (Moser, Kriwet et al. 2001). Overall, the present studies showed feasibility of topical application of temperature-responsive liposomes to enhance the drug release within skin membrane.

2.5. Conclusion

Liposomes composed of DPPC, MPPC and sorbitan monooleate showed a transition temperature relevant for clinical applications. These temperature-sensitive liposomes were also found to be flexible with high elasticity value. Both water soluble imatinib and water insoluble tamoxifen were encapsulated in liposomes with high encapsulation efficiency. About 80% of the drugs released within 30 min above the transition temperature of 39°C. These liposomal systems were rapidly taken up by breast cancer cell lines, MCF-7 and MDA-MB-231, within 30 min. This

property of temperature-responsive drug release allowed for evaluation of cell viability when the drugs were released before and after cell uptake. Tamoxifen with the intracellular target site showed greater growth inhibition when it was released after cell uptake. Meanwhile, imatinib with cell membrane target showed greater cancer cell growth inhibition, when it was released before the cell uptake. Overall, the combination of tamoxifen and imatinib showed synergistic growth inhibition in both the breast cancer cell lines used. Furthermore, the flexible liposomes penetrated the excised porcine skin and improved the skin drug disposition in response to temperature stimulus. Taken together, the findings from this study support the development of flexible temperature sensitive liposomes for transcutaneous co-delivery of tamoxifen and imatinib for effective breast cancer treatment.

Since the depth of skin permeation of drug solution as well as liposome loaded drugs were comparable in case of these temperature sensitive liposomes, we have evaluated the feasibility of using flexible cationic liposomes in our further studies. These liposomes were loaded with micro and macro molecules and applied topically with the help of iontophoresis for the treatment of skin cancer.

Chapter 3

Co-delivery of curcumin and STAT3 siRNA using deformable cationic liposomes to treat skin cancer

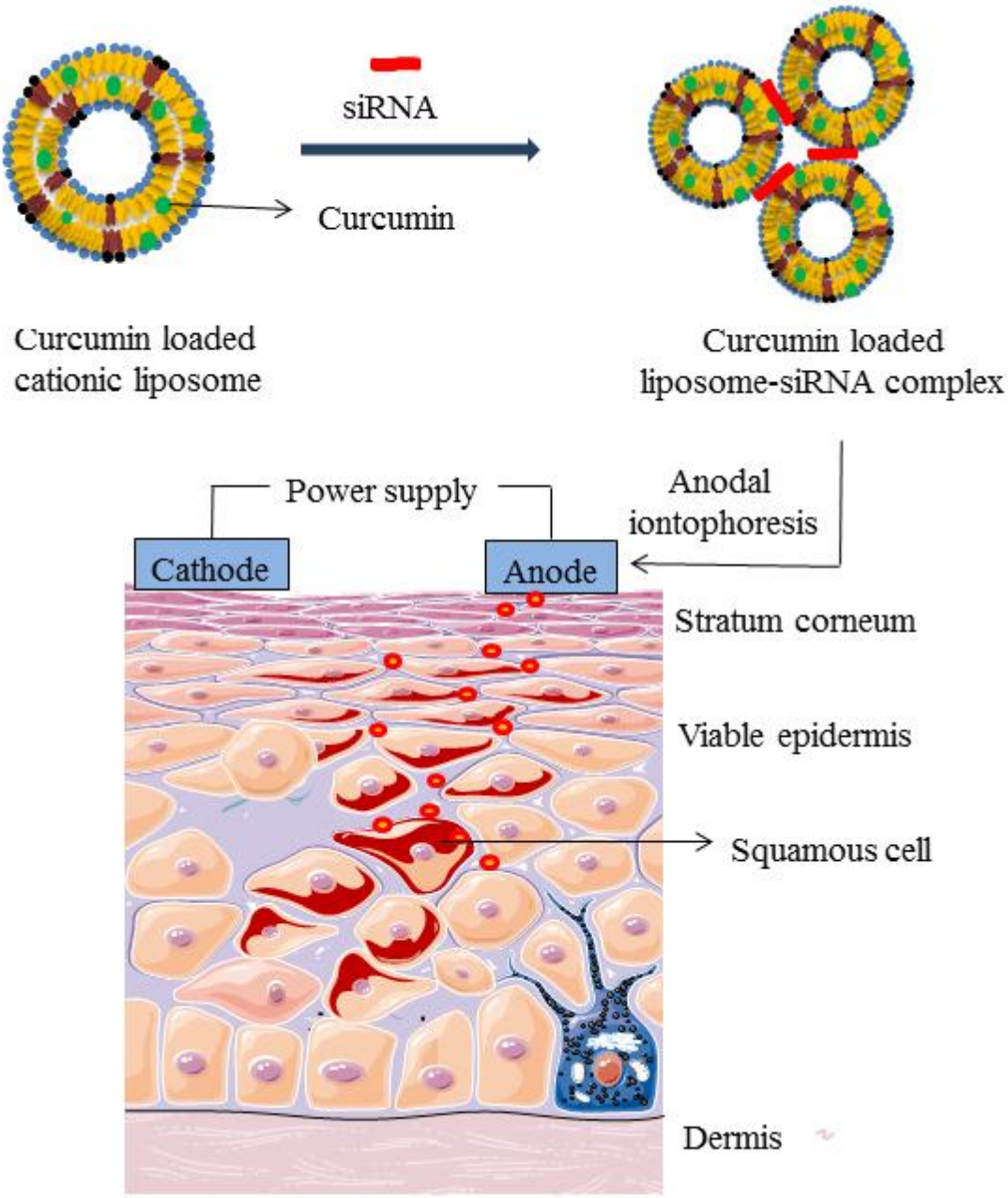
siRNA
Curcumin
Curcumin loaded
cationic liposome
Curcumin loaded
liposome-siRNA complex
Power supply
Anodal
iontophoresis
Cathode
Anode
Stratum corneum
Viable epidermis
Squamous cell
Dermis

3.1. Introduction

Skin cancer is the most widely prevalent cancer type with over two million new cases diagnosed each year in the United States alone (Rogers, Weinstock et al. 2010). Skin cancer is characterized as malignant melanoma and non-melanoma skin cancer. Non-melanoma skin cancers are further divided into squamous cell carcinoma (SCC) and basal cell carcinoma (BCC). The major causative factor for skin cancer is exposure to UV-radiation apart from genetic factors (Diepgen and Mahler 2002). Skin cancer is managed initially through surgical resection followed by chemotherapy. The widely used chemotherapeutic agents include 5-fluorouracil, imiquimod, bleomycin and interferon alpha among others (Kirby and Miller 2010). More recently natural compounds such as curcumin have been shown to improve the tumor regression (Phillips, Clark et al. 2011, Mangalathillam, Rejinold et al. 2012).

Furthermore, gene silencing strategies including RNA interference to suppress the expression of oncogenic proteins has been widely studied with reasonable preclinical success (Wittrup and Lieberman 2015). This successful preclinical studies using small interference RNA (siRNA) lead to multiple ongoing clinical trials (Zuckerman and Davis 2015). Signal transducer and activator of transcription 3 (STAT3) is a transcription factor found to be activated in multiple cancer types including skin cancer (Pedranzini, Leitch et al. 2004, Yu, Pardoll et al. 2009). STAT3 is involved in progression of cell growth, metastasis and inhibition of apoptosis (Thomas, Snowden et al. 2015). It has been found to activate vascular epidermal growth factor, survivin, cyclin D and Bcl-XL family signaling molecules (Niu, Wright et al. 2002). To that end, STAT3 represents a potential target for skin cancer treatment that can be suppressed using siRNA.

However, the clinical development of siRNA therapeutics is limited by its in vivo stability, ability to cross the membrane barriers and localize in intracellular compartments. To overcome these barriers, siRNA has been complexed with various carrier molecules to form nanoparticles (Wang, Lu et al. 2010). In general, cationic polymers or cationic liposomal vesicles have been utilized to complex negatively charged siRNA (Wang, Lu et al. 2010). While the polymer-based carrier systems such as polyethylene imine and poly(amidoamine) dendrimer showed efficient gene silencing, they are cytotoxic and non-biodegradable (Choi, Kang et al. 2010). Meanwhile, cationic liposomal carriers are less cytotoxic and are efficient carriers of siRNA (Kim, Davaa et al. 2010). The commonly used cationic lipids to prepare positively charged liposomes include 1,2-dioleoyil-3-trimethylammonium propane (DOTAP) and 1,2-di-O-octadecenyl-3-trimethylammonium propane (DOTMA) (Schroeder, Levins et al. 2010).

Most of the nanocarrier formulations for chemotherapy are developed as injectable formulations (Brigger, Dubernet et al. 2002). The chemotherapeutic agent is distributed to the whole body resulting in unwanted adverse drug reactions. To overcome the adverse effects of chemotherapeutic agents and localize the drug deposition, topical application of chemotherapeutics is advantageous (Desai, Marepally et al. 2013, Venuganti, Saraswathy et al. 2015). Transport of chemotherapeutics through topical non-invasive route is attractive to treat skin cancer. However, skin forms a formidable membrane barrier for transport of therapeutics attributed to its outer most layer, stratum corneum (SC) (Prausnitz and Langer 2008). Multiple chemical and physical enhancement methods have been developed to improve the skin permeation of drugs (Prausnitz and Langer 2008).

More recently, nanoparticle systems have been shown to be potential carriers for drug transport inside skin (Neubert 2011). Among the different types of nanocarriers, liposomes have been

widely studied for their topical and transcutaneous delivery of variety of drugs including small molecules and nucleic acids (Neubert 2011, Prow, Grice et al. 2011). However, liposomes have only been shown to penetrate the superficial skin layers after passive application. Meanwhile, deformable liposomes containing edge activators such as sodium cholate have been shown to penetrate intact skin under occluding conditions.

Similarly, cationic liposomes can also be transported into skin using physical penetration enhancement technique such as iontophoresis. Iontophoresis enhances the skin penetration of charged particles through a combination of electro-repulsion and electro-osmosis (Wu, Todo et al. 2007). Here, we have used deformable liposomes to complex curcumin loaded STAT3 siRNA and applied anodal iontophoresis to enhance the skin penetration of positively charged lipoplexes (liposome-siRNA complexes).

It is hypothesized that iontophoresis and deformability would enhance the skin penetration of positively charged liposome-siRNA complex, and cationic nano complex would itself be rapidly taken up by the keratinocytes. To that end, the objective was to investigate the co-delivery of curcumin and STAT3 siRNA using cationic liposomes to treat skin cancer.

3.2. Materials and methods

3.2.1. Materials

1, 2-Dioleoyl-3-trimethylammonium propane (DOTAP), 1, 2-dioleoyl-*sn*-glycero-3-phospho-ethanolamine (DOPE) and C6 ceramide were purchased from Avanti Polar lipids, USA. STAT3 siRNA (sense sequence: 5′-AAAUGAAGGUGGUGGAGAAUU-3′; antisense sequence: 5′ UUCUCCACCACCUUCAUUUUU-3′) was purchased from Dharmacon Inc.,

USA. Scrambled siRNA, STAT3 monoclonal antibody, β-actin primary antibody and horseradish peroxidase-conjugated secondary antibody were obtained from Santa Cruz Biotechnology Inc., USA. *Silencer*® Cy™3 labeled siRNA was purchased from Life Technologies Inc., USA. Sodium cholate, curcumin, sodium dodecyl sulfate (SDS), Tris base, agarose, paraformaldehyde, Triton X-100, DAPI and nitrocellulose membrane were purchased from Sigma Aldrich Chemical Company (Bangalore, India). Dulbecco's modified Eagle's medium, fetal bovine serum, Dulbecco's phosphate buffered saline, trypsin EDTA solution, HEPES buffer, chlorpromazine, β-methyl cyclodextrin and thiazolyl blue tetrazolium bromide (MTT) were purchased from Himedia laboratories (Mumbai, India). All the chemicals were used without further purification. Milli-Q water (Millipore, USA) with 18 MΩ cm^{-1} resistivity was used for all the experiments.

3.2.2. Preparation of the curcumin loaded cationic liposome-siRNA complex

Cationic liposomes were prepared using thin film hydration method. Cationic liposomes were prepared using DOTAP, DOPE, sodium cholate and C6 ceramide at 50: 30: 10: 10 w/w proportions, respectively. DOTAP, DOPE and C6 ceramide were dissolved in chloroform at 5 mg/ml and mixed with sodium cholate (5 mg/ml in ethanol). Then, the organic solvent was removed using rotary evaporator at 45±2^{o}C and 80 rpm under reduced pressure. The dried lipid film was then hydrated using 20 mM HEPES buffer (pH 7.4) to obtain a final lipid concentration of 10 mg/ml. Later, the liposome suspension was sonicated for 3 min using bath sonicator and extruded through 100 nm pore size polycarbonate membrane for 15-times (Miniextruder, Avanti Polar Lipids Inc., USA).

The elasticity value of cationic liposomes (DOTAP: DOPE: C6 ceramide - 50: 40: 10 w/w) was compared with that of deformable cationic liposomes (DOTAP: DOPE: NaChol: C6 ceramide - 50: 30: 10: 10 w/w). Elasticity value of liposomes was calculated using Equation (1) (Hiruta, Hattori et al. 2006).

$$\text{Elasticity value} = Jflux \times \left(\frac{rv}{rp}\right)^2 \quad (1)$$

Where J_{flux} is the rate of penetration through a membrane (mg sec^{-1} cm^{-2}), r_v is the mean diameter of liposomes after extrusion (nm) and r_p is the membrane pore size (nm). In order to measure J_{flux}, extruded the liposomes through a polycarbonate membrane (Nuclepore, Whatman Inc., USA) with a pore size of 100 nm (r_p), at a pressure of 0.5 MPa for 5 min. Later, the extrudate was weighed and the mean diameter of vesicles after extrusion (r_v) was determined using zetasizer, (Nano ZS, Malvern Instruments, UK) at 25°C.

The curcumin encapsulation efficiency was studied at different lipid to curcumin ratios (5: 1, 10: 1 and 15: 1 w/w). Curcumin loaded liposomes were prepared similar to the thin film hydration method described above. Curcumin was dissolved in chloroform: methanol in 2: 1 ratio in combination with the lipids.

The encapsulation efficiency of curcumin within the cationic liposomes was determined after separating the un-entrapped free curcumin from the liposome suspension. The liposome suspension was centrifuged using Amicon 10 kDa filters at 6000 rpm for 12 min. In order to determine total curcumin concentration (free as well as entrapped in liposomes), the liposomes were lysed using 6% v/v Triton X-100. The concentration of curcumin was then determined using HPLC system equipped with UV-detector (Shimadzu, Japan). The HPLC analysis was performed using a Phenomenex C8 column with mobile phase consisting of acetonitrile: 0.1%

formic acid (80: 20% v/v). 10 µl sample was injected at a flow rate of 0.5 ml/min and curcumin was detected at 420 nm wavelength. The encapsulation efficiency was determined using Equation (2).

$$Encapsulation\ efficiency\ (\%) = \left(1 - \frac{Concentration\ of\ free\ curcumin}{Concentration\ of\ total\ curcumin}\right) x100 \quad (2)$$

Among the three different lipid: curcumin ratios evaluated, the 10: 1 w/w lipid to curcumin ratio showed greatest encapsulation efficiency and desirable particle size (Table 3.1). Therefore, the liposomes prepared at 10: 1 ratio of lipid: curcumin were further used to complex with siRNA.

Cationic liposomes were complexed with siRNA at N/P (DOTAP: siRNA) ratio of 10: 1. Lipoplexes were prepared by mixing the free or curcumin loaded liposomes with siRNA diluted in 20 mM HEPES buffer (pH 7.4). The mixture was vortexed for 30 sec and incubated for 20 min at room temperature.

The encapsulation of curcumin within liposomes does not affect the siRNA loading efficiency as the curcumin is entrapped within lipid bilayers of liposomal vesicles and the siRNA molecules get attached to the surface of cationic liposome with the help of electrostatic interaction.

3.2.3. Characterization of the cationic liposome-siRNA complex

The free and siRNA complexed liposomes were characterized for average particle size, PDI and zeta-potential by dynamic light scattering. Before measurement, the cationic liposomes and liposome-siRNA complex were diluted with 20 mM HEPES buffer (pH 7.4). To determine zeta-potential, 0.75 ml of the sample was injected into clear folded capillary cell (DTS 1060) and measurement was carried out using Smoluchowski model in automatic mode.

Polyacrylamide gel electrophoresis was performed to study the cationic liposome-siRNA complex formation at 10: 1 (N/P) ratio. Liposome-siRNA complex (10 µl) was mixed with 2 µl of 6X loading buffer containing 10 mM Tris HCl (pH 7.6), 0.03% bromophenol blue, 0.03% xylene cyanol FF, 60% glycerol and 60 mM EDTA. This mixture was then loaded onto 10% polyacrylamide gel. Electrophoresis was performed using a vertical gel electrophoresis unit (Hoefer, Inc., USA) at 50 V for 2 h. Later, visualized the bands using Gel Doc XR^{++} Imaging system (BIORAD, USA) after staining with ethidium bromide (10 µg/ml) for 10 min.

3.2.4. *In vitro* release of curcumin from cationic liposomes

In vitro release of curcumin from cationic liposomes was determined using Franz diffusion cell apparatus as described in our earlier report (Jose, Mandapalli et al. 2016). Briefly, a synthetic cellulose acetate membrane was sandwiched between the donor and receptor compartments of the Franz diffusion cell. PBS containing 20% ethanol maintained at 37±0.5°C using heated water circulator was used as the receptor medium. Ethanol was added to enhance the solubility of curcumin in the receptor medium. The curcumin release from cationic liposomes was compared with diffusion of free curcumin across the membrane. Curcumin loaded liposomes (200 µl) containing 200 µg of curcumin were spiked in the donor compartment. Samples (300 µl) were withdrawn from receptor compartment at predetermined time points (0.25, 0.5, 1, 2, 3, 4, 6, 8, 12, 24, 48 and 72 h). The collected samples were analyzed using HPLC method described above. The amount of curcumin released was determined using a standard calibration curve with a concentration range of 1 to 20 µg/ml and a correlation coefficient of 0.998.

The release profile of curcumin loaded liposomes was fitted to five different drug release models: zero order, first order, Higuchi, Korsmeyer-Peppas and Hixon-Crowell. Out of these, the

model that exhibited the adjusted R -square closest to unity was selected as the best fit model. The details of the models considered are as follows.

(1) Zero order model :

$$Q_t = Q_0 + K_0 t, \quad (3)$$

where Q_t is the amount of drug dissolved in time t, Q_0 is the initial amount of drug in solution, and K_0 is zero order release constant.

(2) First-order model :

$$\text{Log } C_t = \log C_0 - K_t/2.303, \quad (4)$$

where C_0 is the initial drug concentration, C_t is the concentration of drug at time t, and K_t is first-order rate constant.

(3) Higuchi model :

$$Q = K_H t^{1/2}, \quad (5)$$

where Q is the amount of drug released in time t/unit area, K_H is Higuchi dissolution constant, and t is time.

(4) Hixson-Crowell model :

$$W_0^{1/3} - W_t^{1/3} = kt, \quad (6)$$

where W_0 is the initial amount of drug in the dosage form, W_t is the remaining amount of drug at time t , and k is constant incorporating surface-volume relation.

(5) Korsmeyer-Peppas model :

$$M_t/M_\infty = Kt^n, \quad (7)$$

where M_t/M_∞ is the fraction of drug released at time t , K is release rate constant and n is release exponent.

3.2.5. Stability of the cationic liposome-siRNA complex

The stability of liposomal formulations including liposome-siRNA complex, curcumin loaded liposome and curcumin loaded liposome-siRNA complex was evaluated for up to three months. The formulations were stored in an amber colored glass vial closed with screw caps at 2-8°C for three months. Samples were withdrawn at 7, 14, 30, 60 and 90 days, and were analyzed for particle size, zeta-potential and curcumin encapsulation efficiency.

3.2.6. Cell uptake studies

Cell culture studies were performed in human epidermoid carcinoma cells (A431) obtained from National Centre for Cell Science (Pune, India). The cells were cultured in DMEM supplemented with 10% FBS and 1% antibiotic solution (penicillin and streptomycin). The cultured cells were incubated at 37°C, 95% humidity and 5% CO_2.

To study the cell uptake of the lipoplexes, curcumin loaded cationic liposomes were complexed with Cy3 labeled siRNA. A431 cells were seeded in a 12 well plate (1×10^5 cells/well). After 24 h, the cells were treated with curcumin loaded liposomes and curcumin loaded liposome-Cy3 siRNA complex at different time periods including 30, 60 and 120 min. Then, washed the cells with ice cold PBS and fixed using 4% paraformaldehyde. Later, the cells were permeabilized

using 0.1% Triton X-100 and incubated with 4, 6-diamidino-2-phenylindole (DAPI, 1 µg/mL) for 5 min. The cells were observed under fluorescence microscope (Olympus IX53, Olympus Corporation, Japan) and images were acquired after excitation of DAPI, curcumin and Cy3-siRNA using 358, 488 and 550 nm laser, respectively under 20X objective lens. Image analysis was performed using Image J software (version 1.47 V, National Institutes of Health, USA).

The mechanism of cell uptake of curcumin loaded liposomes and curcumin loaded liposome-Cy3 siRNA complex was evaluated using endocytosis uptake inhibitors. Chlorpromazine hydrochloride and methyl-β-cyclodextrin were used for selective inhibition of clathrin-mediated and caveolae-mediated endocytosis, respectively. A431 cells were seeded in a 6-well plate (2 x 10^5 cells/well) and incubated for 24 h at 37ºC. Then the cells were separately treated with chlorpromazine hydrochloride (0.028 mM) and methyl-β-cyclodextrin (5 mM) for 1 h. Later, washed the cells with PBS followed by incubation with curcumin loaded liposomes and curcumin loaded liposome-Cy 3 siRNA complex for 2 h. The cells were washed with PBS and analyzed using fluorescence microscope and flow cytometer. For flow cytometer analysis, cells were treated with trypsin followed by centrifugation at 1200 rpm for 10 min. The cell pellet was resuspended in PBS and analyzed using flow cytometer (Flow Sight, Amnis, Millipore, Germany).

3.2.7. Cell viability study

For cell viability studies, A431 cells were seeded in a 96 well plate (1 x 10^4 cells/well) and incubated for 24 h. Later, the cells were treated with different formulations including free cationic liposomes, free siRNA, free curcumin (150, 250 and 350 µM per well dissolved in 1% DMSO), liposome-siRNA complex (0.25, 0.5 and 1 nM siRNA) and curcumin loaded liposome-

siRNA complex (250 µM curcumin and 0.5 nM siRNA). The formulations were diluted using DMEM and incubated with cells for 8 h at 37ºC. Later, the medium containing formulations was replaced with complete medium and incubated for 48 h. Cell viability was determined using MTT assay. The absorbance of DMSO solubilized formazan crystals was measured at 572 nm wavelength using multimode plate reader (SpectraMax M4, Molecular Devices, USA).

Initial cell viability studies with different concentrations of liposome-siRNA complex (0.25 nM, 0.5 nM & 1.0 nM) showed that 0.5 nM siRNA has significantly higher inhibitory effect compared to 0.25 nM. Whereas, the inhibitory effect shown by 1.0 nM siRNA complex was not significantly different from .05 nM. So we have decided to perform further studies with 0.5 nM siRNA. As per our formulation, 33.064 µl of liposome-siRNA complex contains 0.5 nM siRNA and approximately 250 µM of curcumin entrapped within the liposomes. In order to show the effect of curcumin at levels lower as well as higher than that of the optimized formulation, we have performed cell viability studies at 150, 250 and 350 µM of curcumin.

3.2.8. Apoptosis assay

The apoptosis induction by STAT3 siRNA delivered using cationic liposomes and in combination with curcumin was evaluated using FITC-Annexin V/PI apoptosis assay (Molecular Probes Inc., USA). A431 cells were seeded in a 6-well plate (2 x 10^5 cells/well) and incubated for 24 h at 37ºC. Later, the cells were treated with different formulations containing curcumin (150 and 250 µM curcumin/well) and STAT3 siRNA (0.5 nM). After 8 h treatment, trypsinized the cells, centrifuged and the cell pellet was resuspended in 1X annexin binding buffer (5 mM HEPES, 2.5 mM $CaCl_2$, 140 mM NaCl, pH 7.4). Then, FITC-annexin V (5 µl) and propidium iodide (1 µl of 100 µg/ml) were added to 100 µl of cell suspension and incubated for 15 min. The

cells were analyzed using flow cytometer, where the fluorescence emission of FITC and PI was recorded at 530 nm and 575 nm wavelength, respectively. The total cell population (%) was divided into four groups: live cells (Annexin V-/ PI-), early apoptotic cells (Annexin V+/ PI-), late apoptotic cells (Annexin V+/ PI+) and dead cells (Annexin V-/ PI+).

3.2.9. STAT3 protein suppression

Western blotting was performed to evaluate the *in vitro* gene silencing effect of STAT3 siRNA before and after combination with curcumin loaded cationic liposomes. After treatment of A431 cells with different formulations for 8 h, the cells were harvested using trypsin and total protein was extracted using lysis buffer (50 mM Tris-HCl, 150 mM NaCl, 0.1% Triton X-100, 1 mM sodium orthovenadate, 0.5% sodium deoxycholate, 1 mM sodium fluoride, 1 µg/ml pepstatin and 1 µg/ml leupeptin). The total protein content was estimated by Bradford's assay. Sodium dodecyl sulfate-polyacrylamide gel electrophoresis (SDS-PAGE) was performed to separate the proteins. Sample (10 µl containing 40 µg protein) was mixed with loading buffer and spiked in sample well. Electrophoresis was ran at 50 V for 2 h. Later, the protein bands were electrophoretically transferred to nitrocellulose membrane using transfer unit at 100 V for 1 h. The nitrocellulose membrane was incubated with STAT3 and β-actin primary antibody followed by HRP-conjugated secondary antibody. Later, the membrane was incubated with enhanced chemiluminescent substrate solution (ECL reagent, Super signal Pro, Thermo scientific, USA) and bands were visualized by autoradiography technique (Mandapalli, Labala et al. 2016).

3.2.10. Skin permeation studies

Skin permeation of curcumin loaded cationic liposomes was studied using excised porcine ear skin. The porcine ears were obtained and processed for experimentation as described in our earlier report (Jose, Mandapalli et al. 2016).

The skin permeation of free curcumin and curcumin loaded cationic liposomes was performed by mounting the skin between the receptor and donor compartments of a diffusion cell with stratum corneum facing the donor compartment. PBS containing 20% ethanol and maintained at 37±0.5^{o}C was used as the receptor medium. Free curcumin (200 µl of 1 mg/ml curcumin in ethanol) or curcumin loaded cationic liposome formulation (200 µg curcumin) was spiked in the donor compartment. Samples (300 µl) were withdrawn at predetermined time points (0.25, 0.5, 1, 2, 4, 6, 8, 12, 24, 30, 36 and 48 h) from receptor compartment and immediately replaced with fresh media. The samples were then analyzed using HPLC method described above.

Tape stripping was performed to determine the amount of curcumin retained within skin samples (Jose, Mandapalli et al. 2016). Curcumin retained within stratum corneum and viable epidermis was extracted after incubation with 1 ml methanol for 12 h in a microcentrifuge tube. The extracted curcumin was then analyzed using HPLC method.

3.2.11. Iontophoresis application

Anodal iontophoresis was applied to enhance the skin penetration of curcumin loaded cationic liposomes. A current density of 0.47 mA/cm^2 was applied using a direct current power supply unit (V-care Meditech Pvt. Ltd., Bengaluru, India) for 4 h with silver and silver chloride electrodes placed in the donor and receptor compartments, respectively. A salt bridge made up of

1% of agarose containing 2 mM NaCl was used to avoid direct contact of silver wire with cationic liposomes.

3.2.12. Skin permeation of siRNA

The skin penetration of curcumin loaded liposome-siRNA complex was evaluated using porcine ear skin after passive and anodal iontophoretic application. In order to visually observe the depth of permeation of siRNA, Cy3 labeled siRNA was complexed with curcumin loaded cationic liposomes.

Skin samples were treated with curcumin loaded liposome-siRNA complex in the presence and absence of iontophoresis for 4 h. Later, the skin samples were washed and embedded in optimal cutting temperature (OCT) compound. Thin skin sections (10 μm thickness) were prepared using cryotome (Leica CM 1520, Leica biosciences, *Germany*). The skin cryosections were then visualized using fluorescence microscope. Fluorescence images were acquired after excitation of curcumin using 488 nm and Cy3-siRNA using 550 nm laser under 10X objective lens.

3.2.13. Statistical Analysis

All the results were presented as mean (n=3-4) ± standard deviation. Statistical analysis was performed using analysis of variance (ANOVA) (GraphPad Prism V6), where $p<0.05$ was considered to be minimum level of significance.

3.3. Results

3.3.1. Characterization of the cationic liposome-siRNA complex

The average particle size of cationic liposomes immediately after preparation was found to be 255.9±12.4 nm (PDI: 0.482±0.002). After extrusion through polycarbonate membrane (100 nm pore size) 15-times, the particle size of vesicles reduced to 104.1±7.2 nm (PDI: 0.162±0.004) with a zeta-potential of 53.8±4.0 mV. After complexation of cationic liposomes with negatively charged siRNA molecules, the particle size and zeta-potential of the vesicles increased to 157.0±11.0 nm (PDI: 0.464±0.003) and 70.5±7.0 mV, respectively (Figure 3.1a). The elasticity value of sodium cholate containing liposomes (20.2±1.5 mg sec^{-1} cm^{-2}) was found to be 4-fold greater than that of cationic liposomes without sodium cholate (4.6±0.5 mg sec^{-1} cm^{-2}).

Table 3.1. Particle size, zeta-potential and encapsulation efficiency of curcumin loaded cationic liposomes.

Formulation code	Lipid: curcumin (w/w)	Particle size (nm)	PDI	Zeta-potential (mV)	Encapsulation efficiency (EE %)
F1	5:1	152.4±5.0	0.244±0.002	57.9±6.0	34.1±3.0
F2	10:1	146.7±7.0	0.224±0.004	45.1±4.0	87.5±4.0
F3	15:1	152.2±6.0	0.222±0.002	53.7±4.0	88.9±5.0

Data are presented as mean (n=3) ± standard deviation. PDI – polydispersity index.

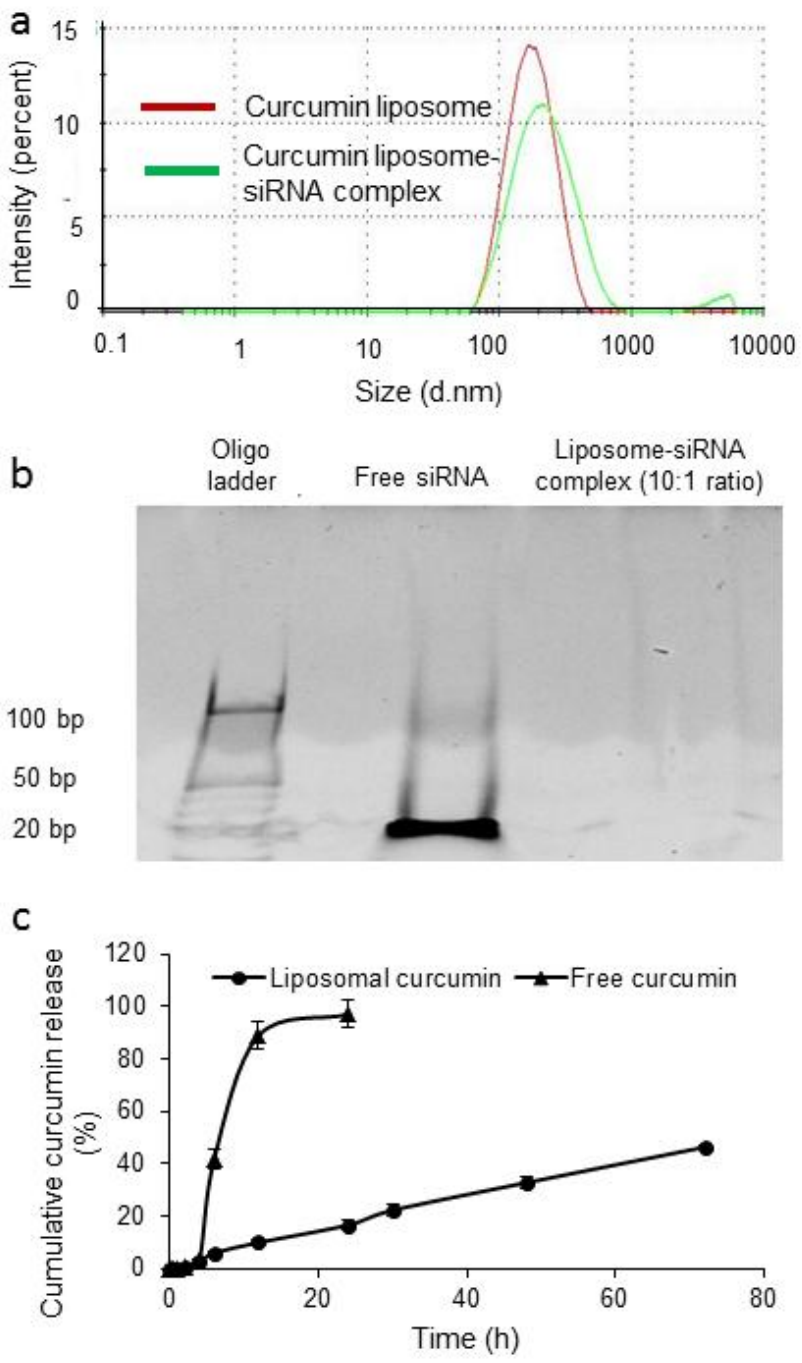

Fig.3.1. a. Particle size distribution of curcumin loaded liposomes and curcumin loaded liposome-siRNA complex. **b.** Polyacrylamide gel electrophoresis of liposome-siRNA complex. **c.** *In vitro* release of curcumin from liposomes.

Curcumin loaded cationic liposomes were prepared at three different lipid to curcumin ratios to optimize the maximum encapsulation efficiency (EE %). Table 3.1 shows the particle size, zeta-potential and EE% of liposomes loaded with curcumin at different lipid to curcumin ratios. At 5: 1 lipid to curcumin ratio, the EE% was found to be 34.1±3.0. The EE% increased to 87.5±4.0 with increase in lipid to curcumin ratio of 10: 1. Further increase in lipid amount to 15: 1 did not show significant enhancement in EE%.

Figure 3.1b shows the polyacrylamide gel electrophoresis of liposome-siRNA complex. There was no corresponding band observed for liposome-siRNA complex compared with free siRNA. This represents complete complexation of liposome-siRNA at 10: 1 (lipid: curcumin) ratio. We have chosen DOTAP: siRNA at 10:1 N/P ratio because there were previous reports of higher loading efficiency of siRNA to cationic liposomes at N/P ratio of more than 6:1. So we have prepared the complex at 10:1 N/P ratio and as per the gel electrophoresis result, there were no free siRNA in the liposome siRNA complex indicating high loading efficiency of siRNA loaded curcumin liposomes.

Figure 3.1c shows the diffusion of free curcumin and release of curcumin from liposomes. The free curcumin diffused across the dialysis membrane within 24 h, whereas only 47% of the total loaded curcumin was released from the liposomes even after 72 h.

Drug release kinetic studies were performed to select a model that better describes the release mechanism of curcumin loaded liposomes. Five different models were tested and their adjusted R -square values are summarized in table 3.2.

Table 3.2. Kinetic models with their R-square values for the release of curcumin from cationic liposomes.

S.No.	Kinetic model	R-square value
1	Zero order	0.9935
2	First-order	0.9974
3	Higuchi model	0.9473
4	Hixson-Crowell	0.995
5	Korsmeyer-Peppas	0.9321

As per the results, zero order model, first order model or Hixson-Crowell model can be used to describe the release kinetics of the curcumin loaded liposomes used in this study.

3.3.2. Stability of the curcumin loaded liposome-siRNA complex

The stability of liposome-siRNA complex, curcumin loaded liposome and curcumin loaded liposome-siRNA complex was determined after storage at 2-8°C for up to 90 days. Table 3.3 shows the average particle size, zeta-potential and percentage of curcumin retained at different storage times.

There was no significant change in particle size and zeta-potential for both the formulations up to 30 days of storage. The percentage of curcumin retained within liposome-siRNA complex decreased from 100 to 92% after one month of storage. On the other hand, there was a significant ($p<0.05$) change in the average particle size and zeta-potential of all the formulations after 30 days of storage.

Table 3.3: Stability of different liposomal formulations stored at 2-8^{o}C for a period of 90 days. Data are presented as mean (n=3) ± standard deviation. PDI – polydispersity index.

	Day 1	**Day 7**	**Day 14**	**Day 30**	**Day 60**	**Day 90**
Liposome-siRNA complex						
Size (nm)	157.0±11.0	158.6±8.0	154.5±8.0	146.7±9.0	482.3±14.0	1071±12
PDI	0.464±0.003	0.312±0.005	0.387±0.007	0.307±0.005	0.462±0.016	0.659±0.014
Zeta-potential (mV)	70.5±7.0	55.7±5.0	45.3±5.0	37.4±7.0	11.6±8.0	-9.3±7.0
Curcumin loaded liposomes						
Size (nm)	146.7±7.0	153.8±6.0	157.3±8.0	168.1±6.0	286.8±16.0	411.5±8.0
PDI	0.224±0.004	0.248±0.005	0.245±0.003	0.249±0.006	0.342±0.016	0.512±0.008
Zeta-potential (mV)	45.1±4.0	40.2±6.0	51.8±4.0	42.7±6.0	33.4±8.0	31.5±5.0
Curcumin retained (%)	100.00	97.46±4.00	96.82±3.00	92.26±5.00	86.87±4.00	71.73±6.00
Curcumin loaded liposome-siRNA complex						
Size (nm)	195.0±9.0	198.6±7.0	192.3±6.0	197.4±7.0	341.3±11.0	987.0±21.0
PDI	0.240±0.005	0.225±0.003	0.280±0.007	0.311±0.006	0.432±0.016	0.643±0.021
Zeta-potential (mV)	58.8±6.0	53.2±7.0	41.3±5.0	33.4±6.0	17.6±4.0	4.3±0.8

3.3.3. Cell uptake studies

Cell uptake of liposome-Cy3 siRNA complex and curcumin loaded liposomal formulations by A431 cells was evaluated using fluorescence microscope. Figure 3.2 shows the images of A431 cells after incubation with free as well as curcumin loaded liposomes for 30 and 120 min.

Images show that there was no cell uptake of free curcumin even after 120 min. On the other hand, curcumin loaded liposomes were taken up by cells within 30 min and proportion of cell uptake increased for up to 120 min. Background corrected fluorescence image analysis showed significant increase in cell associated fluorescence intensity with the increase in incubation time from 30 to 120 min (Figure 3.2).

The merged images indicate that the curcumin loaded liposomes were localized in cytoplasm of A431 cells after incubation for 120 min. Similarly, the cell-associated fluorescence intensity measured by flow cytometer increased with the increase in incubation time indicating enhanced uptake of curcumin loaded liposomes.

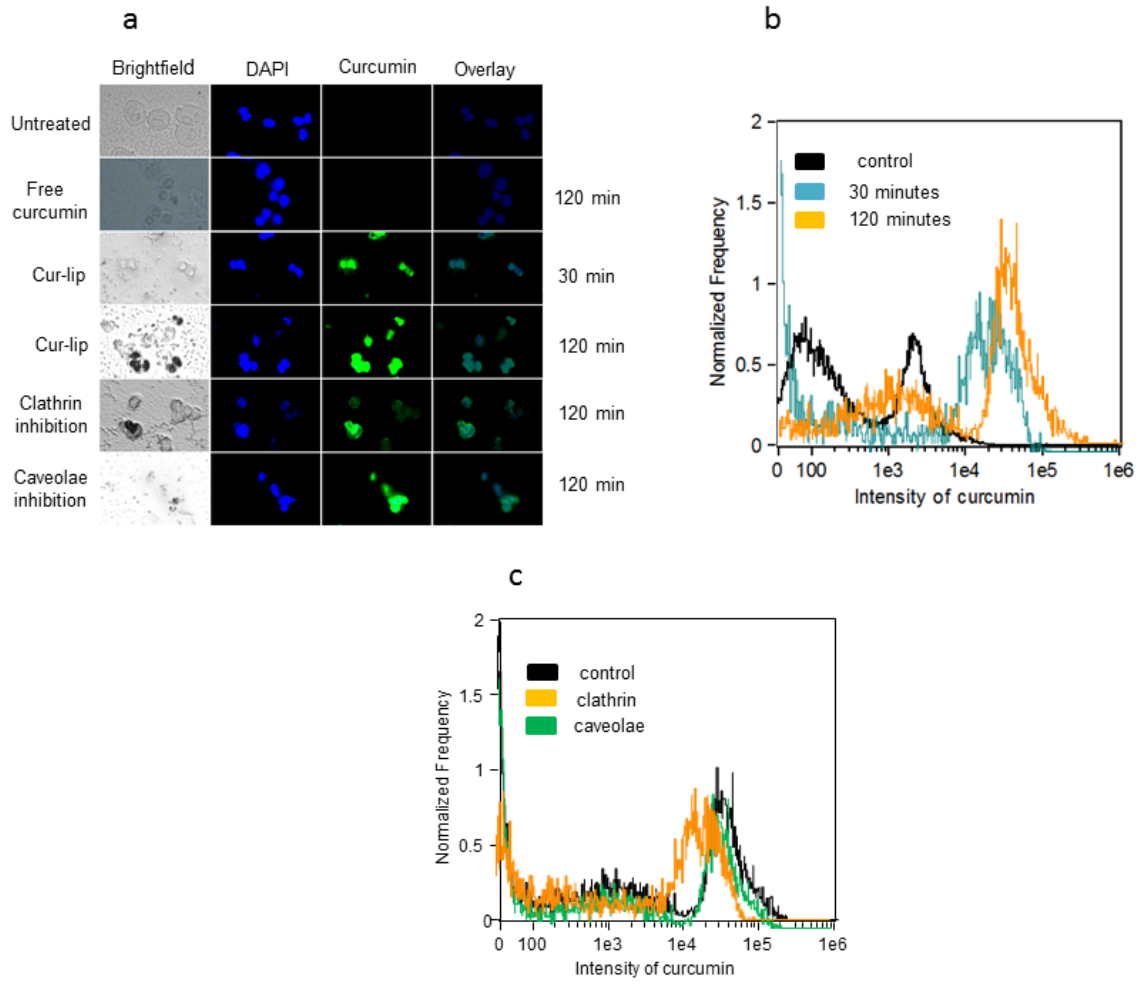

Fig.3.2. a. A431 cell uptake of curcumin loaded liposomes after 30 and 120 min incubation time. Images were representative of at least three experimental groups **b**. Flow cytometer analysis of time dependent A431 cell uptake of curcumin loaded liposomes **c**. Flow cytometer analysis of A431 cell uptake of curcumin loaded liposomes after pretreatment with endocytosis uptake inhibitors including chlorpromazine and methyl β-cyclodextrin.

Figure 3.3 shows the cell uptake of curcumin loaded liposome-Cy3 siRNA complex incubated for 30 and 120 min. There was no cell associated fluorescence after treatment with free Cy3 siRNA. Liposome-Cy3 siRNA complex showed significant cell associated fluorescence within 30 min and it significantly ($p<0.05$) increased after 120 min of incubation. Figure 3.4a shows flow cytometer results of increased uptake of cationic liposome-Cy3 siRNA complex upon increasing the incubation time from 30 to 120 minutes. Similarly, the geometrical mean fluorescence intensity of cells increased with increase in incubation time indicating enhanced cell uptake of curcumin loaded liposome-Cy3 siRNA complex (Figure 3.4b).

The mechanism of cellular uptake of liposomal formulations was elucidated using specific endocytosis inhibitors for clathrin and caveolae mediated pathways. There was a reduced uptake of curcumin loaded liposomes and curcumin loaded liposome-Cy3 siRNA complex after pre-treatment with chlorpromazine and methyl-β-cyclodextrin compared to control cells (without inhibitor pretreatment) (Figure 3.3a). Background corrected fluorescence image analysis showed significant ($p>0.05$) decrease in cell associated fluorescence after treatment with chlorpromazine to inhibit clathrin mediated endocytosis compared to control cells (Figure 3.3c). Similarly, flow cytometer results showed greater cell uptake inhibition after treatment with chlorpromazine compared with methyl-β-cyclodextrin (Figure 3.4b and 3.4d).

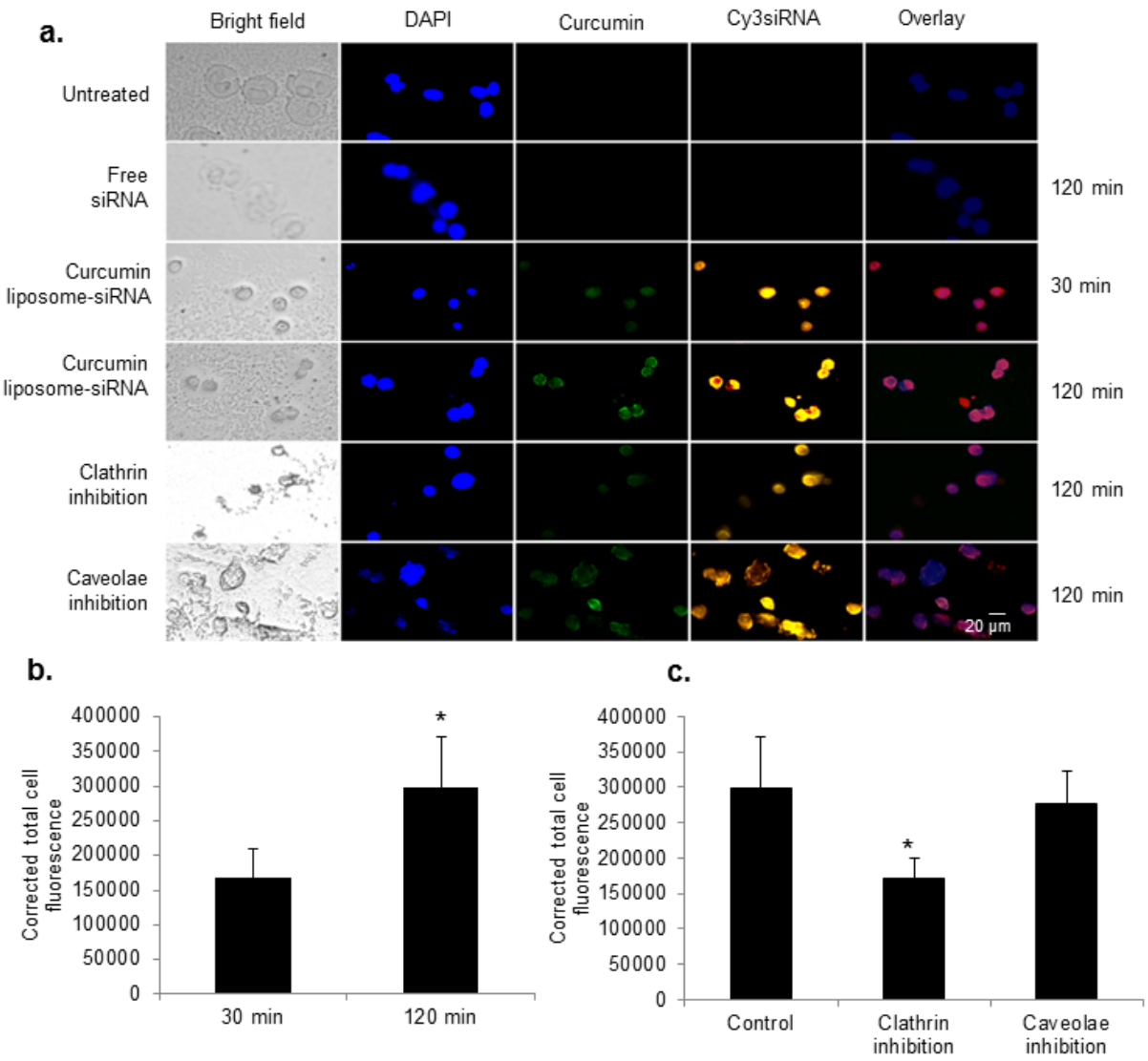

Fig.3.3. a. A431 cell uptake of curcumin loaded liposome-siRNA complex after 30 and 120 min incubation time. Images were representative of at least three experimental groups. **b.** Corrected total cell fluorescence after pretreatment with endocytosis uptake inhibitors including chlorpromazine and methyl β-cyclodextrin calculated using Image J image analysis software. **c.** Corrected total cell fluorescence after 30 and 120 min treatment. Data represents mean (n =3) ± standard deviation. Scale bar represents 20 µm. Asterisk (*) indicates that the value is significantly ($p<0.05$) different in comparison to other values.

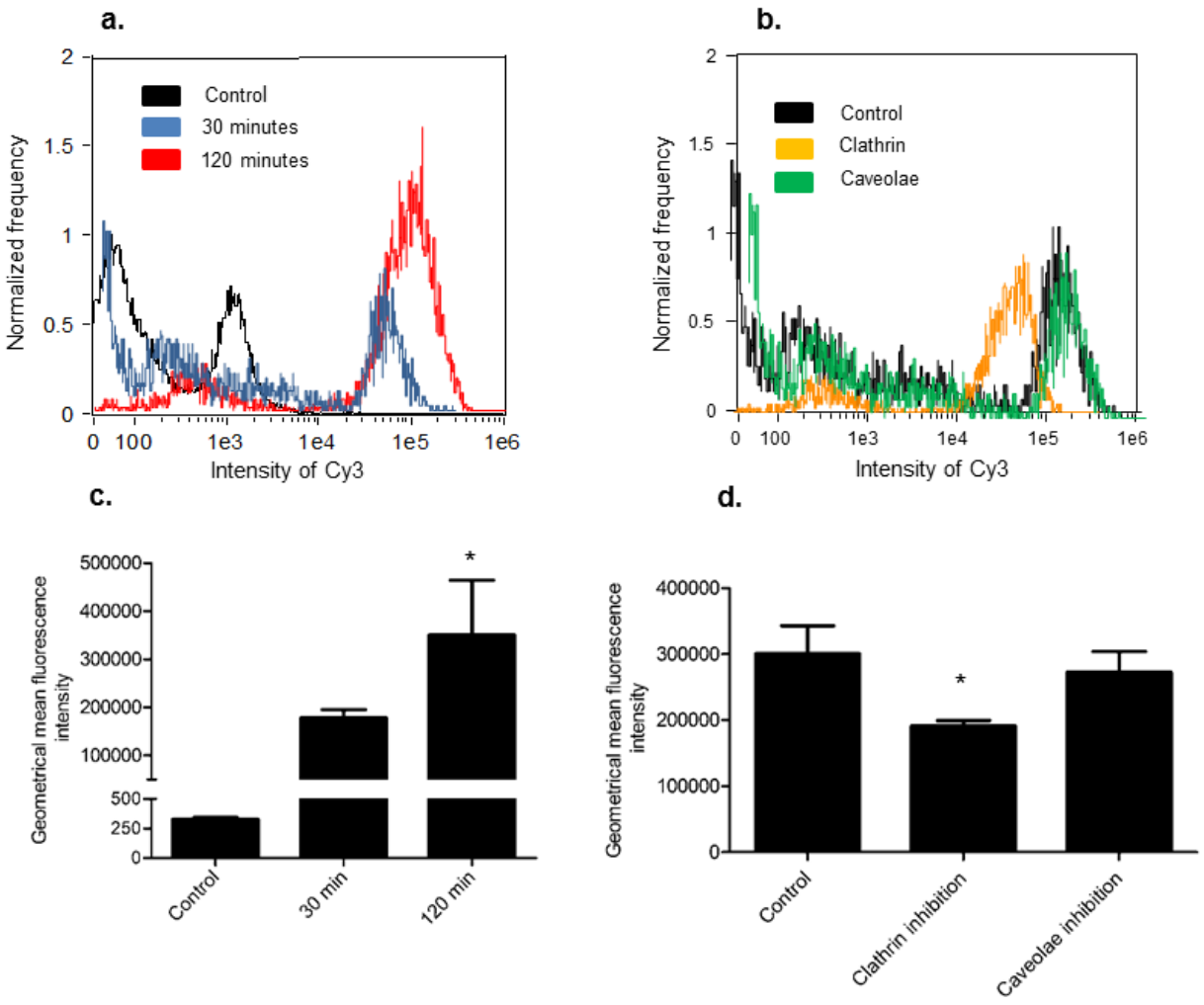

Fig.3.4. **a**. Flow cytometer analysis of time dependent A431 cell uptake of curcumin loaded liposome-siRNA complex. **b.** Flow cytometer analysis of A431 cell uptake of curcumin loaded liposome-siRNA complex after pretreatment with endocytosis uptake inhibitors including chlorpromazine and methyl β-cyclodextrin. **c** and **d.** The geometrical mean fluorescence of cells obtained using Ideas software. Data represents mean (n =3) ± standard deviation. Asterisk (*) indicates that the value is significantly ($p<0.05$) different in comparison to other values.

3.3.4. Cell viability studies

Figure 3.5 shows A431 cell growth inhibition after treatment with different formulations. The cell growth inhibition shown by free STAT3 siRNA was 5.1±1.3%. Free curcumin showed growth inhibition of 12.9±1.7%, 24.5±4.3% and 32.2±2.8% at 150 μM, 250 μM and 350 μM concentrations, respectively. Meanwhile, liposomal curcumin showed 29.9±1.5%, 44.9±3.1% and 54.8±2.4% inhibition at 150 μM, 250 μM and 350 μM concentrations, respectively. Treatment with liposome-STAT3 siRNA complex resulted in 43.3±2.9% (0.25 nM), 53.4±2.7% (0.5 nM) and 56.9±2.0% (1 nM) growth inhibition at respective siRNA concentrations. The co-delivery of curcumin and STAT3 siRNA using liposomes (250 μM curcumin and 0.5 nM siRNA) showed the greatest growth inhibition of 72.9±2.3%.

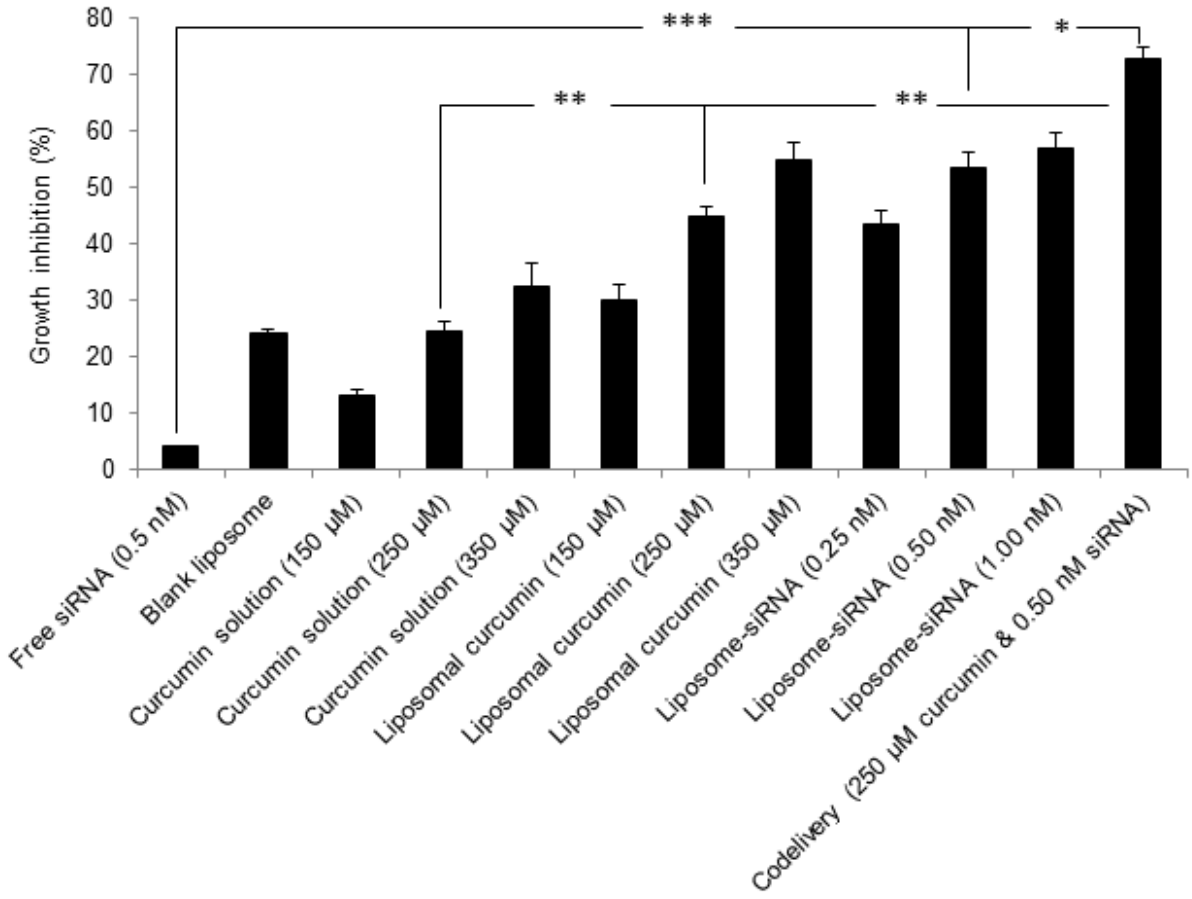

Fig.3.5. Inhibition of A431 cancer cell growth after treatment with different formulations of curcumin and STAT3 siRNA. Results are presented as mean (n=3) ± standard deviation. ***, ** and * indicates that the value is significantly different at $p < 0.001$, $p < 0.01$ and $p < 0.05$, respectively.

3.3.5. Apoptosis assay

Figure 3.6 shows the apoptosis events of cells treated with different formulations. The selected cell population (3000 cells) was divided into four quadrants as live cells, early apoptotic, late apoptotic and dead cells. It was observed that there was a significant difference in the percentage of the early and late apoptotic events after treatment with formulations containing STAT3 siRNA and curcumin compared to untreated cells. Control cells (untreated), cells treated with free STAT3 siRNA and those treated with scrambled siRNA did not show any apoptotic events. Increase in the concentration of free curcumin (150 μM and 250 μM) showed increase in the number of cells undergoing late apoptosis from 5.69±0.88% to 12.73±2.15%, respectively. On the other hand, treatment with curcumin (250 μM) loaded liposome and liposome-STAT3 siRNA complex showed 66.60±4.59% and 47.37±3.43% late apoptotic events. The late apoptotic events increased to 67.27±3.02% after treatment with co-delivery system containing both curcumin and STAT3 siRNA.

3.3.6. STAT3 protein suppression

Figure 3.7 shows the STAT3 protein expression measured by Western blot analysis. There was a concentration dependent suppression of STAT3 protein expression after treatment with cationic liposome-STAT3 siRNA complex at 0.25 nM, 0.5 nM and 1 nM siRNA. Free curcumin (150 μM and 250 μM) did not show any significant reduction in STAT3 protein expression; whereas curcumin loaded cationic liposomes (250 μM curcumin) showed suppression of STAT3 proteins. Curcumin loaded cationic liposome-STAT3 siRNA complex produced further reduction of STAT3 protein expression.

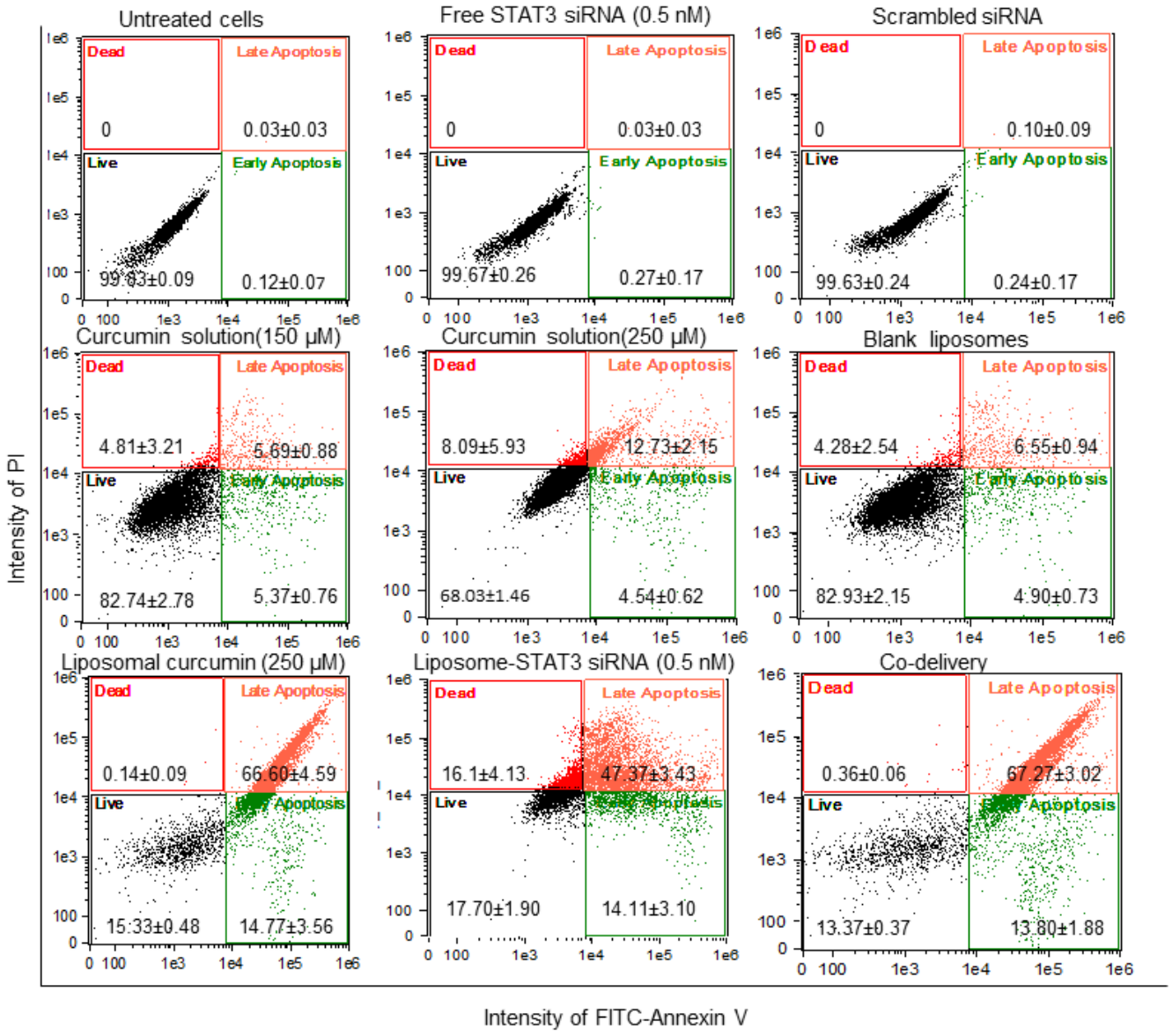

Fig.3.6. Apoptosis events observed in A431 cells after treatment with different formulations. Dot plots are representative of three independent experiments.

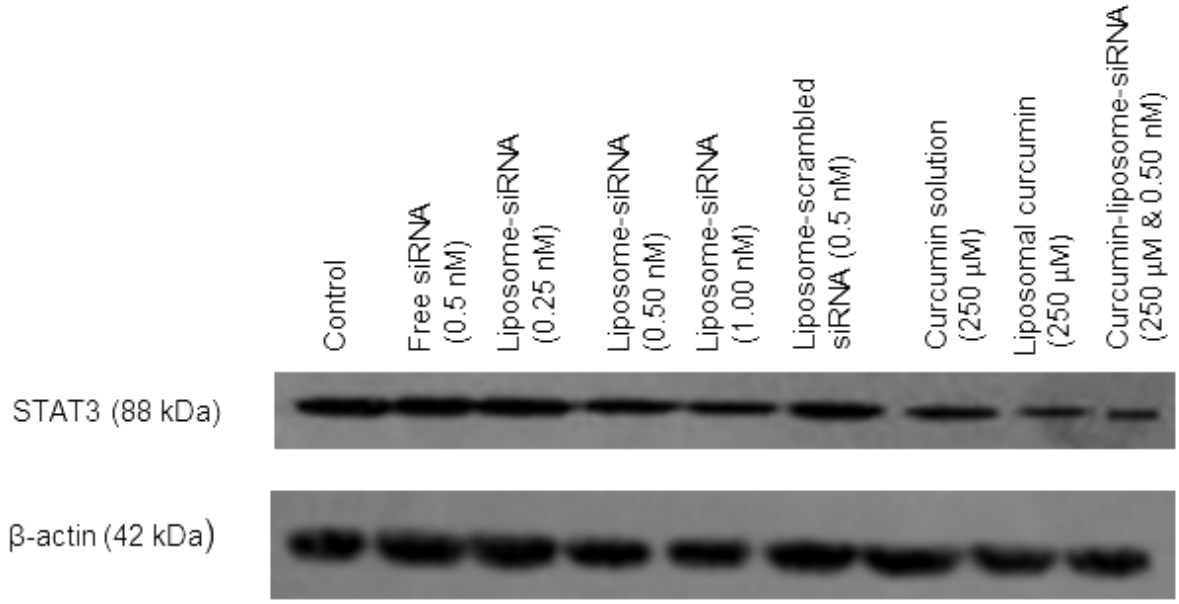

Fig.3.7. Western blot analysis of STAT3 protein expression in A431 cells after treatment with different formulations. β-actin was used as loading control.

3.3.7. Skin permeation studies

The average thickness of porcine ear skin used for *in vitro* permeation studies was found to be 0.87±0.08 mm. The integrity of skin samples before application of formulation was determined by measuring electric resistance and it was found to be 5.68±1.76 kΩ. There was no curcumin detected in the receptor medium after passive treatment of skin with free and liposomal curcumin for 48 h. Similarly, free or liposomal curcumin was not detected in the receptor medium after 4 h of iontophoresis application.

Tape stripping was performed to evaluate the amount of curcumin retained within SC and viable epidermis after treatment with free and liposomal curcumin. Complete stripping of SC was ensured by measuring skin resistance. The resistance values decreased to 3.07±0.55 kΩ after complete removal of SC. Figure 3.8 shows the amount of curcumin retained within SC and viable epidermis after treatment for 4 h. In general, curcumin was retained more within viable epidermis compared with SC.

The cumulative amount of curcumin retained in stratum corneum was comparable after 48 h treatment with free curcumin (9.06±1.20 μg) and liposomal curcumin (7.08±1.22 μg). Similarly, after 4 h passive treatment, there was no significant difference between the free and liposomal curcumin. On the other hand, iontophoresis application significantly ($p<0.05$) enhanced the SC penetration of liposomal curcumin (38.91±5.42 μg) compared with passive application.

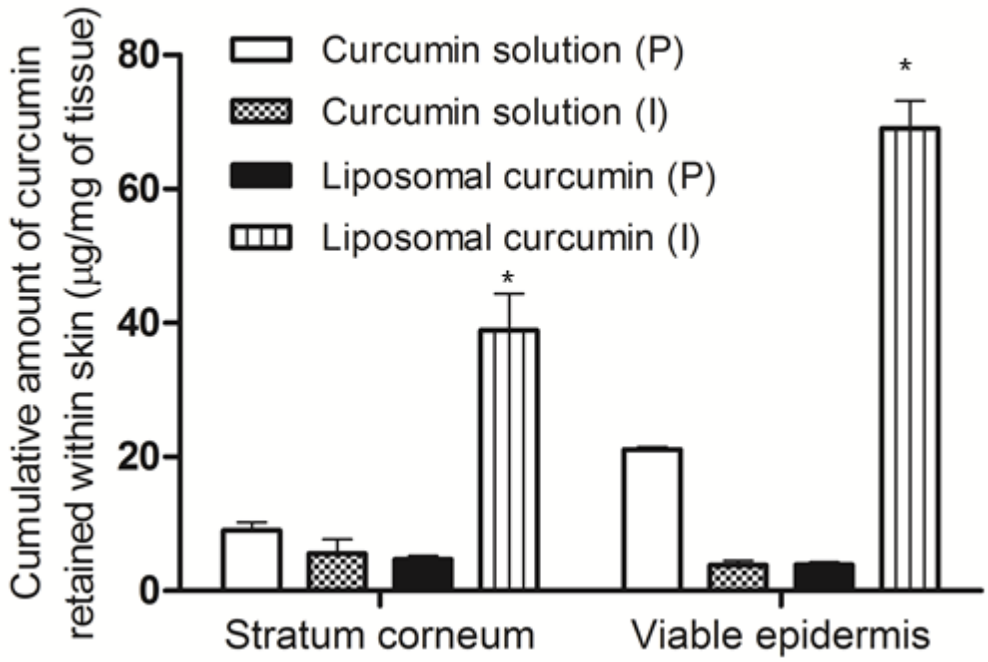

Fig.3.8. Cumulative amount of curcumin retained within stratum corneum and viable epidermis after 4 h passive (P) as well as iontophoretic (I) application of free and liposomal curcumin. Results are presented as mean (n=3) ± standard deviation. Asterisk (*) represents that the values are significantly ($p < 0.05$) different compared with all other treatment groups.

Iontophoretic application of liposomal curcumin resulted in 5-fold greater deposition of curcumin in viable skin compared with 4 h passive application of free curcumin. It was found that passive application of free curcumin showed greater viable skin deposition compared with passive application of liposomal curcumin. This could be attributed to the permeation enhancement effect of ethanol in which free curcumin was dissolved.

Figure 3.9 shows the fluorescence micrographs of skin sections after permeation studies. It was found that passive application of curcumin loaded liposome-Cy3 siRNA complex did not penetrate the viable epidermis and was retained within stratum corneum. After 4 h iontophoresis, the curcumin loaded cationic liposome-Cy3 siRNA complex was able to penetrate the SC and reach the viable epidermis. The fluorescence intensity of both curcumin and Cy3 siRNA were significantly higher in viable epidermis after treatment with iontophoresis.

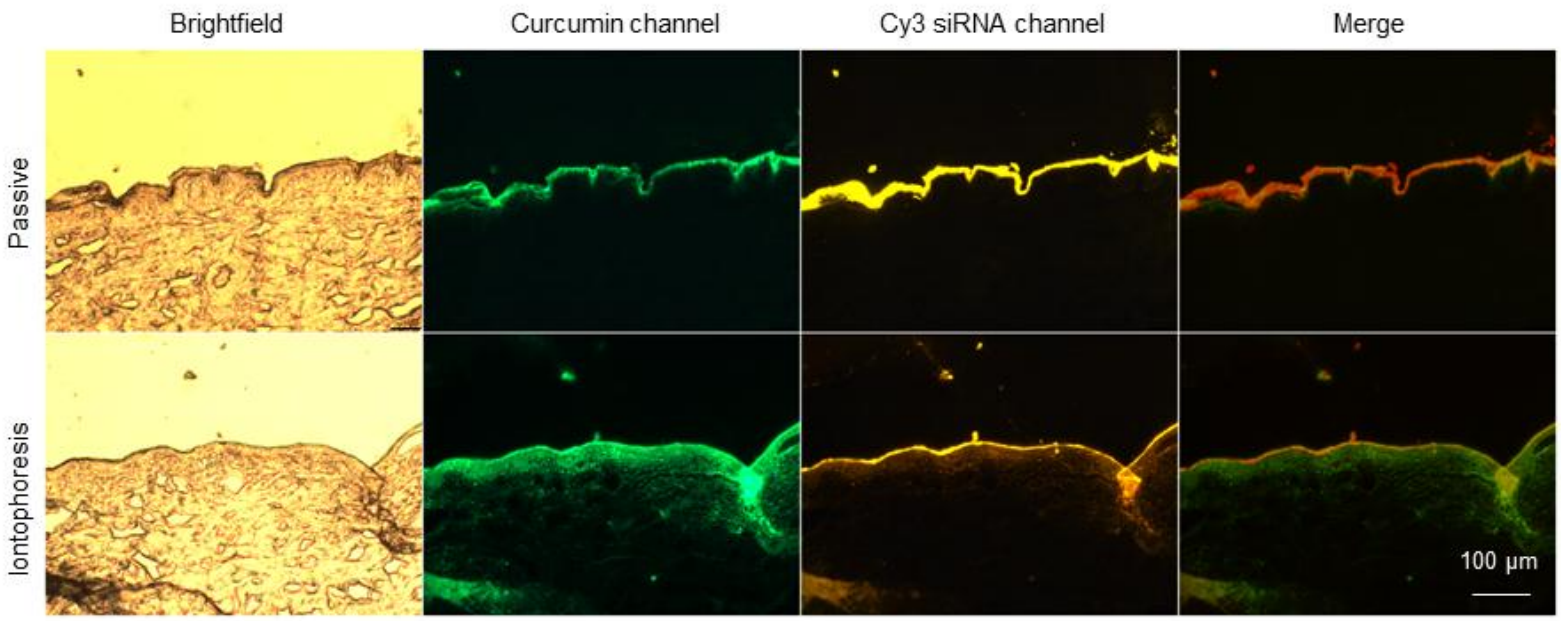

Fig.3.9. Micrographs of skin cryosections after treatment with curcumin loaded liposome-siRNA complex in the presence and absence of iontophoresis. Images were representative of at least three experiments. Scale bar represents 100 µm.

3.4. Discussion

Curcumin is a natural compound obtained from the roots of Curcuma longa. Curcumin has been widely reported to show anti-inflammatory, anti-oxidant and anti-cancer properties (Wilken, Veena et al. 2011). It has been studied in a wide variety of tumor types both in vitro cell studies and in vivo cancer models (Aggarwal, Kumar et al. 2003). Furthermore, curcumin has been shown to possess both chemo preventive action and chemotherapeutic activity in skin cancer models (Aggarwal, Kumar et al. 2003, Shehzad, Wahid et al. 2010). The anti-cancer activity of curcumin is attributed to its effect on PPARγ, STAT3, MAPK, p53, NFκB pathways leading to apoptosis of cancer cells (Aggarwal, Kumar et al. 2003, Epstein, Sanderson et al. 2010). On the other hand, curcumin possesses poor physico-chemical properties limiting its further development as therapeutic formulation. Curcumin is poorly water soluble and shows less bioavailability after oral administration (Hu, Shi et al. 2015). Moreover, curcumin shows little permeability across the skin barrier (Chen, Wu et al. 2012).

Different strategies to enhance curcumin solubility includes cyclodextrin complexation, encapsulation in micelles, liposomes, and polymeric nanoparticles among others (Yallapu, Jaggi et al. 2012, Salem, Rohani et al. 2014). Of these, liposomal system is a good vehicle for curcumin encapsulation and transport through skin (Zhao, Lu et al. 2013). This is because of improved stability of liposomes compared to micelles, while retaining flexibility to penetrate the skin pores (Ogunsola, Kraeling et al. 2012). The deformable liposomes containing widely reported sodium cholate as edge activator provided sufficient flexibility to penetrate the stratum corneum.

Furthermore, the lipophilic nature of curcumin allowed greater encapsulation within the liposomal phospholipid bilayer (Yallapu, Jaggi et al. 2012, Zhao, Lu et al. 2013). The anti-cancer activity of curcumin requires its cytoplasmic translocation. It was found that the cell uptake of liposomal curcumin is more efficient than that of curcumin in solution form (Kunwar, Barik et al. 2006). This has resulted in greater cancer cell growth inhibition and increased apoptosis after encapsulation of curcumin in liposomes.

STAT3 is a signal transduction agent over-expressed in multiple cancer types including skin cancer (Pedranzini, Leitch et al. 2004). It has been shown that over-expression of STAT3 results in deregulation of Bcl-XL, cyclin D and c-Myc pathways leading to enhanced cell growth and multiplication (Yu, Pardoll et al. 2009). Suppression of STAT3 expression has been reported to inhibit the cancer cell growth by increased expression of caspase 3 and interleukin 6 and decreasing the vascular endothelial growth factor (Alshamsan, Hamdy et al. 2010). However, to the best of our knowledge, no specific small molecule inhibitors of STAT3 protein were reported. To that end, RNA interference strategy was chosen to inhibit STAT3 protein expression. siRNA is a gene silencing agent which can bind to target mRNA in a sequence specific manner and inhibit the protein translation.

The efficient delivery of gene silencing agents requires the nucleic acids to be delivered inside the cell to bind to target mRNA. Moreover, the high molecular weight and negative charge of siRNA limits its transport across negatively charged skin (Hsu and Mitragotri 2011). Furthermore, free siRNA is rapidly degraded and shows poor cell uptake. Complexation of siRNA into nano sized particle using cationic liposomes allowed it to be rapidly taken up by the cancer cells. While the lipoplexes uptake was not completely reduced after inhibiting clathrin or caveolae mediated endocytosis, clathrin mediated endocytosis could be predominant cell uptake

pathway for lipoplexes (Rejman, Bragonzi et al. 2005). DOTAP based cationic lipid vesicles have been shown to efficiently translocate from endo-lysosomal system to cytosol (Rehman, Hoekstra et al. 2013). Lipoplexes are shown to gradually translocate through the transient pores of endosomes and cause destabilization of endosomes through lipid mixing (Rehman, Hoekstra et al. 2013).

The STAT3 siRNA upon binding to the target STAT3 mRNA prevents the translation of STAT3 transcription factor. We have shown a concentration dependent decrease in the STAT3 protein expression and increase in the percentage of apoptotic cells after treatment with liposome-siRNA nanocomplex.

A431 cancer cell growth inhibition was found to be 44.9±3.1% and 53.4±2.7% after treatment with liposomal curcumin and liposome-STAT3 siRNA complex, respectively. We hypothesized that the co-delivery of curcumin and STAT3 siRNA using cationic liposomes would further enhance the cancer cell growth inhibition. This combination resulted in significantly ($p<0.05$) greater cancer cell growth inhibition (72.9±2.3%) compared with individual treatments. While, the mechanism of action of STAT3 siRNA is to inhibit the STAT3 signaling for promoting cell growth and multiplication, curcumin mechanism also involves the inhibition of STAT3 pathway among other mechanisms (Bill, Nicholas et al. 2012).

It has been well reported that in general, nanoparticle systems do not penetrate deep inside the skin and localize within the stratum corneum (Dreier, Sørensen et al. 2016). However, liposomes containing edge activators show greater vesicular flexibility and show enhanced skin penetration (Hasan, Belhaj et al. 2014). Cevc et al. showed that intact transfersomes permeated across the skin (Cevc, Gebauer et al. 1998). However, lipoplexes did not penetrate viable epidermis after

passive application. This could be attributed to the increased particle size after complexation of liposome with siRNA. To improve the skin penetration, anodal iontophoresis was applied to reach a target depth of up to 100 μm inside skin. The objective of this work is to reach viable epidermal layers to treat squamous cell and basal cell carcinoma, which was achieved after iontophoresis application.

3.5. Conclusions

Cationic liposomes made of DOTAP and DOPE phospholipids can entrap curcumin with high encapsulation efficiency and also form stable complex with siRNA at 10: 1 (lipid to siRNA) ratio. This nanocomplex is rapidly taken up by A431 cancer cells resulting in growth inhibition, STAT3 protein suppression and induction of apoptosis. The combination delivery of curcumin and STAT3 siRNA was more efficient in cancer cell inhibition compared to individual treatments. Furthermore, the liposomal nanocomplex can be topically delivered in a non-invasive fashion using iontophoresis technique to reach target skin cancer site within viable epidermis. This is the first time that a co-delivery system for curcumin and STAT3 siRNA using liposomes was studied.

Chapter 4

Transcutaneous iontophoretic co-delivery of curcumin and STAT3 siRNA using flexible cationic liposomes: Proof of concept in mouse skin cancer model

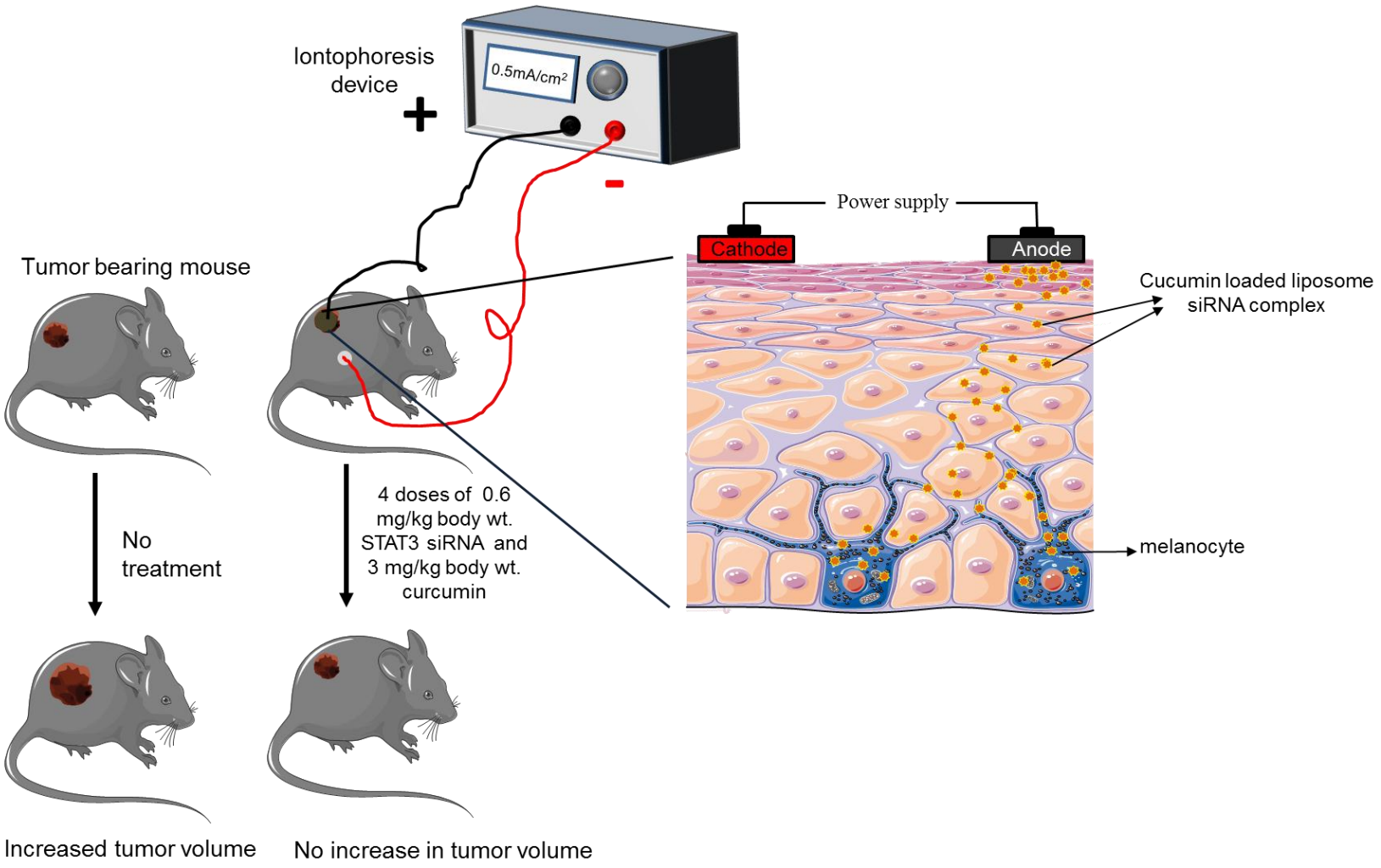
Iontophoresis device
0.5mA/cm²
+
-
Power supply
Cathode
Anode
Tumor bearing mouse
Cucumin loaded liposome siRNA complex
melanocyte
No treatment
4 doses of 0.6 mg/kg body wt. STAT3 siRNA and 3 mg/kg body wt. curcumin
Increased tumor volume
No increase in tumor volume

4.1. Introduction

Skin is an attractive site for the delivery of therapeutics with large surface area and better patient compliance. However, only a limited number of drug compounds are clinically available as topical and transcutaneous dosage forms (Ghosh*, Abraham et al. 2004). This is attributed to the formidable barrier property of skin that would limit the transport of active molecules (Naik, Kalia et al. 2000). The drug compounds with optimal physico-chemical properties can only diffuse through the skin (Wang, Thakur et al. 2005). Multiple skin penetration enhancement techniques have been developed to overcome this limitation (Benson 2005, Paudel, Milewski et al. 2010). These techniques could be broadly classified as chemical and physical skin permeation enhancement techniques. The chemical permeation enhancement method utilizes different classes of chemicals such as solvents, terpenes, fatty acids to alter the skin barrier and enhance the skin penetration of therapeutics (Pathan and Setty 2009). However, only a limited number of chemical permeation enhancers made their entry into the market. This is due to the challenges in incorporating chemical enhancer within a dosage form in acceptable levels to the user, and retaining the activity of the enhancer for the required time intervals (Finnin and Morgan 1999). The physical permeation enhancement techniques such as iontophoresis, electroporation, ultrasound and microneedles utilize electrical current, ultrasound energy or physical disruption of stratum corneum to enhance the skin penetration of therapeutics (Ting, Vest et al. 2004, Nanda, Nanda et al. 2006, Mitragotri 2013). Among these physical techniques, only iontophoresis and microneedles have been clinically approved for delivery of therapeutics (Prausnitz and Langer 2008, Kim, Park et al. 2012).

Recently, nanocarrier-based systems have been developed for efficient skin transport of therapeutics (Gupta, Agrawal et al. 2012). These include liposomes, polymeric and metal-based nanoparticles (Neubert 2011). Among these nanocarriers, liposomes have been widely reported to penetrate the SC, the outermost layer of skin (Benson 2005). Similarly, liposomes containing edge activators (transfersomes) or composed of ethanol (ethosomes) have been shown to penetrate deep inside the skin membrane (Elsayed, Abdallah et al. 2006). To further improve this penetration, nanocarrier-based drug delivery systems have been combined with physical enhancement techniques (Souza, Dias et al. 2014). For example, application of anodal iontophoresis enhanced the skin penetration of cationic liposomes containing various therapeutics (Han, Kim et al. 2004, Kajimoto, Yamamoto et al. 2011). Similarly, iontophoresis has been combined with charged polymeric and metal-based carriers to enhance their skin penetration (Eljarrat-Binstock, Orucov et al. 2008).

The delivery of molecules through skin offers potentially high localized concentration. The localized drug delivery would be beneficial for local skin diseases such as psoriasis, dermatitis, acne and skin cancer among others (Zhang, Tsai et al. 2013). Skin cancer is one of the most widely reported cancer type worldwide. Skin cancer may include the proliferation of basal cells, squamous cells or melanocytes (Franceschi, Levi et al. 1996). The excessive proliferation of melanocytes is particularly important because of low survival rate of patients beyond five years after diagnosis of melanoma (Balch, Soong et al. 2001). Most of the currently approved melanoma targeted therapeutics encounter drug resistance offered by cancer cells after long term therapy (La Porta 2007). Combination therapy using drug and gene is a potent alternate strategy to overcome the limitations associated with individual molecules in cancer therapy (Kang, Gao et al. 2015, Yang, Gao et al. 2015, Teo, Cheng et al. 2016). Here, we hypothesize that a

combination of an anticancer drug curcumin along with anti-STAT3 siRNA would inhibit the cancer progression, while iontophoresis would enhance the skin penetration of topically applied formulation.

Earlier, we have shown that liposomes loaded with curcumin and STAT3 siRNA can penetrate the excised porcine skin to reach epidermis (Jose et al., 2017). Here, we have evaluated the effectiveness of iontophoretically delivered curcumin loaded cationic liposome-STAT3 siRNA complex in controlling the melanoma tumor progression in a mouse melanoma model. The topical iontophoretic application was compared with intra-tumoral administration of formulations.

4.2. Materials and methods

4.2.1. Materials

1, 2-Dioleoyl-3-trimethylammonium propane (DOTAP), 1, 2-dioleoyl-*sn*-glycero-3-phospho-ethanolamine (DOPE) and C6 ceramide were purchased from Avanti Polar lipids, USA. STAT3 siRNA (sense sequence: 5′-AAAUGAAGGUGGUGGAGAAUU-3′; antisense sequence: 5′ UUCUCCACCACCUUCAUUUUU-3′) was purchased from Dharmacon Inc., USA. STAT3 monoclonal antibody, β-actin primary antibody, scrambled siRNA and horseradish peroxidase-conjugated secondary antibody were obtained from Santa Cruz Biotechnology Inc., USA. Curcumin, sodium cholate, agarose, sodium dodecyl sulfate (SDS), Tris base, paraformaldehyde, Triton X-100, DAPI and nitrocellulose membrane were purchased from Sigma Aldrich Chemical Company (Bangalore, India). DMEM, FBS, PBS, trypsin EDTA solution, HEPES buffer, thiazolyl blue tetrazolium bromide (MTT) and RNA-XPress™ reagent were purchased from Himedia laboratories (Mumbai, India). All the chemicals were used

without further purification. Milli-Q water (Millipore, USA) with 18 MΩ cm^{-1} resistivity was used for all the experiments.

4.2.2. Preparation of the curcumin loaded cationic liposome-siRNA complex

Curcumin loaded cationic liposomes were prepared using thin film hydration method and complexed with STAT3 siRNA as described in our previous report (Jose, Labala et al. 2016). Briefly, solutions of DOTAP, DOPE, C6 ceramide, sodium cholate (50: 30: 10: 10 w/w) and weighed quantity of curcumin (10:1 lipid: drug ratio) were mixed in a round bottom flask and the organic solvent was removed using rotary evaporator at 45±2^{o}C and 80 rpm under reduced pressure. The dried lipid film was then hydrated using 20 mM HEPES buffer (pH 7.4) to obtain a final lipid concentration of 10 mg/ml. Bath sonicated the liposome suspension for 3 min and extruded through 100 nm pore size polycarbonate membrane for 15-times (Miniextruder, Avanti Polar Lipids Inc., USA).

The encapsulation efficiency of curcumin within the liposomes was determined after separating the free curcumin from the liposome suspension by centrifuging the liposomes using Amicon 10 kDa filters at 6000 rpm for 12 min. The total amount of curcumin in liposome suspension (free as well as entrapped in liposomes) was determined by lysing the liposomes using 6% v/v Triton X-100. Then, the concentration of curcumin in filtrate (free curcumin) and total liposome was determined using HPLC system equipped with UV-detector (Shimadzu, Japan). The HPLC analysis was performed using a Phenomenex C8 column with mobile phase (acetonitrile: 0.1% formic acid (80: 20% v/v)) at a flow rate of 0.5 ml/min. 10 µl of sample was injected and curcumin was detected at 420 nm wavelength. The encapsulation efficiency was determined using Equation (1).

$$Encapsulation\ efficiency\ (\%) = \left(1 - \frac{Concentration\ of\ free\ curcumin}{Concentration\ of\ total\ curcumin}\right) x100 \quad (1)$$

The complexation of cationic liposomes with STAT3 siRNA was performed at N/P (DOTAP: siRNA) ratio of 10: 1. Lipoplexes were prepared by mixing curcumin loaded liposomes with siRNA diluted in 20 mM HEPES buffer (pH 7.4), vortexed for 30 sec and incubated at room temperature for 20 min.

4.2.3. Characterization of the cationic liposome-siRNA complex

The curcumin loaded liposomes and curcumin loaded liposome-STAT3 siRNA complex were characterized for average particle size, PDI and zeta-potential by dynamic light scattering. The cationic liposomes and liposome-siRNA complex were diluted with 20 mM HEPES buffer (pH 7.4) prior to the measurement. 0.75 ml of the sample was injected into clear folded capillary cell (DTS 1060) and zeta potential measurement was carried out using Smoluchowski model in automatic mode.

4.2.4. Cell culture studies

Mice melanoma cells (B16F10) obtained from National Centre for Cell Science (Pune, India) was used for cell culture studies. DMEM supplemented with 10% FBS and 1% antibiotic solution (penicillin and streptomycin) was used for cell culture. Incubated the cultured cells at 37°C, 95% humidity and 5% CO_2.

4.2.5. Cell viability study

For cell viability studies, B16F10 cells were seeded in a 96 well plate (1 x 10^4 cells/well) and incubated for 24 h. Later, the cells were exposed to different formulations including free siRNA (0.5 nM), curcumin solution (150, 250 and 350 µM per well dissolved in 1% DMSO), curcumin loaded liposome (150, 250 and 350 µM of curcumin), liposome-siRNA complex (0.25, 0.5 and 1 nM siRNA) and curcumin loaded liposome-siRNA complex (250 µM curcumin and 0.5 nM siRNA). The formulations were added after diluting with DMEM and the cells were incubated for 8 h at 37ºC. Later, aspirated the medium containing formulations and the cells were incubated for 48 h in complete media. Thiazolyl blue tetrazolium bromide (MTT) assay was used for determining the cell viability. After solubilising the formazan crystals in DMSO, measured the absorbance at 572 nm wavelength using multimode plate reader (SpectraMax M4, Molecular Devices, USA). The concentrations of curcumin and siRNA used in in this experiment is selected based on our previous experiments using same formulations (Jose, Labala et al. 2016).

4.2.6. Cell uptake studies

Uptake of curcumin loaded cationic liposomes by B16F10 cells were studied by seeding the cells in a 12 well plate (1 x 10^5 cells/well). After 24 h of incubation, the cells were treated with curcumin loaded liposome (250 µM of curcumin) for different time periods including 30, 60 and 120 minutes. Later, washed the cells with ice cold PBS and fixed using 4% paraformaldehyde. 0.1% Triton X-100 was used to permeabilize the cells and then incubated the cells with 4, 6-diamidino-2-phenylindole (DAPI, 1 µg/mL) for 5 min. Later, the cells were observed under fluorescence microscope (Olympus IX53, Olympus Corporation, Japan) and images were acquired after excitation of DAPI and curcumin using 358 and 488 nm laser, respectively under

20X objective lens. Image analysis was performed using Image J software (version 1.47 V, National Institutes of Health, USA).

4.2.7. Skin permeation studies

The depth of skin permeation of curcumin loaded cationic liposomes was studied using excised porcine ear skin. Porcine ears were obtained and processed for permeation experiments as mentioned in our earlier report (Jose, Mandapalli et al. 2016).

The processed skin samples were mounted between the receptor and donor compartments of a Franz diffusion cell with stratum corneum facing the donor compartment. PBS with 20% ethanol maintained at 37±0.5^{o}C was used as the receptor medium. Curcumin loaded cationic liposome formulation (200 µg curcumin) was spiked in the donor compartment. Skin samples were treated with curcumin loaded liposomes (both passive as well as iontophoretic) for a time period of 4 hours.

Anodal iontophoresis was carried out at a current density of 0.47 mA/cm^2 using a direct current power supply unit (V-care Meditech Pvt. Ltd., Bengaluru, India) for 4 h with silver and silver chloride electrodes placed in the donor and receptor compartments, respectively. In order to avoid the direct contact of silver wire with cationic liposomes, a salt bridge made up of 1% agarose containing 2 mM NaCl was used. After completion of 4 h treatment (both passive and iontophoretic), skin samples were removed and carefully washed with PBS to remove all adsorbed liposomes. Air dried the skin samples and mounted on microscopic glass slides with cover slip.

The impact of iontophoresis in enhancing the skin permeation of liposomes was studied by visualizing the skin samples under confocal microscope (Leica TCS SP8, Leica Microsystems CMS, Germany). Curcumin was excited using Argon laser at an excitation wavelength of 488 nm and the images were acquired using 40X/0.30 oil (HCPL APO CS2) objective lens. Optically sectioned the skin sample from 0-200 µm depth at a step size of 1 µm/scan, in order to analyze the skin distribution and depth of penetration of curcumin loaded liposomes. All the images were acquired at constant gain and offset and the mean fluorescence intensity of images was analyzed using Leica LAS X software.

4.2.8. In-vivo studies

In-vivo studies were carried out on C57BL/6 mice melanoma models. Melanoma tumor model was created by the subcutaneous injection of B16F10 mice melanoma cells to C57BL/6 mice. Female C57BL/6 mice (4-6 weeks old) were purchased from the National Centre for Laboratory Animal Science (NCLAS), Hyderabad, India. All animal experiments were performed in accordance with guidelines of Committee for the Purpose of Control and Supervision of Experiments on Animals (CPCSEA) and after getting approval from the Institutional Animal Ethics Committee of BITS Pilani, Hyderabad, India.

In order to induce tumor, mice were shaven and subcutaneously injected with B16F10 cells (1 x 10^6 cells/mice) suspended in Hank's balanced salt solution in the upper left flank region. Then the animals were allowed to grow under normal conditions supported with food and water. They were regularly monitored for weight of the animal and appearance of tumor lesions on the injected area. After a period of approximately 15 -20 days, small tumors started appearing on the

mice skin. Measured the tumor length and breadth at regular intervals using a digital vernier caliper and calculated the volume using equation (2).

$$\text{Tumor volume } (mm^3) = \frac{Longitudinal\ diameter\ (mm) \times (transverse\ diameter\ (mm))\text{^}2}{2} \quad (2)$$

Once the tumor volume reached approximately 200 mm^3, tumor bearing mice were divided into 10 groups with 5 animals in each group. Each group of animals was treated with different formulations of siRNA (0.6 mg/kg body weight) and curcumin (3 mg/kg body weight). The formulations were applied topically (either passive or iontophoresis assisted) or by intratumoral injection.

For passive topical application, spread 75 µl of the formulation carefully upon the skin covering the tumor. In case of iontophoresis assisted topical delivery, the liposomal formulations were dispersed in 0.4 % agarose gel containing 2 mM sodium chloride. The gel with formulation was applied above the tumor and another placebo gel (without formulation) was placed on the skin nearer to tumor area. Anodal iontophoresis (current density of 0.5 mA/cm^2) was applied wherein anode dipped in gel containing formulation and cathode in placebo gel for a period of 2 h. The mice were immobilized under isoflurane anesthesia throughout the iontophoresis treatment. For intratumoral injection, 75 µl of the formulation was injected into the tumor tissue using a 30 gauge needle. Each formulation was administered once in 3 days for 4 times.

Three days after the administration of 4^{th} dose, sacrificed the animal by exposing to ether over dose. Isolated the tumor tissue immediately, measured the tumor weight & volume and submerged in RNA later solution. These tumor tissues were preserved at -80^oC for further studies.

4.2.9. Western blot analysis

Total protein in tumor tissue was extracted using RNA-XPress™ reagent and the level of STAT3 protein was estimated by Western blot analysis. The total protein content in each tumor sample was estimated by Bradford's assay. Separated the proteins using SDS-PAGE. Protein sample (18 µl containing 40 µg protein) was mixed with loading buffer and spiked in sample well. Performed the gel electrophoresis at 50 V for 2 h. Later, transferred the protein bands electrophoretically on to nitrocellulose membrane using transfer unit at 100 V for 1 h. Incubated the nitrocellulose membrane with STAT3 and β-actin primary antibody followed by HRP-conjugated secondary antibody. Further, incubated the membrane with enhanced chemiluminescent substrate solution (ECL reagent, Super signal Pro, Thermo scientific, USA) and visualized the bands using autoradiography technique.

4.2.10. Histological evaluations

Cryosectioned the tumor tissues and examined for the level of STAT3 expression using immunofluorescence reagents. Briefly, mounted the cryostat sections on glass slides, air dried and fixed using ice cold acetone. After removal of acetone, washed the sample with PBS followed by blocking with 5% BSA. Drained off blocking buffer and incubated the sample with STAT3 primary antibody overnight. Washed and incubated with FITC-conjugated secondary antibody and visualized under confocal microscope. Further, the overall cell density was analyzed by staining the cryosectioned tumor samples with haematoxylin and eosin and visualized under confocal microscope.

4.2.11. Statistical Analysis

All the experimental results are presented as mean (n=3-5) ± standard deviation. Statistical analysis was performed using analysis of variance (ANOVA) (GraphPad Prism V6), where $p<0.05$ was considered to be minimum level of significance.

4.3. Results

4.3.1. Characterization of cationic liposome-siRNA complex

The average particle size of curcumin loaded cationic liposomes immediately after preparation was found to be 276.9±14.4 nm (PDI: 0.641±0.002). The particle size of vesicles reduced to 142.4±5.2 nm (PDI: 0.242±0.004) with a zeta-potential of 42.8±5.0 mV after extrusion through polycarbonate membrane (100 nm pore size) for 15-times. The encapsulation efficiency (EE %) of curcumin loaded liposomes was found to be 86.8±6.0. After complexation of curcumin loaded cationic liposomes with negatively charged siRNA molecules, the particle size and zeta-potential of the vesicles increased to 192.6±9.0 nm (PDI: 0.326±0.004) and 56.4±8.0 mV, respectively.

4.3.2. Cell viability study

Figure 4.1 shows the growth inhibition of B16F10 cells after treatment with different formulations of curcumin and STAT3 siRNA. Free STAT3 siRNA (0.5 nM) showed growth inhibition of 3.4±0.7% whereas blank cationic liposomes showed 16.4±2.4% growth inhibition. Curcumin solutions at different concentrations of 150 μM, 250 μM and 350 μM showed growth inhibition of 18.6±3.9%, 29.8±3.8% and 36.5±3.3% respectively. On the other hand, curcumin loaded cationic liposomes showed 34.9±2.6%, 46.0±3.4% and 51.1±3.9% inhibition at 150 μM, 250 μM and 350 μM concentrations, respectively. Cationic liposome-STAT3 siRNA complex at

different concentrations of 0.25 nM, 0.5 nM and 1 nM resulted in cell growth inhibition of 46.9±3.5%, 58.4±3.0% and 62.7±4.6% respectively. Co-delivery of curcumin and STAT3 siRNA using cationic liposomes (250 μM curcumin and 0.5 nM siRNA) resulted in maximum cell growth inhibition of 76.3±4.0%.

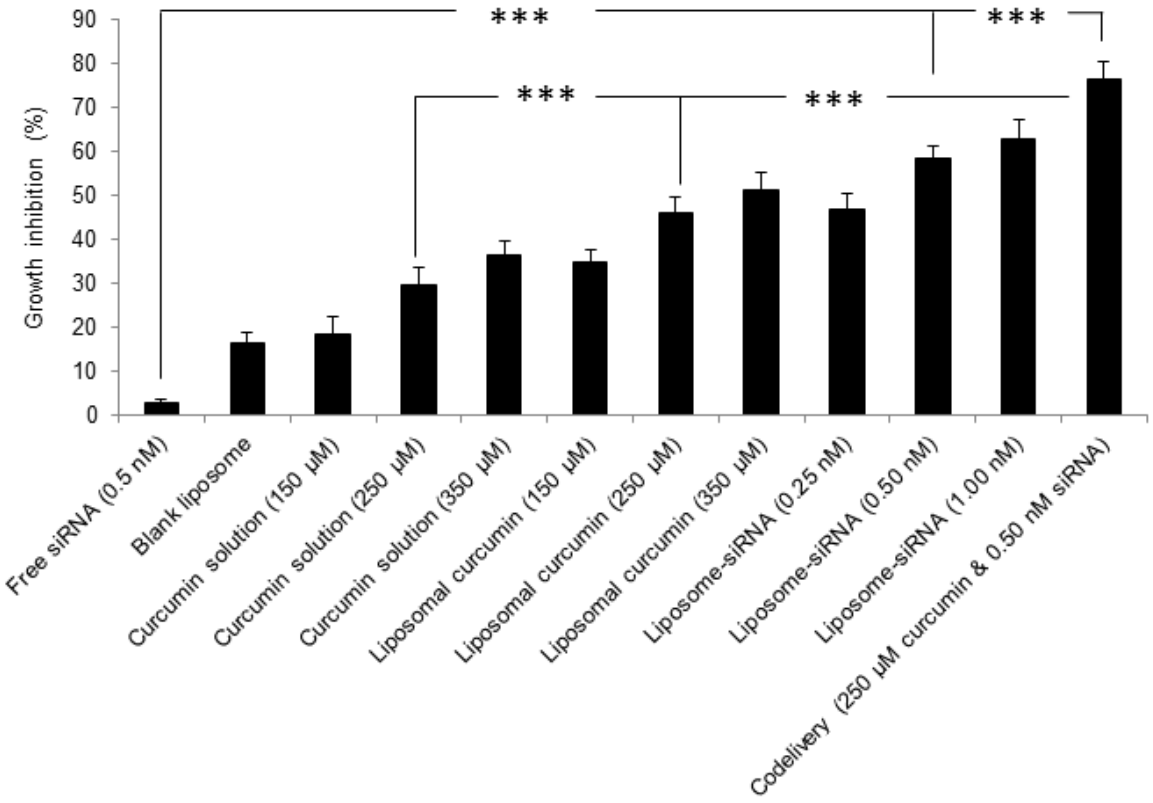

Fig.4.1. Inhibition of B16F10 cancer cell growth after treatment with different formulations of curcumin and STAT3 siRNA. Results are presented as mean (n=5) ± standard deviation. *** indicates that the value is significantly different at $p < 0.001$.

4.3.3. Cell uptake studies

The cellular uptake of curcumin loaded cationic liposomes by B16F10 cells was evaluated using fluorescence microscope.

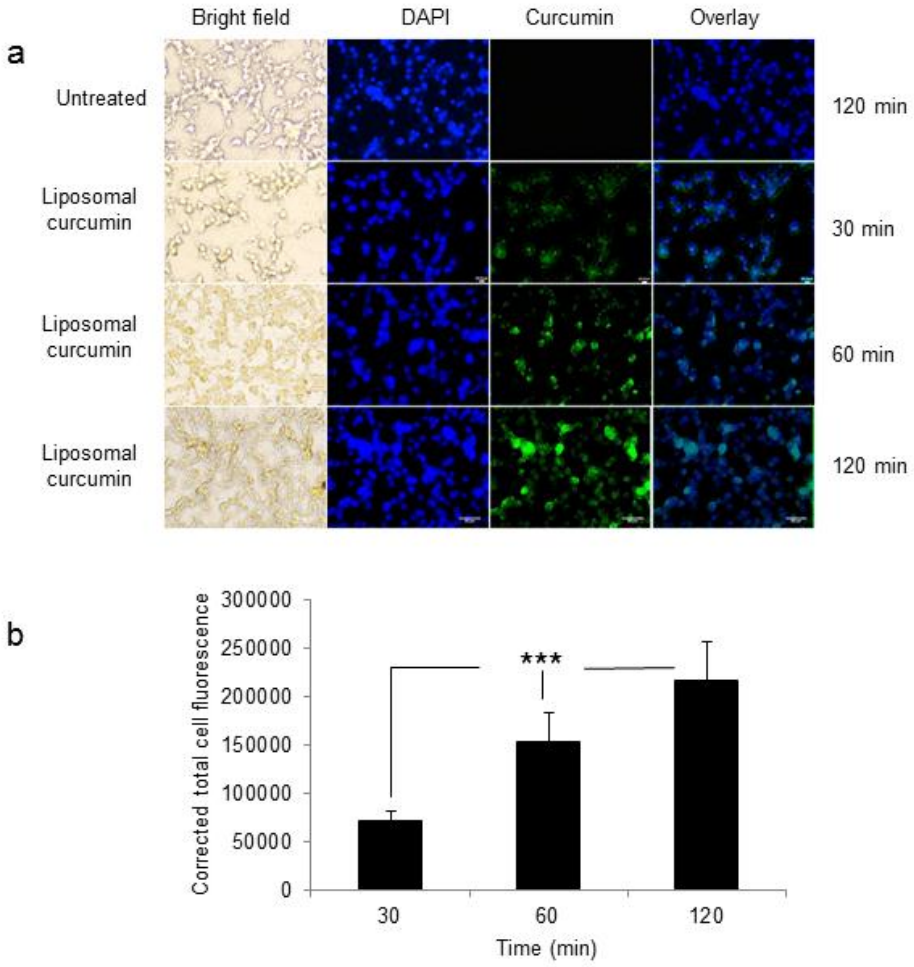

Fig.4.2. a. B16F10 cell uptake of curcumin loaded liposomes after 30, 60 and 120 min incubation time. Images were representative of at least three experimental groups. **b.** Corrected total cell fluorescence calculated using Image J image analysis software. Data represents mean (n =3) ± standard deviation. Asterisk (***) indicates that the value is significantly ($p<0.001$) different in comparison to other values.

Figure 4.2a shows the images of B16F10 cells after incubation with free and liposomal curcumin for a period of 30, 60 and 120 min. Background corrected fluorescence image analysis showed significant increase in cell associated fluorescence intensity with the increase in incubation time from 30 to 120 min (Figure 4.2b). From the images, it was observed that liposome encapsulated curcumin was able to get inside the cells at 30 min of incubation and the fluorescence intensity of curcumin inside the cells got significantly higher at 60 and 120 min. The merged images show that the curcumin loaded liposomes was able to cross the cell membrane and got localized in the cytoplasm. Similarly, there was increased corrected total fluorescence intensity of cells with increase in incubation time from 30 to 120 min indicating enhanced cell uptake of curcumin loaded liposomes upon increasing the incubation time.

4.3.4. Skin permeation studies

Depth of skin penetration of curcumin loaded liposomes after passive and anodal iontophoresis was determined using porcine ear skin samples having thickness of 0.92±0.6 mm and electrical resistance of 4.86±0.14 kΩ. Fig.4.4 shows the confocal microscopic images of skin samples after passive and iontophoretic application of curcumin loaded liposomes for 4 h. From the images, it is clear that passive application of curcumin loaded liposomes was not able to permeate to the deeper skin layers. Here the vesicles were able to reach only up to 50 µm into the skin. Whereas iontophoresis assisted skin permeation of liposomes delivered the vesicles up to a depth of 160 µm inside the skin layers.

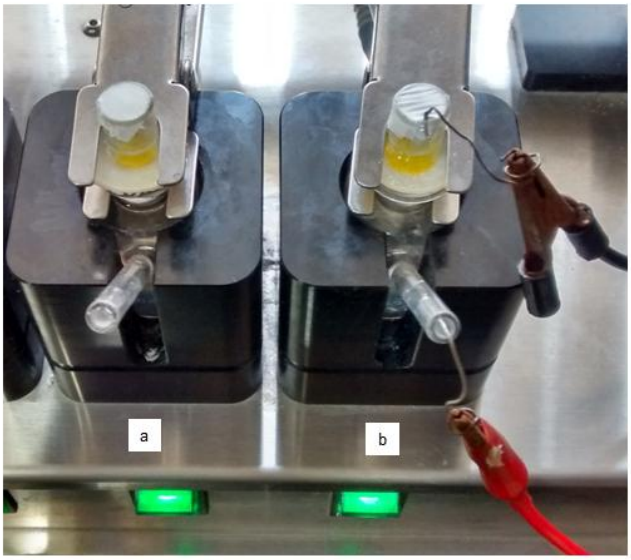

Fig.4.3. Photograph of skin permeation experiments conducted using Franz diffusion cell apparatus. **a.** Passive permeation of curcumin loaded liposomes. **b.** Iontophoresis assisted permeation of curcumin loaded liposomes.

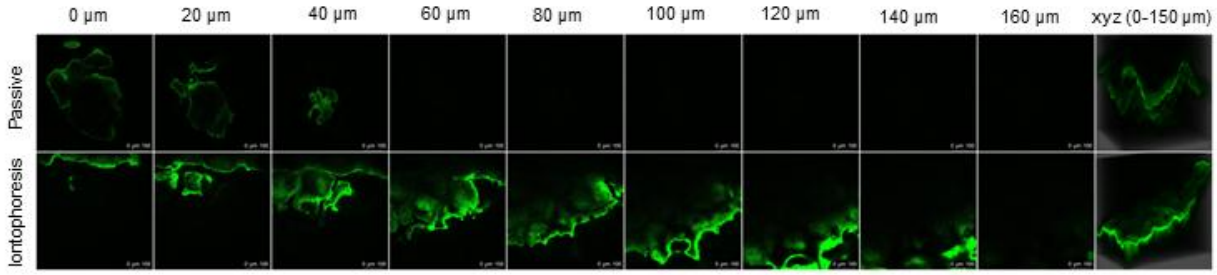

Fig.4.4. Confocal microscopic images of skin samples after passive and iontophoretic treatment with curcumin loaded liposomes for 2 h. Images were shown from surface to 150 µm depth inside skin in XYZ sections. All the images were representative of at least three experiments.

4.3.5. In-vivo studies

Table 4.1 shows the groups of animals with the treatments given. Figure 4.7 shows the tumors isolated from animals after completion of treatment with different formulations. Each tumor image is a representative image from a treatment group consisting of 5 animals. Immediately after isolation of tumor from the sacrificed animal, tumor weight and volume were measured. Figure 4.8 shows the change in tumor volume in different treatment groups during the period of treatment. Figures 4.9a and 4.9b represents the average volume and average weight of tumors isolated from the animals in each treatment group. The average volume and average weight of tumors isolated from untreated group of animals were 3225.17±557.91 $mm^3$and 4.61±0.49 g respectively. Other treatment groups like passive administration of liposome-STAT3 siRNA, passive administration of curcumin loaded liposomes and iontophoretic administration of liposome-scrambled siRNA complex did not show much reduction in tumor weight and tumor volume, compared with that of untreated control group. Intratumoral injection of curcumin solution showed reduction in tumor volume (2172.54±167.27 mm^3) and tumor weight (2.61±0.40 g).

Table 4.1.Groups of animals with treatment given. P-Passive, I-Iontophoresis & ITI-Intratumoral injection

Treatment group	Treatment given
1	Untreated control
2	Liposome-siRNA (P)
3	Liposomal curcumin (P)
4	Liposomal curcumin(ITI)
5	Liposomal curcumin-siRNA (I)
6	Liposomal curcumin-siRNA (ITI)
7	Liposomal curcumin (I)
8	Liposome-siRNA (I)
9	Curcumin solution (ITI)
10	Liposome-scrambled siRNA (I)

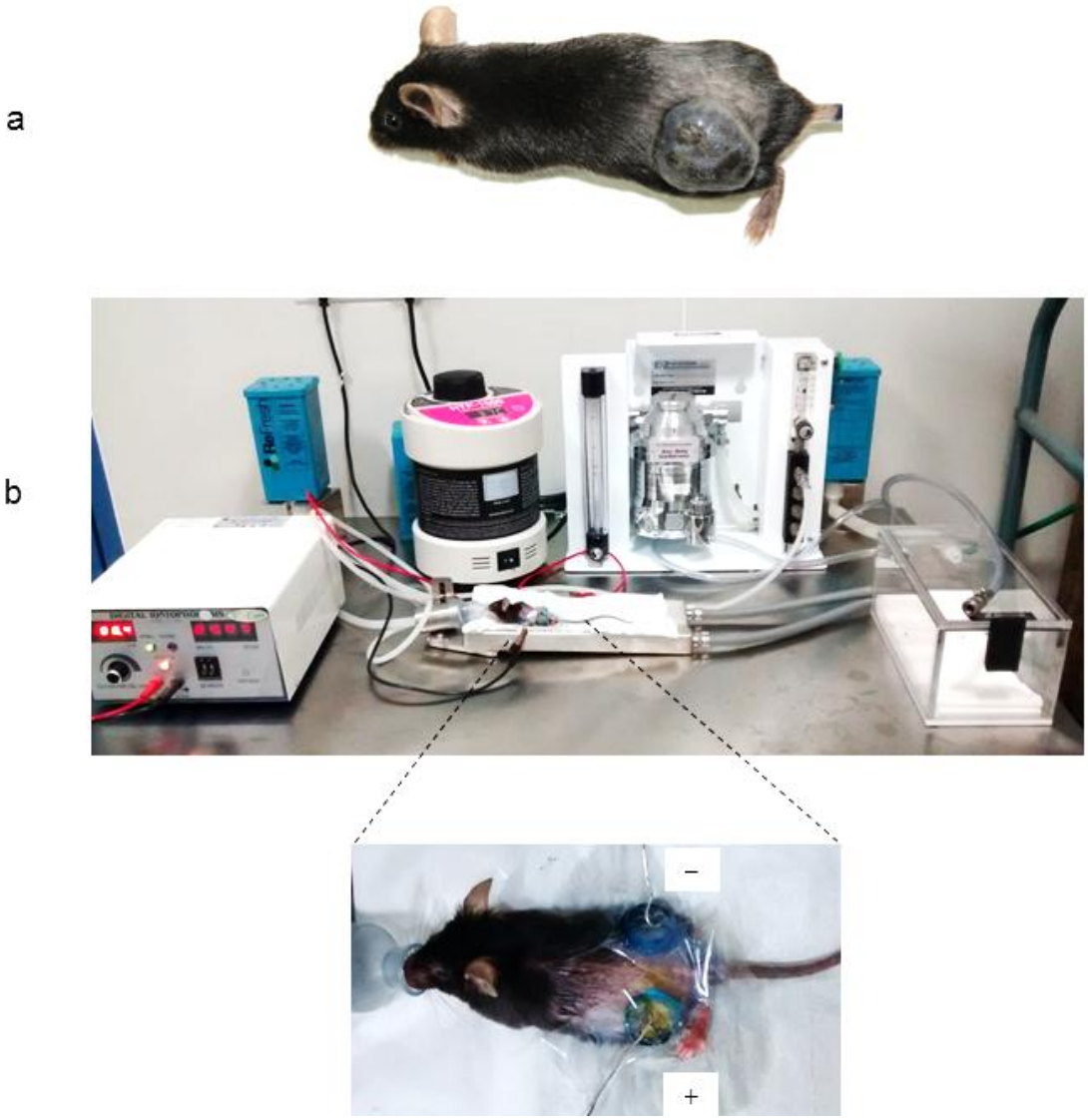

Fig.4.5. a. Photograph of melanoma tumor bearing C57BL/6 mouse. **b.** Photograph of tumor bearing mouse undergoing transcutaneous iontophoretic co-delivery of curcumin and STAT3 siRNA using cationic liposomes under anesthesia.

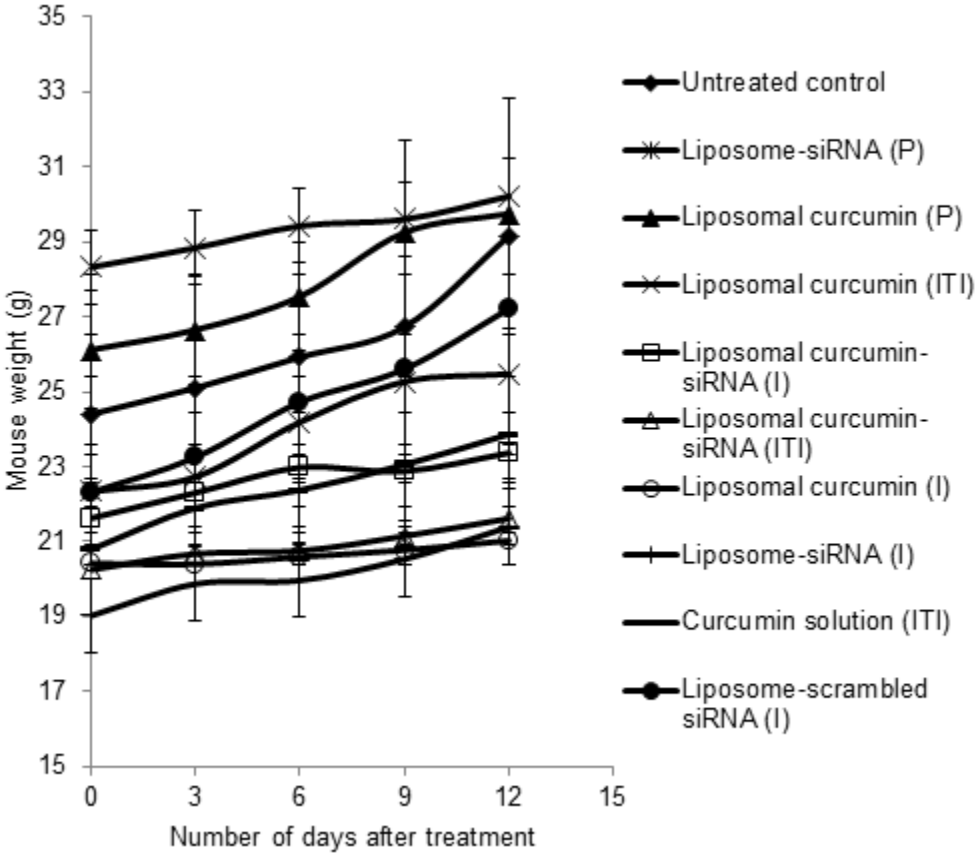

Fig.4.6. Weight of mice during treatment with different formulations. Data represents mean ± standard deviation (n =5).

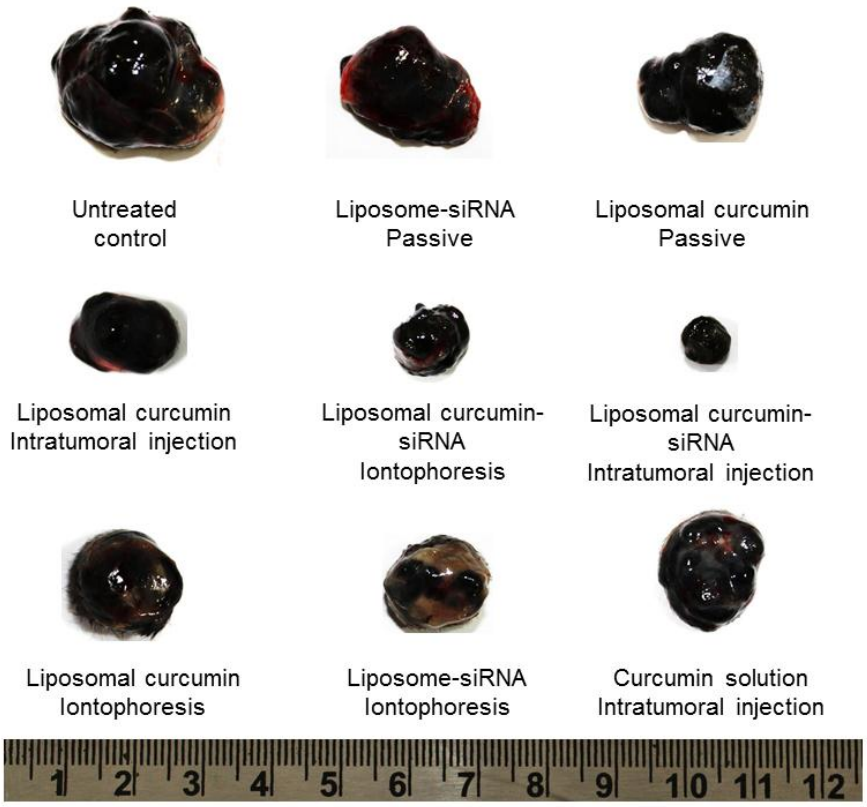

Fig.4.7. Photograph of tumors isolated from tumor bearing C57BL/6 mice after treatment with different formulations. All the images were representative of tumors isolated from five different animals in same treatment group.

Iontophoretic administration of liposome-STAT3 siRNA and curcumin loaded liposomes caused significant reduction in tumor volume (1682.32±414.42 mm^3 and 1502.80±159.86 mm^3) and weight (1.84±0.49 g and 1.75±0.12 g) compared to control group. Intratumoral administration of curcumin loaded liposomes also showed significant reduction in tumor volume (1316.35±419.37 mm^3) and tumor weight (1.59±0.69 g). The group of animals treated with intratumoral injection of curcumin loaded liposome-STAT3 siRNA complex showed maximum reduction in tumor volume (502.89±101.42 mm^3) and tumor weight (0.53±0.21 g). Similarly, the group of animals treated with iontophoretic administration of curcumin loaded liposome-STAT3 siRNA complex also caused significant ($p<0.05$, Student's t-test) reduction in tumor volume (726.23±128.40 mm^3) and tumor weight (0.88±0.10 g) compared to untreated control group of animals.

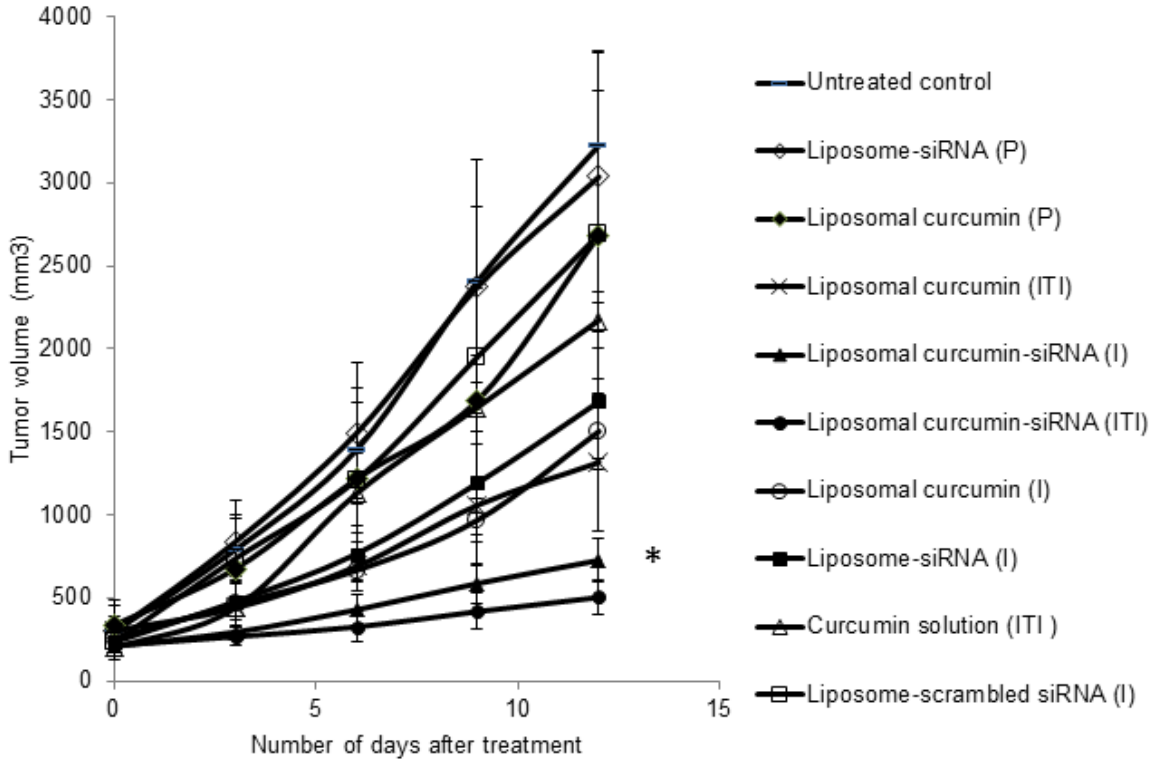

Fig.4.8. Average tumor volume after initiation of treatment with different formulations. Data represents mean ± standard deviation (n =5). * Represents the value is significantly different from all other treatment groups except liposomal curcumin-siRNA (ITI) at $p < 0.05$. (P-Passive, I-Iontophoresis & ITI-Intratumoral injection).

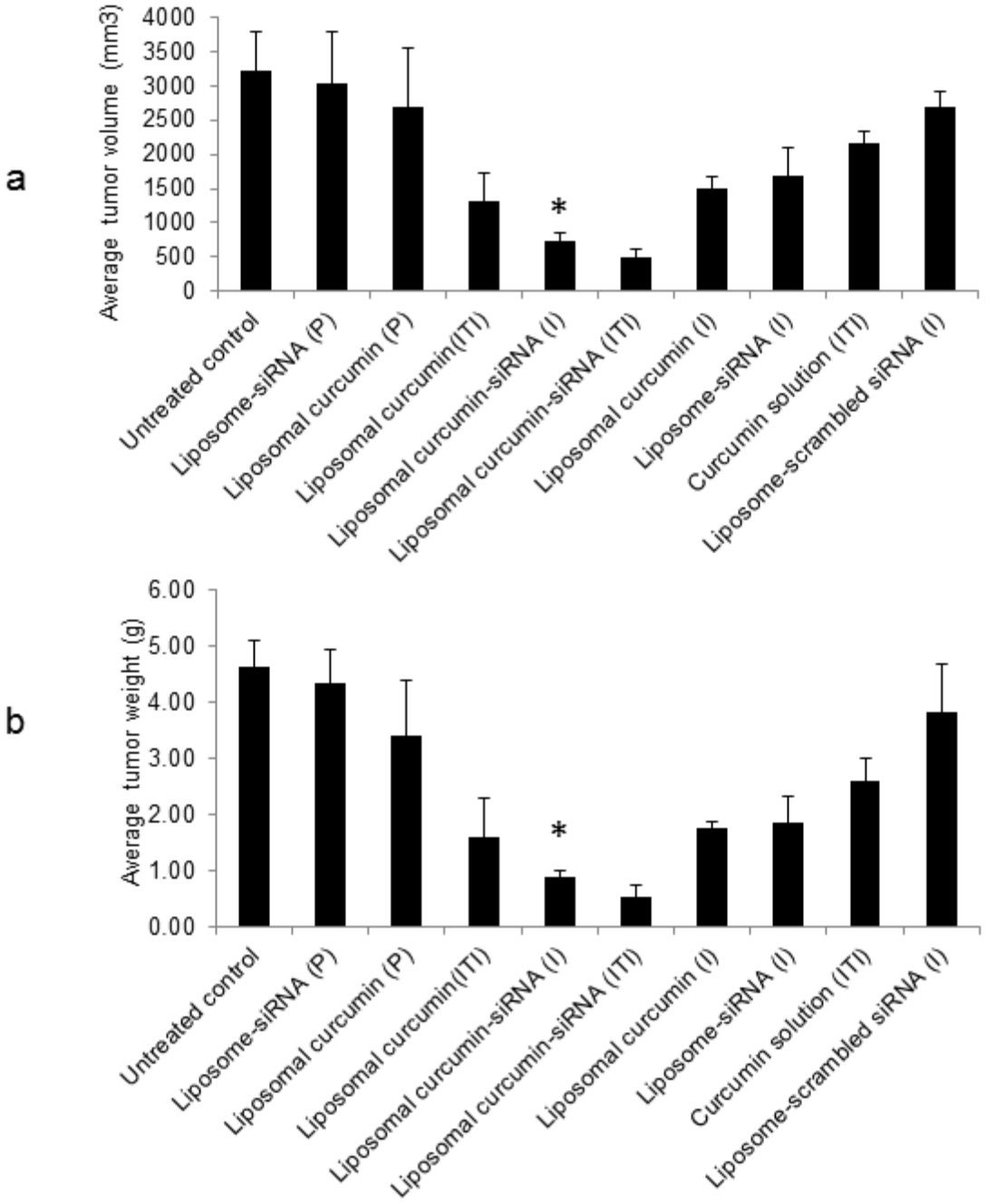

Fig.4.9. a. Average volume of tumors isolated from C57BL/6 tumor bearing mice after treatment with different formulations. **b.** Average weight of tumors isolated from C57BL/6 tumor bearing mice after treatment with different formulations. Data represents mean ± standard deviation (n =5). * represents that the values are significantly different from all other treatment groups except intratumoral injection of curcumin loaded liposome-siRNA complex, at $p < 0.001$.

4.3.6. Western blot analysis

Suppression of STAT3 protein by different treatment approaches in tumor bearing mice were evaluated using Western blot analysis and the results are as shown in figure 4.10.

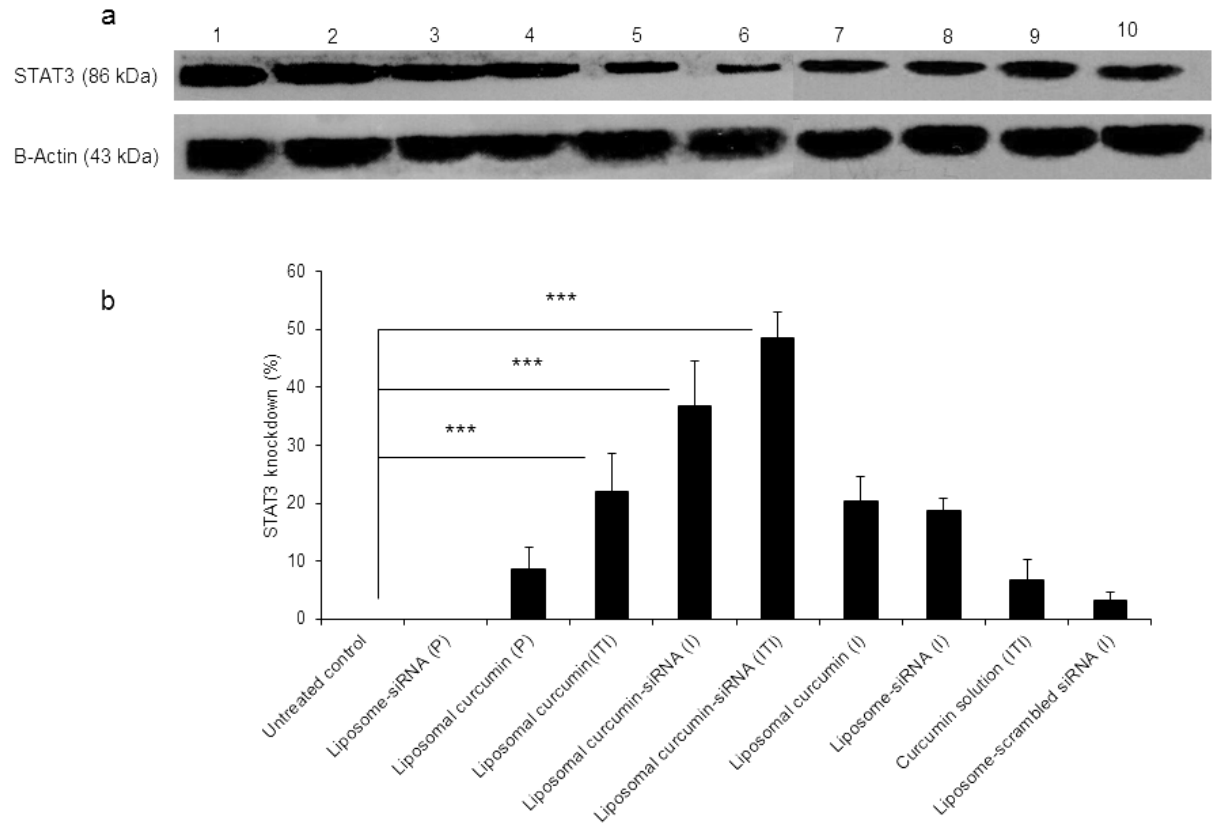

Fig.4.10. a. Expression of STAT3 protein in C57BL/6 tumor bearing mice after treatment with different formulations (1:untreated control, 2:liposome-siRNA (P), 3:liposomal curcumin (P), 4:liposomal curcumin (ITI), 5:liposomal curcumin-siRNA (I), 6:liposomal curcumin-siRNA (ITI), 7:liposomal curcumin (I), 8:liposome-siRNA (I), 9:curcumin solution (ITI), 10:liposome-scrambled siRNA (I)). β-actin was used as loading control. Data represents mean ± standard deviation (n =5). **b.** STAT3 knockdown (%) after treatment with different formulations. *** represents that the values are significantly different at $p < 0.05$. (P-Passive, I-Iontophoresis & ITI-Intratumoral injection).

It was observed that intratumoral injection of curcumin loaded liposome-siRNA complex showed 48.55±4.40 % reduction in STAT3 expression whereas iontophoretic delivery of the same showed 36.81±7.66% reduction. The group treated with passive application of liposome-siRNA complex did not show any reduction in STAT3 expression. Passive application of liposomal curcumin resulted in 8.68±3.76% reduction whereas intratumoral injection of the same formulation showed 22.06±6.60 % reduction in STAT3 protein expression. Iontophoretic application of liposomal curcumin and liposome-siRNA complex showed STAT3 protein suppression of 20.25±4.33 and 18.67±2.27 % respectively. On the other hand, intratumoral injection of curcumin solution showed 6.72±3.54% and iontophoretic application of liposome-scrambled siRNA complex showed only 3.09±1.41% STAT3 protein suppression.

4.3.7. Histological evaluations

Figure 4.11 shows the confocal microscopic images of tumor cryosections after treatment with FITC labeled anti-STAT3 monoclonal antibody. It was observed that the fluorescence intensity was highest in the cryosections of untreated control, passive application of liposome-siRNA complex and iontophoretic application of liposome-scrambled siRNA complex. Fluorescence intensity was minimum for those groups treated with intratumoral injection and iontophoretic application of curcumin loaded liposome-siRNA complex indicating maximum suppression of STAT3 protein. Iontophoretic application of curcumin loaded liposomes and liposome-siRNA complex also showed STAT3 protein suppression. On the other hand, intratumoral injection of curcumin solution and iontophoretic administration of liposome-scrambled siRNA showed very slight to no suppression of STAT3 protein expression.

Figure 4.12 shows the microscopic images of haematoxylin and eosin stained cryosections of tumor samples isolated from mice of different treatment groups. The difference in cell density of

untreated tumor sections and those treated with formulations indicates the suppression of tumor growth after treatment. Those samples obtained from mice treated with intratumoral administration or iontophoretic application of curcumin loaded liposome-siRNA complex showed lesser cell density compared to untreated and passive treatment groups.

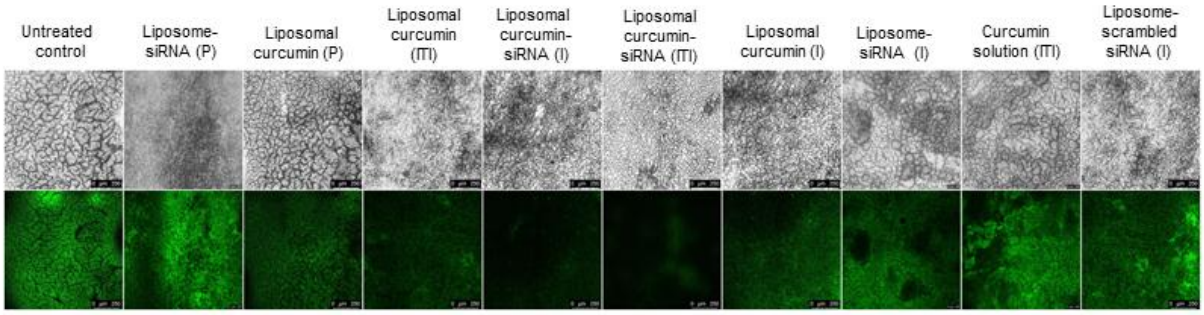

Fig.4.11. Confocal microscopic images of tumor cryosections after treatment with FITC labeled STAT3 secondary antibody. All the images were representative of tumors isolated from five different animals in same treatment group.

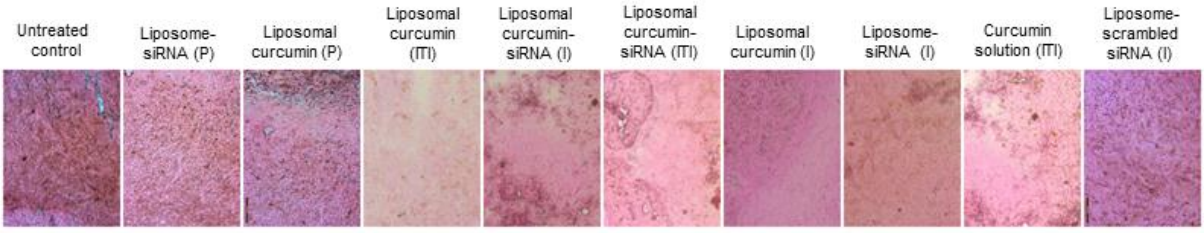

Fig.4.12. Microscopic images of tumor cryosections after staining with haematoxylin and eosin. All the images were representative of tumors isolated from five different animals in same treatment group.

4.4. Discussion

Curcumin is a natural compound obtained from the roots of curcuma longa (Kim, Choi et al. 2003). It possesses multiple properties including anti-inflammatory, anti-oxidant and cytotoxic activity (Ruby, Kuttan et al. 1995, Chainani-Wu 2003, Maheshwari, Singh et al. 2006). The clinical application of curcumin is limited by its poor aqueous solubility (Kim, Jiang et al. 2011). Various methods have been adopted to improve curcumin solubility (Yallapu, Jaggi et al. 2012). Among these, encapsulation of curcumin in liposomes helps in the delivery of therapeutic concentrations at target sites (Bansal, Goel et al. 2011). In general, lipophilic molecules can be better encapsulated in liposomes compared with hydrophilic molecules (Schreier and Bouwstra 1994). When the thin lipid film is hydrated using aqueous medium to prepare lipid vesicles, the hydrophilic molecules partition into the extra-vesicular region, while the lipophilic molecules interact with the hydrophobic phospholipids to get encapsulated within the lipid bilayer of vesicles. Furthermore, curcumin was shown to get embedded in the phospholipid bilayer (Karewicz, Bielska et al. 2011). It was observed that there was no significant ($p>0.05$) increase in the average particle size after encapsulation of curcumin in liposomes. As the curcumin is not a charged molecule, its encapsulation also did not alter the zeta-potential. On the other hand, the positive surface charge of liposomes attributed to DOTAP allowed for electrostatic complexation with negatively charged STAT3 siRNA. The nitrogen/ phosphate (N/P) ratio is an important material attribute for efficient complexation and further cell interaction. The N/P ratio of 10:1 was employed based on our earlier reports using same liposomes and siRNA (Jose, Labala et al. 2016). As the siRNA complexes with the surface of the liposome, and multiple vesicles could be involved in complexation, the average particle size after siRNA complexation increased by 30%. A similar trend was reported earlier by our group and others (Geusens, Lambert et al. 2009). The

release kinetics of curcumin from cationic liposomes was reported in our earlier publication (Jose, Labala et al. 2016).

STAT3 is a transcription factor that would enhance the transcription and translation of growth and migratory factors including vascular epidermal growth factor (VEGF), B-cell lymphoma 2 (BCL2), interleukin 17 (IL-17) and interleukin 23 (IL-23) upon stimulation (Yu, Pardoll et al. 2009). The suppression of STAT3 has been shown to inhibit the tumor progression in multiple cancer types including melanoma (Kortylewski, Jove et al. 2005). The curcumin loaded liposome-STAT3 siRNA complex was taken up by A431 cancer cells within 30 mins (Jose, Labala et al. 2016). The intracellularly released STAT3 siRNA silences the STAT3 protein expression. Meanwhile, the curcumin will show its anticancer activity through various mechanisms including STAT3 suppression (Yang, Liu et al. 2012). Therefore, the combination of curcumin and STAT3 siRNA resulted in significantly ($p<0.05$) greater cancer cell growth inhibition compared with either the curcumin or STAT3 siRNA alone. There are similar reports of enhanced tumor growth inhibition where a small molecule anti-cancer agent is co-administered with siRNA using a nanocarrier (Labala, Jose et al. 2017).

In general, most of the anticancer therapeutic loaded nanocarriers are administered intravenously to evaluate the effectiveness after cancer progression (Hervella, Lozano et al. 2008). In case of cancers that are accessible though topical route, the transcutaneous administration is preferred to minimize the unwanted adverse effects (Schreier and Bouwstra 1994, Prausnitz and Langer 2008). To that end, here we have compared the tumor growth suppression after topical application compared with intratumoral administration in mouse melanoma model. However, the barrier property of skin did not allow the passive diffusion of the curcumin loaded liposome-siRNA complex to penetrate deep inside the skin. To overcome the skin barrier property, anodal

iontophoresis was applied. Iontophoresis enhances the skin penetration of charged molecules and particles by a combination of electrorepulsion and electroosmosis (Guy, Kalia et al. 2000). Especially, anodal iontophoresis was shown to enhance the skin penetration of cationic particles, taking advantage of the solvent migration in the direction of anode to cathode in the presence of electric current.

The application of cationic liposomes for dual delivery of curcumin and STAT3 siRNA did not decrease the overall body weight of mice up to 15 days of treatment (Figure 4.6). Similar to earlier reports, the present study corroborates the effectiveness of topical iontophoresis application to deliver chemotherapeutic agents using nanocarriers to suppress the tumor progression (Venuganti, Saraswathy et al. 2015). The suppression of STAT3 protein by formulations containing STAT3 siRNA indicates that the tumor growth suppression is specific to the STAT3 siRNA. In the group administered with scrambled siRNA there was no reduction in STAT3 protein expression. This was also supported by the immunohistochemicals analysis where the STAT3 protein expression was determined using fluorescent dye labeled anti-STAT3 antibody. Taken together, the co-delivery of curcumin and STAT3 siRNA provided greater tumor growth suppression, while the cationic liposomal nanocarrier system allowed for non-invasive topical iontophoretic application.

The proposed topical iontophoretic co-delivery of curcumin and siRNA using cationic liposomes is a clinically feasible approach for the treatment of skin cancer. There are various examples of clinically approved iontophoresis assisted drug delivery systems like fentanyl ((Ionsys®; Janssen, Beerse, Belgium), sumatriptan (Zecuity®, formerly Zelrix®; NuPathe Inc., Conshohocken, PA, USA), combination of lidocaine and epinephrine (Lidosite®; Vyteris Inc., Fair Lawn, NJ, USA) (Roustit, Blaise et al. 2014). Similarly, our previous investigations proved

that iontophoretic topical co-delivery of imatinib and siRNA using gold nanoparticles is a promising approach to the effective treatment of melanoma (Labala, Jose et al. 2017).

4.5. Conclusion

Cationic liposomes made up of DOTAP and DOPE can be used as a nanocarrier for the co-delivery of curcumin and siRNA. The cationic liposomes can further be transported through skin after application of anodal iontophoresis. The combination of curcumin and STAT3 siRNA resulted in greater B16F10 cancer cell growth inhibition compared with individual agents, while the blank cationic liposomes did not show cytotoxicity. Similarly, co-administration of curcumin and STAT3 siRNA was effective in controlling the melanoma tumor progression compared with either liposomal curcumin or STAT3 siRNA alone. Furthermore, the topical non-invasive application of curcumin loaded cationic liposome-STAT3 siRNA complex using iontophoresis showed similar tumor suppression compared with intratumoral administration.

Chapter 5

Summary and conclusions

5. Summary and conclusions

In the present work, we have investigated the feasibility of transcutaneous co-delivery of two micro-molecules, tamoxifen and imatinib mesylate using temperature sensitive liposomes to treat breast cancer. Additionally, cationic liposomes containing surface active agents were investigated for the co-delivery of a small molecule, curcumin along with a macro-molecule, STAT3 siRNA for the treatment of skin cancer.

Temperature sensitive liposomes made up of DPPC, MPPC and span 80 co-encapsulated tamoxifen and imatinib mesylate with sufficient loading and encapsulation efficiency. Inclusion of span 80 in the liposomal composition enhanced the elasticity of liposomes and thereby improved skin permeation. Average particle size of liposomes remained less than 200 nm, ideal for transdermal application and the nano-carriers were found to be stable for more than one month when stored at 2-8^{o}C. Temperature dependent release studies showed more than 80% release of both tamoxifen and imatinib from the liposomes at temperature above 39^{o}C.

These liposomes were taken up by both MCF-7 and MDA-MB-231 cells within 30 minutes of incubation. Cell viability studies showed that co-delivery of tamoxifen and imatinib significantly enhanced cell growth inhibition of MCF-7 and MDA-MB-231 cells compared to individual agents. Liposomes heated at 40^{o}C to release the drugs outside the cells showed enhanced cell growth inhibition compared to those at 37^{o}C. Skin permeation studies showed significant increase in the amount of drug retained in SC and viable epidermis after application of mild hyperthermia.

Further, to improve the skin permeation by iontophoresis and to incorporate negatively charged siRNA, cationic liposomes were prepared using DOTAP, DOPE and sodium cholate. The

encapsulation efficiency of curcumin within cationic liposomes was more than 80% and sodium cholate significantly improved the elasticity of liposomes. N/P ratio of 10:1 resulted in sufficient complexation of siRNA with curcumin loaded cationic liposomes. The liposome-siRNA complex remained stable for more than one month when stored at 2-8^{o}C.

Cell uptake studies showed that curcumin loaded liposome-siRNA complex was taken up by A431 cells within 30 minutes, predominantly through clathrin mediated pathway. Cell viability, apoptosis and in-vitro gene silencing studies showed significant enhancement in cell growth inhibition and protein suppression by the co-delivery of curcumin and STAT3 siRNA compared to individual agents. Skin permeation studies showed significant enhancement in skin permeation upon iontophoresis compared to passive application.

In-vivo studies showed significant reduction in tumor weight and tumor volume by iontophoretic application of curcumin loaded liposome-siRNA complex compared with individual agents. Iontophoresis significantly reduced tumor progression compared with passive application of the same formulations. Results of in-vivo gene silencing and immunohistochemistry studies showed significant STAT3 suppression in those animals treated with iontophoretic application of curcumin loaded liposome-siRNA complex compared with individual agents.

Overall, this study demonstrates that liposomes can be utilized for topical iontophoretic co-delivery of small and macro-molecules for the treatment of various cancers including skin and breast cancer.

Future scope and directions

The direct outcome of this research led to the development of lipid based nanocarriers for the transcutaneous co-delivery of therapeutic agents for the treatment of various types of cancer.

In case of co-delivery of tamoxifen and imatinib using temperature sensitive liposomes, results of cell viability studies are promising as the co-delivery significantly enhanced the cell growth inhibition compared to individual agents. But, the amount of drugs permeated across the skin after ex-vivo experiments did not show much improvement compared to drug solution. This can be improved by passive methods like inclusion of chemical permeation enhancers or by active physical permeation enhancement techniques like iontophoresis.

Future studies based on this work could include in-vivo studies with mild hyperthermia to verify the efficacy of this delivery system in improving the therapeutic outcome of breast cancer chemotherapy.

Transcutaneous iontophoretic co-delivery of curcumin and STAT3 siRNA significantly reduced the tumor weight and tumor volume compared to individual therapies in mice melanoma model. Based on the results of our investigations, cationic liposomes containing surface active agents could be used for the transcutaneous iontophoretic co-delivery of hydrophilic or hydrophobic anticancer drugs along with genes to improve the therapeutic outcome of cancer therapy in various types of cancer.

Future studies based on this work could include investigation of pharmacokinetic parameters of curcumin and STAT3 siRNA upon transcutaneous co-delivery using liposomes.

References

"<Skin Cancer Prevention and Early detection.pdf>."

Abraham, W. and D. T. Downing (1992). "Lamellar structures formed by stratum corneum lipids in vitro: a deuterium nuclear magnetic resonance (NMR) study." Pharmaceutical research **9**(11): 1415-1421.

Aggarwal, B. B., A. Kumar and A. C. Bharti (2003). "Anticancer potential of curcumin: preclinical and clinical studies." Anticancer res **23**(1A): 363-398.

Akomeah, F., T. Nazir, G. P. Martin and M. B. Brown (2004). "Effect of heat on the percutaneous absorption and skin retention of three model penetrants." European Journal of Pharmaceutical Sciences **21**(2): 337-345.

Allen, T. M. and P. R. Cullis (2004). "Drug delivery systems: entering the mainstream." Science **303**(5665): 1818-1822.

Allen, T. M. and P. R. Cullis (2013). "Liposomal drug delivery systems: from concept to clinical applications." Advanced drug delivery reviews **65**(1): 36-48.

Almeida, A. J. and E. Souto (2007). "Solid lipid nanoparticles as a drug delivery system for peptides and proteins." Advanced drug delivery reviews **59**(6): 478-490.

Alshamsan, A., S. Hamdy, J. Samuel, A. O. El-Kadi, A. Lavasanifar and H. Uludağ (2010). "The induction of tumor apoptosis in B16 melanoma following STAT3 siRNA delivery with a lipid-substituted polyethylenimine." Biomaterials **31**(6): 1420-1428.

Aparajita, V. and P. Ravikumar (2014). "Liposomes as carriers in skin ageing." Int J Curr Pharm Res **6**(3): 1-7.

Armstrong, B. K. and A. Kricker (2001). "The epidemiology of UV induced skin cancer." Journal of Photochemistry and Photobiology B: Biology **63**(1): 8-18.

Ashara, K. C., J. S. Paun, M. M. Soniwala, J. R. Chavada and N. M. Mori (2014). "Micro-emulsion based emulgel: a novel topical drug delivery system." Asian Pacific Journal of Tropical Disease **4**: S27-S32.

Athar, M., X. Tang, J. L. Lee, L. Kopelovich and A. L. Kim (2006). "Hedgehog signalling in skin development and cancer." Experimental dermatology **15**(9): 667-677.

Aungst, B. J., J. A. Blake and M. A. Hussain (1990). "Contributions of drug solubilization, partitioning, barrier disruption, and solvent permeation to the enhancement of skin permeation of various compounds with fatty acids and amines." Pharmaceutical research **7**(7): 712-718.

Balch, C. M., S.-J. Soong, J. E. Gershenwald, J. F. Thompson, D. S. Reintgen, N. Cascinelli, M. Urist, K. M. McMasters, M. I. Ross and J. M. Kirkwood (2001). "Prognostic factors analysis of 17,600 melanoma patients: validation of the American Joint Committee on Cancer melanoma staging system." Journal of Clinical Oncology **19**(16): 3622-3634.

Bansal, S. S., M. Goel, F. Aqil, M. V. Vadhanam and R. C. Gupta (2011). "Advanced drug delivery systems of curcumin for cancer chemoprevention." Cancer prevention research **4**(8): 1158-1171.

Barry, B. W. (2001). "Novel mechanisms and devices to enable successful transdermal drug delivery." European journal of pharmaceutical sciences **14**(2): 101-114.

Benson, H. A. (2005). "Transdermal drug delivery: penetration enhancement techniques." Current drug delivery **2**(1): 23-33.

Bhavsar, D., K. Subramanian, S. Sethuraman and U. Maheswari Krishnan (2012). "Translational siRNA therapeutics using liposomal carriers: prospects & challenges." Current gene therapy **12**(4): 315-332.

Bill, M. A., C. Nicholas, T. A. Mace, J. P. Etter, C. Li, E. B. Schwartz, J. R. Fuchs, G. S. Young, L. Lin and J. Lin (2012). "Structurally modified curcumin analogs inhibit STAT3 phosphorylation and promote apoptosis of human renal cell carcinoma and melanoma cell lines." PloS one **7**(8): e40724.

Bisby, R. H., C. Mead and C. G. Morgan (2000). "Wavelength-programmed solute release from photosensitive liposomes." Biochemical and biophysical research communications **276**(1): 169-173.

Bish, A., A. Ramirez, C. Burgess and M. Hunter (2005). "Understanding why women delay in seeking help for breast cancer symptoms." Journal of psychosomatic research **58**(4): 321-326.

Bitounis, D., R. Fanciullino, A. Iliadis and J. Ciccolini (2012). "Optimizing druggability through liposomal formulations: new approaches to an old concept." ISRN pharmaceutics **2012**.

Bonilla, X., L. Parmentier, B. King, F. Bezrukov, G. Kaya, V. Zoete, V. B. Seplyarskiy, H. J. Sharpe, T. McKee and A. Letourneau (2016). "Genomic analysis identifies new drivers and progression pathways in skin basal cell carcinoma." Nature genetics.

Bonneterre, J., A. Buzdar, J. M. A. Nabholtz, J. F. Robertson, B. Thürlimann, M. von Euler, T. Sahmoud, A. Webster and M. Steinberg (2001). "Anastrozole is superior to tamoxifen as first-line therapy in hormone receptor positive advanced breast carcinoma." Cancer **92**(9): 2247-2258.

Borst, P., R. Evers, M. Kool and J. Wijnholds (2000). "A family of drug transporters: the multidrug resistance-associated proteins." Journal of the National Cancer Institute **92**(16): 1295-1302.

Bos, J. D. and M. M. Meinardi (2000). "The 500 Dalton rule for the skin penetration of chemical compounds and drugs." Experimental dermatology **9**(3): 165-169.

Bouwes Bavinck, J., B. Vermeer, F. Claas and J. Schegget (1994). "Skin cancer and renal transplantation." Journal of nephrology **7**: 261-261.

Bracke, S., M. Carretero, S. Guerrero-Aspizua, E. Desmet, N. Illera, M. Navarro, J. Lambert and M. Del Rio (2014). "Targeted silencing of DEFB4 in a bioengineered skin-humanized mouse model for psoriasis: development of siRNA SECosome-based novel therapies." Experimental dermatology **23**(3): 199-201.

Brash, D. E., J. A. Rudolph, J. A. Simon, A. Lin, G. J. McKenna, H. P. Baden, A. J. Halperin and J. Ponten (1991). "A role for sunlight in skin cancer: UV-induced p53 mutations in squamous cell carcinoma." Proceedings of the National Academy of Sciences **88**(22): 10124-10128.

Brigger, I., C. Dubernet and P. Couvreur (2002). "Nanoparticles in cancer therapy and diagnosis." Advanced drug delivery reviews **54**(5): 631-651.

Bromberg, J. (2002). "Stat proteins and oncogenesis." The Journal of clinical investigation **109**(9): 1139-1142.

Brown, M. B., G. P. Martin, S. A. Jones and F. K. Akomeah (2006). "Dermal and transdermal drug delivery systems: current and future prospects." Drug delivery **13**(3): 175-187.

Burkoth, T. L., B. J. Bellhouse, G. Hewson, D. J. Longridge, A. G. Muddle and D. F. Sarphie (1999). "Transdermal and transmucosal powdered drug delivery." Critical Reviews™ in Therapeutic Drug Carrier Systems **16**(4).

Cevc, G. and G. Blume (1992). "Lipid vesicles penetrate into intact skin owing to the transdermal osmotic gradients and hydration force." Biochimica et Biophysica Acta (BBA)-Biomembranes **1104**(1): 226-232.

Cevc, G., D. Gebauer, J. Stieber, A. Schätzlein and G. Blume (1998). "Ultraflexible vesicles, Transfersomes, have an extremely low pore penetration resistance and transport therapeutic

amounts of insulin across the intact mammalian skin." Biochimica et Biophysica Acta (BBA)-Biomembranes **1368**(2): 201-215.

Chainani-Wu, N. (2003). "Safety and anti-inflammatory activity of curcumin: a component of tumeric (Curcuma longa)." The Journal of Alternative & Complementary Medicine **9**(1): 161-168.

Chaudhary, P. M. and I. B. Roninson (1993). "Induction of multidrug resistance in human cells by transient exposure to different chemotherapeutic drugs." JNCI: Journal of the National Cancer Institute **85**(8): 632-639.

Chen, Y., Q. Wu, Z. Zhang, L. Yuan, X. Liu and L. Zhou (2012). "Preparation of curcumin-loaded liposomes and evaluation of their skin permeation and pharmacodynamics." Molecules **17**(5): 5972-5987.

Choi, Y. J., S. J. Kang, Y. J. Kim, Y.-b. Lim and H. W. Chung (2010). "Comparative studies on the genotoxicity and cytotoxicity of polymeric gene carriers polyethylenimine (PEI) and polyamidoamine (PAMAM) dendrimer in Jurkat T-cells." Drug and chemical toxicology **33**(4): 357-366.

Chou, T.-C. (2010). "Drug combination studies and their synergy quantification using the Chou-Talalay method." Cancer research **70**(2): 440-446.

Clarys, P., K. Alewaeters, A. Jadoul, A. Barel, R. O. Manadas and V. Préat (1998). "In vitro percutaneous penetration through hairless rat skin: influence of temperature, vehicle and penetration enhancers." European journal of pharmaceutics and biopharmaceutics **46**(3): 279-283.

Cleator, S., W. Heller and R. C. Coombes (2007). "Triple-negative breast cancer: therapeutic options." The lancet oncology **8**(3): 235-244.

Cohen, M. H., G. Williams, J. R. Johnson, J. Duan, J. Gobburu, A. Rahman, K. Benson, J. Leighton, S. K. Kim and R. Wood (2002). "Approval summary for imatinib mesylate capsules in the treatment of chronic myelogenous leukemia." Clinical Cancer Research **8**(5): 935-942.

Cristofanilli, M., P. Morandi, S. Krishnamurthy, J. Reuben, B.-N. Lee, D. Francis, D. Booser, M. Green, B. Arun and L. Pusztai (2008). "Imatinib mesylate (Gleevec®) in advanced breast cancer-expressing C-Kit or PDGFR-β: clinical activity and biological correlations." Annals of oncology: mdn352.

Crocker, P., K. Maynard and M. Little (2001). "Pain free blunt needle injection technology." Innov. Pharmaceut. technol **9**: 111-115.

Danhier, F., O. Feron and V. Préat (2010). "To exploit the tumor microenvironment: passive and active tumor targeting of nanocarriers for anti-cancer drug delivery." Journal of Controlled Release **148**(2): 135-146.

Darnell, J. E. (2002). "Transcription factors as targets for cancer therapy." Nature Reviews Cancer **2**(10): 740-749.

Darnell Jr, J. E., I. M. Kerr and G. R. Stark (1994). "Jak-STAT pathways and transcriptional activation in response to IFNs and other extracellular signaling proteins." Science-AAAS-weekly paper edition-including guide to scientific information **264**(5164): 1415-1420.

Davies, H., G. R. Bignell, C. Cox, P. Stephens, S. Edkins, S. Clegg, J. Teague, H. Woffendin, M. J. Garnett and W. Bottomley (2002). "Mutations of the BRAF gene in human cancer." Nature **417**(6892): 949-954.

Deinlein, T., G. Richtig, C. Schwab, F. Scarfi, E. Arzberger, I. Wolf, R. Hofmann-Wellenhof and I. Zalaudek (2016). "The use of dermatoscopy in diagnosis and therapy of nonmelanocytic skin cancer." JDDG: Journal der Deutschen Dermatologischen Gesellschaft **14**(2): 144-151.

del Pozo-Rodríguez, A., D. Delgado, M. Á. Solinís, J. L. Pedraz, E. Echevarría, J. M. Rodríguez and A. R. Gascón (2010). "Solid lipid nanoparticles as potential tools for gene therapy: in vivo protein expression after intravenous administration." International journal of pharmaceutics **385**(1): 157-162.

Demetri, G. D., M. Von Mehren, C. D. Blanke, A. D. Van den Abbeele, B. Eisenberg, P. J. Roberts, M. C. Heinrich, D. A. Tuveson, S. Singer and M. Janicek (2002). "Efficacy and safety of imatinib mesylate in advanced gastrointestinal stromal tumors." New England Journal of Medicine **347**(7): 472-480.

Denet, A.-R., R. Vanbever and V. Préat (2004). "Skin electroporation for transdermal and topical delivery." Advanced drug delivery reviews **56**(5): 659-674.

Desai, P. R., S. Marepally, A. R. Patel, C. Voshavar, A. Chaudhuri and M. Singh (2013). "Topical delivery of anti-TNFα siRNA and capsaicin via novel lipid-polymer hybrid nanoparticles efficiently inhibits skin inflammation in vivo." Journal of Controlled Release **170**(1): 51-63.

Desmet, E., M. Van Gele and J. Lambert (2017). "Topically applied lipid-and surfactant-based nanoparticles in the treatment of skin disorders." Expert Opinion on Drug Delivery **14**(1): 109-122.

Deveraux, Q. L., N. Roy, H. R. Stennicke, T. Van Arsdale, Q. Zhou, S. M. Srinivasula, E. S. Alnemri, G. S. Salvesen and J. C. Reed (1998). "IAPs block apoptotic events induced by caspase-8 and cytochrome c by direct inhibition of distinct caspases." The EMBO journal **17**(8): 2215-2223.

Dhote, V., P. Bhatnagar, P. K. Mishra, S. C. Mahajan and D. K. Mishra (2011). "Iontophoresis: a potential emergence of a transdermal drug delivery system." Scientia pharmaceutica **80**(1): 1-28.

Dienstmann, R., J. Rodon, V. Serra and J. Tabernero (2014). "Picking the point of inhibition: a comparative review of PI3K/AKT/mTOR pathway inhibitors." Molecular cancer therapeutics **13**(5): 1021-1031.

Diepgen, T. L. and V. Mahler (2002). "The epidemiology of skin cancer." British Journal of Dermatology **146**(s61): 1-6.

Dolcet, X., D. Llobet, J. Pallares and X. Matias-Guiu (2005). "NF-kB in development and progression of human cancer." Virchows archiv **446**(5): 475-482.

Domb, A. J. (2005). Lipospheres for controlled delivery of substances. Microencapsulation: Methods and Industrial Applications, Second Edition, Informa Healthcare**:** 297-316.

Dreier, J., J. A. Sørensen and J. R. Brewer (2016). "Superresolution and fluorescence dynamics evidence reveal that intact liposomes do not cross the human skin barrier." PloS one **11**(1): e0146514.

Duan, D., C. Moeckly, J. Gysbers, C. Novak, G. Prochnow, K. Siebenaler, L. Albers and K. Hansen (2011). "Enhanced delivery of topically-applied formulations following skin pre-treatment with a hand-applied, plastic microneedle array." Current drug delivery **8**(5): 557-565.

Dubey, S. and Y. Kalia (2010). "Non-invasive iontophoretic delivery of enzymatically active ribonuclease A (13.6 kDa) across intact porcine and human skins." Journal of controlled release **145**(3): 203-209.

Dudala, T. B., P. R. Yalavarthi, H. C. Vadlamudi, J. Thanniru, G. Yaga, N. L. Mudumala and V. K. Pasupati (2014). "A perspective overview on lipospheres as lipid carrier systems." International journal of pharmaceutical investigation **4**(4): 149-155.

Dunne, M., J. Zheng, J. Rosenblat, D. A. Jaffray and C. Allen (2011). "APN/CD13-targeting as a strategy to alter the tumor accumulation of liposomes." Journal of controlled release **154**(3): 298-305.

Elias, P. M. (1983). "Epidermal lipids, barrier function, and desquamation." Journal of Investigative Dermatology **80**.

Eljarrat-Binstock, E., F. Orucov, Y. Aldouby, J. Frucht-Pery and A. J. Domb (2008). "Charged nanoparticles delivery to the eye using hydrogel iontophoresis." Journal of Controlled Release **126**(2): 156-161.

Elsayed, M. M., O. Y. Abdallah, V. F. Naggar and N. M. Khalafallah (2006). "Deformable liposomes and ethosomes: mechanism of enhanced skin delivery." International journal of pharmaceutics **322**(1): 60-66.

Epstein, J., I. R. Sanderson and T. T. MacDonald (2010). "Curcumin as a therapeutic agent: the evidence from in vitro, animal and human studies." British journal of nutrition **103**(11): 1545-1557.

Erdő, F., N. Hashimoto, G. Karvaly, N. Nakamichi and Y. Kato (2016). "Critical evaluation and methodological positioning of the transdermal microdialysis technique. A review." Journal of Controlled Release **233**: 147-161.

Esfand, R. and D. A. Tomalia (2001). "Poly (amidoamine)(PAMAM) dendrimers: from biomimicry to drug delivery and biomedical applications." Drug discovery today **6**(8): 427-436.

Etheridge, M. L., S. A. Campbell, A. G. Erdman, C. L. Haynes, S. M. Wolf and J. McCullough (2013). "The big picture on nanomedicine: the state of investigational and approved nanomedicine products." Nanomedicine: nanotechnology, biology and medicine **9**(1): 1-14.

Fan, L., F. Li, H. Zhang, Y. Wang, C. Cheng, X. Li, C.-h. Gu, Q. Yang, H. Wu and S. Zhang (2010). "Co-delivery of PDTC and doxorubicin by multifunctional micellar nanoparticles to achieve active targeted drug delivery and overcome multidrug resistance." Biomaterials **31**(21): 5634-5642.

Feingold, K. R. (2007). "Thematic review series: skin lipids. The role of epidermal lipids in cutaneous permeability barrier homeostasis." Journal of lipid research **48**(12): 2531-2546.

Finnin, B. C. and T. M. Morgan (1999). "Transdermal penetration enhancers: applications, limitations, and potential." Journal of pharmaceutical sciences **88**(10): 955-958.

Fireman, S., O. Toledano, K. Neimann, N. Loboda and N. Dayan (2011). "A look at emerging delivery systems for topical drug products." Dermatologic therapy **24**(5): 477-488.

Fisher, B., J. P. Costantino, D. L. Wickerham, C. K. Redmond, M. Kavanah, W. M. Cronin, V. Vogel, A. Robidoux, N. Dimitrov and J. Atkins (1998). "Tamoxifen for prevention of breast cancer: report of the National Surgical Adjuvant Breast and Bowel Project P-1 Study." Journal of the National Cancer Institute **90**(18): 1371-1388.

Fleige, E., M. A. Quadir and R. Haag (2012). "Stimuli-responsive polymeric nanocarriers for the controlled transport of active compounds: concepts and applications." Advanced drug delivery reviews **64**(9): 866-884.

Florence, A. (1993). "Nonionic surfactant vesicles: preparation and characterization." Liposome technology **2**: 157-176.

Forouzanfar, M. H., A. Afshin, L. T. Alexander, H. R. Anderson, Z. A. Bhutta, S. Biryukov, M. Brauer, R. Burnett, K. Cercy and F. J. Charlson (2016). "Global, regional, and national comparative risk assessment of 79 behavioural, environmental and occupational, and metabolic risks or clusters of risks, 1990-2015." Lancet.

Forslind, B. (1994). "A domain mosaic model of the skin barrier." Acta dermatovenereologica-stockholm- **74**: 1-1.

Franceschi, S., F. Levi, L. Randimbison and C. La Vecchia (1996). "Site distribution of different types of skin cancer: new aetiological clues." International journal of cancer **67**(1): 24-28.

Gandhi, N. S., R. K. Tekade and M. B. Chougule (2014). "Nanocarrier mediated delivery of siRNA/miRNA in combination with chemotherapeutic agents for cancer therapy: current progress and advances." Journal of Controlled Release **194**: 238-256.

Gandini, S., F. Sera, M. S. Cattaruzza, P. Pasquini, O. Picconi, P. Boyle and C. F. Melchi (2005). "Meta-analysis of risk factors for cutaneous melanoma: II. Sun exposure." European journal of cancer **41**(1): 45-60.

Garg, T. and A. Kumar Goyal (2012). "Iontophoresis: drug delivery system by applying an electrical potential across the skin." Drug delivery letters **2**(4): 270-280.

Garg, T., B. Malik, G. Rath and A. K. Goyal (2014). "Development and characterization of nano-fiber patch for the treatment of glaucoma." European Journal of Pharmaceutical Sciences **53**: 10-16.

Garg, T., S. Singh and A. K. Goyal (2013). "Stimuli-sensitive hydrogels: an excellent carrier for drug and cell delivery." Critical Reviews™ in Therapeutic Drug Carrier Systems **30**(5).

Garnett, M. J. and R. Marais (2004). "Guilty as charged: B-RAF is a human oncogene." Cancer cell **6**(4): 313-319.

Geusens, B., J. Lambert, S. De Smedt, K. Buyens, N. Sanders and M. Van Gele (2009). "Ultradeformable cationic liposomes for delivery of small interfering RNA (siRNA) into human primary melanocytes." Journal of Controlled Release **133**(3): 214-220.

Geusens, B., M. Van Gele, S. Braat, S. C. De Smedt, M. C. Stuart, T. W. Prow, W. Sanchez, M. S. Roberts, N. N. Sanders and J. Lambert (2010). "Flexible nanosomes (SECosomes) enable efficient siRNA delivery in cultured primary skin cells and in the viable epidermis of ex vivo human skin." Advanced Functional Materials **20**(23): 4077-4090.

Ghaffarian, R. and S. Muro (2013). "Models and methods to evaluate transport of drug delivery systems across cellular barriers." JoVE (Journal of Visualized Experiments)(80): e50638-e50638.

Ghafouri-Fard, S. and S. Ghafouri-Fard (2012). "Immunotherapy in nonmelanoma skin cancer."

Ghosh*, T. K., W. Abraham and B. R. Jasti (2004). Transdermal and topical drug delivery systems. Theory and practice of contemporary pharmaceutics, CRC Press**:** 423-455.

Giavedoni, P., S. Puig and C. Carrera (2016). Noninvasive imaging for nonmelanoma skin cancer. Seminars in cutaneous medicine and surgery, Frontline Medical Communications.

Gilchrest, B. A., M. S. Eller, A. C. Geller and M. Yaar (1999). "The pathogenesis of melanoma induced by ultraviolet radiation." New England Journal of Medicine **340**(17): 1341-1348.

Goldberg, L. H. (1996). "Basal cell carcinoma." The Lancet **347**(9002): 663-667.

Göppner, D. and M. Leverkus (2010). "Basal cell carcinoma: from the molecular understanding of the pathogenesis to targeted therapy of progressive disease." Journal of skin cancer **2011**.

Gottesman, M. M., T. Fojo and S. E. Bates (2002). "Multidrug resistance in cancer: role of ATP–dependent transporters." Nature Reviews Cancer **2**(1): 48-58.

Goyal, R., L. K. Macri, H. M. Kaplan and J. Kohn (2016). "Nanoparticles and nanofibers for topical drug delivery." Journal of Controlled Release **240**: 77-92.

Gray-Schopfer, V., C. Wellbrock and R. Marais (2007). "Melanoma biology and new targeted therapy." Nature **445**(7130): 851-857.

Greene, G. L., N. B. Sobel, W. King and E. V. Jensen (1984). "Immunochemical studies of estrogen receptors." Journal of steroid biochemistry **20**(1): 51-56.

Guo, J., L. Si, Y. Kong, K. T. Flaherty, X. Xu, Y. Zhu, C. L. Corless, L. Li, H. Li and X. Sheng (2011). "Phase II, open-label, single-arm trial of imatinib mesylate in patients with metastatic melanoma harboring c-Kit mutation or amplification." Journal of Clinical Oncology **29**(21): 2904-2909.

Gupta, M., U. Agrawal and S. P. Vyas (2012). "Nanocarrier-based topical drug delivery for the treatment of skin diseases." Expert opinion on drug delivery **9**(7): 783-804.

Guy, R. H., Y. N. Kalia, M. B. Delgado-Charro, V. Merino, A. Lopez and D. Marro (2000). "Iontophoresis: electrorepulsion and electroosmosis." Journal of controlled release **64**(1): 129-132.

Haftek, M., M. H. Teillon and D. Schmitt (1998). "Stratum corneum, corneodesmosomes and ex vivo percutaneous penetration." Microscopy research and technique **43**(3): 242-249.

Han, I., M. Kim and J. Kim (2004). "Enhanced transfollicular delivery of adriamycin with a liposome and iontophoresis." Experimental dermatology **13**(2): 86-92.

Hannon, G. J. (2002). "RNA interference." Nature **418**(6894): 244-251.

Hasan, M., N. Belhaj, H. Benachour, M. Barberi-Heyob, C. Kahn, E. Jabbari, M. Linder and E. Arab-Tehrany (2014). "Liposome encapsulation of curcumin: physico-chemical characterizations and effects on MCF7 cancer cell proliferation." International journal of pharmaceutics **461**(1): 519-528.

Hawrot, A., M. Alam and D. Ratner (2003). "Squamous cell carcinoma." Current Problems in Dermatology **15**(3): 91-133.

Heinrich, M. C., K. Owzar, C. L. Corless, D. Hollis, E. C. Borden, C. D. Fletcher, C. W. Ryan, M. Von Mehren, C. D. Blanke and C. Rankin (2008). "Correlation of kinase genotype and clinical outcome in the North American Intergroup Phase III Trial of imatinib mesylate for treatment of advanced gastrointestinal stromal tumor: CALGB 150105 Study by Cancer and Leukemia Group B and Southwest Oncology Group." Journal of clinical oncology **26**(33): 5360-5367.

Herr, N. R., B. M. Kile, R. M. Carelli and R. M. Wightman (2008). "Electroosmotic flow and its contribution to iontophoretic delivery." Analytical chemistry **80**(22): 8635-8641.

Hervella, P., V. Lozano, M. Garcia-Fuentes and M. J. Alonso (2008). "Nanomedicine: new challenges and opportunities in cancer therapy." Journal of Biomedical Nanotechnology **4**(3): 276-292.

Hiruta, Y., Y. Hattori, K. Kawano, Y. Obata and Y. Maitani (2006). "Novel ultra-deformable vesicles entrapped with bleomycin and enhanced to penetrate rat skin." Journal of controlled release **113**(2): 146-154.

Hsu, T. and S. Mitragotri (2011). "Delivery of siRNA and other macromolecules into skin and cells using a peptide enhancer." Proceedings of the National Academy of Sciences **108**(38): 15816-15821.

Hu, F., K. Neoh and E. Kang (2006). "Synthesis and in vitro anti-cancer evaluation of tamoxifen-loaded magnetite/PLLA composite nanoparticles." Biomaterials **27**(33): 5725-5733.

Hu, L., Y. Shi, J. H. Li, N. Gao, J. Ji, F. Niu, Q. Chen, X. Yang and S. Wang (2015). "Enhancement of oral bioavailability of curcumin by a novel solid dispersion system." Aaps Pharmscitech **16**(6): 1327-1334.

Hua, S. (2015). "Lipid-based nano-delivery systems for skin delivery of drugs and bioactives." Frontiers in pharmacology **6**: 219.

Hui, S. W., M. Langner, Y.-L. Zhao, P. Ross, E. Hurley and K. Chan (1996). "The role of helper lipids in cationic liposome-mediated gene transfer." Biophysical journal **71**(2): 590-599.

Huzil, J. T., S. Sivaloganathan, M. Kohandel and M. Foldvari (2011). "Drug delivery through the skin: molecular simulations of barrier lipids to design more effective noninvasive dermal and transdermal delivery systems for small molecules, biologics, and cosmetics." Wiley Interdiscip Rev Nanomed Nanobiotechnol **3**(5): 449-462.

Igney, F. H. and P. H. Krammer (2002). "Death and anti-death: tumour resistance to apoptosis." Nature Reviews Cancer **2**(4): 277-288.

Immordino, M. L., F. Dosio and L. Cattel (2006). "Stealth liposomes: review of the basic science, rationale, and clinical applications, existing and potential." International journal of nanomedicine **1**(3): 297.

Iwamoto, T. (2013). "Clinical application of drug delivery systems in cancer chemotherapy: review of the efficacy and side effects of approved drugs." Biological and Pharmaceutical Bulletin **36**(5): 715-718.

Jain, K. K. (2008). "Drug delivery systems-an overview." Drug delivery systems: 1-50.

Jain, M. (2017). "Past, present, and future of molecular oncology in India." International Journal of Molecular and Immuno Oncology **2**(1): 1-3.

Jain, S., N. Patel, M. K. Shah, P. Khatri and N. Vora (2016). "Recent Advances in Lipid-Based Vesicles and Particulate Carriers for Topical and Transdermal Application." Journal of Pharmaceutical Sciences.

Jain, S., N. Patel, M. K. Shah, P. Khatri and N. Vora (2017). "Recent Advances in Lipid-Based Vesicles and Particulate Carriers for Topical and Transdermal Application." J Pharm Sci **106**(2): 423-445.

Jemal, A., F. Bray, M. M. Center, J. Ferlay, E. Ward and D. Forman (2011). "Global cancer statistics." CA: a cancer journal for clinicians **61**(2): 69-90.

Jensen, L. B., K. Petersson and H. M. Nielsen (2011). "In vitro penetration properties of solid lipid nanoparticles in intact and barrier-impaired skin." European Journal of Pharmaceutics and Biopharmaceutics **79**(1): 68-75.

Jiang, Q., S. Zheng and G. Wang (2013). "Development of new estrogen receptor-targeting therapeutic agents for tamoxifen-resistant breast cancer." Future **5**(9): 1023-1035.

Jose, A., S. Labala and V. V. K. Venuganti (2016). "Co-delivery of curcumin and STAT3 siRNA using deformable cationic liposomes to treat skin cancer." Journal of Drug Targeting: 1-15.

Jose, A., P. K. Mandapalli and V. V. K. Venuganti (2016). "Liposomal hydrogel formulation for transdermal delivery of pirfenidone." Journal of liposome research **26**(2): 139-147.

Joy, A., M. Ghosh, R. Fernandes and M. Clemons (2015). "Systemic treatment approaches in her2-negative advanced breast cancer—guidance on the guidelines." Current Oncology **22**(Suppl 1): S29.

Kajimoto, K., M. Yamamoto, M. Watanabe, K. Kigasawa, K. Kanamura, H. Harashima and K. Kogure (2011). "Noninvasive and persistent transfollicular drug delivery system using a combination of liposomes and iontophoresis." International journal of pharmaceutics **403**(1): 57-65.

Kalderon, D. (2005). The mechanism of hedgehog signal transduction, Portland Press Limited.

Kalepu, S. and V. Nekkanti (2015). "Insoluble drug delivery strategies: review of recent advances and business prospects." Acta Pharmaceutica Sinica B **5**(5): 442-453.

Kamel Hassan, A. O. and A. H. Elshafeey (2010). "Nanosized particulate systems for dermal and transdermal delivery." Journal of biomedical nanotechnology **6**(6): 621-633.

Kang, L., Z. Gao, W. Huang, M. Jin and Q. Wang (2015). "Nanocarrier-mediated co-delivery of chemotherapeutic drugs and gene agents for cancer treatment." Acta Pharmaceutica Sinica B **5**(3): 169-175.

Karewicz, A., D. Bielska, B. Gzyl-Malcher, M. Kepczynski, R. Lach and M. Nowakowska (2011). "Interaction of curcumin with lipid monolayers and liposomal bilayers." Colloids and Surfaces B: Biointerfaces **88**(1): 231-239.

Kay, M. A. (2011). "State-of-the-art gene-based therapies: the road ahead." Nature Reviews Genetics **12**(5): 316-328.

Khan, M., Z. Y. Ong, N. Wiradharma, A. B. E. Attia and Y. Y. Yang (2012). "Advanced materials for co-delivery of drugs and genes in cancer therapy." Advanced healthcare materials **1**(4): 373-392.

Kim, H.-K., E. Davaa, C.-S. Myung and J.-S. Park (2010). "Enhanced siRNA delivery using cationic liposomes with new polyarginine-conjugated PEG-lipid." International journal of pharmaceutics **392**(1): 141-147.

Kim, M.-J., H. J. Lee, I.-A. Lee, I.-Y. Kim, S.-K. Lim, H.-A. Cho and J.-S. Kim (2008). "Preparation of pH-sensitive, long-circulating and EGFR-targeted immunoliposomes." Archives of pharmacal research **31**(4): 539-546.

Kim, M.-k., G.-j. Choi and H.-s. Lee (2003). "Fungicidal property of Curcuma longa L. rhizome-derived curcumin against phytopathogenic fungi in a greenhouse." Journal of agricultural and food chemistry **51**(6): 1578-1581.

Kim, T. H., H. H. Jiang, Y. S. Youn, C. W. Park, K. K. Tak, S. Lee, H. Kim, S. Jon, X. Chen and K. C. Lee (2011). "Preparation and characterization of water-soluble albumin-bound curcumin nanoparticles with improved antitumor activity." International journal of pharmaceutics **403**(1): 285-291.

Kim, Y.-C., J.-H. Park and M. R. Prausnitz (2012). "Microneedles for drug and vaccine delivery." Advanced drug delivery reviews **64**(14): 1547-1568.

Kirby, J. S. and C. J. Miller (2010). "Intralesional chemotherapy for nonmelanoma skin cancer: a practical review." Journal of the American Academy of Dermatology **63**(4): 689-702.

Klareskog, L., U. M. Tjernlund, U. Forsum and P. A. Peterson (1977). "Epidermal Langerhans cells express Ia antigens."

Klemsdal, T., K. Gjesdal and J.-E. Bredesen (1992). "Heating and cooling of the nitroglycerin patch application area modify the plasma level of nitroglycerin." European journal of clinical pharmacology **43**(6): 625-628.

Korkola, J. E., S. DeVries, J. Fridlyand, E. S. Hwang, A. L. Estep, Y.-Y. Chen, K. L. Chew, S. H. Dairkee, R. M. Jensen and F. M. Waldman (2003). "Differentiation of lobular versus ductal breast carcinomas by expression microarray analysis." Cancer research **63**(21): 7167-7175.

Kortylewski, M., R. Jove and H. Yu (2005). "Targeting STAT3 affects melanoma on multiple fronts." Cancer and Metastasis Reviews **24**(2): 315-327.

Kortylewski, M., H. Xin, M. Kujawski, H. Lee, Y. Liu, T. Harris, C. Drake, D. Pardoll and H. Yu (2009). "Regulation of the IL-23 and IL-12 balance by Stat3 signaling in the tumor microenvironment." Cancer cell **15**(2): 114-123.

Krag, D., D. Weaver, J. Alex, J. Fairbank and et al. (1993). "Surgical resection and radiolocalization of the sentinel lymph node in breast cancer using a gamma probe." Surgical oncology **2**(6): 335-340.

Kricker, A., B. K. Armstrong and D. R. English (1994). "Sun exposure and non-melanocytic skin cancer." Cancer Causes & Control **5**(4): 367-392.

Kulkarni, S., G. Betageri and M. Singh (1995). "Factors affecting microencapsulation of drugs in liposomes." Journal of microencapsulation **12**(3): 229-246.

Kunwar, A., A. Barik, R. Pandey and K. I. Priyadarsini (2006). "Transport of liposomal and albumin loaded curcumin to living cells: an absorption and fluorescence spectroscopic study." Biochimica et Biophysica Acta (BBA)-General Subjects **1760**(10): 1513-1520.

La Porta, C. A. (2007). "Drug resistance in melanoma: new perspectives." Current medicinal chemistry **14**(4): 387-391.

La Thangue, N. B. and D. J. Kerr (2011). "Predictive biomarkers: a paradigm shift towards personalized cancer medicine." Nature reviews Clinical oncology **8**(10): 587-596.

Labala, S., A. Jose, S. Chawla, M. S. Khan, S. Bhatnagar, O. P. Kulkarni and V. V. K. Venuganti (2017). "Effective melanoma cancer suppression by iontophoretic co-delivery of STAT3 siRNA and imatinib using gold nanoparticles." International Journal of Pharmaceutics.

Lamparski, H., U. Liman, J. A. Barry, D. A. Frankel, V. Ramaswami, M. F. Brown and D. F. Obrien (1992). "Photoinduced destabilization of liposomes." Biochemistry **31**(3): 685-694.

Lampe, M. A., M. L. Williams and P. M. Elias (1983). "Human epidermal lipids: characterization and modulations during differentiation." Journal of Lipid Research **24**(2): 131-140.

Larsen, R. H., F. Nielsen, J. A. Sørensen and J. B. Nielsen (2003). "Dermal Penetration of Fentanyl: Inter-and Intraindividual Variations." Basic & Clinical Pharmacology & Toxicology **93**(5): 244-248.

Lee, W.-R., S.-C. Shen, H.-H. Lai, C.-H. Hu and J.-Y. Fang (2001). "Transdermal drug delivery enhanced and controlled by erbium: YAG laser: a comparative study of lipophilic and hydrophilic drugs." Journal of controlled release **75**(1): 155-166.

Lee, W.-R., S.-C. Shen, K.-H. Wang, C.-H. Hu and J.-Y. Fang (2003). "Lasers and microdermabrasion enhance and control topical delivery of vitamin C." Journal of investigative dermatology **121**(5): 1118-1125.

Li, C. I., B. O. Anderson, J. R. Daling and R. E. Moe (2003). "Trends in incidence rates of invasive lobular and ductal breast carcinoma." Jama **289**(11): 1421-1424.

Li, H.-F., C. Wu, M. Xia, H. Zhao, M.-X. Zhao, J. Hou, R. Li, L. Wei and L. Zhang (2015). "Targeted and controlled drug delivery using a temperature and ultra-violet responsive liposome with excellent breast cancer suppressing ability." RSC Advances **5**(35): 27630-27639.

Lin, Y.-L., C.-H. Chen, H.-Y. Wu, N.-M. Tsai, T.-Y. Jian, Y.-C. Chang, C.-H. Lin, C.-H. Wu, F.-T. Hsu and T. K. Leung (2016). "Inhibition of breast cancer with transdermal tamoxifen-encapsulated lipoplex." Journal of nanobiotechnology **14**(1): 11.

Longbridge, D., P. Sweeney, T. Burkoth and B. Bellhouse (1998). Effects of particle size and cylinder pressure on dermal powderject delivery of testosterone to conscious rabbits. Proc Int Symp Control Rel Bioact.

Lucks, J. and R. Müller (1991). "Medication vehicles made of solid lipid particles (solid lipid nanospheres SLN)." EP0000605497.

Mahato, R. I., A. Rolland and E. Tomlinson (1997). "Cationic lipid-based gene delivery systems: pharmaceutical perspectives." Pharmaceutical research **14**(7): 853-859.

Maheshwari, R. K., A. K. Singh, J. Gaddipati and R. C. Srimal (2006). "Multiple biological activities of curcumin: a short review." Life sciences **78**(18): 2081-2087.

Mandapalli, P. K., S. Labala, J. Bojja and V. V. K. Venuganti (2016). "Effect of pirfenidone delivered using layer-by-layer thin film on excisional wound healing." European Journal of Pharmaceutical Sciences **83**: 166-174.

Mangalathillam, S., N. S. Rejinold, A. Nair, V.-K. Lakshmanan, S. V. Nair and R. Jayakumar (2012). "Curcumin loaded chitin nanogels for skin cancer treatment via the transdermal route." Nanoscale **4**(1): 239-250.

Mangasarian, O. L., W. N. Street and W. H. Wolberg (1995). "Breast cancer diagnosis and prognosis via linear programming." Operations Research **43**(4): 570-577.

Manna, S. and M. K. Holz (2016). "Tamoxifen Action in ER-Negative Breast Cancer." Signal transduction insights **5**: 1.

Marais, R., Y. Light, H. Paterson and C. Marshall (1995). "Ras recruits Raf-1 to the plasma membrane for activation by tyrosine phosphorylation." The EMBO journal **14**(13): 3136.

Marais, R., Y. Light, H. F. Paterson, C. S. Mason and C. J. Marshall (1997). "Differential regulation of Raf-1, A-Raf, and B-Raf by oncogenic ras and tyrosine kinases." Journal of Biological Chemistry **272**(7): 4378-4383.

Marin, S., G. Mihail Vlasceanu, R. Elena Tiplea, I. Raluca Bucur, M. Lemnaru, M. Minodora Marin and A. Mihai Grumezescu (2015). "Applications and toxicity of silver nanoparticles: a recent review." Current topics in medicinal chemistry **15**(16): 1596-1604.

Marks, R. (1996). "Squamous cell carcinoma." The Lancet **347**(9003): 735-738.

Martinez, J.-C. and C. C. Otley (2001). The management of melanoma and nonmelanoma skin cancer: a review for the primary care physician. Mayo Clinic Proceedings, Elsevier.

Martins, S., B. Sarmento, D. C. Ferreira and E. B. Souto (2007). "Lipid-based colloidal carriers for peptide and protein delivery-liposomes versus lipid nanoparticles." International journal of nanomedicine **2**(4): 595.

Marwah, H., T. Garg, A. K. Goyal and G. Rath (2016). "Permeation enhancer strategies in transdermal drug delivery." Drug delivery **23**(2): 564-578.

McCubrey, J. A., M. Milella, A. Tafuri, A. M. Martelli, P. Lunghi, A. Bonati, M. Cervello, J. T. Lee and L. S. Steelman (2008). "Targeting the Raf/MEK/ERK pathway with small-molecule inhibitors." Current opinion in investigational drugs (London, England: 2000) **9**(6): 614-630.

McIntosh, T., S. Advani, R. Burton, D. Zhelev, D. Needham and S. Simon (1995). "Experimental tests for protrusion and undulation pressures in phospholipid bilayers." Biochemistry **34**(27): 8520-8532.

McManus, M. T. and P. A. Sharp (2002). "Gene silencing in mammals by small interfering RNAs." Nature reviews genetics **3**(10): 737-747.

McPherson, K., C. Steel and J. Dixon (2000). "ABC of breast diseases: breast cancer—epidemiology, risk factors, and genetics." BMJ: British Medical Journal **321**(7261): 624.

McPherson, K., C. Steel and J. Dixon (2000). "Breast cancer-epidemiology, risk factors, and genetics." BMJ: British Medical Journal **321**(7261): 624.

Meeran, S. M., T. Punathil and S. K. Katiyar (2008). "IL-12 deficiency exacerbates inflammatory responses in UV-irradiated skin and skin tumors." Journal of Investigative Dermatology **128**(11): 2716-2727.

Menon, G. K. (2015). "Skin Basics; Structure and Function." 9-23.

Mezei, M. and V. Gulasekharam (1982). "Liposomes—a selective drug delivery system for the topical route of administration: gel dosage form." Journal of Pharmacy and Pharmacology **34**(7): 473-474.

Mikszta, J., J. Britingham, J. Alarcon, R. Pettis and J. Dekker (2001). "Applicator having abraded surface coated with substance to be applied." Patent WO **1**(89622): A1.

Mikszta, J. A., J. M. Brittingham, J. Alarcon, R. J. Pettis and J. P. Dekker III (2003). Topical delivery of vaccines, Google Patents.

Mills, J. K. and D. Needham (2005). "Lysolipid incorporation in dipalmitoylphosphatidylcholine bilayer membranes enhances the ion permeability and drug release rates at the membrane phase transition." Biochimica et Biophysica Acta (BBA)-Biomembranes **1716**(2): 77-96.

Ming, J. E., E. Roessler and M. Muenke (1998). "Human developmental disorders and the Sonic hedgehog pathway." Molecular medicine today **4**(8): 343-349.

Mitragotri, S. (2013). "Devices for overcoming biological barriers: the use of physical forces to disrupt the barriers." Advanced drug delivery reviews **65**(1): 100-103.

Monteagudo, E., Y. Gándola, L. González, C. Bregni and A. Carlucci (2012). "Development, characterization, and in vitro evaluation of tamoxifen microemulsions." Journal of drug delivery **2012**.

Moser, K., K. Kriwet, A. Naik, Y. N. Kalia and R. H. Guy (2001). "Passive skin penetration enhancement and its quantification in vitro." European journal of pharmaceutics and Biopharmaceutics **52**(2): 103-112.

Moses, M. A., H. Brem and R. Langer (2003). "Advancing the field of drug delivery: taking aim at cancer." Cancer cell **4**(5): 337-341.

Muhrer, J. C. (2009). "Melanoma: current incidence, diagnosis, and preventive strategies." The Journal for Nurse Practitioners **5**(1): 35-41.

Murphy, M. and A. J. Carmichael (2000). "Transdermal drug delivery systems and skin sensitivity reactions." American journal of clinical dermatology **1**(6): 361-368.

Murthy, S. N. (1999). "Magnetophoresis: an approach to enhance transdermal drug diffusion." Die Pharmazie **54**(5): 377-379.

Murthy, S. N. and S. R. R. Hiremath (2001). "Physical and chemical permeation enhancers in transdermal delivery of terbutaline sulphate." AAPS PharmSciTech **2**(1): 1-5.

Nagarajan, S., E. E. Schuler, K. Ma, J. T. Kindt and R. B. Dyer (2012). "Dynamics of the gel to fluid phase transformation in unilamellar DPPC vesicles." The Journal of Physical Chemistry B **116**(46): 13749-13756.

Naik, A., Y. N. Kalia and R. H. Guy (2000). "Transdermal drug delivery: overcoming the skin's barrier function." Pharmaceutical science & technology today **3**(9): 318-326.

Nanda, A., S. Nanda and N. Khan Ghilzai (2006). "Current developments using emerging transdermal technologies in physical enhancement methods." Current drug delivery **3**(3): 233-242.

Needham, D., G. Anyarambhatla, G. Kong and M. W. Dewhirst (2000). "A new temperature-sensitive liposome for use with mild hyperthermia: characterization and testing in a human tumor xenograft model." Cancer research **60**(5): 1197-1201.

Nelson, B. R., D. Railan and S. Cohen (1997). "Mohs' micrographic surgery for nonmelanoma skin cancers." Clinics in plastic surgery **24**(4): 705-718.

Neubert, R. H. (2011). "Potentials of new nanocarriers for dermal and transdermal drug delivery." European journal of pharmaceutics and biopharmaceutics **77**(1): 1-2.

Neville, J. A., E. Welch and D. J. Leffell (2007). "Management of nonmelanoma skin cancer in 2007." Nature clinical practice Oncology **4**(8): 462-469.

Nguyen, T. H. and D. Q.-D. Ho (2002). "Nonmelanoma skin cancer." Current treatment options in oncology **3**(3): 193-203.

Nitta, S. K. and K. Numata (2013). "Biopolymer-based nanoparticles for drug/gene delivery and tissue engineering." International journal of molecular sciences **14**(1): 1629-1654.

Niu, G., K. L. Wright, M. Huang, L. Song, E. Haura, J. Turkson, S. Zhang, T. Wang, D. Sinibaldi and D. Coppola (2002). "Constitutive Stat3 activity up-regulates VEGF expression and tumor angiogenesis." Oncogene **21**(13): 2000.

O'Regan, R. M. and V. C. Jordan (2002). "The evolution of tamoxifen therapy in breast cancer: selective oestrogen-receptor modulators and downregulators." The lancet oncology **3**(4): 207-214.

Ogiso, T., T. Hirota, M. Iwaki, T. Hino and T. Tanino (1998). "Effect of temperature on percutaneous absorption of terodiline, and relationship between penetration and fluidity of the stratum corneum lipids." International journal of pharmaceutics **176**(1): 63-72.

Ogunsola, O. A., M. E. Kraeling, S. Zhong, D. J. Pochan, R. L. Bronaugh and S. R. Raghavan (2012). "Structural analysis of “flexible” liposome formulations: new insights into the skin-penetrating ability of soft nanostructures." Soft Matter **8**(40): 10226-10232.

Oh, Y.-K. and T. G. Park (2009). "siRNA delivery systems for cancer treatment." Advanced drug delivery reviews **61**(10): 850-862.

Olszanski, A. J. (2014). "Current and future roles of targeted therapy and immunotherapy in advanced melanoma." Journal of Managed Care Pharmacy **20**(4): 346-356.

Otberg, N., H. Richter, H. Schaefer, U. Blume-Peytavi, W. Sterry and J. Lademann (2004). "Variations of hair follicle size and distribution in different body sites." Journal of Investigative Dermatology **122**(1): 14-19.

Panwar, P., B. Pandey, P. Lakhera and K. Singh (2010). "Preparation, characterization, and in vitro release study of albendazole-encapsulated nanosize liposomes." Int J Nanomedicine **5**(101): 8.

Parnami, N., T. Garg, G. Rath and A. K. Goyal (2014). "Development and characterization of nanocarriers for topical treatment of psoriasis by using combination therapy." Artificial cells, nanomedicine, and biotechnology **42**(6): 406-412.

Pathan, I. B. and C. M. Setty (2009). "Chemical penetration enhancers for transdermal drug delivery systems." Tropical Journal of Pharmaceutical Research **8**(2).

Pattni, B. S., V. V. Chupin and V. P. Torchilin (2015). "New developments in liposomal drug delivery." Chemical reviews **115**(19): 10938-10966.

Paudel, K. S., M. Milewski, C. L. Swadley, N. K. Brogden, P. Ghosh and A. L. Stinchcomb (2010). "Challenges and opportunities in dermal/transdermal delivery." Therapeutic delivery **1**(1): 109-131.

Pedranzini, L., A. Leitch and J. Bromberg (2004). "Stat3 is required for the development of skin cancer." The Journal of clinical investigation **114**(5): 619-622.

Petersen, K. K., M. L. Rousing, C. Jensen, L. Arendt-Nielsen and P. Gazerani (2011). "Effect of local controlled heat on transdermal delivery of nicotine." International journal of physiology, pathophysiology and pharmacology **3**(3): 236-242.

Pfeifer, G. P. and A. Besaratinia (2012). "UV wavelength-dependent DNA damage and human non-melanoma and melanoma skin cancer." Photochemical & Photobiological Sciences **11**(1): 90-97.

Phillips, J. M., C. Clark, L. Herman-Ferdinandez, T. Moore-Medlin, X. Rong, J. R. Gill, J. L. Clifford, F. Abreo and C.-A. O. Nathan (2011). "Curcumin inhibits skin squamous cell carcinoma tumor growth in vivo." Otolaryngology--Head and Neck Surgery **145**(1): 58-63.

Prabha, S., R. Vyas, N. Gupta, B. Ahmed, R. Chandra and S. Nimesh (2016). "RNA interference technology with emphasis on delivery vehicles—prospects and limitations." Artificial cells, nanomedicine, and biotechnology **44**(6): 1391-1399.

Pradhan, M., D. Singh and M. R. Singh (2013). "Novel colloidal carriers for psoriasis: current issues, mechanistic insight and novel delivery approaches." Journal of Controlled Release **170**(3): 380-395.

Prausnitz, M. R. and R. Langer (2008). "Transdermal drug delivery." Nat Biotechnol **26**(11): 1261-1268.

Prausnitz, M. R. and R. Langer (2008). "Transdermal drug delivery." Nature biotechnology **26**(11): 1261-1268.

Prow, T. W., J. E. Grice, L. L. Lin, R. Faye, M. Butler, W. Becker, E. M. Wurm, C. Yoong, T. A. Robertson and H. P. Soyer (2011). "Nanoparticles and microparticles for skin drug delivery." Advanced drug delivery reviews **63**(6): 470-491.

Rehman, Z. u., D. Hoekstra and I. S. Zuhorn (2013). "Mechanism of polyplex-and lipoplex-mediated delivery of nucleic acids: real-time visualization of transient membrane destabilization without endosomal lysis." ACS nano **7**(5): 3767-3777.

Reithmeier, H., J. Herrmann and A. Göpferich (2001). "Lipid microparticles as a parenteral controlled release device for peptides." Journal of Controlled Release **73**(2): 339-350.

Rejman, J., A. Bragonzi and M. Conese (2005). "Role of clathrin-and caveolae-mediated endocytosis in gene transfer mediated by lipo-and polyplexes." Molecular Therapy **12**(3): 468-474.

Robertson, G. P. (2005). "Functional and therapeutic significance of Akt deregulation in malignant melanoma." Cancer and metastasis reviews **24**(2): 273-285.

Rogers, H. W., M. A. Weinstock, A. R. Harris, M. R. Hinckley, S. R. Feldman, A. B. Fleischer and B. M. Coldiron (2010). "Incidence estimate of nonmelanoma skin cancer in the United States, 2006." Archives of dermatology **146**(3): 283-287.

Rosko, A. J., K. K. Vankoevering, S. A. McLean, T. M. Johnson and J. S. Moyer "Contemporary Management of Early-Stage Melanoma: A Systematic Review." JAMA Facial Plastic Surgery.

Roustit, M., S. Blaise and J. L. Cracowski (2014). "Trials and tribulations of skin iontophoresis in therapeutics." British journal of clinical pharmacology **77**(1): 63-71.

Rubin, A. I., E. H. Chen and D. Ratner (2005). "Basal-cell carcinoma." New England Journal of Medicine **353**(21): 2262-2269.

Ruby, A., G. Kuttan, K. D. Babu, K. Rajasekharan and R. Kuttan (1995). "Anti-tumour and antioxidant activity of natural curcuminoids." Cancer letters **94**(1): 79-83.

Russo, A., B. Ficili, S. Candido, F. M. Pezzino, C. Guarneri, A. Biondi, S. Travali, J. A. McCubrey, D. A. Spandidos and M. Libra (2014). "Emerging targeted therapies for melanoma treatment (Review)." International journal of oncology **45**(2): 516-524.

Russo, A. E., E. Torrisi, Y. Bevelacqua, R. Perrotta, M. Libra, J. A. McCubrey, D. A. Spandidos, F. Stivala and G. Malaponte (2009). "Melanoma: molecular pathogenesis and emerging target therapies (Review)." International journal of oncology **34**(6): 1481.

Saladi, R. N. and A. N. Persaud (2005). "The causes of skin cancer: a comprehensive review." Drugs of Today **41**(1): 37-54.

Salem, M., S. Rohani and E. R. Gillies (2014). "Curcumin, a promising anti-cancer therapeutic: a review of its chemical properties, bioactivity and approaches to cancer cell delivery." Rsc Advances **4**(21): 10815-10829.

Sammeta, S. M., S. R. K. Vaka and S. N. Murthy (2010). "Transcutaneous electroporation mediated delivery of doxepin-HPCD complex: a sustained release approach for treatment of postherpetic neuralgia." Journal of controlled release **142**(3): 361-367.

Samson, K. (2014). "More Evidence Tamoxifen Gel Works as Well as Oral Form but with Fewer Side Effects." Oncology Times **36**(18): 46-47.

Sarasin, A. (1999). "The molecular pathways of ultraviolet-induced carcinogenesis." Mutation Research/Fundamental and Molecular Mechanisms of Mutagenesis **428**(1): 5-10.

Scales, S. J. and F. J. de Sauvage (2009). "Mechanisms of Hedgehog pathway activation in cancer and implications for therapy." Trends in pharmacological sciences **30**(6): 303-312.

Schoellhammer, C. M., D. Blankschtein and R. Langer (2014). "Skin permeabilization for transdermal drug delivery: recent advances and future prospects." Expert opinion on drug delivery **11**(3): 393-407.

Schreier, H. and J. Bouwstra (1994). "Liposomes and niosomes as topical drug carriers: dermal and transdermal drug delivery." Journal of controlled release **30**(1): 1-15.

Schroeder, A., C. G. Levins, C. Cortez, R. Langer and D. G. Anderson (2010). "Lipid-based nanotherapeutics for siRNA delivery." Journal of internal medicine **267**(1): 9-21.

Schwartz, R. A. (1988). Squamous cell carcinoma. Skin Cancer, Springer**:** 36-47.

Schwendener, R. A. and H. Schott (2010). "Liposome formulations of hydrophobic drugs." Liposomes: Methods and Protocols, Volume 1: Pharmaceutical Nanocarriers: 129-138.

Sedda, A., G. Rossi, C. Cipriani, A. Carrozzo and P. Donati (2008). "Dermatological high-dose-rate brachytherapy for the treatment of basal and squamous cell carcinoma." Clinical and experimental dermatology **33**(6): 745-749.

Sercombe, L., T. Veerati, F. Moheimani, S. Y. Wu, A. K. Sood and S. Hua (2015). "Advances and challenges of liposome assisted drug delivery." Frontiers in pharmacology **6**: 286.

Sezer, A. D. (2012). Recent Advances in Novel Drug Carrier System, InTech.

Sharma, N., G. Agarwal, A. Rana, Z. A. Bhat and D. Kumar (2011). "A review: Transdermal drug delivery system: A tool for novel drug delivery system." International Journal of Drug Development and Research.

Shehzad, A., F. Wahid and Y. S. Lee (2010). "Curcumin in cancer chemoprevention: molecular targets, pharmacokinetics, bioavailability, and clinical trials." Archiv der Pharmazie **343**(9): 489-499.

Shiau, A. K., D. Barstad, P. M. Loria, L. Cheng, P. J. Kushner, D. A. Agard and G. L. Greene (1998). "The structural basis of estrogen receptor/coactivator recognition and the antagonism of this interaction by tamoxifen." Cell **95**(7): 927-937.

Shim, G., M.-G. Kim, J. Y. Park and Y.-K. Oh (2013). "Application of cationic liposomes for delivery of nucleic acids." Asian Journal of Pharmaceutical Sciences **8**(2): 72-80.

Siegel, R. L., K. D. Miller and A. Jemal (2016). "Cancer statistics, 2016." CA: a cancer journal for clinicians **66**(1): 7-30.

Singh, I. and A. P. Morris (2011). "Performance of transdermal therapeutic systems: Effects of biological factors." Int J Pharm Investig **1**(1): 4-9.

Singh, K., N. Arora and T. Garg (2012). "Superbug: antimicrobial resistance due to NDM-1." Int J Inst Pharm Life Sci **2**(2): 58-66.

Singh, R., U. U. Shedbalkar, S. A. Wadhwani and B. A. Chopade (2015). "Bacteriagenic silver nanoparticles: synthesis, mechanism, and applications." Applied microbiology and biotechnology **99**(11): 4579-4593.

Singhal, G. B., R. P. Patel, B. Prajapati and N. A. Patel (2011). "Solid lipid nanoparticles and nano lipid carriers: as novel solid lipid based drug carrier." Int Res J Pharm **2**(2): 20-52.

Sinico, C. and A. M. Fadda (2009). "Vesicular carriers for dermal drug delivery." Expert opinion on drug delivery **6**(8): 813-825.

Slamon, D. J., B. Leyland-Jones, S. Shak, H. Fuchs, V. Paton, A. Bajamonde, T. Fleming, W. Eiermann, J. Wolter and M. Pegram (2001). "Use of chemotherapy plus a monoclonal antibody against HER2 for metastatic breast cancer that overexpresses HER2." New England Journal of Medicine **344**(11): 783-792.

Sober, A. J. (1983). "Diagnosis and management of skin cancer." Cancer **51**(S12): 2448-2452.

Society, A. C. (2012). American Cancer Society: Cancer Facts and Figures 2012, American Cancer Society Atlanta, GA.

Souza, J. G., K. Dias, T. A. Pereira, D. S. Bernardi and R. F. Lopez (2014). "Topical delivery of ocular therapeutics: carrier systems and physical methods." Journal of Pharmacy and Pharmacology **66**(4): 507-530.

Stahl, J. M., A. Sharma, M. Cheung, M. Zimmerman, J. Q. Cheng, M. W. Bosenberg, M. Kester, L. Sandirasegarane and G. P. Robertson (2004). "Deregulated Akt3 activity promotes development of malignant melanoma." Cancer research **64**(19): 7002-7010.

Steiner, A., H. Pehamberger and K. Wolff (1987). "In vivo epiluminescence microscopy of pigmented skin lesions. II. Diagnosis of small pigmented skin lesions and early detection of malignant melanoma." Journal of the American Academy of Dermatology **17**(4): 584-591.

Steinsträsser, I. and H. P. Merkle (1995). "Dermal metabolism of topically applied drugs: pathways and models reconsidered." Pharmaceutica Acta Helvetiae **70**(1): 3-24.

Strickland, F. M. and M. L. Kripke (1997). "Immune response associated with nonmelanoma skin cancer." Clinics in plastic surgery **24**(4): 637-647.

Sultana, S., M. R. Khan, M. Kumar, S. Kumar and M. Ali (2013). "Nanoparticles-mediated drug delivery approaches for cancer targeting: a review." Journal of drug targeting **21**(2): 107-125.

Svedman, P. (1995). Transdermal perfusion of fluids, Google Patents.

Svedman, P., S. Lundin, P. Höglund, C. Hammarlund, C. Malmros and N. Pantzar (1996). "Passive drug diffusion via standardized skin mini-erosion; methodological aspects and clinical findings with new device." Pharmaceutical research **13**(9): 1354-1359.

Svedman, P., C. Svedman and S. Lundin (1991). "Administration of antidiuretic peptide (DDAVP) by way of suction de-epithelialised skin." The Lancet **337**(8756): 1506-1509.

Szakács, G., J. K. Paterson, J. A. Ludwig, C. Booth-Genthe and M. M. Gottesman (2006). "Targeting multidrug resistance in cancer." Nature reviews Drug discovery **5**(3): 219-234.

Szmigielski, S., H. Zielinski, B. Stawarz, J. Gil, J. Sobczynski, G. Sokolska, J. Jeljaszewicz and G. Pulverer (1988). "Local microwave hyperthermia in treatment of advanced prostatic adenocarcinoma." Urological research **16**(1): 1-7.

Tan, P. and A. Billis (2004). "Basal cell carcinoma." World Health Organization classification of tumours: pathology and genetics of tumours of the urinary system and male genital organs. International Agency for Research on Cancer, Lyon **206**.

Teo, P. Y., W. Cheng, J. L. Hedrick and Y. Y. Yang (2016). "Co-delivery of drugs and plasmid DNA for cancer therapy." Advanced drug delivery reviews **98**: 41-63.

Testa, J. R. and A. Bellacosa (2001). "AKT plays a central role in tumorigenesis." Proceedings of the National Academy of Sciences **98**(20): 10983-10985.

Thomas, S., J. Snowden, M. Zeidler and S. Danson (2015). "The role of JAK/STAT signalling in the pathogenesis, prognosis and treatment of solid tumours." British journal of cancer **113**(3): 365-371.

Thomson, T. M., M. J. Mattes, L. Roux, L. J. Old and K. O. Lloyd (1985). "Pigmentation-associated glycoprotein of human melanomas and melanocytes: definition with a mouse monoclonal antibody." Journal of Investigative Dermatology **85**(2): 169-174.

Ting, W. W., C. D. Vest and R. D. Sontheimer (2004). "Review of traditional and novel modalities that enhance the permeability of local therapeutics across the stratum corneum." International journal of dermatology **43**(7): 538-547.

Tojo, K. (1987). "Random brick model for drug transport across stratum corneum." Journal of pharmaceutical sciences **76**(12): 889-891.

Tsouris, V., M. K. Joo, S. H. Kim, I. C. Kwon and Y.-Y. Won (2014). "Nano carriers that enable co-delivery of chemotherapy and RNAi agents for treatment of drug-resistant cancers." Biotechnology advances **32**(5): 1037-1050.

Tsuruo, T., M. Naito, A. Tomida, N. Fujita, T. Mashima, H. Sakamoto and N. Haga (2003). "Molecular targeting therapy of cancer: drug resistance, apoptosis and survival signal." Cancer science **94**(1): 15-21.

Ulrich, A. S. (2002). "Biophysical aspects of using liposomes as delivery vehicles." Bioscience reports **22**(2): 129-150.

van den Bergh, B. A., J. Vroom, H. Gerritsen, H. E. Junginger and J. A. Bouwstra (1999). "Interactions of elastic and rigid vesicles with human skin in vitro: electron microscopy and two-photon excitation microscopy." Biochimica et Biophysica Acta (BBA)-Biomembranes **1461**(1): 155-173.

van Leeuwen, R. W., T. van Gelder, R. H. Mathijssen and F. G. Jansman (2014). "Drug–drug interactions with tyrosine-kinase inhibitors: a clinical perspective." The Lancet Oncology **15**(8): e315-e326.

Vanhaesebroeck, B. and D. R. Alessi (2000). "The PI3K–PDK1 connection: more than just a road to PKB." Biochemical Journal **346**(3): 561-576.

Venuganti, V. V. and O. P. Perumal (2009). Nanosystems for dermal and transdermal drug delivery. Drug Delivery Nanoparticles Formulation and Characterization, CRC Press**:** 126-155.

Venuganti, V. V. K., M. Saraswathy, C. Dwivedi, R. S. Kaushik and O. P. Perumal (2015). "Topical gene silencing by iontophoretic delivery of an antisense oligonucleotide–dendrimer nanocomplex: the proof of concept in a skin cancer mouse model." Nanoscale **7**(9): 3903-3914.

Walters, K. A. (2002). Dermatological and transdermal formulations, CRC Press.

Wang, C.-Y., M. W. Mayo, R. G. Korneluk, D. V. Goeddel and A. S. Baldwin (1998). "NF-κB antiapoptosis: induction of TRAF1 and TRAF2 and c-IAP1 and c-IAP2 to suppress caspase-8 activation." Science **281**(5383): 1680-1683.

Wang, H., Y. Zhao, Y. Wu, Y.-l. Hu, K. Nan, G. Nie and H. Chen (2011). "Enhanced anti-tumor efficacy by co-delivery of doxorubicin and paclitaxel with amphiphilic methoxy PEG-PLGA copolymer nanoparticles." Biomaterials **32**(32): 8281-8290.

Wang, J., Z. Lu, M. G. Wientjes and J. L.-S. Au (2010). "Delivery of siRNA therapeutics: barriers and carriers." The AAPS journal **12**(4): 492-503.

Wang, Y., R. Thakur, Q. Fan and B. Michniak (2005). "Transdermal iontophoresis: combination strategies to improve transdermal iontophoretic drug delivery." European journal of pharmaceutics and biopharmaceutics **60**(2): 179-191.

Watson, D. S., A. N. Endsley and L. Huang (2012). "Design considerations for liposomal vaccines: influence of formulation parameters on antibody and cell-mediated immune responses to liposome associated antigens." Vaccine **30**(13): 2256-2272.

Weigelt, B. and J. S. Reis-Filho (2009). "Histological and molecular types of breast cancer: is there a unifying taxonomy?" Nature reviews Clinical oncology **6**(12): 718-730.

Wilken, R., M. S. Veena, M. B. Wang and E. S. Srivatsan (2011). "Curcumin: A review of anti-cancer properties and therapeutic activity in head and neck squamous cell carcinoma." Molecular cancer **10**(1): 12.

Wittrup, A. and J. Lieberman (2015). "Knocking down disease: a progress report on siRNA therapeutics." Nature Reviews Genetics **16**(9): 543-552.

Wong, C., R. Strange and J. Lear (2003). "Basal cell carcinoma." BMJ: British Medical Journal **327**(7418): 794.

Wu, X.-M., H. Todo and K. Sugibayashi (2007). "Enhancement of skin permeation of high molecular compounds by a combination of microneedle pretreatment and iontophoresis." Journal of controlled release **118**(2): 189-195.

Xie, Y., B. Xu and Y. Gao (2005). "Controlled transdermal delivery of model drug compounds by MEMS microneedle array." Nanomedicine: Nanotechnology, Biology and Medicine **1**(2): 184-190.

Xiong, F., Z. Mi and N. Gu (2011). "Cationic liposomes as gene delivery system: transfection efficiency and new application." Die Pharmazie-An International Journal of Pharmaceutical Sciences **66**(3): 158-164.

Xu, S., D. Robbins, J. Frost, A. Dang, C. Lange-Carter and M. H. Cobb (1995). "MEKK1 phosphorylates MEK1 and MEK2 but does not cause activation of mitogen-activated protein kinase." Proceedings of the National Academy of Sciences **92**(15): 6808-6812.

Yallapu, M. M., M. Jaggi and S. C. Chauhan (2012). "Curcumin nanoformulations: a future nanomedicine for cancer." Drug discovery today **17**(1): 71-80.

Yang, C.-L., Y.-Y. Liu, Y.-G. Ma, Y.-X. Xue, D.-G. Liu, Y. Ren, X.-B. Liu, Y. Li and Z. Li (2012). "Curcumin blocks small cell lung cancer cells migration, invasion, angiogenesis, cell cycle and neoplasia through Janus kinase-STAT3 signalling pathway." PloS one **7**(5): e37960.

Yang, Y., J. Bugno and S. Hong (2013). "Nanoscale polymeric penetration enhancers in topical drug delivery." Polymer Chemistry **4**(9): 2651.

Yang, Z., D. Gao, Z. Cao, C. Zhang, D. Cheng, J. Liu and X. Shuai (2015). "Drug and gene co-delivery systems for cancer treatment." Biomaterials science **3**(7): 1035-1049.

Yano, T., A. Nakagawa, M. Tsuji and K. Noda (1986). "Skin permeability of various non-steroidal anti-inflammatory drugs in man." Life sciences **39**(12): 1043-1050.

Yu, H. and R. Jove (2004). "The STATs of cancer—new molecular targets come of age." Nature Reviews Cancer **4**(2): 97-105.

Yu, H., H. Lee, A. Herrmann, R. Buettner and R. Jove (2014). "Revisiting STAT3 signalling in cancer: new and unexpected biological functions." Nature reviews Cancer **14**(11): 736-746.

Yu, H., D. Pardoll and R. Jove (2009). "STATs in cancer inflammation and immunity: a leading role for STAT3." Nature Reviews Cancer **9**(11): 798-809.

Zhang, Z., P. C. Tsai, T. Ramezanli and B. B. Michniak-Kohn (2013). "Polymeric nanoparticles-based topical delivery systems for the treatment of dermatological diseases." Wiley Interdisciplinary Reviews: Nanomedicine and Nanobiotechnology **5**(3): 205-218.

Zhao, Y.-Z., C.-T. Lu, Y. Zhang, J. Xiao, Y.-P. Zhao, J.-L. Tian, Y.-Y. Xu, Z.-G. Feng and C.-Y. Xu (2013). "Selection of high efficient transdermal lipid vesicle for curcumin skin delivery." International journal of pharmaceutics **454**(1): 302-309.

Zorec, B., S. Becker, M. Reberšek, D. Miklavčič and N. Pavšelj (2013). "Skin electroporation for transdermal drug delivery: the influence of the order of different square wave electric pulses." International journal of pharmaceutics **457**(1): 214-223.

Zuckerman, J. E. and M. E. Davis (2015). "Clinical experiences with systemically administered siRNA-based therapeutics in cancer." Nature Reviews Drug Discovery **14**(12): 843-856.

List of publications and presentations

From thesis

1. Jose A., S. Labala and V. V. K. Venuganti (2017). "Co-delivery of curcumin and STAT3 siRNA using deformable cationic liposomes to treat skin cancer." *Journal of Drug Targeting 25(4):* 330-341.
2. Jose A, S.Labala, K.M. Ninave, S.K. Gade and V. V. K. Venuganti (2017). "Effective skin cancer treatment by topical co-delivery of curcumin and STAT3 siRNA using cationic liposomes" *AAPS PharmScitech*: 1-10.
3. Jose A, K.M. Ninave, K S Ravali and V. V. K. Venuganti (2017)." Temperature-sensitive liposomes for topical codelivery of tamoxifen and imatinib for synergistic breast cancer treatment". (under communication)

Other publications

1. Jose A., P. K. Mandapalli and V. V. K. Venuganti (2016). "Liposomal hydrogel formulation for transdermal delivery of pirfenidone." *Journal of liposome research* 26(2): 139-147.
2. Labala S., Jose A. and Venuganti, V.V.K. (2016). "Transcutaneous iontophoretic delivery of STAT3 siRNA using layer-by-layer chitosan coated gold nanoparticles to treat melanoma". *Colloids and Surfaces B: Biointerfaces*, 146, 188-197.
3. Labala S, Jose A, S R Chawla, M S Khan, S Bhatnagar, O P Kulkarni and V V K Venuganti (2017). Effective melanoma cancer suppression by iontophoretic co-delivery of STAT3 siRNA and imatinib using gold nanoparticles. *International Journal of Pharmaceutics* 525 (2), 407-417.

4. P K Mandapalli, Labala S, Jose A, Bhatnagar S, R Janupally, D Sriram and V V K Venuganti (2017). "Layer-by-layer thin films for codelivery of TGF-beta siRNA and epidermal growth factor to improve excisional wound healing". *AAPS PharmSciTech* 18(3), 809-820.

Conference presentations

1. Anup Jose, Suman Labala, Venkata Vamsi K. Venuganti. Topical iontophoretic co-delivery of curcumin and STAT3 siRNA using liposomes to treat skin cancer. AAPS Annual Meeting and Exposition 2016, Nov' 2016, Denver, USA.
2. Anup Jose, Suman Labala, Venkata Vamsi K. Venuganti. Preparation, characterization and in-vitro evaluation of ceramide containing liposome - STAT3 siRNA complex to treat skin cancer. AAPS Annual Meeting and Exposition 2015, Oct' 2015, Orlando, USA.
3. Anup Jose, Praveen K. Mandapalli, Venkata Vamsi K. Venuganti. Feasibility study for transdermal delivery of pirfenidone using liposomes. 66th Indian Pharmaceutical Congress, Jan' 2015, Hyderabad, India.

Awards and honors

1. International Travel Award by Amgen (USA) to present a paper at AAPS Annual Meeting and Exposition 2016, Nov 2016, Denver, USA.
2. International Travel Support (ITS) Grant by Science and Engineering Research Board (SERB), Department of Science and Technology (DST), Govt. of India to present a paper at AAPS Annual Meeting and Exposition 2015, Oct 2015, Orlando, USA.

3. International Travel Award by Centre for International Co-operation in Science (CICS), Govt. of India to present a paper at AAPS Annual Meeting and Exposition 2015, Oct 2015, Orlando, USA.

Biography of Anup Jose

Mr. Anup Jose has completed his B.Pharm from College of Pharmaceutical Sciences, Govt. Medical College, Trivandrum, Kerala (2009). He has obtained his M.Pharm (Pharmaceutics) from Pondicherry University, Pondicherry (2011). Later, he worked as a formulation scientist in Formulation Research & Development department of Zydus Cadila, Mumbai (2011-2013). He joined BITS Pilani Hyderabad campus in August 2013 to pursue his doctoral degree under the supervision of Dr.Venkata Vamsi Krishna Venuganti. He has authored/co-authored research papers in renowned national and international peer-reviewed journals and presented his research works at various national and international conferences. He has qualified GATE-2009, GPAT-2010, GPAT-2011 and GPAT-2013. Mr. Anup received international travel awards from Department of Science and Technology (DST), Govt. of India (2015), Centre for International Co-operation in Science (CICS), Govt. of India (2015) and Amgen, USA (2016) to present his research works in various international conferences.

Biography of Dr. Venkata Vamsi Krishna Venuganti

Dr. Venkata Vamsi Krishna Venuganti is currently working as Assistant Professor in department of pharmacy, BITS Pilani, Hyderabad campus. He has completed his B.Pharm from Kakatiya University, Andhra Pradesh (2004). He obtained his Ph.D in Pharmaceutical Sciences from South Dakota State University, USA (2010). Later, he joined as faculty member, department of pharmacy, BITS Pilani, Hyderabad campus in July 2010. He has one Indian patent to his credit and several publications in various renowned international peer-reviewed journals. He has also written a book chapter "Nanosystems for dermal and transdermal drug delivery" in Drug Delivery Nanoparticels Formulation and Characterization published by Informa Healthcare Inc, New York, NY, USA. His areas of research include nano/micro-carrier mediated drug delivery for transdermal/topical applications, non-viral carriers for gene-based drug delivery and development of biomaterials for drug delivery. Currently he has seven ongoing projects funded by government agencies and pharmaceutical industries. He has successfully completed four projects funded by various research funding agencies.